UNIVERSITEIT VAN PRETORIA
UNIVERSITY OF PRETORIA
YUNIBESITHI YA PRETORIA

Fischer and N-heterocyclic carbene complexes of chromium(0)

by

Roan Fraser

Submitted in partial fulfilment of the requirements for the degree

Magister Scientiae

in the Faculty of Natural and Agricultural Sciences

University of Pretoria

Pretoria

Supervisor:

Dr M. Landman

June 2012

© University of Pretoria

Declaration

The synthesis, characterisation and molecular modelling outlined in this dissertation were carried out at the Department of Chemistry, University of Pretoria, between January 2011 and March 2012. Dr Marilé Landman served as supervisor for the entire duration of the research project and I, Roan Fraser, declare that all work published on my behalf is my own and has not previously been submitted by myself or in my authority for the degree Magister Scientiae at this or any other tertiary institution.

.....

Roan Fraser

June 2012

© University of Pretoria

ABSTRACT

Fischer and N-heterocyclic carbene complexes of chromium(0)

by

Roan Fraser

Supervisor: Dr M. Landman

Submitted in partial fulfilment of the requirements for the degree Magister Scientiae, Department of Chemistry, University of Pretoria, Pretoria

The central focus of this study was the synthesis, structural investigation and characterisation of multiple chromium carbene complexes. Fifteen novel chromium(0) complexes were synthesised. The synthesis of the primary monocarbene starting material [$Cr(CO)_5${C(OEt)(heteroaryl)}], heteroaryl = thiophene, furan, 2,2'-bithiophene, was carried out utilising typical Fischer methodology. A wide variation of spacer ligands were reacted to obtain different carbene substituents. The ligand substitution reaction between carbonyl ligands and the bidentate ligands followed the techniques proposed in literature and produced distinctive chelated monocarbene complexes with the resulting structure *mer*-[$Cr(CO)_3$(dppe){carbene)}]. An extensive collection of more sophisticated monocarbene complexes was synthesised via modification pathways (aminolysis). Conversion of original ethoxy-bearing monocarbenes through aminolysis provided the corresponding amine analogues, possessing both novel structure and unique chemical reactivity. The aminolysis reactions involved different sized amino reagents; both ammonia and cyclohexyl amine (bulky, cyclic chair amines) were employed to produce derivatives of the monocarbene starting complexes. Lastly, the synthesis of unique N-heterocyclic carbene (NHC) complexes was envisaged. Synthesis of both the pentacarbonyl-bearing and phosphine-bearing NHC complexes was attempted utilising an adapted version of a methodology proposed in literature. The synthesis of chelate NHC complexes, however, proved difficult and the resulting products were not obtained.

All Fischer and N-heterocyclic carbene complexes were characterised using infrared spectroscopy, nuclear magnetic resonance spectroscopy and mass spectrometry. In cases where single crystals were obtained, X-ray crystallography was used to confirm molecular structures. X-ray crystallographic studies indicated that carbonyl substitution reactions

© University of Pretoria

performed on monocarbene starting material, will favour the formation of the meridonial isomer in molecules where the carbene substituents are less bulky. Due to steric considerations, the substitution of labile carbonyl ligands in the *trans* position to the carbene moiety will be favoured. Density functional theory (DFT) calculations were performed on the complexes synthesised in this study. The results obtained indicated the favoured isomeric form to be facial in some cases whereas crystallographic data signified the meridonial isomer as the more stable product, irrespective of the bulkiness of the carbene substituents. Bond lengths, geometry and bond angles were all comparable to those of the single-crystal X-ray data. Single-point energy calculations show clearly that modelling methods provide good estimations of energetically favourable geometries, and accurate DFT calculations also predict the HOMO and LUMO orientations around the metal or ligand spheres. The majority of the structures provided by the computed model, illustrated that the 3d atomic orbitals of the metal contributed significantly to the HOMO, whereas the LUMO was mostly orientated around the carbene carbon atom. Metathesis and polymerisation catalytic reactions were attempted on [$Cr(CO)_3$(dppe){C(OEt)(thiophene)}], **2**, whereas only metathesis studies were employed for [$Cr(CO)_3$(dppe){C(NHCy)(thiophene)}], **6**. Both complexes presented as inert to either reaction and no catalytic capability was witnessed. Gas chromatography was used to indicate the level of progression of the reaction and the chromatogram verified that neither pre-catalyst found application in metathesis or, in the case of **2**, in polymerisation.

© University of Pretoria

Acknowledgments

I would like to thank the following individuals for their contribution to either my personal or professional life:

First and foremost Dr Marilé Landman, for all her hard work, compassion and wisdom. Without her expert leadership neither this research nor my dissertation would have been feasible.

My extended family – Elmari and Johan Fraser, Chantelle and Janus van Rooyen and Emile and Ria Fraser. They offer a truly diverse family model, built on pillars of loyalty, trust and love.

My inspirational lab partner, René Pretorius, who is an expert hexane and DCM distiller with a swiftness of character and wit matched only by the greatness of her intellect.

My best friends – Ruan de Bruin, Madelize Oosthuizen, Shalene Bothma, Nelda Breedt, Liezl Ebersohn, André van der Westhuizen, Hansie van Staden and Frikkie Malan. Different qualifications and specialities did not pose any obstacle to my loyal friends in providing innovative solutions to any problems that presented themselves throughout the course of my research.

Dr Cornie van Sittert and Quinten of North West University, Potchefstroom, for assistance with the catalytic study.

Prof P.H. van Rooyen, Dave Liles and Eric Palmer - our crystallography and NMR experts, respectively.

And lastly with special thanks to the entire University of Pretoria's Chemistry Department.

© University of Pretoria

CONTENTS

ABSTRACT ..... **III**

LIST OF COMPLEXES ..... **X**

LIST OF ABBREVIATIONS ..... **XIV**

1 INTRODUCTION **1**

1.1 Overview of Carbene Complexes 1

1.2 Fischer Carbene Complexes 3

1.2.1 Overview 3

1.2.2 Synthesis 4

1.2.3 Theoretical bonding model and coordination 7

1.2.4 Reactivity 9

1.2.5 Applications 12

1.3 Schrock Carbene Complexes 14

1.3.1 Overview 14

1.3.2 Synthesis 15

1.3.3 Theoretical bonding model and coordination 17

1.3.4 Reactivity and application 18

1.4 N-Heterocyclic Carbene (NHC) Complexes 21

1.4.1 Overview 21

1.4.2 Synthesis 22

1.4.3 Theoretical bonding model and coordination 26

1.4.4 Reactivity and application 27

1.5 Coordination Complexes 31

1.5.1 Overview 31

1.5.2 Isomers 31

1.5.3 Denticity 32

1.5.4 The chelate effect 33

1.6 Aim of the study 333

2 BIDENTATE LIGATED CARBENE COMPLEXES **35**

2.1 Background 35

2.1.1 Fischer carbene complexes containing aromatic substituents 35

2.1.2 Fischer carbene complexes containing heteroaromatic substituents 37

2.1.3 Thiophene as heteroaromatic substituent 37

2.1.4 Furan as heteroaromatic substituent 39

© University of Pretoria

2.1.5 Polythiophenes as heteroaromatic substituent 39
2.1.6 Theoretical synthetic methodology 39
2.2 Synthesis 41
2.2.1 Focus 41
2.2.2 Synthetic methodology 42
2.3 Characterisation and Crystallographic Data 46
2.3.1 NMR spectroscopy 46
2.3.2 Infrared spectroscopy 59
2.3.3 X-ray crystallography 62
2.3.4 Mass spectroscopy 168
3 EVOLUTION OF MONOCARBENES: AMINOLYSIS 73
3.1 Background 73
3.2 Synthesis 77
3.2.1 Focus 77
3.2.2 Synthetic methodology 79
3.3 Characterisation 81
3.3.1 NMR spectroscopy 81
3.3.2 Infrared spectroscopy 98
3.3.3 X-ray crystallography 99
3.3.4 Mass spectrometry 105
4 SYNTHESIS OF N-HETEROCYCLIC CARBENE COMPLEXES 106
4.1 Background and Theoretical Synthesis 106
4.1.1 Abnormal NHC complexes 107
4.1.2 Remote NHC complexes (rNHCs) 108
4.1.3 Synthesis of NHC complexes 109
4.2 Synthesis 112
4.2.1 Focus 112
4.2.2 Synthetic methodology 113
4.3 Characterisation 116
4.3.1 NMR spectroscopy 116
4.3.2 Infrared spectroscopy 120
4.3.3 X-ray crystallography 120
4.3.4 Mass spectrometry 124
5 APPLICATION STUDY: CATALYTIC ABILITY 125
5.1 Application Background 125

© University of Pretoria

5.1.1 Fischer carbenes 125
5.1.2 N-heterocyclic carbene complexes 127
5.1.3 Focus of the study 128
5.2 Methodology 130
5.2.1 Metathesis and polymerisation reactions 130
5.2.2 Analysis: gas chromatography 131
5.3 Results 131
5.3.1 Metathesis reactions 131
5.3.2 Polymerisation reactions 134
5.4 Discussion 135
6 THEORETICAL STUDY: MOLECULAR MODELLING 138
6.1 Theoretical Modelling 138
6.1.1 Modelling methods 138
6.1.2 Theoretical calculations: Fischer carbenes 139
6.1.3 Theoretical calculations: N-heterocyclic carbenes 140
6.2 Intention of this Study 142
6.3 Structural Study 144
6.3.1 Structures investigated 144
6.3.2 Bidentate coordination 145
7 CONCLUSIONS 159
7.1 Synthesis 159
7.2 Characterisation 161
7.2.1 NMR spectroscopy 161
7.2.2 Infrared spectroscopy 162
7.2.3 X-ray crystallography 163
7.2.4 Mass spectrometry 163
7.3 Theoretical modelling 164
7.4 Catalytic studies 164
8 EXPERIMENTAL: STANDARD OPERATIONAL PROCEDURES AND SPECIFICATIONS 165
8.1 Products 165
8.2 Information and Specifications 166
8.2.1 NMR spectroscopy 166
8.2.2 Infrared spectroscopy 167
8.2.3 X-ray crystallography 167
8.2.4 Gas chromatography 167

© University of Pretoria

8.2.5 Mass spectroscopy 168
8.2.6 Reactions 168
8.3 Preparation of Bidentate-containing Fischer Carbene Complexes 169
8.3.1 1,2-Bis(diphenylphosphino)ethane chelated monocarbene complexes (**1**-**3**) 169
8.3.2 2,2'-Bipyridine chelated monocarbene complex 170
8.3.3 TEMED chelated monocarbene complex 170
8.4 Preparation of Aminocarbene Complexes 171
8.4.1 Ammonia aminocarbene complexes (**A** and **B**) 171
8.4.2 Mono aminocarbene complexes (**4**, **5**, **8**, **10** and **11**) 171
8.4.3 Bidentate ligated aminocarbene complexes (**6**, **7** and **9**) 172
8.5 Preparation of N-Heterocyclic Carbene Complexes 173
8.5.1 Formation of NHC complex (**12**) 173
8.6 Preparation of Coordination Complexes 175
8.6.1 Formation of complex **14** 175
APPENDICES: All crystal data tables available on the included CD 176
Appendix A: Crystal data and structure refinement for complex **1** 176
Appendix B: Crystal data and structure refinement for complex **2** 177
Appendix C: Crystal data and structure refinement for complex **3** 178
Appendix D: Crystal data and structure refinement for complex **14** 179
Appendix E: Crystal data and structure refinement for complex **B** 180
Appendix F: Crystal data and structure refinement for complex **A** 181
Appendix G: Crystal data and structure refinement for complex **6** 182
Appendix H: Crystal data and structure refinement for complex **13** 183
Appendix I: Crystal data and structure refinement for complex **15** 184
Appendix J: Crystal data and structure refinement for complex **F** 185

© University of Pretoria

LIST OF COMPLEXES

Fischer Carbenes

Complex 1

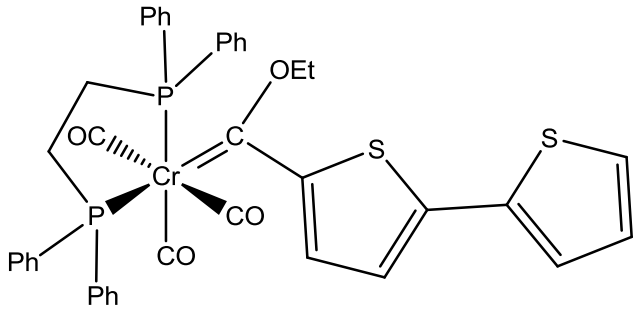

Complex 2

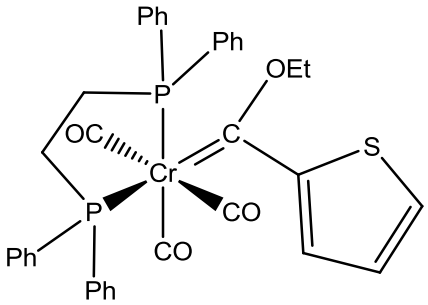

Complex 3

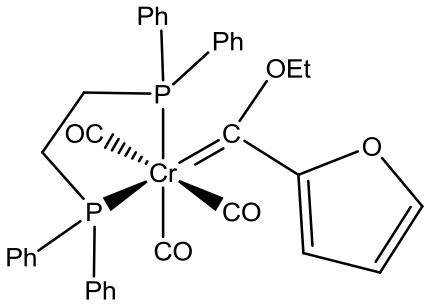

Amino Fischer Carbenes

Complex A

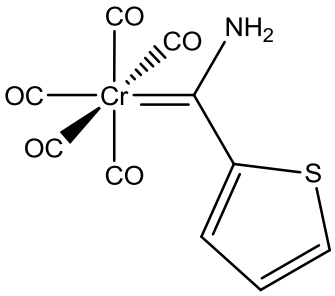

Complex B

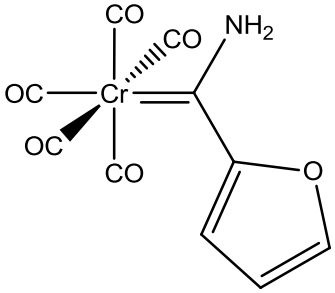

Complex 4

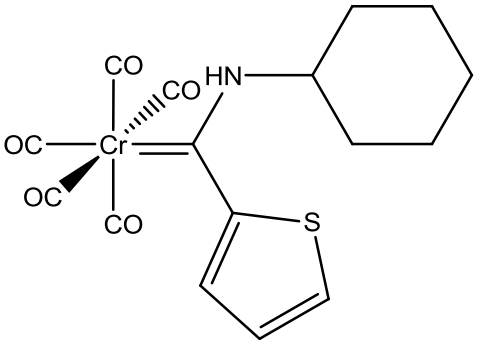

Complex 5

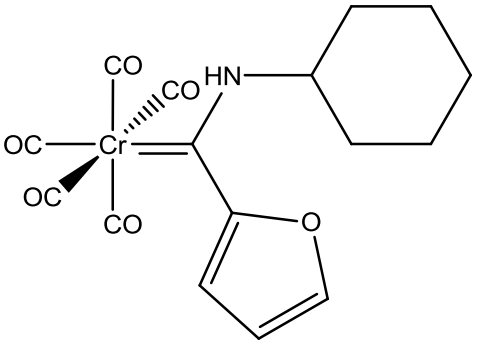

© University of Pretoria

Amino Fischer Carbenes (*Cont.*)

Complex 6

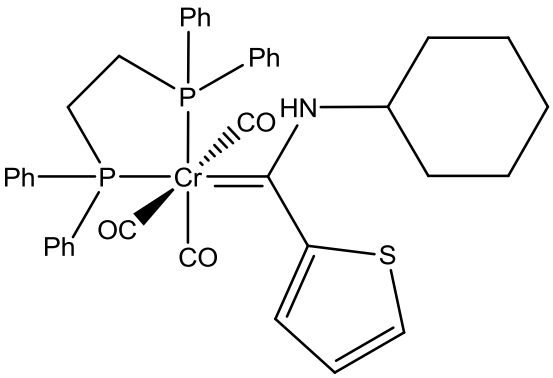

Complex 9

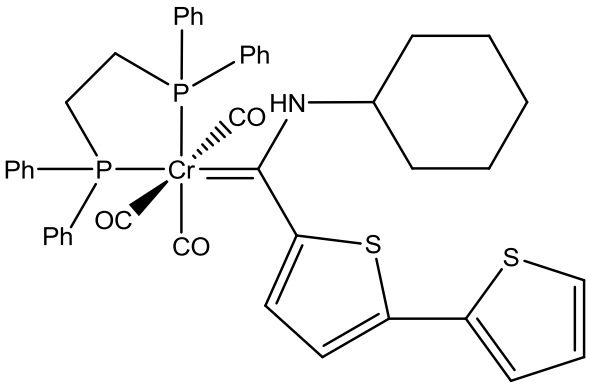

Complex 7

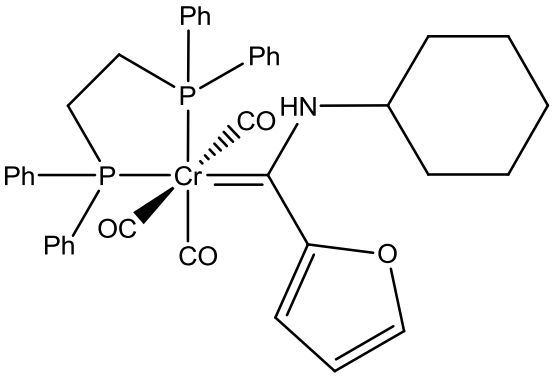

Complex 10

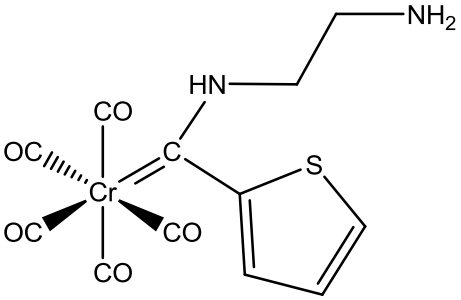

Complex 8

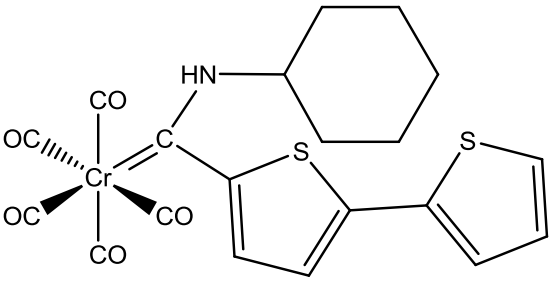

Complex 11

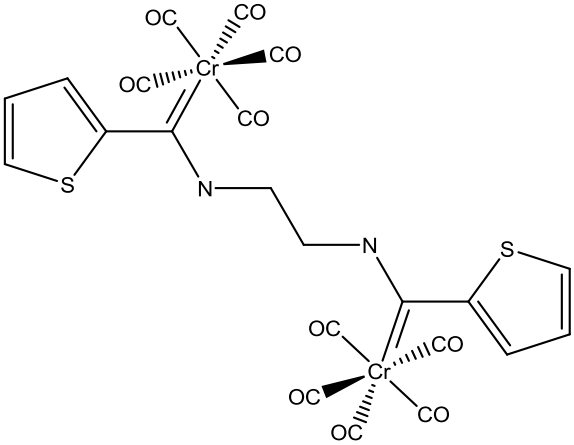

© University of Pretoria

N-Heterocyclic Carbenes

Complex 12

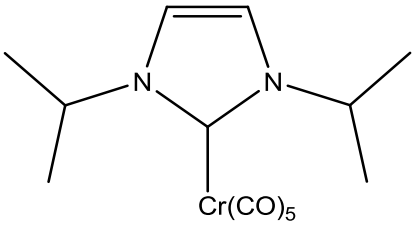

Coordination Complexes

Complex 13

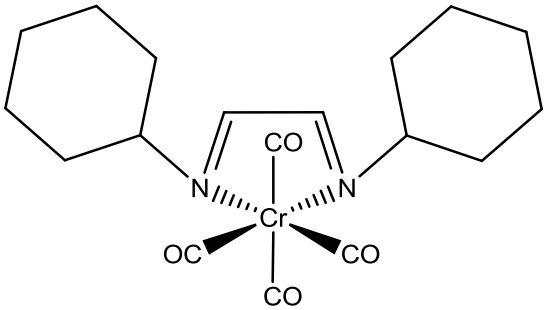

Complex 14

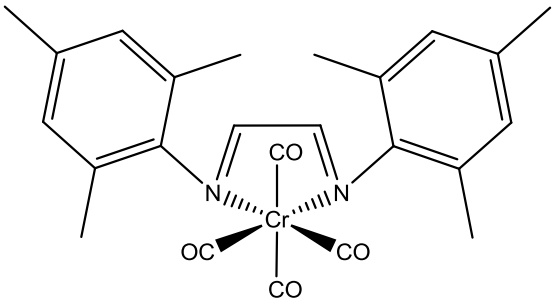

Known Complexes

Complex C

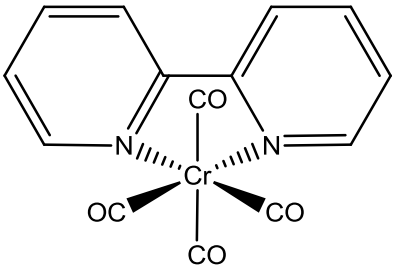

Complex D

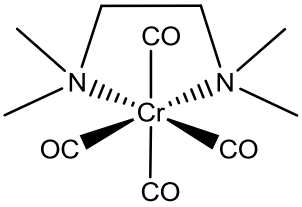

Complex E

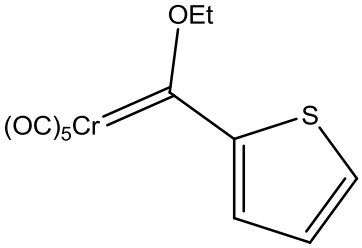

Complex F

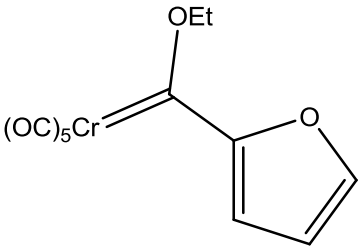

Complex G

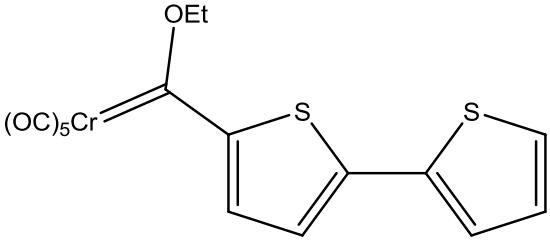

© University of Pretoria

LIST OF ABBREVIATIONS

Å	Angstrom
BDE	bond dissociation energy
bipy	2,2'-bipyridine
Bt	bithiophene
Bu	butyl
cy	cyclohexyl
D	doublet
DCM	dichloromethane
dd	doublet of doublets
ddd	doublet of doublet of doublets
DEE	diethyl ether
DFT	density functional theory
DHC	dihydrocoumarin
dppe	1,2-bis(diphenylphosphino)ethane
E	electrophile
EDTA	ethylenediaminetetraacetic acid
Et	ethyl
Fr	furan
GC	gas chromatography
HOMO	highest occupied molecular orbital
HSQC	heteronuclear single quantum coherence
hv	Planck's constant × frequency
IR	infrared spectroscopy
Im	imidazole
J	coupling constant
LUMO	lowest unoccupied molecular orbital

© University of Pretoria

m	medium (IR spectroscopy)
m	multiplet (NMR spectroscopy)
Me	methyl
MS	mass spectrometry
Naph	naphthalene
NHC	N-heterocyclic carbene
Nu	nucleophile
NMR	nuclear magnetic resonance spectroscopy
Ph	phenyl
PT	polythiophenes
R	alkyl group
ROMP	ring-opening metathesis polymerisation
RT	room temperature
s	strong (IR spectroscopy)
s	singlet (NMR spectroscopy)
SCF	self-consistent field (density)
td	triplet of doublets
TEMED	N'N'N''N''-tetramethylethane-1,2-diamine
Tf	thiophene
THF	tetrahydrofuran
tlc	thin layer chromatography
UV	ultraviolet
vs	very strong (IR spectroscopy)
vis	visible (UV-vis spectroscopy)
w	weak (IR spectroscopy)

© University of Pretoria

1 Introduction

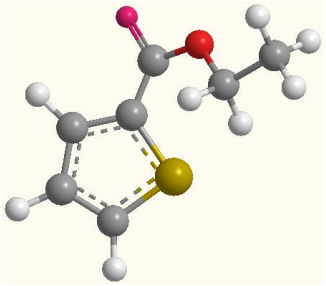

1.1 Overview of Carbene Complexes

In the early 1960s organometallic chemistry introduced an exciting new twist to the already extensive and expanding world of inorganic chemistry. With the synthesis of the first metal-to-carbon double bond, Fischer was not only presented with the Nobel Prize in Chemistry but also broke new ground and produced an entirely new field of research.[1] Carbenes are not only well known in today's scientific community, but are currently also an active research area worldwide with vast applicability and diversity in structure and properties.[2] Currently, one of the most famous examples of application is the Grubbs catalyst used in olefin metathesis, ROMP and ring-closing metathesis reactions.[3] Since the discovery of the vast catalytic applicability of carbene complexes, extensive research has been done and funds made available to investigate a large diversity of these novel complexes for both catalytic ability and other applications.[4] Carbenes can be defined on the basis of their neutral electronic state, which features a divalent carbon atom, and contain diverse reactivity both as naked units and within transition metal complexes.[5] When ligated to a metal component through coordination, the complexes are divided into two major categories based on reactivity and electronic configuration.[6] Named after the pioneers who discovered and characterised them, carbenes of the 'Fischer-type' contain an electrophilic carbene carbon with two electrons in the hybridised sp^2 orbitals, while the second, 'Schrock-type'[7] complexes bear inverted polarity and a single electron in both the sp^2 hybridised orbital and the

[1] Fischer, E. O., Maasböl, A., *Angew. Chem., Int. Ed. Engl.,* **1964**, 3, 580.
[2] Special edition dedicated to carbene and carbyne complexes and their applications, *J. Organomet. Chem*., **2001**, 617–618.
[3] Scholl, M., Ding, S., Lee, C. W., Grubbs, R. H., **1999**, 1(6), 953–956.
[4] Koch, J. K., *Organometallic Mechanisms and Catalysis*, Academic Press, New York, **1978.**
[5] (a) Doering, W. V. E., Hoffmann, A. K., *J. Am. Chem. Soc*., **1954**, 76, 6162. (b) Fischer, E. O., Maasböl, A., *Angew. Chem., Int. Ed. Engl*., **1964**, 3, 580.
[6] Fischer, E. O., Maasböl, A., *Angew. Chem., Int. Ed. Engl.,***1964**, 3, 645.
[7] Schrock R. R., *Acc. Chem. Res.,* **1979**, 12, 98.

© University of Pretoria

unhybridised p-orbital. Table 1.1 summarises the key differences between Fischer type and Schrock-type carbenes.

Table 1.1. Differences between 'Fischer-type' and 'Schrock-type' carbenes

Property	Fischer	Schrock
Nature of carbene	Electrophilic	Nucleophilic
Typical R-groups	π-donor	Alkyl
Typical metals	Cr(0),W(0),Mo(0)	Ta(V), W(VI)
Electron count (covalent model)	$2e^-$	$2e^-$
Electron count (ionic model)	$2e^-$	$4e^-$
Δ Oxidation state to metal complex	0	+2

There is a third derivative class of carbene complexes, termed 'N-heterocyclic carbenes' (NHCs). This class is distinct and is based on a molecular structure in which a carbene carbon is winged by two heteroatoms, one on either side, bearing alkyl groups. NHC complexes are σ-donating ligands and can be compared to classic P-, N-, O-donating ligands rather than to the typical Fischer or Schrock carbenes.[8] The NHCs were developed and the preparation methods published well over 30 years ago independently by Öfele, and Wanzlick and Schönherr.[9,10a]

NHC complexes have developed over recent years to become a robust part of organometallic chemistry. The modification of the Grubbs first-generation catalyst through a substitution reaction of a single phosphine ligand with an NHC carbene produced the corresponding second-generation catalyst with enhanced activity. The vast superiority of the second-generation catalyst over its predecessor illustrates the power and applicability of this class of compounds.[11]

[8] Weskamp, T., Volker, P. W., Wolfgang, A. H., *J.Organomet Chem.,* **2000***,* 600, 12–22.
[9] Öfele, K., *J. Organomet. Chem.,* **1968,** 12, 42.
[10] (a) Wanzlick, H. W. Schönherr, H., J. *Angew. Chem.,* **1968**, 80,154.; *Angew. Chem. Int. Ed. Engl.,* **1968**, 7, 141. (b) Lurger, P., Ruban, G., *Acta Crystallogr., Sect. B.,* **1971**, 27, 2276.
[11] Huang, J., Stevens, E. D., Nolan, S. P., Petersen, J. L., (1999). *J. Am. Chem. Soc.*, **1999**, 121(12), 2674–2678.

© University of Pretoria

Common characteristics of the carbene carbon atom include:[12]

- Approximate sp^2 hybridisation
- Geometry of expected trigonal planar
- Bond distance is shorter than the classic σ-bond but yet still longer than the typical σ-donor/π-acceptor as illustrated by the carbonyl ligand.
- If the carbene carbon atom is bound to a heteroatom (Fischer-type), additional stability is gained through electron density donation from the heteroatom. Thus additional resonance is available to add to the resonance hybrid.
- As the carbene carbon is ligated to different metal complexes, different characteristics are found.
- R-groups such as furan, thiophene and ferrocene may add additional stability to carbene complexes by adding electron density to the carbene carbon.[13]
- Double bond characteristics are added to a nitrogen atom when an amine group serves as a substituent of the carbene carbon.

1.2 Fischer Carbene Complexes

1.2.1 Overview

Fischer and Maasböl discovered the first carbene complex containing a transition metal in 1964 and ever since this revolutionary date, this rich chemistry has been continuously developing.[14] The pentacarbonyl[methoxybenzylidene]tungsten(0) that was originally made by the Fischer group is a key example of a Fischer carbene complex (Schemes 1.1 and 1.2). Fischer carbenes are normally composed of the lower valent transition metals between and including Group 6 to 8 and, in general, have good π-acceptor ligands coordinated to the metal sphere. The presence of the π-acceptor groups aids stability by providing additional

[12] Elschenbroich, C., Salzer, A., *Organometallics: A Concise Introduction,* 2nd edn, **1992**, Verlagsgesellschaft, New York.
[13] Connor, J. A., Jones, E. M., Loyd, J. P., *J. Organometal. Chem.,***1970**, 24, C20–C22.
[14] Fischer, E. O., Maasböl, A., *Angew, Chem., Int. Ed. Engl.,***1964**, 76, 645.

© University of Pretoria

access sites for excess electron density to be stored. By comparison, the carbon of the carbene has electrophilic properties and is stabilised through electron back-donation by metal d-electrons. Additional electron support is also provided through electronic contribution by the heteroatom substituents to the carbene centre.

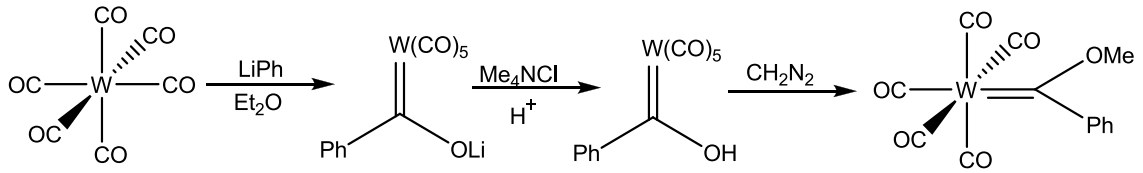

Scheme 1.1. Synthetic pathway utilised by Fischer

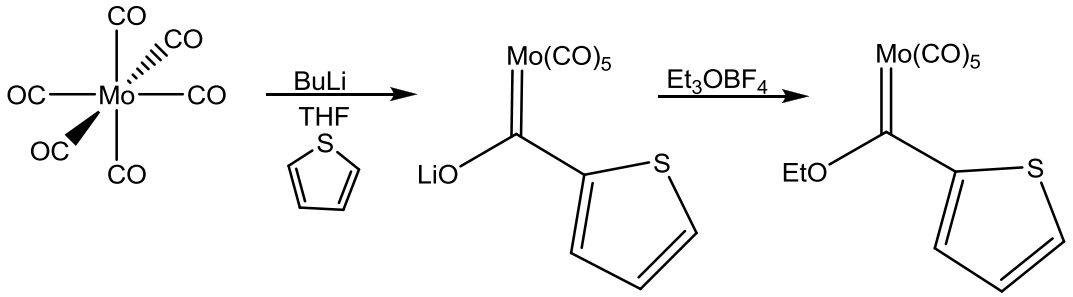

Scheme 1.2. Synthetic pathway of a typical Fischer carbene

1.2.2 Synthesis

Many different synthetic routes are available for Fischer carbene production. The method most commonly preferred today, however, consists of an alkyl lithium attack on a metal carbonyl ligand, followed by the addition of an alkylation source (Scheme 1.3).[15,16]

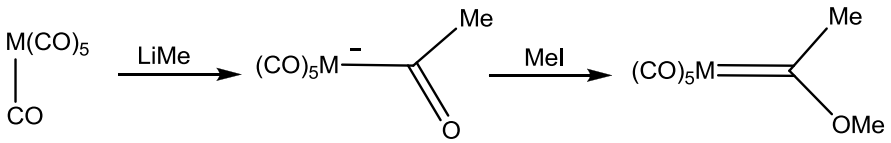

Scheme 1.3. Alkyl lithium attack on metal carbonyl, followed by alkylation

[15] Hartwig, J. F., *Organotransition Metal Chemistry, from Bonding to Catalysis,* University Science Books, New York, **2010**, pp 481–504.
[16] Semmelhack, M. F., *Organometallics in Synthesis*, Schlosser, M. (Ed.), Wiley, Chichester, UK, **2002**, pp 1024–1041.

© University of Pretoria

Fischer carbenes can also be fashioned from hexacarbonyl metal coordination compounds that undergo a reductive route (Scheme 1.4) or, alternatively, via vinylidene and allenylidene intermediates (Scheme 1.5)[15,16].

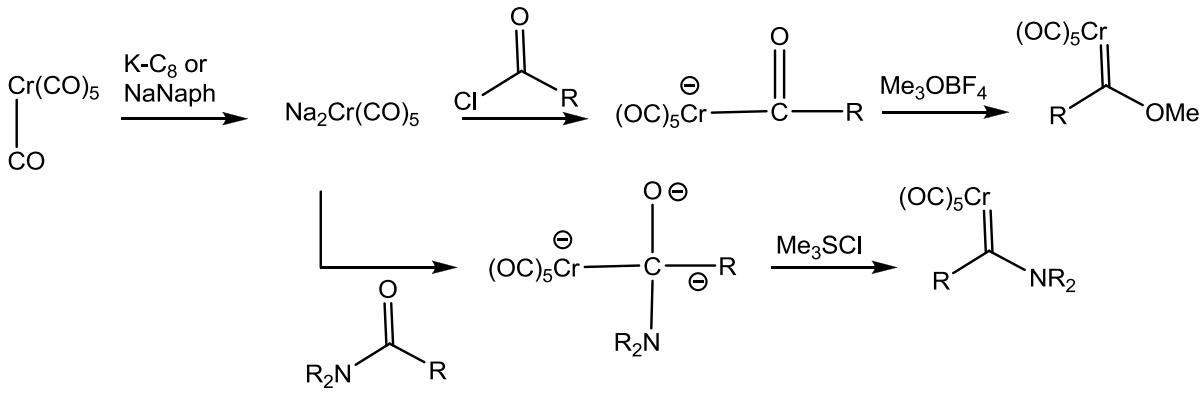

Scheme 1.4. Hexacarbonyl metal undergoing a reductive route

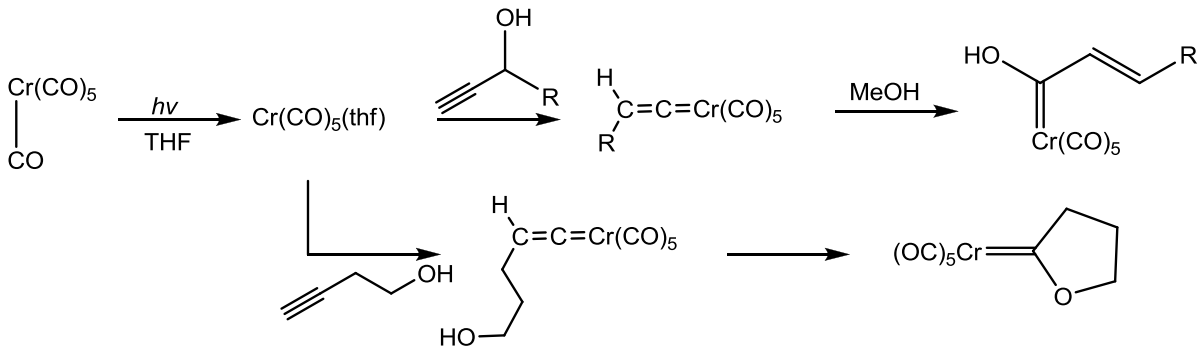

Scheme 1.5. Vinylidene and allenylidene intermediates

Alternative synthetic pathways are based on electronic considerations. Both treatment of an acyl intermediate with an electrophile and the nucleophilic attack of isonitrile groups will result in the production of the corresponding Fischer-type carbene complex (Scheme 1.6). [17]

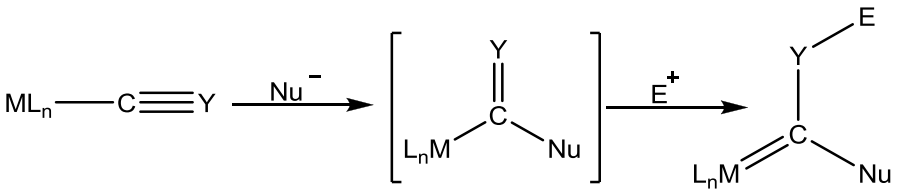

Scheme 1.6. Treatment of an acyl intermediate with an electrophile

[17] Dötz, K. H., *Angew. Chem., Int. Ed. Engl.*, **1984 ,**23, 587.

© University of Pretoria

Additional Fischer carbene synthesis strategies are as follows:

- Cleavage and insertion reactions of metal into an electron-rich olefin (ethene-type molecule): Lappert[18]
- Addition of carbonyl metalate complexes to germinal chlorides: Öfele[19]
- Treatment of isonitrile complexes with nucleophiles: Chatt[20]
- Accommodation of free carbene molecules by metals: Herrmann[21]
- Deprotonation of the α-position of metal-alkyls: Schrock[22]
- Hydride abstraction from metal-alkyls: Gladysz[23]

Many possible reactions have been postulated and carried out, with various levels of success, in an effort to synthesise carbene complexes efficiently. Progress has been made with optimising the yields obtained in the previously mentioned reactions; however, both steric and electronic properties need be taken into consideration.[17]Simple reactions, as in the case of lithiation of thiophene and sequential reaction with metal carbonyl complexes, often yield multiple by-products. Reactions yielding both monocarbene and biscarbene products (side-products) have been reported and the catalytic properties of a variety of these complexes have been studied.[24] Typical biscarbene products can also often show a high degree of symmetry. Fischer-type carbene complexes have been intensively utilised and applied in a large variety of chemical processes.[25,26] The applications of these complexes as catalysts in many reactions over the past decades have increased the popularity of these complexes and the striving to improve on published compounds. In the search to produce a catalyst with increased capability and activity, many new generations of catalysts have been fashioned. Reactions such as the thermal decomposition of Fischer carbenes to produce alkenes,[25] ring-closing and ring-opening metathesis[26] and the Dötz benzannulation reactions

[18] Lappert, M. F., *J. Chem. Soc., Dalton Trans.,* **1977**, 2172.
[19] Öfele, K., *Angew. Chem., Int. Ed. Engl.,* **1968**, 7, 950.
[20] Chatt, J., *J. Chem. Soc., Dalton Trans.,* **1969**, 1322.
[21] Herrmann, W. A., Reiter, B., Biersack, H., *J. Organomet. Chem.,* **1975**, 97, 245.
[22] Schrock, R. R., *J. Am. Chem. Soc.,* **1975**, 97, 6577.
[23] Gladysz, J. A., Kriel, W. A., Yu Lin, G. Bodner, G. S., *J. Chem. Soc.,* **1983**, 105, 4958.
[24] Van Jaarsveld, N. A., MSc Dissertation, *Synthesis and structure of modified thiophene biscarbene complexes,* **2009**, University of Pretoria, Pretoria.

© University of Pretoria

are only a few examples of the applicability of Fischer carbenes in the modern chemical environment.[25,26]

1.2.3 Theoretical bonding model and coordination

Currently, carbenes can be differentiated into two classes based on the multiplicity of the electronic configuration. The multiplicity of the lowest electronic state, the ground state, determines both the chemical properties and the reactivity of the carbene complex.[27]The multiplicity is determined on the basis of the energy of the σ and p_π orbitals, as depicted in Figure 1.1. Fischer carbenes are singlet carbenes with filled σ and empty p_π orbitals and thus show ambiphilic behaviour, whereas the Schrock counterpart (triplet carbenes) can be considered as diradicals, containing a single electron in both the σ and p_π orbitals.[28] As Figure 1.1 indicates, the classic carbene (divalent and bearing six valence electrons) contains a sp^2-hybridised carbon atom and features a bent geometry in its free form. A linear geometry (sp-hybridised) is also theoretically possible and the carbon possesses two energetically degenerate p orbitals (p_x, p_y) with the overall structural geometry being higher in energy. Of the two bent sp^2 geometries, the Fischer type is energetically favoured.[28]

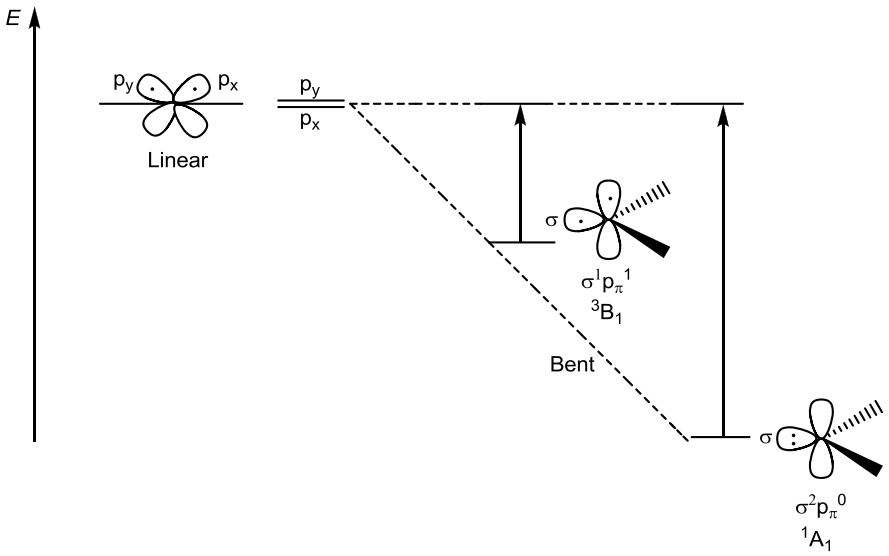

Figure 1.1. Frontier orbitals and corresponding electron configurations of carbenes

[25] Wulff, W.D., *Metal-carbene cycloaddition,* in *Comprehensive Organic Synthesis*, Wiley-Interscience, New York, **1988.**
[26] Hegedus, L. S., *Transition Metals in the Synthesis of Complex Organic Molecules*, **1994**, University Science Books, Mill Valley, CA, US.
[27] Schuster, G. B., *Adv. Phys. Org. Chem..* **1986**, 22, 311–361.
[28] Hahn, F. E., Jahnke, M. C., *Angew. Chem. Int. Ed. Engl.,* **2008,** 47, 3122–3172.

© University of Pretoria

As in the case of alkoxycarbenes, stabilised heteroatom-containing Fischer carbenes have a noticeable gap between their singlet and triplet energy states.[29] The bond or coordination of these carbenes to the metal fragment can be depicted as a σ donor-π acceptor interaction between the singlet carbene fragment ($\sigma^2 p_\pi^0$) and the metal coordination sphere.[28] The σ-donation of the ($^1A_1$) singlet carbene carbon, with back-donation from the metal atom, leaves the carbene carbon electrophilic in nature, creating an electron gap (Figures 1.2 to 1.4). In reality, the carbene carbon can be seen as an LZ ligand (donation of two electrons) with an empty p orbital available to accommodate electron density from metal→ligand donation.

Ab initio calculations performed by Taylor and Hall on the electronic structure of both Fischer carbenes and a large variety of free carbenes, however, indicated that singlet carbenes tend to be stabilised by heteroatom and phenyl substituents.[30]

This is clearly visible in the majority of Fischer carbenes where the heteroatom has the ability to provide additional electronic support to the electrophilic carbene carbon atom.

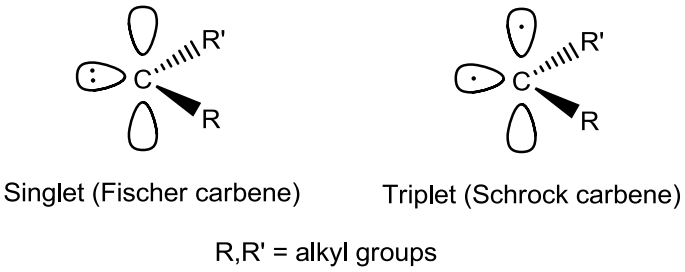

Figure 1.2. Singlet carbene vs. triplet carbene

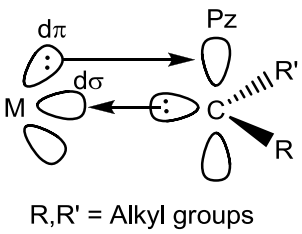

Figure 1.3. Bonding interaction in Fischer carbene complexes

[29] Bourrissou, D., Guerret, O., Gabbaï, F. P., Bertrand, G., *Chem. Rev.,* **2000**, 100, 39.
[30] Taylor, T. E., Hall, M. B., *J. Am. Chem. Soc.,* **1984**, 106, 1576–1584.

© University of Pretoria

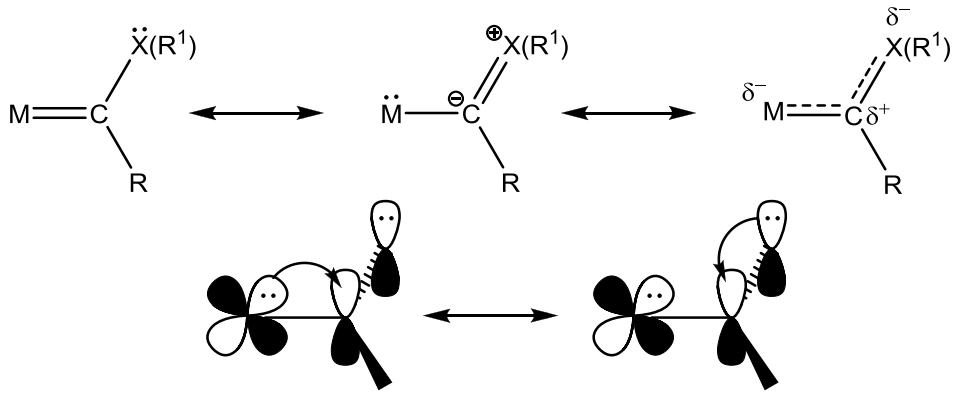

Figure 1.4. Stabilisation of Fischer carbene complexes through the acyl form (resonance effect)

1.2.4 Reactivity

Fischer carbene complexes have found application in several different types of reaction due to their richness in reactive sites (Figure 1.5). The carbene structure not only contains an electrophilic carbene carbon atom, but this centre also contains a winged heteroatom substituent displaying nucleophilic tendencies[31] and can promote electrophilic attacks. Depending on the acidity of protons on the available substituents of the carbene, there may also be deprotonation sites available. The sheer wealth of chemical reactivity displayed by Fischer carbene complexes leaves ample space for modification reactions to be performed on the complex.

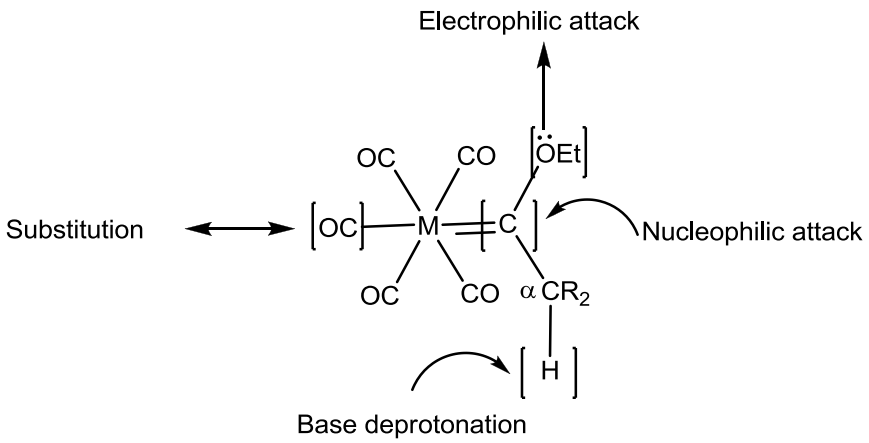

Figure 1.5. Typical reactions and modification of Fischer carbene complexes

[31] Bezuidenhout, D. I., MSc Dissertation, *Synthesis and structural investigation of manganese carbene complexes,* **2006**, University of Pretoria, Pretoria.

© University of Pretoria

The metal-pentacarbonyl moiety is exceptionally electron-draining and thus inhibits the metal-to-carbene carbon π-back-donation.[32] This leads to a polarisation effect resulting in electron density being withdrawn from the carbene carbon and housed on the metal centre itself. The net polarisation effect leaves the carbene carbon electron-deficient and open to nucleophilic attack.[33,34,35]

Aminolysis reactions are typical examples of modification of the original carbene complex and are achieved through a nucleophilic attack by an amine group on the carbene carbon, resulting in displacement of the alkoxy substituent. Sulphide, alkyl and hydroxyl molecules also display nucleophilic characteristics and thus can be commonly applied in substitution reactions on the carbene carbon[17,36] (Scheme 1.7).

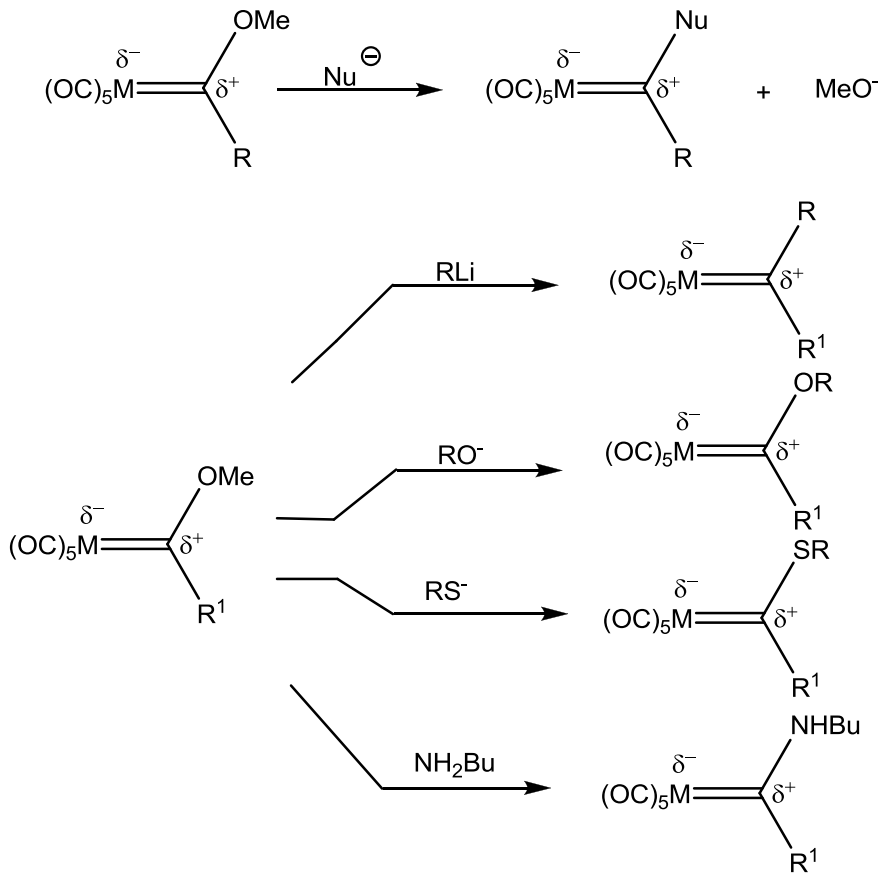

Scheme 1.7. Typical nucleophilic modification of Fischer carbene complexes

[32] Van der Watt, E., MSc Dissertation, *The Synthesis of Fischer carbene complexes with metal-containing substituents,* **2006**, University of Pretoria, Pretoria.
[33] Dötz, K. H., *Metal Carbenes in Organic Synthesis,* **2004**, Springer-Verlag, Germany.
[34] Collman, J. P., Hegedus, L. S., Norton, J. R., Finke, R. G., *Principles and Application of Organotransition Metal Chemistry,* **1987**, University Science Books, Mill Valley, CA, US.
[35] Helling, J. F., Rennison, S. C., Merijan, *J., Am. Chem. Soc.,* **1967**, 89, 7141.
[36] Fischer, E. O., Leopold, M., Kreiter, C. G., Müller, J., *Chem. Ber.*, **1972**, 105, 150.

© University of Pretoria

Since electron lone pairs are available on the oxygen of the ethoxy substituent, these electrons provide the stabilising group with nucleophilic characteristics. Electron-deficient fragments, such as Lewis acids (e.g. BBr_3), can bind to this reaction site and carbene molecules producing nucleophilic attacks on Lewis acids results in metal-containing carbyne complexes[31] (Scheme 1.8).

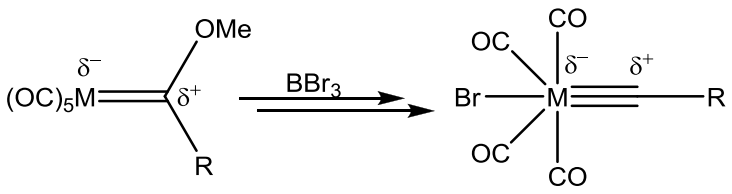

Scheme 1.8. Typical nucleophilic modification of Fischer carbene complexes

In cases where the carbenes contain alkyl substituents and the acidity allows, bases can deprotonate the more acidic α-alkyl group, producing metal carbene anions.[29] Since the carbene carbon atom is electrophilic in nature and gains minimal electron density from the inductive effect of the α-alkyl group (Figure 1.5), polar effects produce protons on the alkyl groups with higher acidity. Bases can thus deprotonate via deprotonation pathways. The most versatile reactions available to Fischer carbene complexes are substitution reactions. The carbonyl ligands are labile and easily undergo substitutions with less labile counterparts to produce highly derivatised complexes.[37] Substitution reactions with both phosphorous-containing and nitrogen-containing ligands are numerous and provide a rich variety of complexes (Scheme 1.9). Even examples of bidentate phosphine ligand coordination with carbenes have been reported.[38,39] There have been interesting developments as a result of the introduction of microwave reactions, in which bidentate ligands can be coordinated to metal centres through induced substitution reactions[40] and may lead to synthetic pathways of subsequent addition of the carbene fragment.

[37] Dötz, K. H., Stendel, J., Jr., *Chem. Rev.*, **2009**, 109, 3227.
[38] Arrieta, A., Cossío, F. P., Fernández, I., Gómez-Gallego, M., Lecea, B., Mancheño, M. J., Sierra, M. A., *J. Am. Chem. Soc.* **2000**, 122, 11509–11510.
[39] Barluenga, J., Muñiz, K., Tomás, M., Ballesteros, A., García-Granda, S., *Organometallics,* **2003**, 22, 1756–1760
[40] Van Atta, S. L., Duclos, B. A., Green, D. B. *Organometallics,* **2000**, 19, 2397–2399.

© University of Pretoria

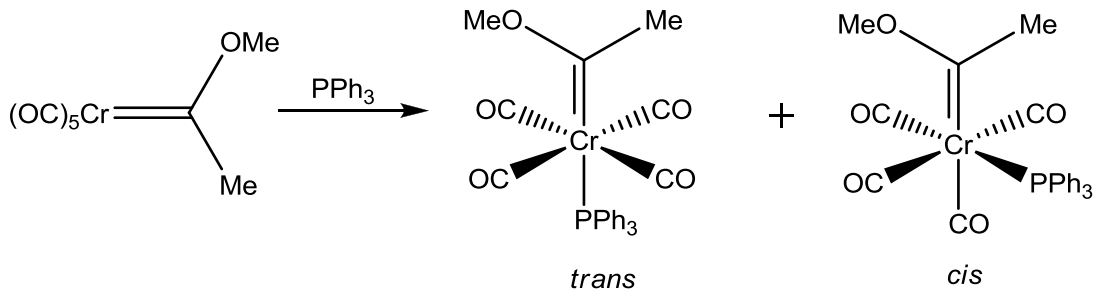

Scheme 1.9. Carbonyl substitution reaction with phosphine ligand[41]

1.2.5 Applications

The applicability of transition metal compounds and especially carbene complexes in synthetic organic chemistry has experienced a noteworthy increase in recent years.[42] Among the numerous metal-containing compounds and carbene complexes as a whole, the Fischer-type carbenes of multiple transition groups, and in particular Group 6 metals, are of major synthetic importance.[43]

Fischer carbenes have been employed in synthetics research and industrial laboratories, aiding in the isolation of multiple important reaction intermediates.[44,45] Fischer carbene complexes are prospective precursors of numerous functionalised carbocycles and heterocycles through thermal and photochemical procedures.[46,47,48]

One of the most important applications of Fischer-type carbenes is the so-called Dötz benzannulation reaction, which was first proposed in 1975[49] (Scheme 1.10). This reaction

[41] Fischer, E. O., Fischer, H., Werner, H., *Angew. Chem., Int. Ed. Engl.,* **1972**, 11, 644.
[42] Beller, M., Bolm, C. (Eds), *Transition Metals for Organic Chemistry,* Wiley-VCH, Weinheim, Germany, **1998.**
[43] (a) Zaragoza-Dörwald, F., *Metal Carbenes in Organic Synthesis,* Wiley-VCH, Weinheim, Germany, **1999**. (b) Dötz, K. H., Fischer, H., Hofmann, P., Kreissl, F. R., Schubert, U., Weiss, K., *Transition Metal Carbene Complexes,* Wiley-VCH, Weinheim, Germany, **1983.**
[44] (a) Bao, J., Wulff, W. D., Dominy, J. B., Fumo, M. J., Grant, E. B., Rob, A. C., Whitcomb, M. C., Yeung, S.–M., Ostrander, R .L., Rheingold, A. L., *J. Am. Chem. Soc.,* **1996**, 118, 3392. (b) Kagoshima, H., Okamura, T., Akiyama, T., *J. Am. Chem. Soc.,* **2001**, 123, 7182. (c) Iwasawa, N., Shido, M., Kusama, H., *J. Am. Chem. Soc.,* **2001**, 123, 5814. (d) Miura, T., Iwasawa, N., *J. Am. Chem. Soc.,* **2002**, 124, 518.
[45] Barluenga, J., Ballesteros, A., Santamaría, J., Bernardo de la Rúa, R., Rubio, E., Tomás, M., *J. Am. Chem. Soc.,* **2000**, 122, 12874.
[46] (a) Barluenga, J., Fañanás, F. J., *Tetrahedron*, **2000**, 112, 4124–4126. (b) Sierra, M. A., *Chem. Rev.,* **2000**, 100, 3591–4002.
[47] Barluenga, J., Santamaría, M., Tomás, M., *Chem. Rev.*, **2004**, 104, 2259–2283.
[48] Herndon, J. W., *Tetrahedron*, **2000**, 56, 1257–1280.
[49] Dötz, K. H., *Angew. Chem.,* **1975**, 87, 672–673; *Angew. Chem., Int. Ed. Engl,.* **1975**, 14, 644–645.

© University of Pretoria

allows the efficient synthesis of antibiotics,[50] natural products[51] and biologically important molecules.[52] The reaction pathways of Fischer carbene complexes are versatile and accordingly a broad range of products is accessible.[31] One unique characteristic often utilised in synthetic approaches is the fact that in the above-mentioned pathways, either the metal-carbon bond is retained in the end-product while a ligand is adapted, or the bond itself undergoes reactions.[31]

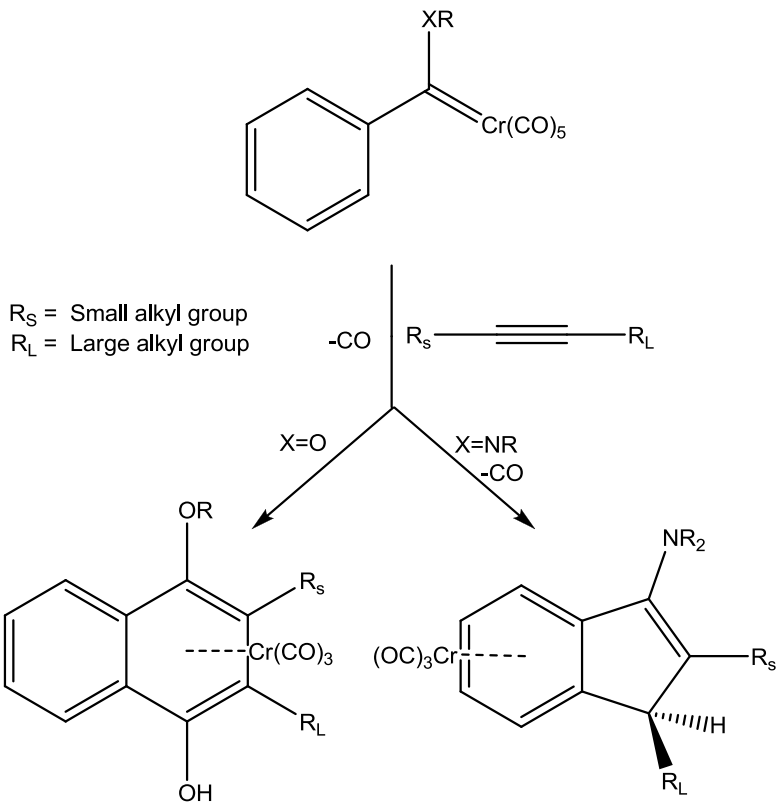

Scheme 1.10. Dötz benzannulation versus cyclopentannulation[53]

Additional applications in organic chemistry include the following:

- Serving as blocking groups in organic synthesis[54]
- Improvement in reactivity and selectivity[55]

[50] Boger, D. L., Hunter, O., Mbiya, K., Zhang, M. S., *J. Am. Chem. Soc.,* **1998**, 117, 11839–11849.
[51] Anderson, J. C., Denton, R. M., Hickin, H. G., Wilson, C., *Tetrahedron*, **2004**, 60, 2327–2335.
[52] Dötz, K. H., Kuhn, W., *Angew. Chem.,* **1983**, 95, 750–751.
[53] Oscar, J., Jimenez-Halla, C., Solá, M., *Chem. Eur. J.,* **2009**, 15, 12503–12520.
[54] Barluenga, J., *J. Am. Chem. Soc.,* **2002**, 124, 9056–9057.
[55] Wulff, W., *J. Am. Chem. Soc.,* **1990**, 112, 3642.

© University of Pretoria

- Reaction with olefins[56]
- General annulations with alkynes and alkenes[57]
- Catalytic carbene transfer reactions[58]

1.3 Schrock Carbene Complexes

1.3.1 Overview

In 1974 the first synthesis of a high oxidation state (d^0) metal-alkylidene complex[59] was proposed. The synthesis of the complex was accomplished by α-hydrogen abstraction on a tris(2,2-dimethylpropyl)methyl tantalum(V) dichloride precursor to produce what is the now the world-famous Schrock carbene[60] (Scheme 1.11). The tantalum neopentylidene complex was novel in many aspects and was the only known example of a stable M=CHR carbene complex. As mentioned before, the carbene was formed through a new reaction route via an intermolecular α-hydrogen abstraction by an alkyl group and differed from the Fischer carbene in the key aspect of being highly electron-lacking (10 electrons in the metal-based bonding orbitals). The complex displayed noteworthy properties and illustrated a metal presiding in the highest oxidation state with the metal-carbon bond so severely polarised as to leave the metal positively charged and the carbene carbon nucleophilic in nature.[61]

Schrock carbenes are generally highly thermally stable and resistant to intermolecular decomposition reactions, which suggests that numerous other high-oxidation states, for highly steric coordinated ligand complexes, are producible. These compounds are afforded by using early transition metals in high oxidation states with strong donor and weak π-acceptor ligands.[32] Schrock-type carbenes have been incorporated into well-known catalysts, as in the case of the Grubbs catalyst, and multiple new derivatives are now in existence.

[56] Grubbs, R. H., *Organometallics,* **2002**, 21, 2153–2164.
[57] Barluenga, J., *Org. Lett.,* **2006**, 8, 2703–2706.
[58] Sierra, M. A., *J. Am. Chem. Soc.,* **2001**, 123, 851–861.
[59] Schrock, R. R., *J. Am. Chem. Soc.,* **1974**, 96, 6796.
[60] De Frémont, P., Marion, N., Nolan, S. P., *Coord. Chem. Rev.,* **2009**, 253, 862–892
[61] Schrock, R. R., *Angew. Chem., Int. Ed. Engl.,* **2006**, 45, 3748–3759.

© University of Pretoria

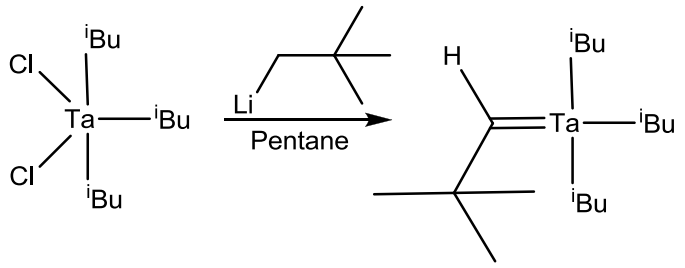

Scheme 1.11. Synthesis of first alkylidene–metal (d^0) complex

1.3.2 Synthesis

Similar to the case of Fischer carbenes, there are also several different synthetic routes available for the production of Schrock carbenes. Three main synthetic routes are currently utilised to full exploitation to produce these complexes. Synthesis through metal alkyl complexes seems increasingly popular since these compounds are easily afforded and prepared by the reaction of metal halides with lithiated alkyl reagents or Grignard reagents.[62] Early transition metals with saturated coordination spheres and dialkyl, trialkyl or polyalkyl ligated groups can form alkylidene complexes through α-deprotonation.[63]

The success of the reaction depends on the vital formation of thermodynamically and kinetically stable leaving groups which, in standard processes, normally consist of either alkanes or weakly conjugated acids. Coordination complexes without β-hydrogens and containing either methyl, neopentyl or *tert*-butyl groups are normally preferred since any competing β-deprotonation reactions will be avoided.[64] The reaction can be promoted through various methods, including thermally and photochemically (Scheme 1.12).

$$L_mM^n(CH_2R)_2 \xrightarrow{\text{UV- light}} L_mM^n{=}CHR + CH_3R$$

$$L_mM^n(CH_2R)_2 + xPR_3 \longrightarrow L_mM^n{=}CHR(PR_3)_x + CH_3R$$

$$L_mM^n(CH_2R)_2 + B^- \longrightarrow L_mM^n{=}CHR + BH + X^-$$

Scheme 1.12. Synthesis of Schrock carbenes via α-hydrogen elimination

[62] Budzelaar, P. H. M., Bart van Oort, A., Orpen, A. G., *Eur. J. Inorg. Chem.,* **1998**, 1485.
[63] (a) Van Asselt, A., Burger, B. J., Gibson, V. C., Bercaw, J. E., *J. Am. Chem. Soc.,* **1986**, 108, 5347. (b) Schrock, R. R., *Acc. Chem. Res.,* **1990**, 23, 158. (c) Li, L., Hung, M., Xue, Z., *J. Am. Chem. Soc.,* **1995**, 117, 12746.
[64] (a) Mindiola, D. J., *Acc. Chem. Res.,* **2006**, 39, 813. (b) Gerber, L. C. H., Watson, L. A., Parkin, S., Weng, W., Foxman, B. M., Ozerov, O. V., *Organometallics*, **2007**, 26, 4866.

© University of Pretoria

Phosphiranes, i.e. phosphorous ylides containing a nucleophilic carbon frequently used for Wittig reactions,[65] react with phosphine-containing reduced-metal complexes of Ti^{2+}, Zr^{2+},V^{3+} and W^{4+} to produce Schrock carbenes via a transfer reaction.[61,66a] The synthetic pathway starts with the metal undergoing the loss of a phosphine ligand prior to nucleophilic attack by the ylide carbon on the metal atom.[66c] A zwitterionic intermediate forms which undergoes rearrangement to produce the corresponding carbene complex. The reaction is promoted by the formation of a carbene with a lower energy state since steric hindrances brought about by the phosphirane group will subside[66c] (Scheme 1.13). Transmetalation from Group 5 metal carbenes have only been reported once. In 1982, Wengrovius *et al*. obtained a series of novel tungsten(VI) oxoneopentylidene complexes by carbene transfer from tantalum(V) carbene starting material.[67] The reaction depended on a tungsten-tantalum dimetal carbene that acted as a bridging intermediate before final ligand (often PR_3) loss to yield the corresponding tungsten carbene.

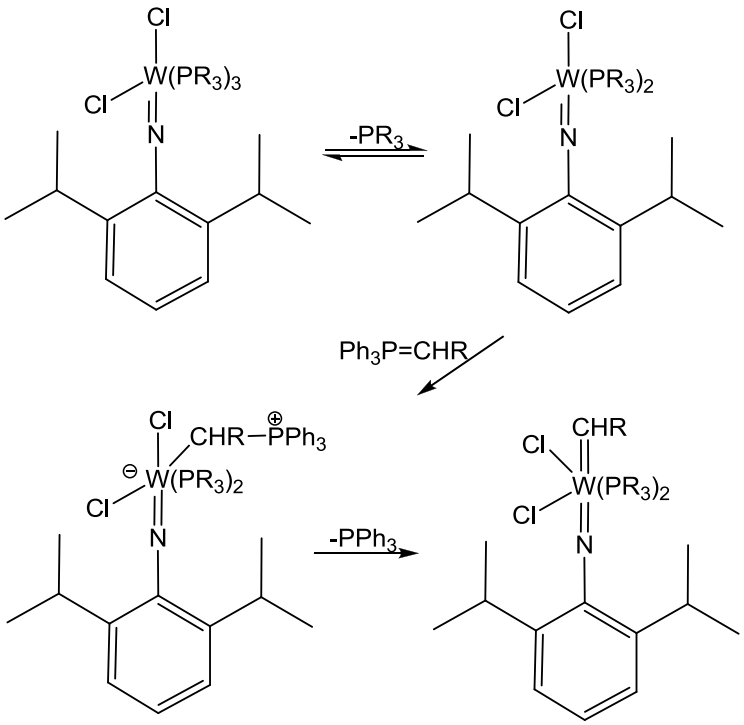

Scheme 1.13. Synthesis of Schrock carbenes via phosphiranes

[65] (a) Wittig, G., Schöllkopf, U., *Chem. Ber.,* **1954**, 87, 1318. (b) Wittig, G., Haag, W., Chem. *Ber.,* **1955**, 88, 1654. (c) Maryanoff, B. E., Reitz, A. B., *Chem. Rev.,* **1989**, 89, 863.
[66] (a) Sharp, P. R., Schrock, R. R., *J. Organomet. Chem.,* **1979**, 171, 43. (b) Schwartz, J., Gell, K. I., *J. Organomet. Chem.,* **1980**, 184, C1. (c) Johnson, L. K., Frey, M., Ulibarri, T. A., Virgil, S. C., Grubbs, R. H., Ziller, J. W., *J. Am. Chem. Soc.,* **1993**, 115, 8167. (d) Buijink, J. K., Teuben, J. H., Kooijman, H., Spek, A. L., *Organometallics,* **1994**, 13, 2922.
[67] Wengrovius, J. H., Schrock, R. R., *Organometallics,* **1982**, 1, 148.

© University of Pretoria

1.3.3 Theoretical bonding model and coordination

Inadequately stabilised carbenes, as in the cases of alkyl and dialkyl carbenes, have small energy gaps involving their singlet and triplet states (Figures 1.6 to 1.8). The metal-carbon bond is covalent in nature and fashioned by the pairing of two triplet fragment pieces.[68,69] Thus triplet carbene fragments will prefer to interact with triplet-state metal components in a covalent fashion. The metal-carbon bond is described as a classic double bond and the π-electrons distribute evenly between the metal and the carbene carbon.[28] Schrock carbene complexes are found almost exclusively in the early transition metals with highest oxidation states (d^0); the carbene carbon is nucleophilic in nature and thus reacts with electrophiles at this reaction centre. The nucleophilic nature of the carbene carbon can be attributed to the polarisation effect that the more electro-negative carbon exerts on the electro-positive metal centre. Ligands coordinated to the metal centre are typically strong σ-donor/weak π-acceptor groups, whereas the substituents on the carbene carbons are typically alkyl or/and hydride groups. *Ab initio* calculations performed by Taylor and Hall indicate that alkyl and hydride substituents stabilise a triplet ground state at the carbene carbon centre.[28] Due to the double bond nature of Schrock carbenes, the carbene fragment is considered to be an X_2-type ligand, as expected. For this reason there will be a net oxidation change of +2 to effect.

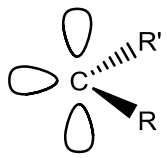

R,R' = Alkyl / Hydride

Schrock Triplet carbene

Figure 1.6. Diagram of a triplet carbene

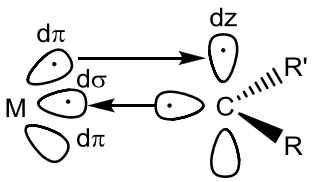

R,R' = Alkyl / Hydride

Figure 1.7. Diagram of Schrock carbene coordination

[68] Canac, Y., Soleilhavoup, S., Conejero, S., Bertrand, G., *J. Organomet. Chem.,* **2004**, 689, 3857.
[69] Vyboishchikov, S. F., Frenking, G., *Chem. Eur. J.,* **1998**, 4, 1428.

© University of Pretoria

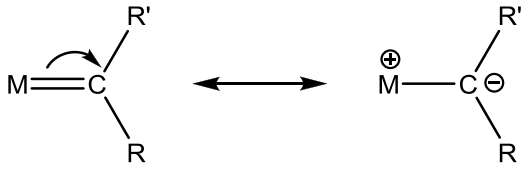

R,R' = Alkyl or Hydride

Figure 1.8. Diagram showing the resonance explanation for the nucleophilic behaviour of the carbene carbon

1.3.4 Reactivity and application

Schrock carbene complexes are utilised mostly in synthetic organic chemistry and have found application in olefin metathesis (Scheme 1.14) and as substitutes for phosphorus ylides in Wittig reactions.[70] In the case of Wittig reactions, Schrock carbenes confer a variety of advantages, including evasion of acid-base side-reactions, capability of olefinating both esters and amides, and being less sensitive to steric effects.[71] Traditionally, the most utilised olefin metathesis reactions (Figure 1.10) consisted of ring-opening metathesis polymerisation (ROMP) for sterically strained cycloalkanes. However, olefin metathesis reactions in terms of organic reactions have only been well defined over the past couple of years.[71] Olefin metathesis reactions have developed exponentially since the discovery of the famous Grubbs catalyst and the so-called Schrock catalyst, which tolerated a larger variety of functionalised substituents (Figure 1.9). Before the synthesis of these catalysts, reports of olefin metathesis reactions for the selective preparation of non-polymeric organic compounds was relatively unknown.[72]

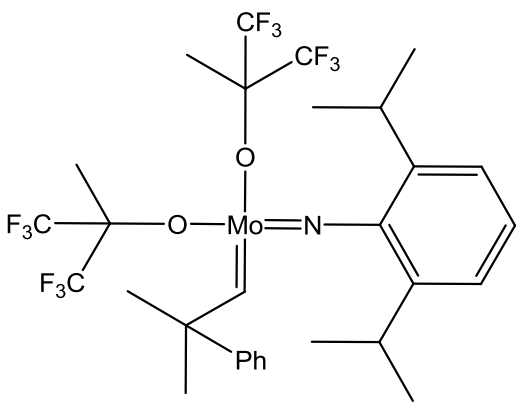

Figure 1.9. Diagram of a Schrock catalyst

[70] Pine, S. H., Shen, G. S., Hoang, H., *Synthesis*, **1991**, 165.
[71] Randall, M. L., Snapper, M. L., *J. Mol. Catal.*,**1998**, 133, 29.
[72] Herndon, J. W., *Coord. Chem. Rev.*, **2000**, 206–207, 237–262.

© University of Pretoria

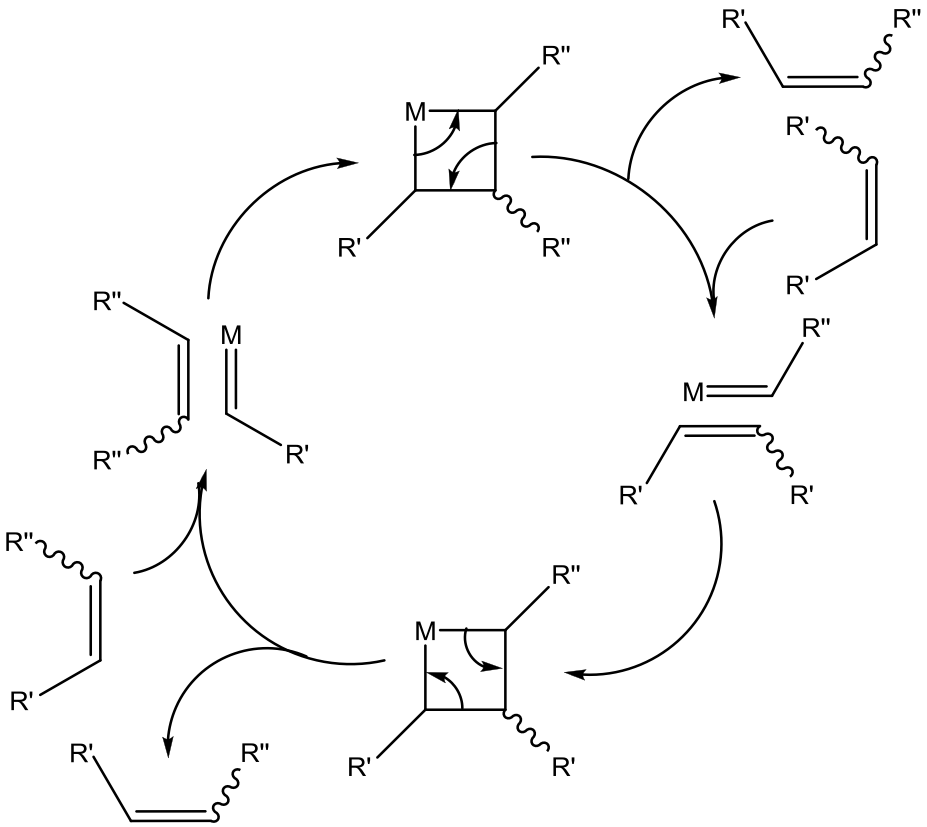

Figure 1.10. Chauvin mechanism of olefin metathesis

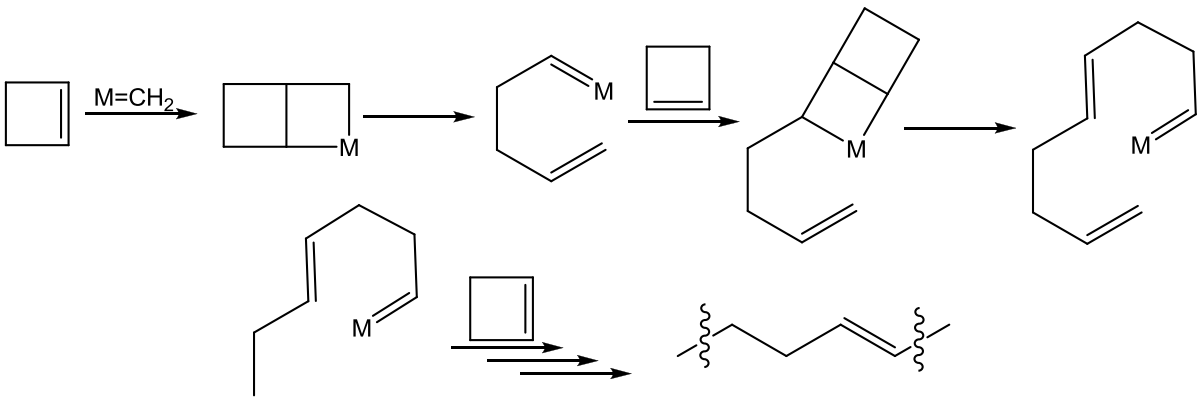

Scheme 1.14. Olefin metathesis for cyclobutene

The Grubbs catalyst is a Schrock-type transition metal carbene complex named after the chemist who originally synthesised the compound, Robert H. Grubbs. Two main generations have been published and numerous derivatives of these generations synthesised. Grubbs

© University of Pretoria

catalysts are exceptionally versatile due to the ability of these complexes to be compatible with a large range of both solvents and functional groups.[73,74]

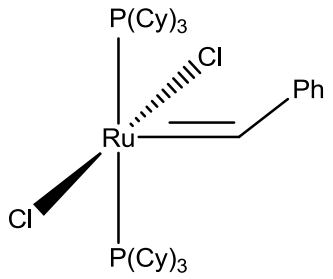

Figure 1.11. Structure of Grubbs' first-generation catalyst

The first-generation Grubbs' catalyst (Figure 1.11) is reasonably uncomplicated to synthesise from $RuCl_2(PPh_3)_3$, phenyldiazomethane and tricyclohexylphosphine in a single-reaction flask method; the product is effortless to handle and stable in air.[75,76] The second-generation version of the celebrated catalyst characteristically has similar application in organic synthesis, however with an additional increase in activity (Figure 1.12). The second-generation derivative is also stable in both moisture and air, thus providing additional incentive for the preferential utilisation of the second over the first.

This second-generation catalyst was produced by the Nolan group in 1999 through modification of the first generation. Modification was achieved by the substitution of a single phosphine substituent by an N-heterocyclic carbene ligand, thus producing the first complex containing both a Schrock carbene and an NHC group ligated to the metal centre.[77] Further modification of the second generation through the use of an extensive series of unique substituents bound to the nitrogen atoms of the NHC fragment produced classes of derivatives with fluctuating catalytic ability.

Applications of the Grubbs catalysts as a whole is vast and still expanding. Recently the aerospace industry has started research on how the catalyst may polymerise dicyclopentadiene to seal micro cracks in the hulls of spaceships.[78]

[73] Vougioukalakis, G. C., Grubbs, R. H., *Chem. Rev.,* **2010**, 110, 3, 1746–1787.
[74] Trnka, T. M., Grubbs, R. H., *Acc. Chem. Res.*, **2003,** 34, 1, 18–29.
[75] Scholl, M., Ding, S., Lee, C. W., Grubbs, R. H., *Org. Lett.,* **1999**, 1(6), 953–956.
[76] Schwab, P., Grubbs, R. H., Ziller, J. W., *J. Am. Chem. Soc.,* **1996,** 118, 1, 100–110.
[77] Huang, J., Stevens, E. D., Nolan, S. P., Peterson, J. L., *J. Am. Chem. Soc.,* **1999,** 121, 12, 2674–2678.
[78] White, S. R., Sottos, N. R., Geubelle, P. H., Moore, J. S., Kessler, M. R., Sriram, S. R., Brown, E. N., Viswanathan, S., *Nature*, **2001,** 409, 6822, 794–797.

© University of Pretoria

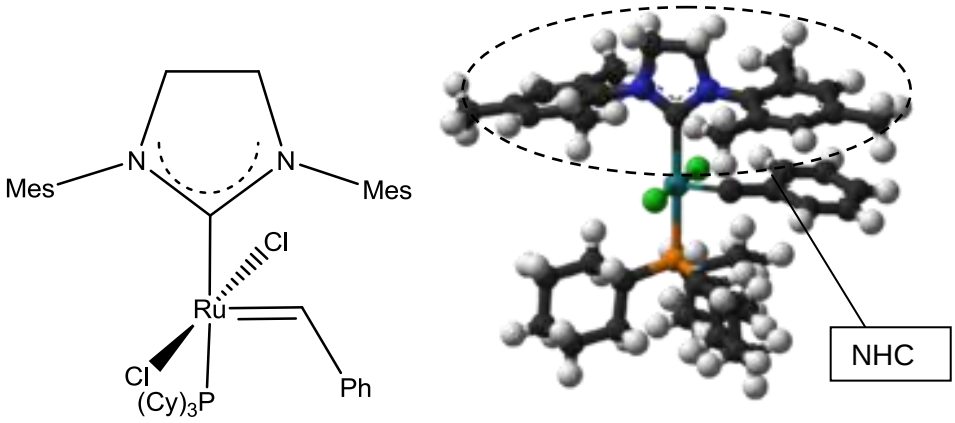

Figure 1.12. Structure of Grubbs' second-generation catalyst

1.4 N-Heterocyclic Carbene (NHC) Complexes

1.4.1 Overview

Nucleophilic N-heterocyclic carbenes (NHCs), also called Arduengo carbenes, have attracted extensive amounts of research since the free analogue was isolated and ligated to transition metal complexes by Arduengo *et al*. in the 1990s.[79] Prior to the findings of Arduengo *et al*., Öfele[9] and Wanzlick and Schönherr[10] were able to produce coordinated NHC complexes but failed to produce the first free NHC carbene. Properties of classic NHCs include strong σ-donating and weak π-acceptor ability, corresponding to that of a phosphine ligand rather than that of the theoretical Fischer or Schrock carbene counterparts.[80]

Primary considerations indicated that NHC carbenes may just simply be mimics of the phosphine ligand. However, it became quite clear that these carbenes present with novel chemistry which has vast applicability and are more complex than originally considered.[81] Minute changes to the NHC design result in remarkable changes in the electronic donor ability of the carbene moieties and inflict geometric constraints on the N-substituents, influencing their steric force.[82] Numerous publications relating to metal coordination, properties and catalytic ability have surfaced over the past 20 years[83] (Figure 1.13) and have

[79] (a) Arduengo, A. J., Harlow, R. L., Kline, M., *J. Am. Chem. Soc.,* **1991**, 113, 361. (b) Arduengo, A. J., Kline, M., Calabrese, J. C., Davidson, F., *J. Am. Chem. Soc.,* **1991**, 113, 9704. (c) Arduengo, A. J., Krafczyk, R., Schmutzler, R., Craig, H. A., Goerlich, J. R., Marshall, W. J., Unverzagt, M., *Tetrahedron*, **1999**, 55, 14523.
[80] Green, J. C., Scurr, R. G., Arnold, P. L., Cloke, F. G. N., *Chem. Commun.,* **1997**, 1963.
[81] Crabtree, R. H., *J. Organomet. Chem.,* **2005**, 690, 5451–5457.
[82] Despagnet-Ayoub, E., Grubbs, R. H., *J. Am. Chem. Soc.,* **2004**, 126, 10198.
[83] Herrmann, W. A., *Angew. Chem., Int. Ed. Engl.,* **2002**, 41, 1290.

© University of Pretoria

particularly commented on the NHC complex's stability towards moisture, heat and oxygen.[84] Recent research advances of employing silver (I) complexes as metal carbene transfer reagents have attracted much interest and application.[85] Pd(II) carbenes have been prepared via silver NHC transfer reactions[86] and a number of these silver transfer reagents show prospective application in material sciences.[87]

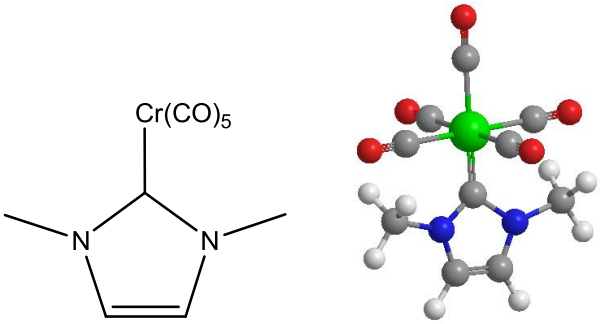

Figure 1.13. Structure of a typical NHC coordinated to chromium(0)

1.4.2 Synthesis

It has been more than 30 years since the first NHC complexes were independently prepared and published by Öfele,[9] and Wanzlick and Schönherr[10a] (Scheme 1.15). In both synthetic pathways, deprotonation of imidazolium salt by a basic metal precursor producing the imidazolin-2-ylidene complex was utilised, as depicted in Scheme 1.15. Later Lappert *et al.* extended the synthetic methodology to include complexes containing imidazolidin-2-ylidene ligands,[88] but it was not until 1991 when the first free NHC carbene was synthesised and crystallised by the Arduengo group by deprotonation of 1,3-bis(adamantyl)imidazolium chloride.[77a] (Scheme 1.16). Today NHC complexes of roughly all transition metals on the periodic table are known and the syntheses of these complexes are achieved by three main routes, namely (1) the in situ deprotonation of a ligand predecessor,[8] (2) the ligation of the free NHC to a metal centre[8] or (3) cleavage of an electron-rich olefin.[8] Although these

[84] Chiu, P. L., Chen, C. Y., Zeng, J. Y., Lu, C. Y., Lee, H. M., *J. Organomet. Chem.,* **2005**, 690, 1682–1687.
[85] (a) Wang, H. M. J., Lin, I. J. B., *Organometallics,* **1998**, 17, 972. (b) Bildstein, B., Malaun, M., Kopacka, H., Wurst, K., Mitterböck, M., Ongania, K.-H., Opromolla, G., Zanello, P., *Organometallics,* **1999**, 18, 4325.
[86] (a) Bonnet, L. G., Douthwaite, R. E., Kariuki, B. M., *Organometallics,* **2003**, 22, 4187. (b) Danopoulos, A. A., Tulloch, A. A. D., Winston, S., Eastham, G., Hursthouse, M. B., *J. Chem Soc., Dalton Trans.,* **2003**, 1009.
[87] (a) Lee, C. K., Lee, K. M., Lin, I. J. B., *Organometallics.* **2002**, 21, 10. (b) Chen, J. C. C., Lin, I. J. B., *J. Chem. Soc., Dalton Trans.,* **2000**, 839.
[88] Lappert, M. F., *J. Organomet. Chem.,* **1988**, 358, 185.

© University of Pretoria

methods are still actively pursued, many additional reactions have been postulated and present formidable evidence of synthetic achievement.

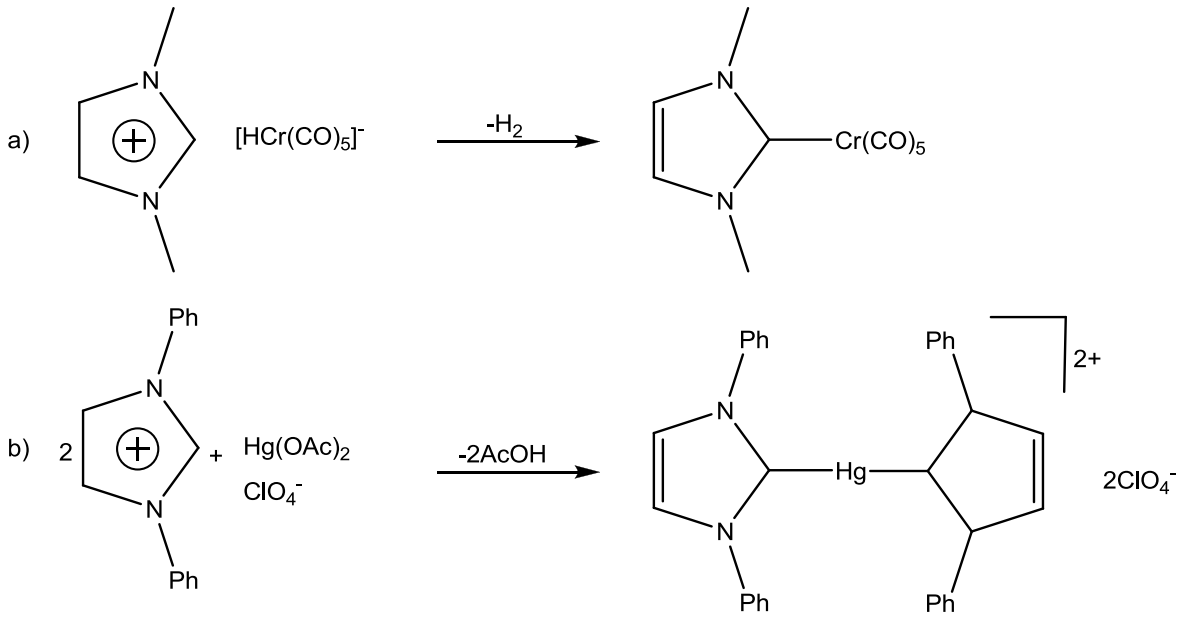

Scheme 1.15. First NHC metal complexes: Synthetic schemes of (a) Öfele[9], and (b) Wanzlick and Schönherr[10a]

The in situ synthesis of the NHC carbene and the complexation to a metal centre offers a key advantage in cases where the free NHC is either unstable, hard to handle or difficult to prepare. A typical example of the in situ methodology is witnessed by the deprotonation of an NHC precursor by a basic metalate. Deprotonation (in situ) of azolium cations by Brönstedt basic metalate anions upon heating is a standard example of this methodology and Öfele and Herberhold were able to prepare the first (NHC)Cr(CO)$_5$ complex utilising this methodology (Scheme 1.16)[89]. It is worth noting that the disadvantage of this method lies in the availability of the metalate precursor, which is determined by both the character and oxidation state of the metal centre of the newly formed complex and the direct environment of the ligand. Deprotonation via basic anions or external basis, such as potassium *tert*-butoxide, or elimination of small molecules from neutral ligand precursors are also imitative of the in situ methodology. Complexation of the free NHC has become an exceedingly common practice since Arduengo *et al*. first published the method, with the applicability of the proposed scheme inducing much awareness and excitement. The power and advantage of this technique is illustrated by the fact that multiple metal precursors, without extraordinary

[89]Öfele, K., Herberhold, M., *Angew. Chem.,* **1970**, 82, 775; *Angew. Chem., Int. Ed. Engl.,* **1970**, 9, 739.

© University of Pretoria

requirements regarding both the ligand sphere and the oxidation state, can be utilised for the synthesis of the NHC complexes. Many unique methods have developed over the time regarding the preparation of free NHC complexes from precursors, such as deprotonation of azolium salts by NaH and KO*t*Bu in THF,[90] but the most general procedure to produce these mentioned free NHC complexes in high yield occurs through deprotonation by NaH in a mixture of liquid ammonia and THF[91,92].

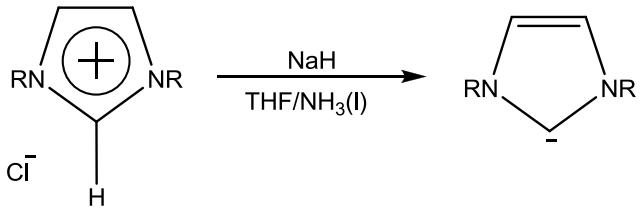

Scheme 1.16. Synthesis of free N-heterocyclic carbene

Cleavage of dimeric complexes with bridging ligands (halogens, CO, acetonitrile, etc.) by nucleophilic free NHC ligands can produce NHC complexes coordinated to metal spheres.[91,92] An additional method is the exchange of coordinated phosphine ligands with isolated free NHCs to produce the corresponding NHC metal ligated complex. The added benefit of this technique resides in the fact that phosphine ligands are readily substituted, even at lower temperature (Scheme 1.17).[93] The Grubbs catalyst is a typical example of a modern complex produced by this process.

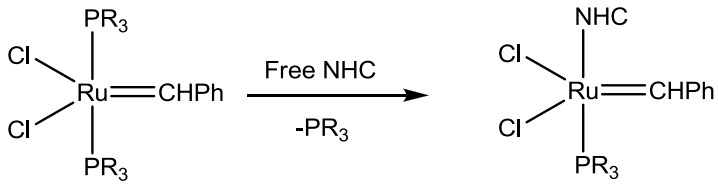

Scheme 1.17. Substitution of a phosphine ligand by an NHC

Electron-rich olefins are nucleophilic in nature and thus subject to thermal cleavage by a large variety of transition metal complexes. Dimerisations of non-stable N-heterocyclic

[90] Arduengo III, A. J., Dias, H. V. R., Harlow, R. L., Kline, M., *J. Am. Chem. Soc.,* **1992**, 114, 5530.
[91] Herrmann, W. A., Köcher, C., Gooβen, L. J., Artus, G. R. J., *Chem. Eur. J.,* **1996**, 2, 1627.
[92] Herrmann, W. A., Elison, M., Fischer, J., Köcher, C., Artus, G. R. J., *Chem. Eur. J.,* **1996**, 2, 772.
[93] Schroll, M., Ding, S., Lee, C. W., Grubbs, R. H., *Org. Lett.,* **1999**, 1, 953.

© University of Pretoria

carbenes in general produce these electron-wealthy olefins.[94] It was only proved in recent years that an equilibrium exists between the free NHC monomer and the olefin dimer.[95] Refluxing tetraaminoethylenes in toluene in the presence of a metal (Fe, Co, Mn, etc.) precursor[18,96] can potentially yield the resultant NHC complex and, in general, up to two carbonyl ligands can be substituted. Higher substitutions are, however, plausible.[97] Apart from these three main synthetic routes, less common reaction routes have also led to the formation of NHC complexes of various metals. Additional requirements for the metal reagent, the NHC ligand or the complex forerunner have, however, prohibited broad application of these less common routes. One method that in recent years has attracted attention is the utilisation of ligand transfer reactions. NHC ligands can be transferred in an intermolecular reaction from one metal centre to another in particular cases.[8] The first reported reaction of this method was a disproportionation reaction of (1,3-dimethylimidazolin-2-ylidene)$Cr(CO)_5$ (Scheme 1.18). The metal complex was heated under a photolysis environment to form[87] (1,3-dimethylimidazolin-2-ylidene)$Cr(CO)_4$ and $Cr(CO)_6$. NHC transfer reactions are possible from imidazolidin-2-ylidene of Group 5 metal pentacarbonyl complexes, and NHC ligands are successfully transferred to rhodium(I), palladium(II), platinum(II), copper(I), silver(I) and gold(I) in this manner.[98,99]

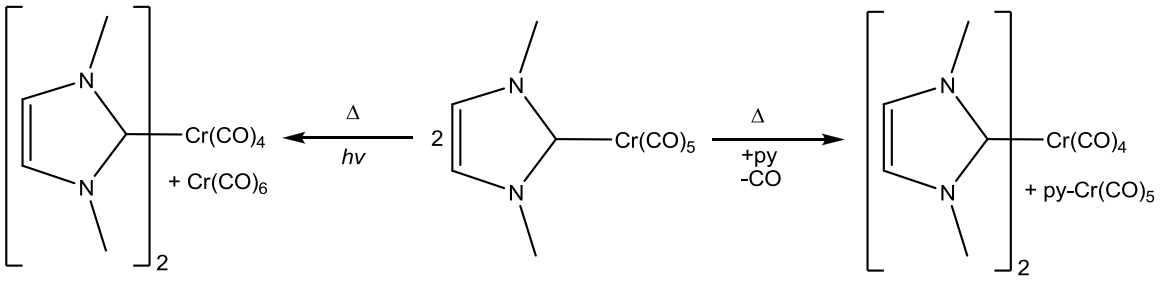

Scheme 1.18. Disproportionation of (NHC)$Cr(CO)_5$

[94]Schumann, H., Glanz, M., Winterfield, J., Hemling, H., Kuhn, N., Kratz, T., *Angew. Chem. Chem.* **1994**, 106, 1829.
[95](a) Liu Y., Linder, P. E., Lemal, D. M., *J. Am. Chem. Soc.* **1999**, 121, 10626. (b) Hahn, F. E., Wittenbacher, L., Le Van, D., Fröhlich, R., *Angew. Chem.,* **2000**, 112, 551.
[96] Hitchcock, P. B., Lappert, M. F., Pye, P. L., *J. Chem. Soc., Dalton Trans.* **1978** , 826.
[97] Coleman, A. W., Hitchcock, P. B., Lappert, M. F., Maskell, R. K., Miffler, J. H., *J.Organomet. Chem.* **1978** , 296, 173
[98]Arduengo III, A. J., Dias, H. V. R., Calabrese, J. C., Davidson, F., *Organometallics.* **1993** , 12, 3405.
[99]Arduengo III, A. J., Gamper, S. F., Calabrese, J. C., Davidson, F., *J. Am. Chem. Soc.* **1994** , 116, 4391.

© University of Pretoria

1.4.3 Theoretical bonding model and coordination

N-heterocyclic carbenes are singlet carbenes and substituted by two π-donors of type X_2C. The carbenes contain a higher bent angle at the carbene carbon atom compared with that of a classic Fischer carbene counterpart due to the ring structure of the moiety. The interaction of the π-electron pairs of the substituent with the p_π orbital of the carbene carbon raises the relative energy of the p_π orbital but does not, however, affect the σ orbital; in effect, the σ-p_π energy cap enlarges, adding additional stability to the bent singlet ground state. π-electron interaction between the electron-rich substituent and the p_π orbital of the carbene carbon results in a π system of four electrons and three centres in which the X-C bonds attain partial multiple bond property.[21] Carbenes such as NHCs that receive electron density from both α-groups (R-groups) attain the right bent geometry with a small valence angle for strongly and effortlessly binding to metal fragments.[100,101] Since NHCs bind so strongly to the metal centre, they display high dissociation energies and the phenomenon is quantified by theoretical calculations for many different metal complexes. The higher dissociation energies are calculated in comparison with typical ligands. [102,103]

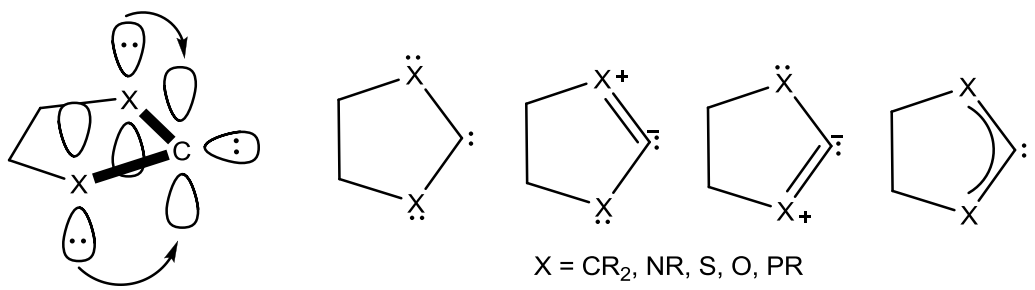

Figure 1.14. Electronic considerations for N-heterocyclic carbenes

The electronic and steric properties of Arduengo carbenes can be controlled by simply modifying either the carbon backbone or the functional groups associated with the ring structure (Figure 1.14).[28]

[100] (a) Harrison, J. F., *J. Am. Chem. Soc.,* **1971**, 93, 4112. (b) Harrison, J. F., Liedtke, C. R., Liebman, J. F., *J. Am. Chem. Soc.,* **1979**, 101, 7162. (c) Pauling, L., *J. Chem. Soc., Chem. Commun.,* **1980**, 688.
[101] Irikura, K. K., Goddard III, W. A., Beauchamp, J. L., *J. Am. Chem. Soc.,* **1992**, 114, 48.
[102] Weskamp, T., Kohl, F. J., Hieringer, W., Gleich, D., Herrmann, W. A., *Angew. Chem.,* **1999**, 111, 2573.
[103] Schwarz, J., Böhm, V. P. W., Gardiner, M. G., Groscher, M., Herrmann, W. A., Hieringer, W., Raudaschl-Sieber, G., *Eur. Chem J., In press.*

© University of Pretoria

Modification of the carbene can lead to complexes with specific solubility or electron-donor properties and since the compounds are mostly used as catalysts, they provide a less odorous alternative to their classic phosphine counterpart.[104] Several molecular structures for NHCs have been determined by single-crystal X-ray diffraction and it was proved that little differentiation exists between the geometric properties of different NHCs .When coordinated to metals, the carbene carbon-metal bond is significantly longer for NHCs (210 pm) than for the typical Fischer and Schrock carbenes (>200 pm).[83] The possibility of determining rotational barriers due to double bond characteristics has been elusive to date and only steric factors have been positively attributed as an influence on rotation.[105] Since the M-C bond does not display absolute double bond characteristics, it may be postulated that the bond itself might have qualities in between those of a classic single or double bond.

1.4.4 Reactivity and application

Complete reports on the preparation of metal-bound NHC complexes applicable to catalysis appeared in 1996 and were followed by multiple new reports in the following decade.[106,107,108] After initial patent reports, catalytic data were released as a series of publications. The earliest publication dated back to 1995.[109] The initial reported utilisation of NHC fragments in catalysis was that of the Heck coupling of aryl bromides and aryl chlorides. A platinum(II) NHC complex containing halogen ligands utilised for typical Heck reactions becomes active under conditions of smooth reduction with hydrazine and thus produces the corresponding Pt(0) species. Numerous highly reactive and stable catalysts utilised for Heck, Suzuki (Scheme 1.19) and Sonogashira reactions contains NHC fragments coordinated to the Pd metal centres. These complexes are exceptionally versatile and the reactions require unexpectedly low catalyst loading to obtain both pure and high yields.[109]

[104] Arnold, P. L., Pearson, S., *Coord. Chem. Rev.,* **2007**, 251, 596–609.
[105] Weskamp, T., Schattenmann, W. C., Spiegler, M., Herrmann, W. A., *Angew. Chem., Int. Ed. Engl.,* **1998**, 37, 2490.
[106] Herrmann, W. A., Fischer, J., Öfele, M., Artus, G. R. J., *J. Organomet. Chem.,* **1997**, 530, 259.
[107] Herrmann, W. A., Gertsberger, G., Spiegler, M., *Organometallics,***1997**, 16, 2209.
[108] Baretta, W., Herdtweck, E., Herrmann, W. A., Ringo, P., Schwartz, J., *Organometallics,* **2002.**
[109] Herrmann, W. A., Elison, M., Fischer, J., Köscher, C., Artus, G. R. J., *Angew. Chem.,* **1995**, 107, 2602.

© University of Pretoria

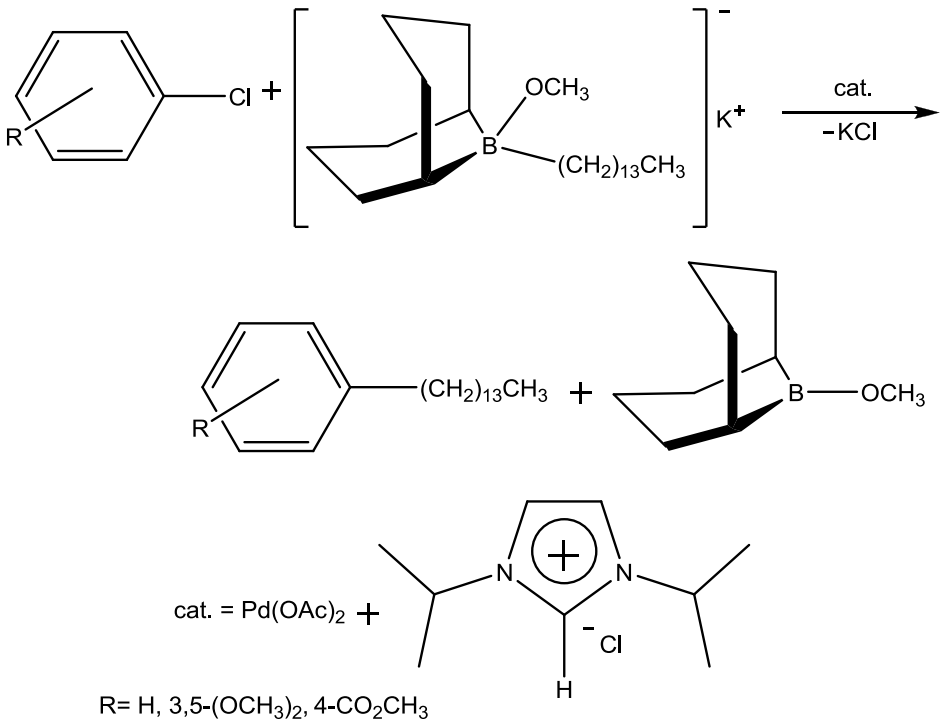

Scheme 1.19. Reaction and catalyst used in Suzuki coupling

Palladium catalysed amination of aryl halides has also been modified in recent years by ligation of NHC fragments to the palladium metal sphere (Scheme 1.20). Advances in both substrate scope and reaction rates have been achieved by palladium NHC complexes and their derivatives. NHCs have also become ever-increasingly popular as ligands in the palladium catalysed α-aryllation of amides.[110] Bulky, sterically hindered ligands are typically used with enhanced performance and quantitative yields. The syntheses of chiral NHCs, coordination to metal fragments and applications of these chiral carbenes were published in 1996.[111]

Chiral NHC complexes are utilised in the hydrosilylation of acetophenol by a rhodium catalyst with an enantiomeric excess of around 70%. One of the most important applications of NHC complexes is for olefin metathesis (Figure 1.15). NHC ligands have adequately demonstrated their catalytic superiority over the classic phosphine ligand. Numerous derivatives have been employed with the aim of producing newer and more versatile catalysts for catalysing olefin metathesis reactions.

[110] Hartwig, J. F., *J. Org. Chem.* **2001**, 66, 3402.
[111] Herrmann, W. A., Köcher, C., Gooβen, L. J., Artus, G. R. J., *Angew. Chem.,* **1996**, 108, 2980.

© University of Pretoria

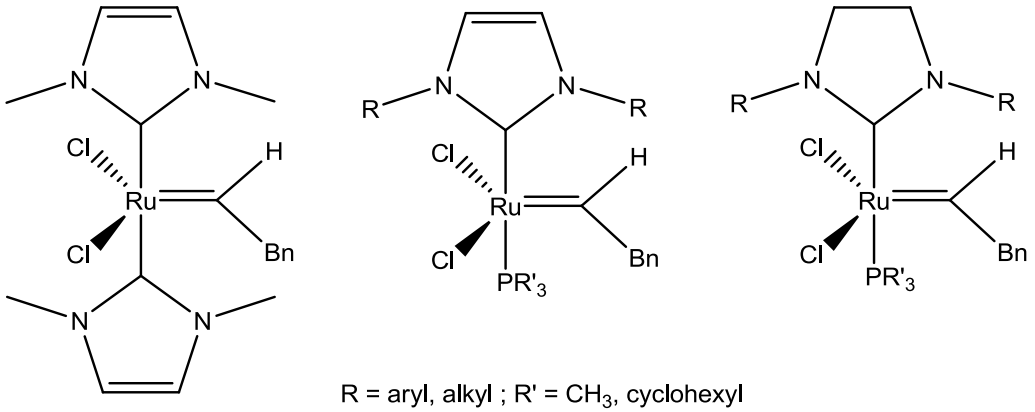

Figure 1.15. NHC complexes in olefin metathesis

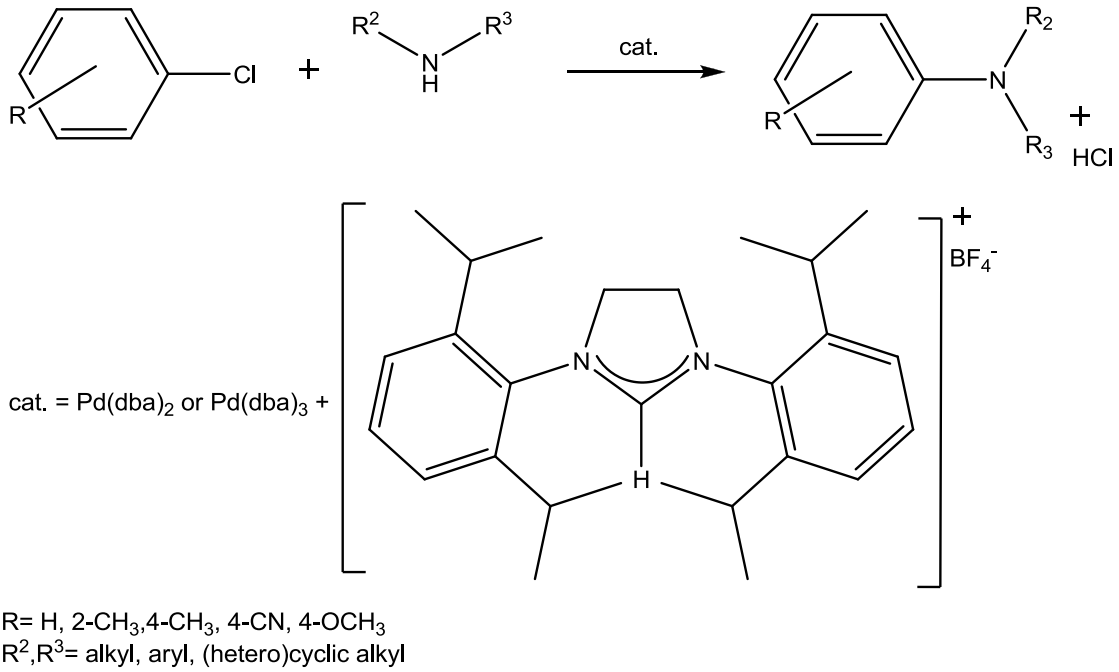

Scheme 1.20. NHC complexes in aryl amination

Both the synthesis of the Grubbs catalyst and the production of the second-generative derivatives allowed higher activity in typical metathesis reactions. In addition, the Grubbs catalyst made ruthenium the most promising metathesis metal due to its tolerance of functional groups and the mild reaction conditions required. Ring-opening polymerisation, acyclic diene metathesis and ring-closing metathesis all typically occur with the addition of the Grubbs catalyst derivatives and are held to be the best understood metathesis varieties to date. Hydroformylation of olefin reactions was historically catalysed utilising the rhodium(I) phosphane complexes. These complexes, however, are required in large excesses (up to 1

© University of Pretoria

000-fold) to avoid decomposition pathways and to obtain realistic ratios of linear and branched products. Stoichiometric quantities of rhodium triphenylphosphane complexes slowly decompose under the required conditions of catalytic hydroformylation.[112] In contrast to the rhodium(I) phosphane complexes, the NHC derivative complex of rhodium has long-term stability which allows stoichiometric quantities to be used and produces compounds over an extended lifespan. It is vital to bear in mind that since there presides a higher electron density on the metal centre of the carbene metal, reduced activity has been noted. High activity in combination with enduring stability have been described in cases of mixed rhodium carbene phosphane complexes.[81] The vast applicability and strength of NHC complexes lies in the immense structural versatility of these carbenes (Figure 1.16), which leads to (a) chirality, (b) functionality, (c) immobilisation, (d) water solubility and (e) the chelate effects.[81] All of these properties are currently being utilised and stable metal complexes are reported in each case.[113,114]

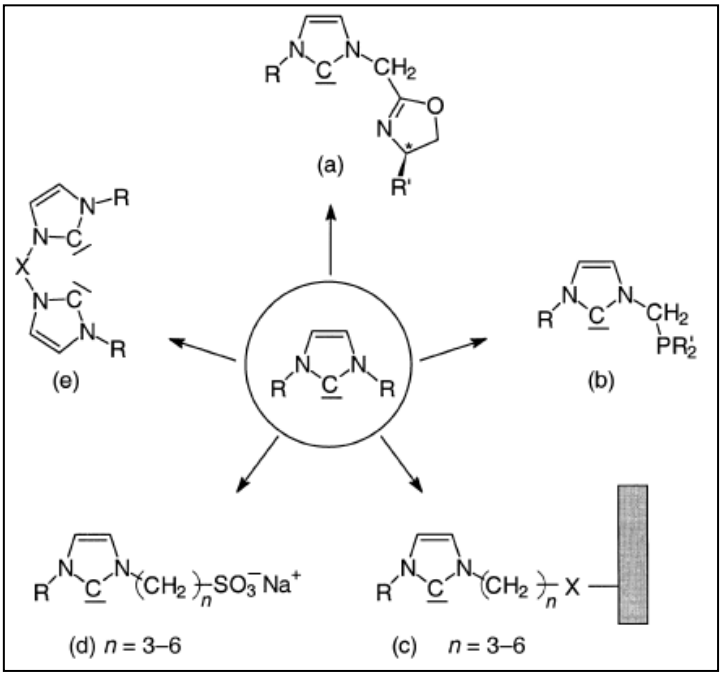

Figure 1.16. Versatility of NHC complexes[83]

[112] Herrmann, W. A., Köcher, C., *Angew. Chem., Int. Ed. Engl.,* **1997**, 36, 2162–2187.
[113] Various PhD theses filed under the supervision of W. A. Herrmann (all Technische Universität München): (a) Mihalios, D., PhD thesis (**1992**). (b) Roesky, P. W., PhD thesis (**1994**). (c) Elison, M., PhD thesis (**1995**). (d) Fischer, J., PhD thesis (**1996**). (e) Artus, G. R. J., PhD thesis (**1996**). (f) Reisinger, C.-P., PhD thesis (**1997**). (g) Köcher, C., PhD thesis (**1997**). (h) Steinbeck, M., PhD thesis (**1997**). (i) Booβen, L. J. PhD thesis (**1997**). (j) Runte, O. PhD thesis (**2000**). (k) Weskamp, T. PhD thesis (**1999**). (l) Schwarz, J. PhD thesis (**2000**). (m) Böhm, V. P. W., PhD thesis (**2000**). (n) Köhl, F., J., PhD thesis (**2000**). (o) Prinz, M., PhD thesis (**2001**).
[114] Böhm, V. P. W., Herrmann, W. A., *Angew. Chem.,* **2000**, 112, 4200.

© University of Pretoria

1.5 Coordination Complexes

1.5.1 Overview

Coordination complexes, or metal complexes, are chemical entities formed between ligands (organic, ionic or uncharged) and metal centres.[115] In reality, almost all conceivable compounds containing metal centres fall under the class of coordination complexes. Bonding between the metal fragment and the complexing ligands is considered weaker than the classic covalent bond. The bond strength is dependent on the metal-ligand interaction, centred mainly on the electron donation from the associated donor ligand. Typically, metal complexes are bound to several donor atoms and the central metal or ions, together with associated ligands, comprise the coordination sphere.[116] Coordination to metal fragments may be reversible or irreversible in character and many ligands bind quite strongly to the metal atom. Coordination complexes, although known throughout history (e.g. Prussian blue), were not fully understood until the first breakthrough by Alfred Werner in 1893.[117] Werner proposed that Co(III) bears six complexing ligands arranged in an octahedral geometry around the central metal atom. His theory allowed understanding of and differentiation between ionic and coordinated ligands in a compound and explained the formation of many different isomers that were previously misunderstood.

Ligands coordinate to metals typically in one of two modes: firstly, by donating a single pair of electrons (σ-donation) or secondly, as in the case of olefins, through filled π-orbitals into a metal's empty orbitals. The complex geometry is typically described by the coordination number, which is defined as the number of donor atoms attached to the metal atom.

1.5.2 Isomers

Isomer formation is also an important concept in coordination complexes. Although the arrangement of ligands around the metal core is fixed in place by coordination, it is possible to modify this arrangement by reactions that form other stable isomers. Stereoisomerism is characterised by the fact that the same bonds migrate to different positions in the coordination sphere. Ligands thus obtain different orientations in terms of other ligands, which differ from the original orientation.

---

[115] PAC. *Glossary of Terms Used in Physical Organic Chemistry (IUPAC Recommendations 1994),* **1994**, *p 1098.*

[116] *Red Book: IUPAC Nomenclature of Inorganic Chemistry,* 3rd edn., Blackwell Scientific Publications, Oxford, **1990**.

[117] Atkins, P., Overton, T., Rourke, J., Weller, M., Armstrong, F., *Inorganic Chemistry,* 4th edn.,Oxford University Pres, Oxford, **2006**, p 219.

© University of Pretoria

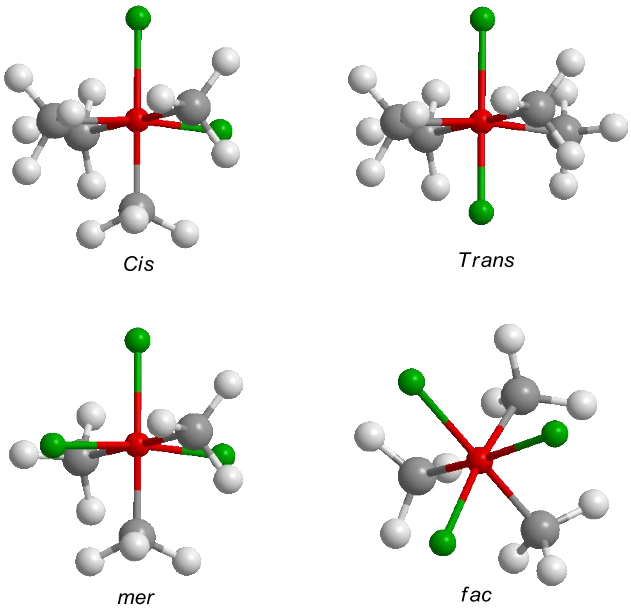

Figure 1.18. Molecular geometry of stereoisomers

Another form of isomer arises when three identical ligands coordinate to form the face of an octahedral complex (labelled facial or *fac* isomers), and when three ligands obtain both *cis* and *trans* geometry simultaneously (called meridonial or *mer* isomers)[118,119] (Figure 1.18).

1.5.3 Denticity

Denticity in a coordination entity is defined as the number of donor groups from a specific ligand that foster the ability to coordinate to a single metal atom.[120] In most cases only a single atom from a given ligand will coordinate, termed a 'monodentate ligand', and thus produce a denticity equal to one, but complexes with bidentate (two donor atoms coordinated from a single ligand) are not uncommon. Ligands with more than one donor atom are also termed 'polydentate' and may produce large bulky complexes. Multidentate ligands are considered chelation agents.[121]

[118] Von Zelewsky, A., *Stereochemistry of Coordination Compounds,* Wiley, Chichester, UK, **1996**.
[119] Kaufman, G. B., *Inorganic Coordination Compounds,* Wiley, New York, **1981**.
[120] *Red Book: IUPAC Nomenclature of Inorganic Chemistry,* 3rd edn., Blackwell Scientific Publications, Oxford, **1990,** p 147.
[121] PAC. *Glossary of Terms Used in Physical Organic Chemistry (IUPAC Recommendations 1994),* **1994**, p 1094.

© University of Pretoria

1.5.4 The chelate effect

The chelate effect describes the amplified affinity of metals for bi- and polydentate ligands in comparison with a collection of related monodentate counterparts. In addition, the effect casts light on the supplementary stability that these ligands bring to the coordination entity. It is clear from thermodynamic considerations that the formation constant (K_{f1}) of a complex with a bidentate chelate ligand, e.g. ethylenediamine, is greater in comparison with the value of β_2 for the bis(ammine) complex (Scheme 1.21).[122]

$$[Cd(OH_2)_6]^{2+}{}_{(aq)} + en_{(aq)} \rightleftharpoons [Cd(en)(OH_2)_4]^{2+}{}_{(aq)} + 2H_2O(l) \qquad \log K_{f1} = 5.84$$

$$[Cd(OH_2)_6]^{2+}{}_{(aq)} + 2\,NH_{3(aq)} \rightleftharpoons [Cd(NH_3)_2(OH_2)_4]^{2+}{}_{(aq)} + 2H_2O(l) \qquad \log \beta_2 = 4.94$$

Scheme 1.21. Formation constants for chelates and monodentate ligands

Considering that in both cases a formal M-N bond is formed, it is obvious that the formation of the chelate complex is more favoured. The chelate effect can be attributed to the differences in reaction entropy between the chelate and non-chelate aqueous complexes. The entropy benefit of chelation extends not only to main bidentate ligands but also, in theory, to multidentate ligands. As a matter of fact, the greater the number of donor sites, the greater the entropy benefit of substituting monodentate ligands. The chelate effect furthermore accounts partly for the superior stability of complexes containing the tetradentate porphyrin ligand or complexes ligated to the hexadentate ligand EDTA. Apart from thermodynamic considerations, the chelate effect also involves kinetic factors that have an effect. When one ligation group is bonded to the metal centre, it is more likely that other donor sites will also bond. This effect is due to the close proximity of sites to the metal atom and thus it favours additional ligation.[123]

1.6 Aim of the study

The aim of this study was the complete synthesis, characterisation and structural investigation of multiple alkoxycarbenes and aminocarbenes with aromatic heteroarene substituents, together with several N-heterocyclic carbenes (NHCs) containing a number of different N-substituents. Thiophene, bithiophene and furan heteroarenes were utilised as

[122] Atkins, P., De Paula, J., *Physical Chemistry,* 8th edn,Oxford University Press, Oxford,UK, **2006**.
[123] Atkins, P., Overton, T., Rourke, J., Weller, M., Armstrong, F., *Inorganic Chemistry,* 4th edn, Oxford University Press, Oxford, **UK, 2006**, pp 494–495.

© University of Pretoria

carbene substituents, while dppe, 2-2'-bipy and TEMED bidentate ligands encompassed the range of metal ligated groups utilised. Focus also fell on:

- The full characterisation of all the complexes synthesised in the study;
- Investigating appropriate application possibilities for the novel carbene complexes;
- Improving on existing synthetic procedures;
- Using computational models for comparison with experimental results.

The syntheses of isopropyl- and cyclohexyl-containing NHCs were attempted. These complexes were also novel and produced insight into the application of this class of compounds. Molecular aspects, such as bond lengths, bond angles and structural energies of the novel carbenes synthesised in this study, were analysed using nuclear magnetic resonance (NMR) spectroscopy, infrared (IR) spectroscopy, mass spectroscopy, X-ray diffraction and DFT calculations. Two of these modified complexes were also investigated for catalytic activity.

Complexes **2** and **6** were both part of the catalytic study. The aim was to determine the extent of catalytic ability of these complexes and both olefin metathesis and polymerisation reactions were attempted. Ideally, the catalytic study would be utilised in conjunction with theoretical modelling with the aim of synthesising a model having the capability of accurately predicting parameters for catalytic functionality.

Computational modelling was employed in conjunction with the abovementioned methods to explore the possibility of producing an accurate, representative technique to compute and predict chemical properties. By utilising computational calculations, theoretical IR stretching frequencies became available to serve as a comparison with the experimentally obtained results. HOMO (highest molecular orbital) and LUMO (lowest unoccupied molecular orbital) density calculations were also attempted and served as indicators of nucleophilic and electrophilic regions within the computed structures.

© University of Pretoria

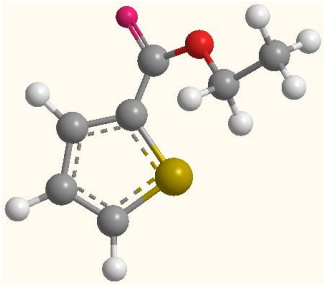

2 Bidentate Ligated Carbene Complexes

2.1 Background

2.1.1 Fischer carbene complexes containing aromatic substituents

Metal-containing carbene structures originated with the synthesis of the novel pentacarbonyl[methoxybenzylidene]tungsten(0) complex by Fischer and Maasböl.[1] This compound not only provided the first evidence of a metal-carbon double bond, but also contained a substituent, attached to the carbene carbon atom, with an aromatic system. The carbene carbon atom is further flanked by a heteroatom with π-donating characteristics, supplying the sp^2 hybridised atom with electron density through both σ and π interactions. Stabilisation through electron migration from this heteroatom produces *cis* and *trans* configurations (Figure 2.1).[2,3] The delocalisation of electrons is thus extensive and distributed through the carbene system, metal centre and phenyl or heteroarene substituent[4] (Figure 2.2).

[1] Fischer, E. O., Maasböl, A., *Angew. Chem.*, **1964**, 76, 645.
[2] Lage, M. L., Fernández, I., Mancheño, M. J., Sierra, M. A., *Inorg. Chem.,* **2008**, 47, 5253–5258
[3] Lage, M. L., Fernández, I., Mancheño, M. J., Gómez-Gallego, M., Sierra, M. A., *Chem. Eur. J.,* **2010**, 16, 6616–6624.
[4] Cardin, D. J., Cetinkaya, B., Lappert, M. F., *Chem. Rev.,* **1972**, 72, 545.

© University of Pretoria

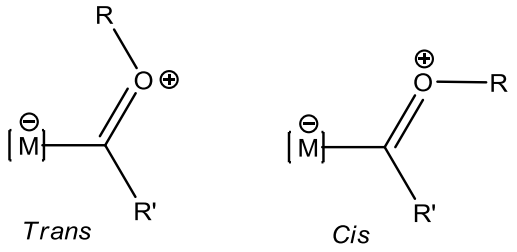

Figure 2.1. *Cis* and *trans* configurations around the heteroatom substituent

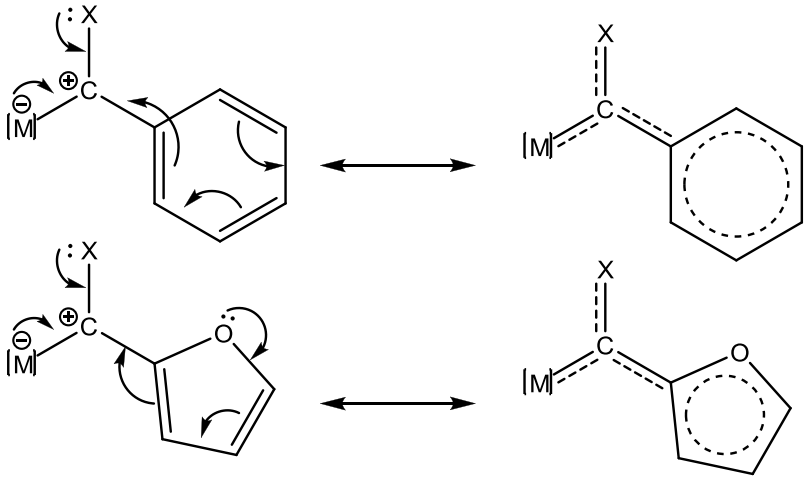

Figure 2.2. Electron π-delocalisation network through the carbene system

Aromatic and heteroarene substituents have been extensively utilised in the synthesis of carbenes for additional stabilisation. There has been general consensus since the 1960s that these moieties exhibit the following unique combination of characteristics: [5]

i. They consist of planar, cyclic delocalised π-electron systems;
ii. These structures contain additional stabilisation energy (resonance energy); providing a more stable alternative to the olefinic counterpart;
iii. Delocalisation of the electrons produces bond lengths between those of a single and a double bond;
iv. Substitution reactions are more favoured than addition reactions;
v. Ring opening and loss of aromaticity is thermodynamically disfavoured;
vi. They show high energy-ultraviolet/visible spectral bands and typically more symmetrical configurations in IR spectroscopy.

[5]Krygowski, T. M., Crañski, M. K., Czarnocki, Z., Häfelinger, G., Katritzky, A. R., *Tetrahedron,* **2000**, 56, 1783.

© University of Pretoria

2.1.2 Fischer carbene complexes containing heteroaromatic substituents

The first in-depth study of the heteroarene derivatives of aromatic Fischer carbenes was done by Connor and Jones.[6] Chromium Fischer-type carbenes containing heteroarenes, such as furan, were the first of this class of carbene complexes to be studied. Experimental studies further confirmed that changing the heteroatom infused in the heteroarene substituent has a direct effect on the extent of the π-stabilisation ability of the substituent on the carbene carbon.[6] Heteroarenes provide electron density to the electron-poor carbene carbon through π-donation and this ability increases in the order of heteroatom = O < S < NMe (Figure 2.3).[6] From considerations in regard to the mentioned heteroarene stabilisation trend, it can be deduced that oxygen-containing heteroarenes will provide the least stabilisation to the carbene carbon and, ultimately, the metal back-bonding to the carbene centre will be excessive, resulting in a stronger metal-carbon bond. Sulfur-containing heteroarenes provide a different picture by infusing the carbene carbon atom with additional electron support to a greater extent than the corresponding furan ring.

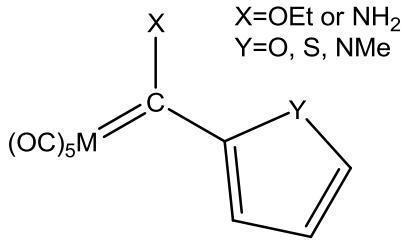

Figure 2.3. Heteroarene substituted Fischer carbene complexes

2.1.3 Thiophene as heteroaromatic substituent

Thiophene is a heterocyclic aromatic ring with the molecular formula of C_4H_4S and consists of a flat five-membered ring with vast substitution reaction properties. Benzene-fused derivatives of this class are well known and both benzothiophene and dibenzothiophene not only contain the moiety, but are also regularly seen in substitution reactions. Both oxygen (furan) and nitrogen (pyrrole) structural analogues exist and are often utilised in conjunction to study electronic and structural characteristics as part of larger reactivity trends. Thiophene was originally discovered as a contaminant in benzene[7] and the pioneer Victor Meyer was responsible for the isolation of the novel aromatic structure. At room temperature, thiophene contains chemical and physical properties similar to those of benzene and is a clear liquid

[6]Connor, J. A., Jones, E. M., *J. Chem. Soc., Part A,* **1971**,1974.
[7] Meyer, V. *Berichte der Deutschen Chemischen Gesellschaft,* **1883**, 16, 1465–1478.

© University of Pretoria

with an aroma similar to that of benzene. Due to the similarity between the boiling points of thiophene and benzene, purification by distillation proves difficult. Owing to it's aromaticity, thiophene is flat in structure with an angle of 93˚ around the sulfur atom. C-C-S angles of 109˚ and approximately 120˚ around the remaining base carbons are observed. C-C bond lengths of 1.35 Å were determined for carbon atoms adjacent to the sulfur atom, while the carbon-sulfur bond length of 1.74 Å is witnessed. The remaining carbon-carbon bond has a length of 1.41Å [8,9,10] (Figure 2.4). On the basis of theoretical calculations it has been suggested that the degree of aromaticity is less than that of benzene and the electron density on the sulfur atom is delocalised into the π-electron system. With reference to reactivity, thiophene is not only reactive towards electrophiles and desulfurisation, but also readily lithiated with butyl lithium to produce 2-lithiothiophene, which serves as a precursor for numerous derivatives. [11] Chemical and physical adaptation and modulations are successfully achieved by the addition of functionalised groups to the parent moiety.[12] Sulfur-containing aromatic systems are often utilised as building blocks or starting material in many agrochemicals and pharmaceuticals. Arene ring-containing biologically active structures can often be substituted by thiophene (Figure 2.4) without any loss in activity[13].

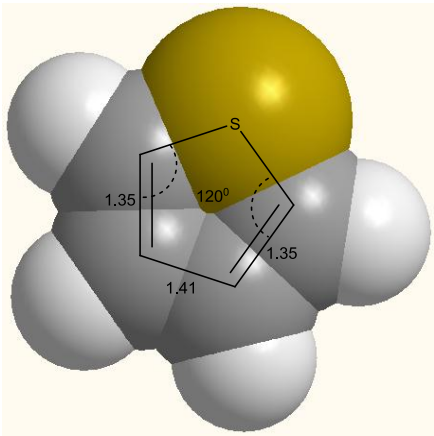

Figure 2.4. Space-filling model of a thiophene molecule

[8] Longuet-Higgins, H. C., *Trans. Faraday Soc.,* **1949**, 45, 173.
[9] Epiotis, N. D., Cherry, W. R., Bernardi, F., Hehre, W. J., *J. Am. Chem. Soc.,* **1976**, 98, 4361.
[10] Angelici, R. J., *Coord. Chem. Rev.,* **1990**, 105, 61.
[11] Jones, E., Moodie, I. M., *Org. Synt.,* **1988**, 6, 979.
[12] Raos, G., Famulari, A., Meille, S. V., Gallazzi, M. C., Allegra, G. *J. Phys. Chem., Part A,* **2004**, 108, 691.
[13] Rauchfuss, T. B., *Prog. Inorg Chem.,* **1991**, 39, 259–311.

© University of Pretoria

2.1.4 Furan as heteroaromatic substituent

Furan is an aromatic five-membered ring containing an oxygen atom. The physical properties of furan include high volatility, low boiling point (close to room temperature) and toxicity. Recent findings indicate that furan molecules are carcinogenic. Furan is colourless and often used as starting material for various reactions to produce speciality chemicals.[14] It shows a molecular structure similar to that of thiophene and also shares the distinctive property of delocalising electron density from the oxygen atom into the aromatic π-system. Due to the aromaticity of furan, its reactivity is more comparable to that of arene derivatives than typical ethers such as tetrahydrofuran, but it claims a higher reactivity than the non-heteroarenes such as benzene. Studies of resonance contributions show the amplified electron density of the ring, ultimately resulting in an advanced rate of electrophilic substitution.[15] Furan also forms lithium derivatives when treated with organolithiums, although in lower yields than thiophene.

2.1.5 Polythiophenes as heteroaromatic substituent

Polythiophenes, e.g. bithiophene, result from polymerisation reactions of the smaller monomeric thiophene. Polythiophenes (PTs) demonstrate noticeable optical characteristics resulting from the conjugation system through the backbone. This is demonstrated by the fluorescence of substituted polythiophene solution under UV irradiation. The study of thiophenes has intensified over the past few decades and PTs have found potential applications in field-effect transistors,[16] electroluminescent devices, batteries and solar cells, diodes and non-linear optics. Bithiophene has reactivity trends similar to those of thiophene.

2.1.6 Theoretical synthetic methodology

For the synthesis of Fischer alkylidene complexes, the most universal procedure utilised is the addition of an alkyl lithium to a metal carbonyl to produce the acyl metalate intermediate, which is subsequently treated with a strong alkylating reagent (O atom alkylation) to produce the stable carbene (Scheme 2.1). Quantum chemical calculations have confirmed that the

[14] Hoydonckx, H. E., Van Rhijn, W. M., De Vos, D. E., Jacobs, P. A. Furfural and derivatives, In *Ullmann's Encyclopedia of Industrial Chemistry,* Wiley-VCH, Weinheim, Germany,, **2005**.
[15] Paula, Y. *Organic Chemistry,* 5th edn,Upper Saddle River, NJ, US, Pearson Prentice Hall, **2007.**
[16] Gamier, F. Field-effect transistors based on conjugated materials. In Müllen, K., Wegner, G. (Eds), *Electronic Materials: The Oligomer Approach,* Wiley-VCH, Weinheim, Germany, **1998**.

© University of Pretoria

carbon atom in the CO coordination ligand holds a larger positive charge than a free carbonyl group and thus a nucleophilic attack should indeed be favoured.[17]

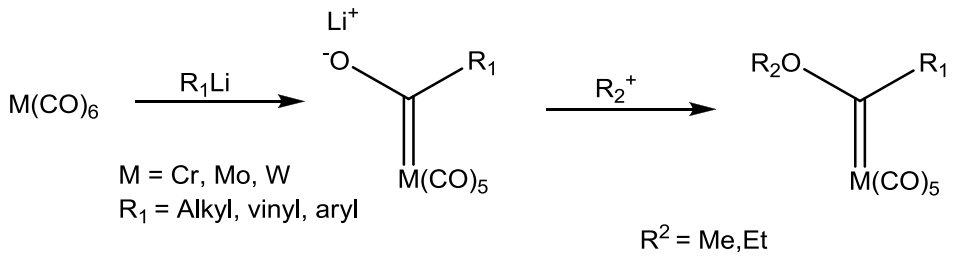

Scheme 2.1. Alkylidene synthesis according to Fischer methodology

An alternative version of this process is the alkylation of a neutral acyl complex.[18] Modifications of carbonyl ligands, attached to metals, are often achieved via thermochemical or photochemical procedures.[19] The last few decades, however, have seen the application of microwave-assisted synthesis to produce the same desired substitution effect, with superior rates and yields accompanying such modifications. Substitutions of multiple carbonyl ligands by bidentate ligands have been reported[19] (Scheme 2.2).

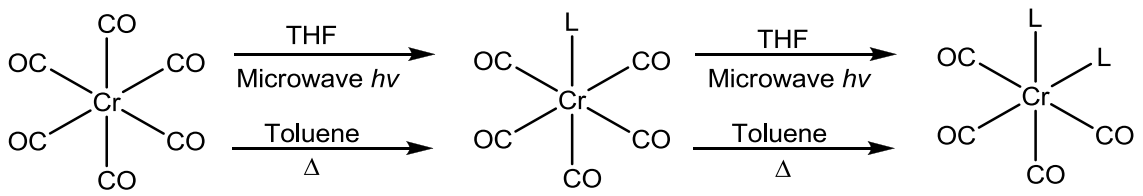

Scheme 2.2. Carbonyl substitution reaction methodology

[17] Elschenbroich, C. *Organometallics,* 3rd edn, Wiley-VCH, Weinheim, Germany, **2005**, p 334.
[18] Gladysz, J. A., Kriel, W. A., Yu Lin, G. Bodner, G. S., *J. Chem. Soc.,* **1983**, 105, 4958.
[19] Van Atta, S. L., Duclos, B. A., Green, D. B., *Organometallics,* **2000**, 19, 2397–2399.

© University of Pretoria

2.2 Synthesis

2.2.1 Focus

The focus of this part of the study was on the synthesis of multiple chromium(0) carbene complexes and further functionalisation of these carbene species by replacing multiple labile coordinated carbonyl ligands with bidentate counterparts. A diverse range of heteroaromatic carbene substituents (thiophene, 2,2'-bithiophene and furan) were employed, and numerous bidentate ligands were used to provide catalytic, structural and electronic insight. Figure 2.5 depicts the complexes that were proposed as the major focus of synthesis described in this chapter.

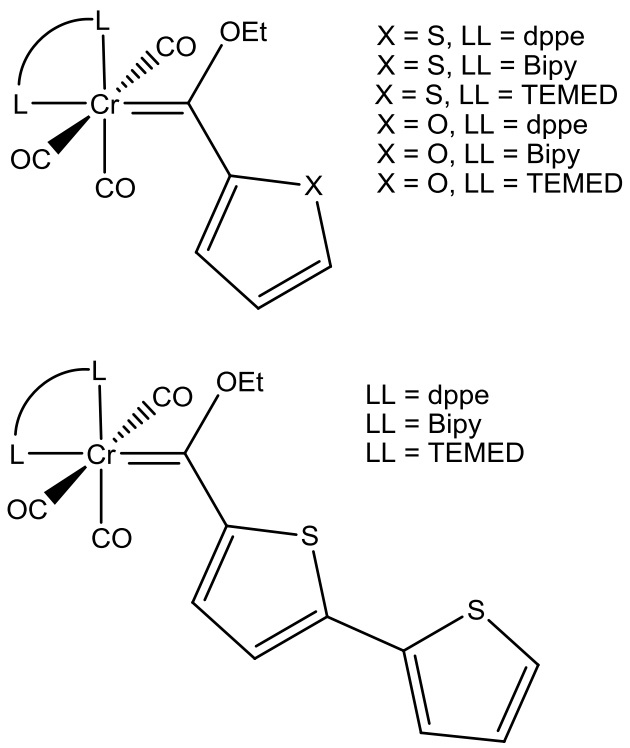

Figure 2.5. Proposed carbene complexes of chromium(0)

Details of synthesis are given in the literature for monocarbene complexes incorporating thiophene[20], furan and bithiophene as heteroarene substituents. (2-Bithienyl)ethoxycarbene pentacarbonyl chromium(0), **G**, has previously been synthesised in our laboratories by van

[20] Terblans, Y. M., PhD Thesis (and references therein), *Thiophene Bimetallic Carbene Complexes,* **1996**, University of Pretoria, Pretoria.

© University of Pretoria

Staden,[21] and the ethoxy furan chromium carbene, **F**, has been prepared by both Crause[22] and, originally, by Connor and Jones.[6] The crystal structure of the ethoxy thiophene monocarbene of chromium, **E**, was determined by Thompson *et al*.[23]

2.2.2 Synthetic methodology

Classic Fischer methodology was employed in the synthesis of the carbene starting material (Scheme 2.3). This process produced carbene complexes [$M(CO)_5$(carbene)] with adequate stability and reactivity to endure further exploitation.

Further functionalisation was accomplished by refluxing the carbene starting material in toluene[24, 25] together with the bidentate ligand to produce the final substituted Fischer carbene complex. The first reaction stage in the multi-step synthesis requires a strong base to deprotonate the α-proton, of suitable acidity, on the heteroarene. The base n-BuLi was selected as appropriate for this function and deprotonation occurred at -78 °C, under inert conditions and with dry THF as solvent. This step was repeated numerous times with the temperature being modified in each case. The results with respect to yields obtained indicated that deprotonation at higher temperatures allowed increased levels of single deprotonation to occur. The net result is thus larger yields of monocarbene complex compared with the biscarbene product. A temperature of -30 °C was found to be optimum. Metalation followed the abovementioned deprotonation step. Chromium hexacarbonyl was added in a single portion at -78 °C and the reaction followed a nucleophilic mechanism in which an electrophilic metal carbonyl carbon is attacked by the newly formed nucleophilic, deprotonated heteroarene ring. The chromium metal acylate is formed as consequential product. The solvent was removed under vacuum and the resulting residue dissolved in dichloromethane, an appropriate alkylation solvent. Alkylation followed through the addition of triethyl oxonium salt to the acylate intermediate at -30 °C with the level of completion being checked with the aid of thin layer chromatography (tlc) analysis. The carbene starting material was purified employing silica gel chromatography with hexane and dichloromethane (DCM) as eluent agent. Yields of 60-72% were obtained.

---

[21] van Staden, M., MSc Dissertation, *Synthesis and structure of bithiophene complexes,* **2001**, University of Pretoria, Pretoria.
[22] Crause, C., *Synthesis and application of carbene complexes with heteroaromatic substituents,* **2004**, University of Pretoria, Pretoria.
[23] Thompson, S., Landman, M., van Rooyen, P., Unpublished results.
[24] Barluenga, J., Muñiz, K., Tomás, M., Ballesteros, A., García-Granda, S., *Organometallics,* **2003**, 22, 1756–1760.
[25] Reinheimer, E. W., Kantardjieff, K. A., Herron, S. R., Tisserat, C. G., Casalnuovo, J. A., *J. Chem. Crystallogr.,* **2003**, 33, 503–512.

© University of Pretoria

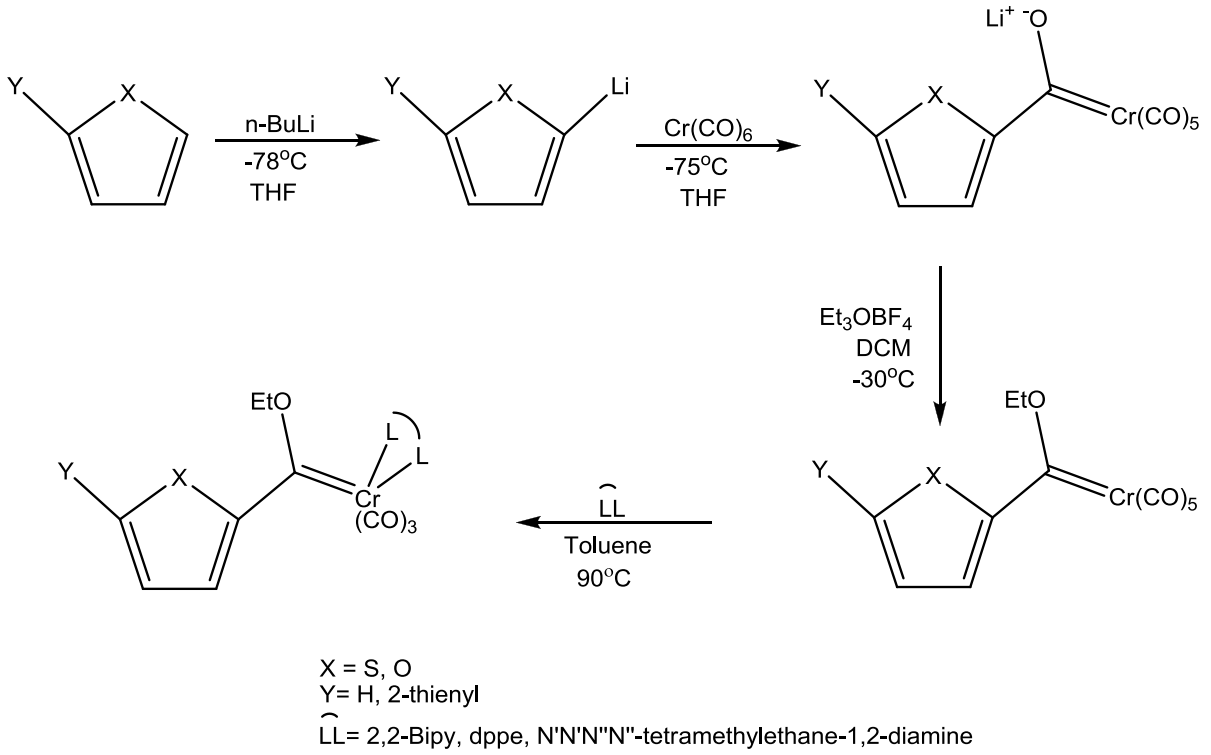

Scheme 2.3. Synthetic methodology of the carbene complexes of chromium(0)

The monocarbene complexes were dissolved in 15 ml of toluene and equivalent quantities of the bidentate ligand added to each reaction flask. The reaction mixture was allowed to reflux at 90 °C until tlc analysis indicated completeness of the reaction. The final reaction step yielded bidentate ligated monocarbene complexes **1–3** with a measured yield of 60–63%. Table 2.1 indicates selected physical properties of complexes **1–3** and **14**. Interestingly, the coordination of the bidentate phosphine ligand occurred *trans* to the carbene fragment and produces the meridonial structure. This coordination mode is contrary to the *fac*-(dppe)$(CO)_3$M=C(OR) isomer proposed by Reinheimer *et al.*[25] (Figure 2.6).

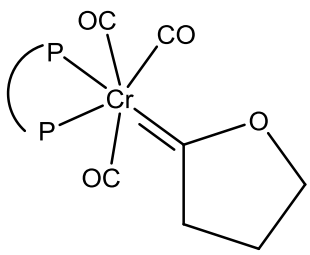

Figure 2.6. *fac*-(dppe)Cr$(CO)_3$=C(OR) structure

© University of Pretoria

Table 2.1. Physical properties of carbene complexes **1**–**3** and **14**

Complex	Yield (%)	Colour
1	60	Purple
2	65	Brown
3	63	Orange-brown
14	45	Blue

All functionalised complexes as well as starting complex **A** were crystallised by diffusion of a DCM solution surrounded by a hexane bath. The synthesis of mono-substituted furan carbene followed a similar reaction to that of the bidentate ligated counterpart. The monocarbene complexes were dissolved in 15 ml of toluene and equivalent quantities of the phosphine ligand added to the reaction flask. The reaction mixture was allowed to reflux at 90 °C until tlc analysis indicated satisfactory yields. The reaction produced inter-converting isomeric products that proved difficult to separate adequately. Since separation was not achieved, both isomers were characterised together. The synthesis of monophosphine-containing carbene complexes has also been reported in the literature and the reaction is normally promoted through thermal or photochemical processes[26] (Scheme 2.4).

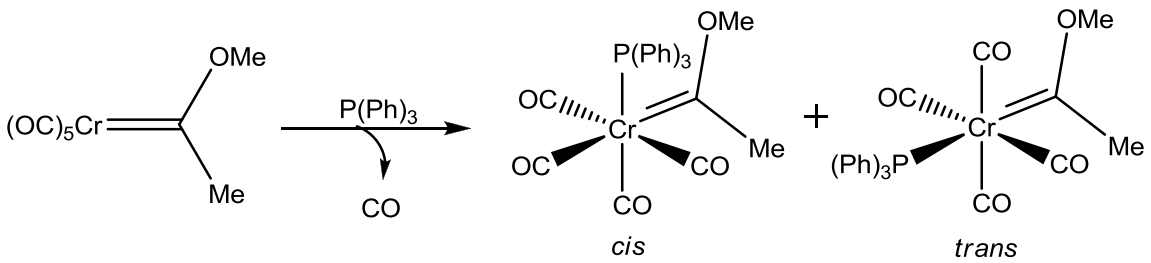

Scheme 2.4. Carbonyl substitution of a chromium carbene complex

The synthetic approach based on temperature-controlled substitution of a carbonyl ligand for a monophosphine ligand was extended later by the Fischer group to include both different metals and different carbene substituents.[27] Fischer *et al.* also later found applications for phosphine-containing carbene complexes in the synthesis and isolation of optically active cyclopropane from a reaction employing [(-) (R)-methylphenylpropylphosphine] (phenylmethoxycarbene).[28] Part of the focus of this chapter was on the synthesis of carbene complexes containing nitrogen-based bidentate analogues of complexes **1**–**3**. However,

[26] Fischer, E. O., Fischer, H., *Angew. Chem., Int. Ed. Engl.,* **1972**, 11, 644.
[27] Fischer, H., Fischer, E. O., Kreissel, F. R., *J. Organomet. Chem.,* **1974**, 64, C41–C44.
[28] Cooke, M. D., Fischer, E. O., *J. Organomet. Chem.,* **1973**, 56, 279–284.

© University of Pretoria

characterisation data indicated failure in the formation of TEMED, 2,2'-bipy and (Z)-N',N',N'',N''-tetramesitylethene-1,2-diamine carbene complexes. The reactions yielded bidentate coordination complexes, which formed through the substitution of the carbene fragment. In view of the products obtained, it was proposed that substitution of ligands tends to occur in a fashion to limit electronic competition. Thus replacing a carbonyl ligand (σ-donor, π-acceptor) with an amine ligand (σ-donor) will result in added electron density being shifted onto the metal centre and eventually to the π-acceptor ligands. Since the trend for π-accepting ability follows the series CO > PPh_3 > Fischer carbene, when the second nitrogen atom coordinates to the metal centre, the carbene moiety would rather be substituted than a carbonyl ligand since the carbene's ability to stabilise electron density from the metal is lower than that of the corresponding carbonyl groups. Scheme 2.5 shows the products obtained for the reactions of the carbene complex starting material with a bidentate amine ligand. Both the TEMED and the 2,2'-bipy complex have previously been synthesised and fully characterised.[29,30]

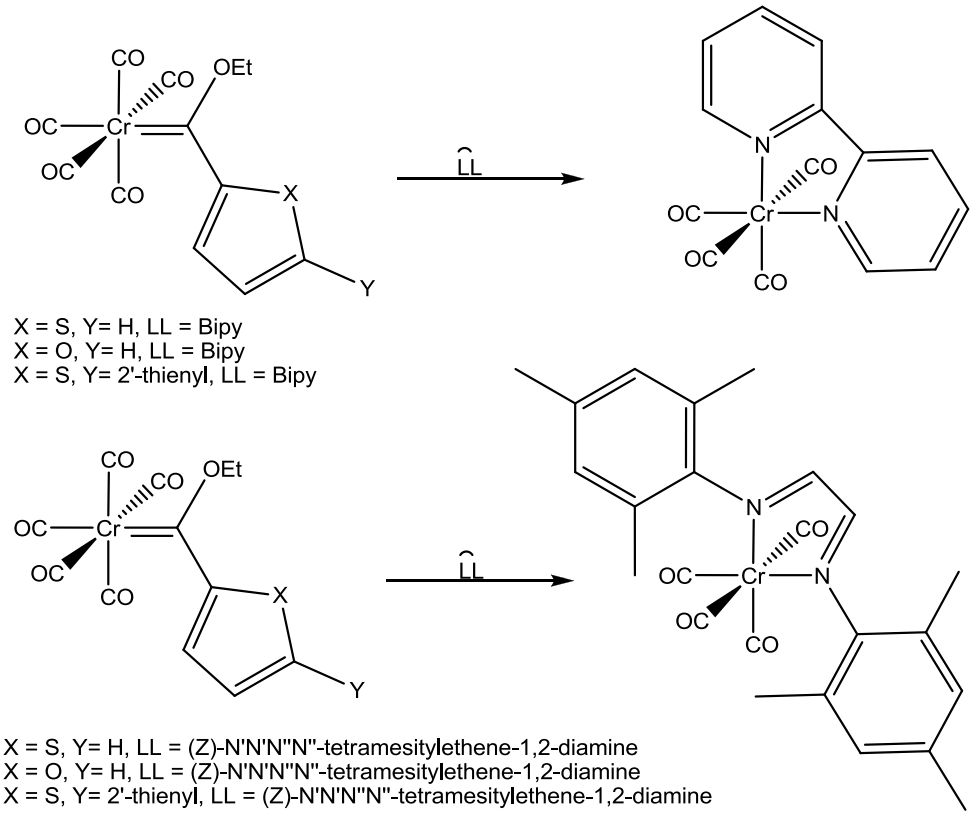

Scheme 2.5. Products obtained from utilising amine bidentate ligands

[29] Le Floch, P., Carmichael, D., Richard, L., Mathey, F., *Organometallics,* **1992**, 11, 2475–2479
[30] Kruger, G. J., Gafner, G., de Villiers, J. P. R., Raubenheimer, H. G., Swanepoel, H., *J. Organomet. Chem.,* **1980**, 187, 333.

© University of Pretoria

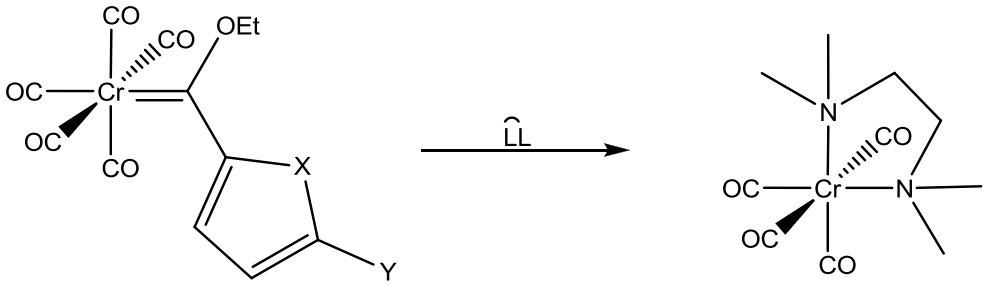

X = S, Y= H, LL = TEMED
X = O, Y= H, LL = TEMED
X = S, Y= 2'-thienyl, LL = TEMED

Scheme 2.5 (continued). Products obtained from utilising amine bidentate ligands

2.3 Characterisation and Crystallographic Data

The novel complexes **1**–**3** and **14** were fully characterised utilising deuterated solutions of CH_2Cl_2 and $CHCl_3$ for NMR spectroscopy, KBr pellets for infrared spectroscopy and the samples in solid, crystal state for X-ray crystallographic data collection. Solid state infrared characterisation limited the solvent effect and thus the problem of solubility could be circumvented.

2.3.1 NMR spectroscopy

^{1}H NMR spectroscopy

Proton NMR spectra were collected for all complexes as well as for the starting material utilised. Proton shifts of pure heteroatom-containing arene rings as well as uncoordinated bidentate ligands were compared with their corresponding ligated carbene complexes and the effect of carbene formation and ligation in each case studied. Tables 2.2 and 2.3 provide the proton chemical shifts of all the free substituents used in the synthesis of the bidentate-containing carbene complexes. The deuterated solvent used is specified at the bottom of the table.

© University of Pretoria

Table 2.2. ^{1}H NMR shifts of unligated heteroarene molecules

Mono-ring arenes

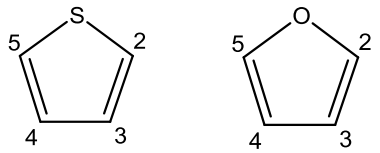

Multi-ring arenes

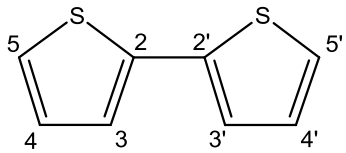

Proton assignment	Thiophene[31]	Furan[32]	**Proton assignment**	2,2'-Bithiophene[21]
	Chemical shift (δ, ppm)	**Chemical shift (δ, ppm)**		**Chemical shift (δ, ppm)**
H_2,H_5	7.20 (d)	7.38	$H_3,H_{3'}$	7.18
H_3,H_4	6.96 (d)	6.30	$H_4,H_{4'}$	7.02
			$H_5,H_{5'}$	7.21

Table 2.3. ^{1}H NMR shifts of unligated bidentate molecules

Bidentate ligands

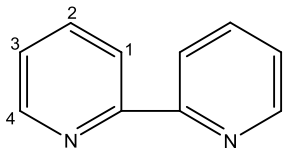

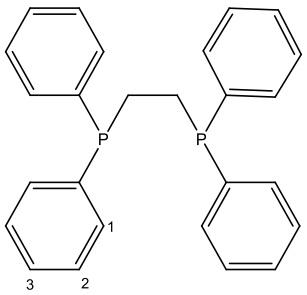

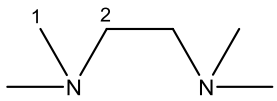

Proton assignment	2,2-Bipyridine **Chemical shift (δ, ppm)**	Bis-(diphenylphosphino) ethane **Chemical shift (δ, ppm)**	TEMED **Chemical shift (δ, ppm)**
H_1	8.64 (ddd)	7.28 (m)	2.24 (s)
H_2	7.78 (td)	7.28 (m)	2.38 (s)
H_3	7,27 (ddd)	7.28 (m)	-
H_4	8.37 (td)	-	-

Solvent : $CDCl_3$

[31] Abrahams, R. J., Fischer, J., Loftus, P., *Introduction to NMR Spectroscopy,* Wiley, New York, **1988**.
[32] Pretch, E., Seible, J., Clerc, T., Simon, W., *Tables for Spectral Data for Structure Determination of Organic Compounds,* 2nd edn, Springer-Verlag, Berlin and Heidelberg, **1989**.

© University of Pretoria

Table 2.3 (continued). ^{1}H NMR shifts of unligated bidentate molecules

Bidentate ligands

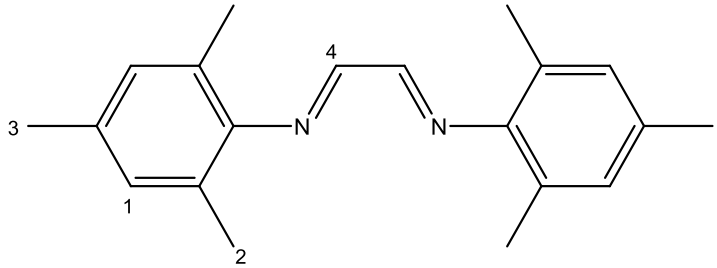

	(Z)-N',N',N'',N''-tetramesitylethene-1,2-diamine[33]
Proton assignment	**Chemical shift (δ, ppm)**
H_1	6.76 (m, 4H)
H_2	2.11 (s, 12H)
H_3	2.14 (s, 6H)
H_4	8.06 (s, 2H)

Comparison of the uncoordinated ligands and heteroarenes with the ligated, functionalised carbene complexes provided valuable insight into the electronic system of the synthesised products. In the formation of the carbene moiety and coordination to the metal sphere, the carbene centre acts as an electron hole with all the electron density draining towards this centre. Both the heteroarene and the metal moiety provide the necessary electron density to stabilise the classic electron-deficient, carbene carbon atom with added resonance stability from the flanking heteroatom. This is evident from the downfield shift of the protons from the coordinated vs. the uncoordinated ring protons of the heteroarene. The coordination shift (Δδ) is definable as the difference in the chemical shift value between the observed chemical shift of the metal-containing complex and the uncoordinated ligand,[34] such that:

$$\Delta\delta = \delta(\text{metal complex}) - \delta(\text{uncoordinated ligand})$$

Protons ligated to metal centres are generally considered hydridic in nature and experience a predominantly overwhelming shielding, resulting in an exceptionally large Δδ value. Group trends are also visible in terms of proton shielding and metals tend to have more shielded protons as the atomic number enlarges (metals belonging to same group). Characteristic

[33] Van der Westhuizen, B., MSc Dissertation, *Synthetic investigation of Mn(I) and Re(I) N-heterocyclic carbene complexes,* **2010**, University of Pretoria, Pretoria.
[34] Elschenbroich, C., Salzer, A., *Organometallics*, *A Concise Introduction*, 2nd edn, VCH Publishers, New York, **1992.**

© University of Pretoria

peaks of both the heteroarene rings and the hydrogen-bearing ethoxy substituent were present and provided sound evidence for the existence of the expected carbene moiety. In comparison with the proton NMR spectra of the pentacarbonyl monocarbene starting material complexes, the spectra for complexes **1–3** indicated multiple new peaks corresponding to the ligation of the bidentate ligands.

Table 2.4 summarises the proton NMR chemical shifts for complexes **1–3** and **14**.

Table 2.4. ^{1}H NMR shifts of complexes **1–3** and **14**

Assignment	**Complexes**		
	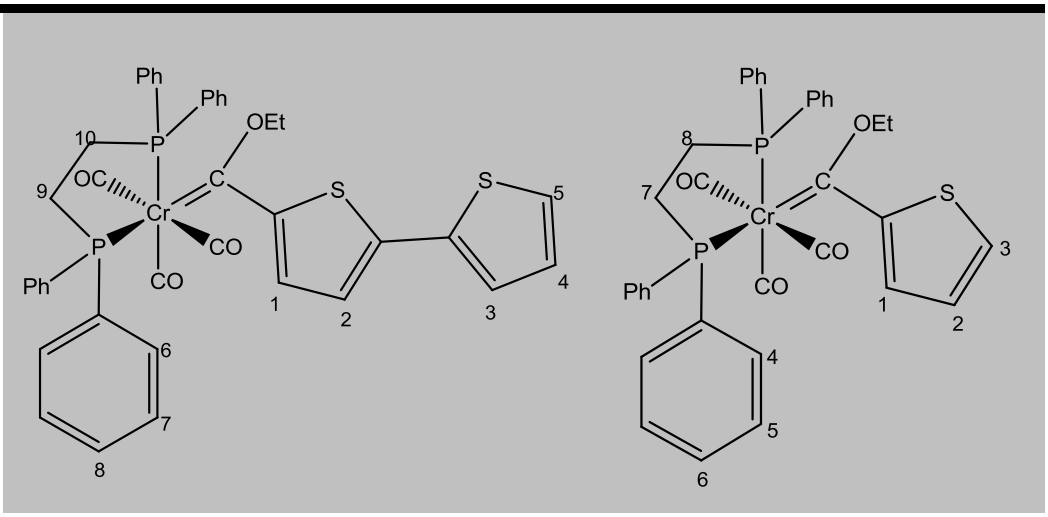		
	1		**2**
Proton	**Chemical shift (δ, ppm)**	**Coupling constant (*J*, Hz)**	**Chemical shift (δ, ppm)**
H_1	7.60 (s, br)	-	7.75 (s, br)
H_2	7.26 (d)	3.3	6,86 (s, br)
H_3	7.32 (d)	3.1	7.60 (s, br)
H_4	7.04 (dd)	4.9, 3.4	7.27-7.63 (m)
H_5	7.47 (d)	4.5	7.27-7.63 (m)
H_6	7.28-7.50 (m) 7.63-7.75 (m)	-	7.27-7.63 (m)
H_7	7.28-7.50 (m) 7.63-7.75 (m)	-	2.51–2.75 (m)
H_8	7.28-7.50 (m) 7.63-7.75 (m)	-	2.51–2.75 (m)
H_9	2.52–2.68 (m)	-	-
H_{10}	2.71-2.86 (m)	-	-
$-OCH_2-$	4.55 (q)	7.2	4.48 (s, br)
$-CH_3$	1.37 (t)	7.0	1.37 (s, br)

Solvent: CD_2Cl_2

© University of Pretoria

Table 2.4 (continued). ^{1}H NMR shifts of complexes **1–3** and **14**

Assignment **Complexes**

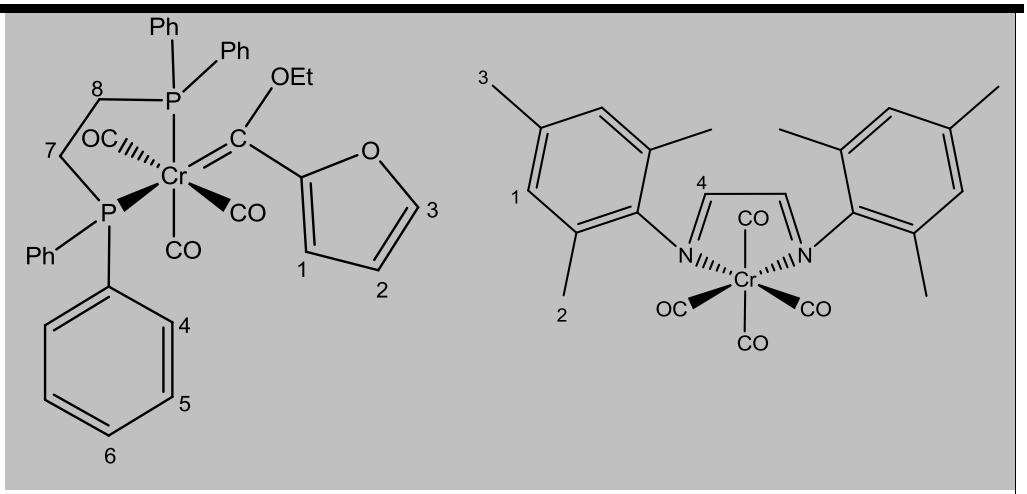

	3		**14**
Proton	**Chemical shift (δ, ppm)**	**Coupling constant (*J*, Hz)**	**Chemical shift (δ, ppm)**
H_1	7.17 (d)	3.1	6.99 (s)
H_2	6.25 (s, br)	-	2.20 (s)
H_3	7.04 (s, br)	6.5	2.33 (s)
H_4-H_6	7.10-7.40 (m) 7.50-7.68 (m)	-	8.16 (s)
H_7	2.59 (m)	-	-
H_8	2.59 (m)	-	-
$-OCH_2$	4.68 (q)	7.0	-
$-CH_3$	1.37(t)	7.1	-

Solvent : $CDCl_3$

Due to electronic constraints and the stability of the complexes in solution, the ^{1}H NMR spectra obtained for the carbenes were of low quality; in many cases the protons were identifiable but it was not possible to determine the coupling constants. The bithiophene-containing complex contains proton signals for H_3 and H_9 further downfield in comparison with H_4 due to the electronic effects of the π-resonance between the two aromatic rings, as shown in Figure 2.7.

© University of Pretoria

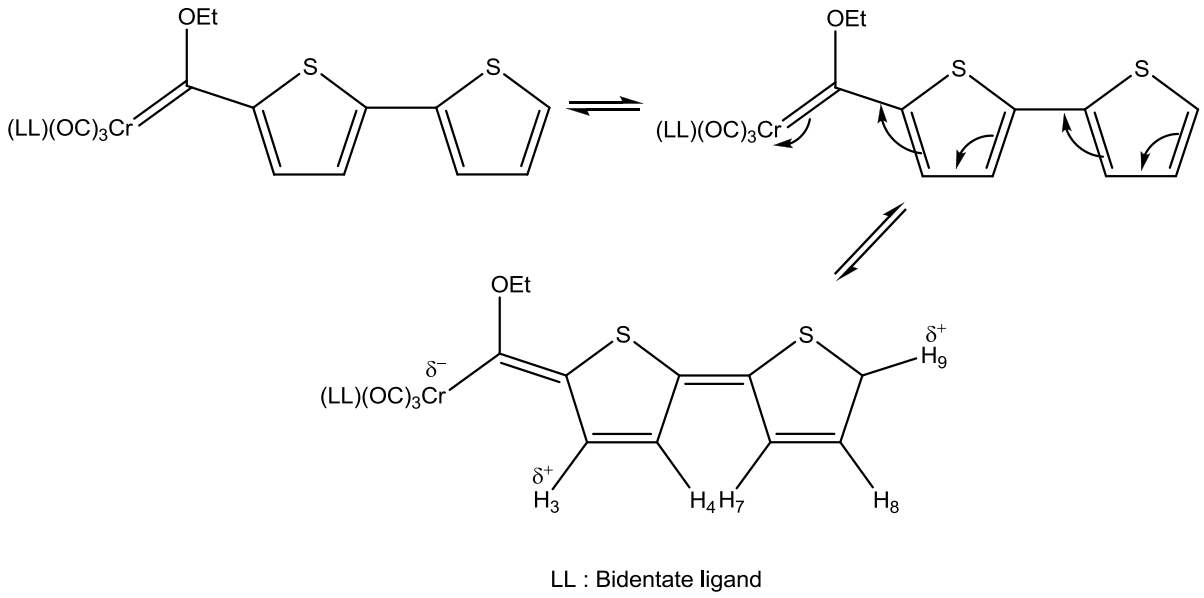

Figure 2.7. Resonance effects in bithiophene carbenes

As Figure 2.8 indicates, protons H_4, H_7 and H_8 are less affected by any delocalisation of the aromatic system, while simultaneously protons H_3 and H_9 become more deshielded and this ultimately results in a downfield shift. The electronic environment of H_3 results in a higher downfield chemical shift for this proton, since the proton is located closer to the electron-draining carbene centre. The delocalised aromatic arene system can be effectively utilised to describe the proton chemical shifts of thiophene and furan. The chemical shift of these protons compares favourably with that of an ester standard (Figure 2.8).[22]

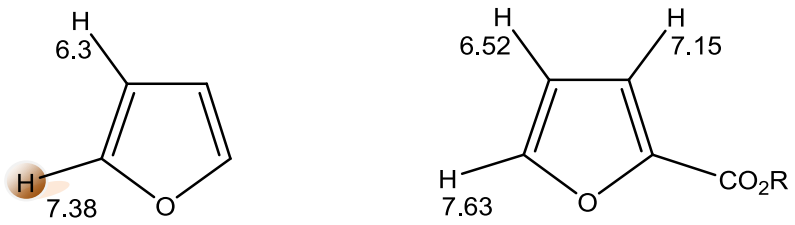

Figure 2.8. Comparison between a furan ligand and a general ester compound

Due to the oxygen atom's additional electronegativity, the encircled proton (Figure 2.8) will also bear the lowest electron density and thus experience a downfield chemical shift.

© University of Pretoria

Thiophene monocarbene complexes, in contrast, display a greater downfield shift for the proton in closer proximity to the carbene centre. On coordination of the bidentate ligands to the metal carbene systems, a general upfield shift of the arene proton systems is expected due to the additional electron support provided by these chelating ligands to the metal centre and eventually through the entire carbene system. On analysis of the NMR spectra, however, the heteroatom protons remained stationary and thus no new chemical shift was witnessed. The proton shifts of the dppe ligand unfortunately overlapped with the heteroarene proton signals and this made it practically impossible to determine shifts for all the protons accurately. The -OCH_2- proton peaks presented as a multiplet instead of the expected quartet.

Since the products had both low solubility and exceptional instability in deuterated solutions, the peaks had low intensities and were in some cases undistinguishable. H_3 of complex **1** illustrated that the presence of a carbene moiety would also influence the chemical shifts of the entire bithiophene substituent. Proton H_3 displayed a chemical shift of δ = 7.33 ppm, which is shifted more downfield in comparison with H_2 which was located at δ = 7.27 ppm. Both protons displayed a doublet since no long-distance coupling could be observed. The protons on the aromatic ring of the phosphine ligand for complexes **1**–**3** displayed multiple differently sized peaks between the regions δ = 7.17 ppm and 7.75 ppm, and the peaks corresponded to 20 protons in total. H_1 complexes **1**, **2** and **3** were shifted further downfield, in comparison to the other heteroarene protons. The proton shifts related to these highly deshielded protons are δ = 7.60 ppm, δ = 7.75 ppm and δ = 7.17 ppm, respectively. H_3 was also shifted downfield with chemical shift values of δ = 7.32 ppm, δ = 7.60 ppm and δ = 7.04 ppm, respectively, for complexes **1**-**3**.

^{13}C NMR spectroscopy

^{13}C NMR chemical shifts are well known and reported for the applied heteroarene substituents, but proved slightly elusive for the bidentate ligands utilised. Data collected with the aim of full characterisation by ^{13}C NMR spectroscopy were collected for all bidentate ligands (Table 2.6) to ensure comprehensiveness and reliable records. Characterisation of the heteroarene substituents is taken from the literature and supplied in Table 2.5.

© University of Pretoria

Table 2.5. ^{13}C NMR shifts of unligated heteroarene molecules

Mono-ring arenes

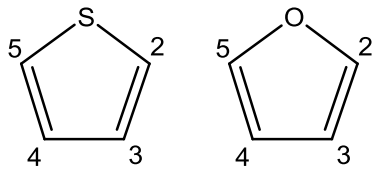

Multi-ring arenes

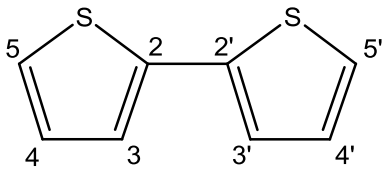

	Thiophene[30]	Furan[31]		2,2'-Bithiophene[21]
Carbon assignment	**Chemical shift (δ, ppm)**	**Chemical shift (δ, ppm)**	**Carbon assignment**	**Chemical shift (δ, ppm)**
C_2,C_5	127.6	143.0	C_2,C_2'	137.4
C_3,C_4	125.8	109.9	C_3,C_3'	123.7
-	-	-	C_4,C_4'	127.7
-	-	-	C_5,C_5'	124.3

Novel bidentate ligated chromium carbene complexes were compared with the unligated literature versions. Fischer-type carbene carbons are electrophilic in nature and thus the carbene carbon atom contains exceptionally low electron density. To remedy the electron deficiency experienced by the carbene carbon, electronic and resonance stabilisation is provided by the acyl-carbene hybrid.

The electronically deficient carbene carbon is extremely deshielded and thus occupies an upfield position comparable to that of ester carbons. The literature provides a broader range of upfield shifts that may be occupied by the carbene carbon. Carbene carbon shifts have been found to be as high as 400 ppm[35] and in other reported cases as low as 200 ppm.[36]

A hypothetical model for shifts and field positions is based on three major concerns, namely (1) the extent of electron donation from alkoxy substituent (π-dative donation), (2) metal back-donation from d-orbital electrons, and (3) the heteroarene ring producing an supplementary electron dosage. Heterocyclic electron supply to the carbene moiety decreases through the series: 2,2'-bithiophene > 2-thiophene > 2-furan. Table 2.6 provides the ^{13}C NMR shifts for the bidentate ligands utilised in this study.

[35] Fischer, E. O., Selmayr, T., Kreissl, F. R., Schubert, U., *Chem. Ber,*. 556, **1988**, 133.
[36] Anderson, B. A., Wulff, W. D., Rahm, A., *J. Am. Chem. Soc.,* 115, **1993**, 4602.

© University of Pretoria

Table 2.6. ^{13}C NMR shifts of unligated bidentate molecules

Bidentate ligands

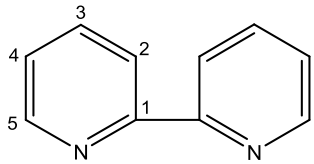

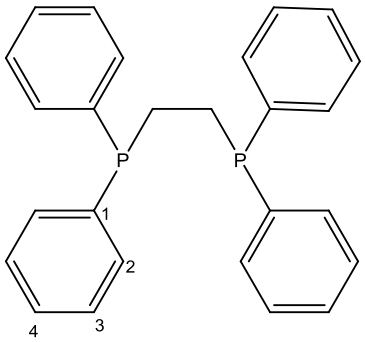

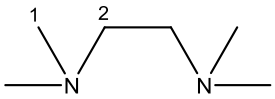

Carbon assignment	2,2-Bipyridine **Chemical shift (δ, ppm)**	Bis(diphenylphosphino) ethane **Chemical shift (δ, ppm)**	TEMED **Chemical shift (δ, ppm)**
C_1	156.1	138.1	45.8
C_2	121.0	132.7	57.7
C_3	136.9	128.4	-
C_4	123.7	128.7	-
C_5	149.2	-	-

Solvent : $CDCl_3$

Bidentate ligands

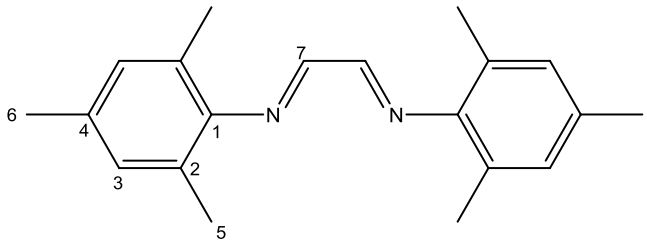

Carbon assignment	(Z)-N',N',N'',N''-tetramesitylethene-1,2-diamine[33] **Chemical shift (δ, ppm)**
C_1	148.2
C_2	129.4
C_3	126.7
C_4	134.1

© University of Pretoria

Table 2.6 (continued). ^{13}C NMR shifts of unligated bidentate molecules

Carbon assignment	Chemical shift (δ, ppm)
C_5	18.3
C_6	20.8
C_7	163.6

Monocarbene pentacarbonyl chromium(0) complexes of thiophene, furan and bithiophene were prepared prior to the substitution of carbonyl ligands for bidentate ligands. ^{13}C NMR data reported the chromium pentacarbonyl carbene carbon peaks at a chemical shift of δ = 316.42 ppm, 310.90 ppm and 312.16 ppm for thiophene, furan and bithiophene carbene complexes, respectively. The heteroarene carbon atom flanking the carbene carbon indicated chemical shifts of δ = 155 ppm (thiophene), δ = 164.06 ppm (furan) and δ = 167.94 ppm (bithiophene).

Literature values exist for compounds with structures similar to the complexes synthesised in this study. Barluenga *et al.*[24] allocated the chemical shifts of the three carbonyl ligands coordinated to a phosphine bidentate-containing carbene complex (meridonial) at 217.6 ppm (dd, $J_{C\text{-}P}$ = 20.7, 17.4 Hz), 218.7 ppm (dd, $J_{C\text{-}P}$ = 22.3, 15.8 Hz) and 220.5 ppm (d, $J_{C\text{-}P}$ = 22.9 Hz). The carbene carbon shift was found to be exceptionally downfield and seen at δ = 352.2 ppm.

Arrieta *et al*[37] reported characterisation data of a *fac* isomer of the dppe coordinated carbene complex. Carbon chemical shifts of the two carbonyl ligands were assigned at 235.2 ppm (t, $J_{C\text{-}P}$ = 5.6 Hz) and 235.6 ppm (t, $J_{C\text{-}P}$ = 5.5 Hz), while the carbene carbon atom signal was observed at δ = 354.4 ppm. The values of both the carbon chemical shift for the carbene carbon and that for the carbonyl ligand are similar to those obtained in this study.

Literature provide C-P coupling values for all carbonyl ligands as well as for the carbene carbon. C-P couplings produced multiplets for both carbonyl ligands as well as for the carbene carbon, whereas normally only singlet peaks are observed.

Table 2.7 provides the ^{13}C chemical shifts for complexes **1, 2, 3** and **14**.

[37] Arrieta, A., Cossío, F. P., Fernández, I., Gómez-Gallego, M., Lecea, B., Mancheño, M. J., Sierra, M. A., *J. Am. Chem. Soc.* **2000**, 122, 11509–11510.

© University of Pretoria

Table 2.7. ^{13}C NMR shifts of complexes **1–3** and **14**

Assignment	**Complexes**	
	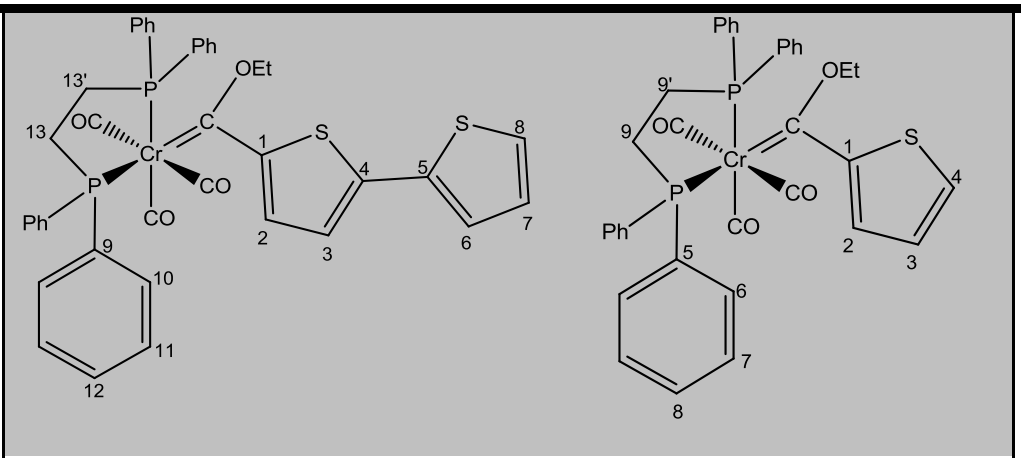	
	1	**2**
Carbon	**Chemical shift (δ, ppm)**	**Chemical shift (δ, ppm)**
Carbene	312.6	315.8
C_1	162.1	157.3
C_2	144.1	144.6
C_3	125.2	125.5
C_4	149.8	141.8
C_5	144.0	138.0
C_6	127.9	132.7
C_7	128.1	130.8
C_8	126.0	131.6
C_9, C_9'	138.0	29.7, 27.7
C_{10}	132.7	-
C_{11}	129.7	-
C_{12}	131.4	-
C_{13}, C_{13}'	35.7, 28.1	-
CO (*1*)	220.1	225.3
CO (*2*)	225.6	227.0
CO (3)	235.4	235.0
$-OCH_2-$	72.2	72.2
$-CH_3$	15.4	15.4

Solvent: $CDCl_3$, CO (1) & CO (2) *trans* to each other, CO (3) *trans* to phosphine

© University of Pretoria

Table 2.7 (continued). ^{13}C NMR shifts of complexes **1–3** and **14**

Assignment	**Complex**	
	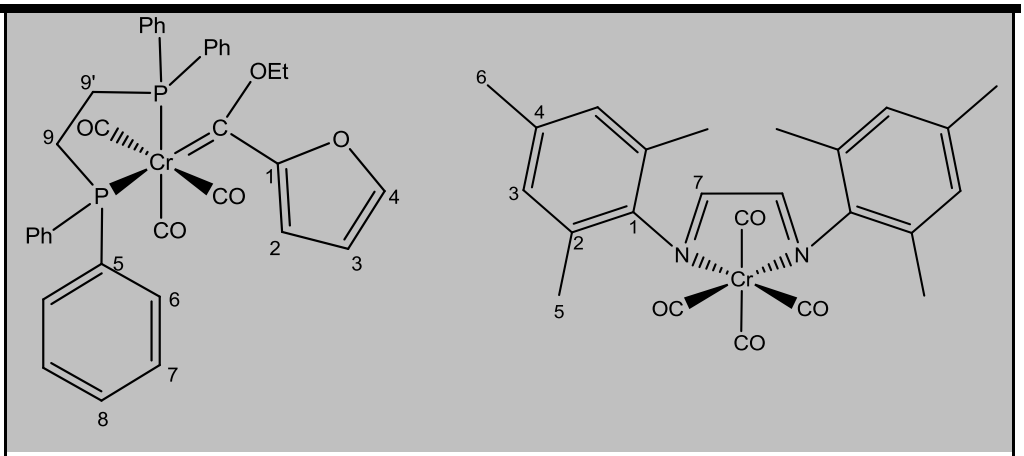	
	3	**14**
Carbon	**Chemical shift (δ, ppm)**	**Chemical shift (δ, ppm)**
Carbene	316.3	-
C_1	164.3	151.4
C_2	112.5	135.7
C_3	111.8	129.3
C_4	146.1	128.1
C_5	138.7	20.8
C_6	132.7	18.2
C_7	130.6	158.9
C_8	131.3	-
C_9/C_9'	30.7, 28.4	-
CO (*1*)	220.1	213.6
CO (*2*)	225.6	224.3
CO (*3*)	235.8	-
$-OCH_2-$	73.7	-
$-CH_3$	15.6	-

Solvent : $CDCl_3$, CO (1) & CO (2) *trans* to each other, CO (3) *trans* to phosphine

A comparison between the pentacarbonyl carbene complex (**E**-**G**) and the bidentate ligated tricarbonyl complex (**1-3**) displays similar chemical shifts. The carbene carbon shifts of **1**, **2** and **3** are 312.50, 315.71 and 310.86 ppm, respectively, which is similar to the shifts of the unsubstituted monocarbene complexes. Three carbonyl shifts are visible on the ^{13}C NMR spectra. The carbonyl ligands *trans* to each other is shifted upfield since they have similar

© University of Pretoria

electron densities, whilst the carbonyl *trans* to a phosphine ligand is shifted more downfield. The *cis* carbonyl ligand is shifted slightly more upfield and is positioned *trans* to the phosphine atom. The substituents on the carbene carbon atom appear to have limited influence on the carbonyl ligands, while the metal carbene seems to be particularly sensitive to changes in the electronic environment.[38] The heteroarene carbons are shifted in accordance with their proximity to the carbene carbon and their position in the extended delocalised system. C_1 occupies the most downfield-shifted position since the atom is located directly next to the carbene carbon atom. The shift for C_1 in complexes **1–3** are δ = 164.9, 157.2 and 164.3 ppm, respectively. Delocalisation of the aromatic system leaves C_4 deshielded and the atom tends to have an unexpectedly upfield shift.

^{31}P NMR spectroscopy

^{31}P NMR spectroscopy was recorded for complexes **1-3** and the chemical shifts reported in Table 2.8.

Table 2.8. ^{31}P NMR shifts of complexes **1–3**

Complex	P_1 Chemical shift (δ, ppm)	P_2 Chemical shift (δ, ppm)
1	84.1	79.1
2	84.2	79.2
3	83.4	78.6

Solvent : $CDCl_3$

Two distinct chemical shifts are observed which corresponds to P_1 (*trans* to the carbene) and P_2 (*trans* to a carbonyl). P_1 is observed further downfield due to the electron withdrawing ability of the carbene centre, leaving the P-atom more deshielded whilst P_2 is slightly more upfield and competing for electron density with a carbonyl ligand. Both phosphine and carbonyl ligands have π-accepting ability, however, the carbonyl ligand is more favoured in terms of back-donation of electron density from the metal.

[38] Mann, B. E., *Adv. Organomet. Chem.,* **1974**, 12, 135.

© University of Pretoria

2.3.2 Infrared spectroscopy

IR spectroscopy has been employed in this study for characterisation of all the novel complexes. Utilising carbonyl stretching frequencies, data on the quantity and position of carbonyl ligands were obtained. Literature values indicated an IR stretching frequency of 2143 cm^{-1} for free carbonyl groups, while a range between 1850 and 2120 cm^{-1} is expected for terminal ligated carbonyl ligands.[39] Carbonyl ligands have stretching frequencies between the C-O bonds, independent of the other vibrating activities of ligands coordinated at a different spatial location. There is a direct correlation between CO stretching vibrational frequencies and the M-C bond order.[34] Increases in the stretching frequency normally mirror an increase in the M-C bond order, with the bond becoming more 'double bond-like' in character. Consideration of the extent of metal→carbonyl back-bonding is of crucial importance. As the degree of back-bonding from the metal to the ligand increases, the M-C bond strength increases and the bond length shortens. The corresponding effect on the C-O bond is evidenced in a higher frequency of vibration, longer bond length and lower bond order, as shown in Figure 2.9. Carbene fragments, phosphine ligands, and ammine and amine ligands either have no π-accepting ability or are weaker π-acceptors than the classic carbonyl ligand, and thus coordination of these groups to metals will in effect increase the M-C bond strength. As electron density shifts to the carbonyl groups and the M-C bond order increases, an IR shift to lower wavenumbers is evident.[32] All synthesised complexes in this study illustrated this effect clearly. Hexacarbonyl chromium shows a carbonyl stretching frequency of 2000 cm^{-1}. The intensities and the number of these vibrations are dependent on the amount and the local symmetry of the ligands around the central atom. In accordance with the method of local symmetry,[40] a monocarbene complex of the type $M(CO)_5L$ belongs to the symmetry C_{4v}, corresponding to only four vibrations, namely $A_1^{(1)}$, $A_1^{(2)}$, B_1 and E. Figure 2.10 demonstrates that only two vibrational frequency bands are IR active, corresponding to the E and $A_1^{(2)}$ bands. A possibility arises, however, for band $A_1^{(1)}$ to become IR active due to coupling to the $A_1^{(2)}$ vibrational mode.[32]

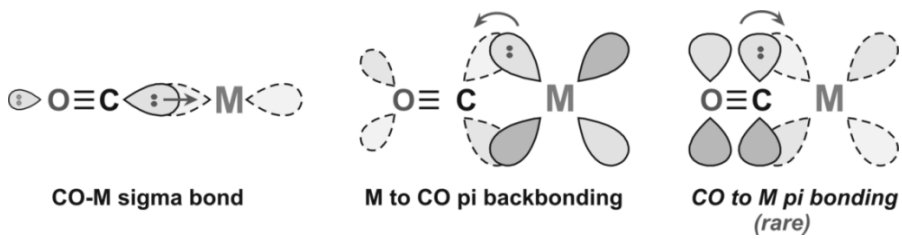

Figure 2.9. Bonding interactions between metal and carbonyl ligand

[39] Braterman, P. S., *Metal Carbonyl Spectra*, Academic Press, London, **1975**.
[40] Haines, L. M., Stiddard, M. H. B., *Adv. Inorg. Chem. Radiochem.*, **1969**, 12, 53.

© University of Pretoria

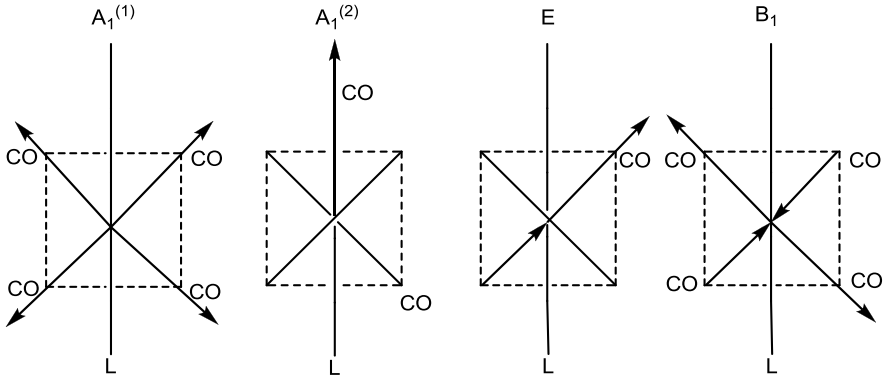

Figure 2.10. Possible IR stretching vibrational modes of $M(CO)_5L$ complexes

From all possible vibration modes it should be clear that the $A_1^{(2)}$ and E band should produce the most prominent peaks on the IR spectrum of $ML(CO)_5$. The $A_1^{(2)}$ is often seen as a contour peak on the higher-frequency side of the E band when a good π-acceptor group ligates to the metal atom or on the lower-frequency side (left of E) when weaker π-acceptor ligands are coordinated.[21] The formation of complexes with fewer carbonyl ligands also produces fewer possible vibrational modes. Further functionalisation of complexes $M(CO)_5L$ through the substitution of two CO ligands gives rise to only two vibrational modes and two visibly active IR bands if the substituting ligands are identical (Figure 2.11). Absolute C_1 symmetry, however, where no symmetry is observed, produces three distinct vibrational modes corresponding to $M(CO)_3L'L''L'''$.

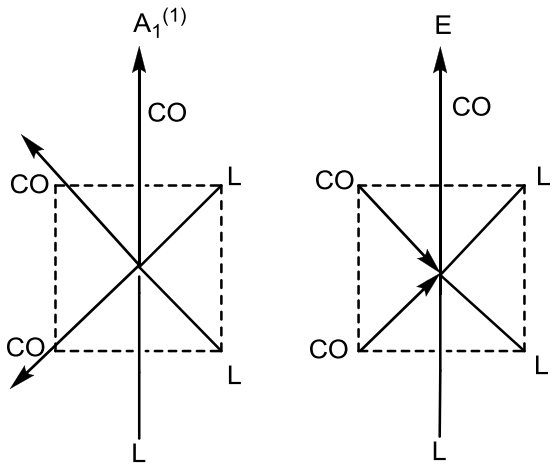

Figure 2.11. Possible IR stretching vibrational moles of $M(CO)_3LLL$ complexes

IR spectroscopy data was obtained for all complexes (**1–3** and **14**). The vibration bands and the intensities are listed in Table 2.9.

© University of Pretoria

Table 2.9. IR data for complexes **1–3** and **14**

Complex	Carbonyl stretching frequencies (ν_{CO}, cm^{-1})			
	$A_1^{(1)}$	$A_1^{(2)}$	B_1	B_2
1	2005 (w)	1850 (s)	1860 (s)	-
2	2005 (w)	1840 (s)	1862 (s)	-
3	2007 (w)	1837 (s)	1863 (s)	-
14	2001 (s)	1902 (s)	1916 (s)	1866 (s)

Complexes **1–3** displayed three distinct IR-active bands. Since no symmetry was observed for the molecular structures, all three remaining carbonyl ligands were in a different chemical environment. Computational studies also confirmed three vibrational modes expected for the complexes with the general formula $Cr(CO)_3L'L''L'''$, (Chapter 6).

Arrieta *et al.*[37] reported three IR-active regions at 1919, 1840 and 1815 cm^{-1} for the isomeric product *fac*-[(ethoxy)(methyl)carbene](1,2-bis(diphenylphosphino)ethane)] (tricarbonyl)-chromium(0). Although the research group produced the *fac* isomer, the IR bands correspond adequately to the *mer* isomeric structure. IR was reported in solid state as a KBr pellet.

Barluenga *et al.*[24] also reported three IR-active bands at 1982, 1961 and 1919 cm^{-1} for a meridonial bidentate phosphine coordinated phenyl carbene complex. Two other meridonial structures containing different carbene substituents were also reported. IR vibrations were witnessed at 2013, 1961 and 1902 cm^{-1} for a carbene complex containing a methyl substituent and at 2004, 1950 and 1896 cm^{-1} for a (*E*)-(CH=CH-2-furyl) substituted complex. Infrared studies were reported in THF.

Complex **14** displayed four active IR bands corresponding to the $A_1^{(1)}A_1^{(2)}$, B_1 and B_2 bands. These IR-active bands typically have similar intensities and frequencies which might cause the $A_1^{(2)}$ and B_1 bands to overlap, producing only three distinguishable bands. Complex **14** displays a similar splitting pattern to that published by Ruminiski *et al.*,[41] which reported four individual bands at 2008, 1906, 1889 and 1825 cm^{-1} for a $Cr(CO)_4$dpp complex (dpp = 2,3-bis(2-pyridyl)pyrazine).

[41] Ruminski, R. R., Wallace, I., *Polyhedron*.,**1987**, 8, 1673–1676.

© University of Pretoria

2.3.3 X-ray crystallography

Single-crystal X-ray diffraction data confirmed the molecular structure of complexes **F**, **1**, **2**, **3** and **14**. X-ray diffraction served as an additional characterisation tool to aid in determining the discrete structures of these complexes and was utilised in conjunction with NMR and IR spectroscopy. The X-ray structure confirmed the presence of bidentate ligated monocarbene complexes bearing only three carbonyl ligands. Complex **14** contained four carbonyl ligands in addition to the chelate. All single crystals were obtained from dichloromethane:hexane and yielded brown crystals for complexes **1**, **2** and **3**. Complex **14** produced blue crystals whist complex **F** produced red-orange crystals.

Figures 2.12, 2.14, 2.16, 2.17 and 2.20 show the ORTEP[42] + POV-Ray[43] plots of these molecules and Figure 2.13 indicates the packing structure of complex **1**. Complexes **1, 2, 3** and **14** all crystallised in the monoclinic crystal system with space group P2(1)/n for **1–3** and *Cc* for complex **14**. Complex **1** contained two definable units in a single unit cell, while complex **2** had four units per cell. Ligation of the bidentate ligand occurs *trans* to the carbene carbon atom and produces the meridonial isomer. For both the thiophene carbene and bithiophene carbene complexes, the sulfur atom of the aromatic rings orientates itself to occupy a space in the same region as the oxygen of the ethoxy substituent (*syn)*, with the furan in an *anti* conformation.

The bithiophene heterorings in complex **1** have a torsion angle of about 180° between the two sulfur atoms. The complex crystallised with dichloromethane units between individual carbene molecules. The $C_{carbene}$-M bond length for complexes **1** and **2** are 1.968(5) Å and 1.9902 Å, respectively. Significant bond lengths and angles for the complexes are presented in Tables 2.10 to 2.12, while the complete crystallographic data on complexes **1**, **2**, **3** and **14** are contained in Appendices A, B, C and D, respectively. Complex **14** was obtained as the major product in the synthesis of a nitrogen-based bidentate carbene complex and contained four carbonyl ligands after the substitution of the carbene moiety, instead of two carbonyl ligands.

The average carbonyl bond length for complexes **1**-**3** were determined to be 1.8687 Å, 1.8709 Å and 1.8677 Å, respectively, and in chapter 6 compared to computed models.

[42] Farrugia, L. J., *J. Appl. Crystallogr.,* **1997**, 30, 565.
[43] The POV-Ray Term, POV-Ray, **2004**, URL: http://www.povray.org/download/

© University of Pretoria

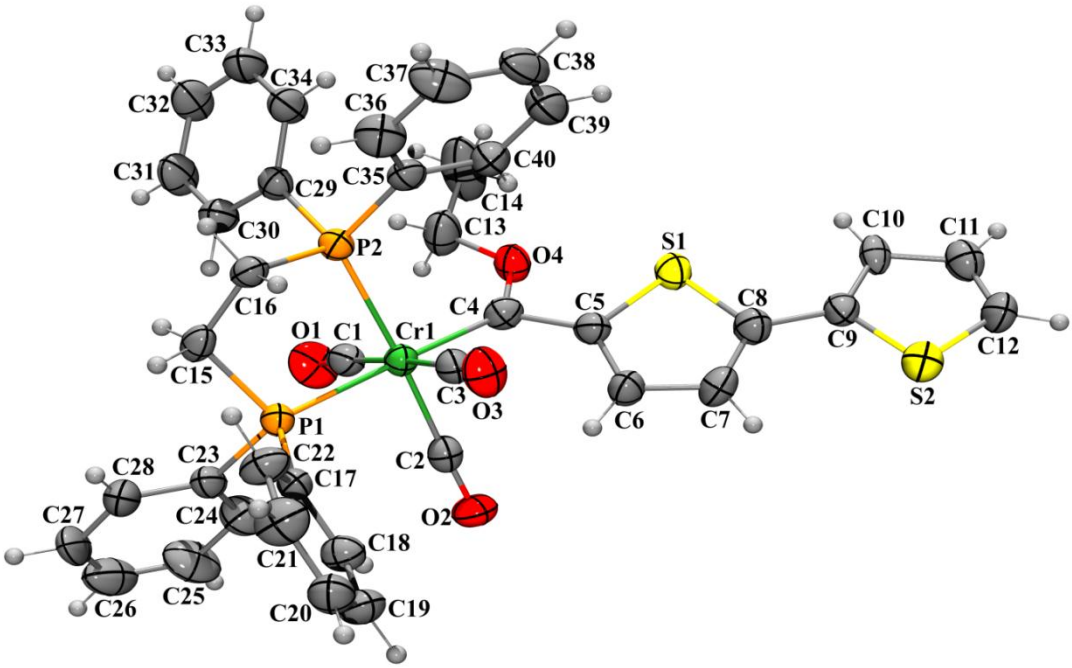

Figure 2.12. ORTEP + POV-Ray plot of the structure of **1**

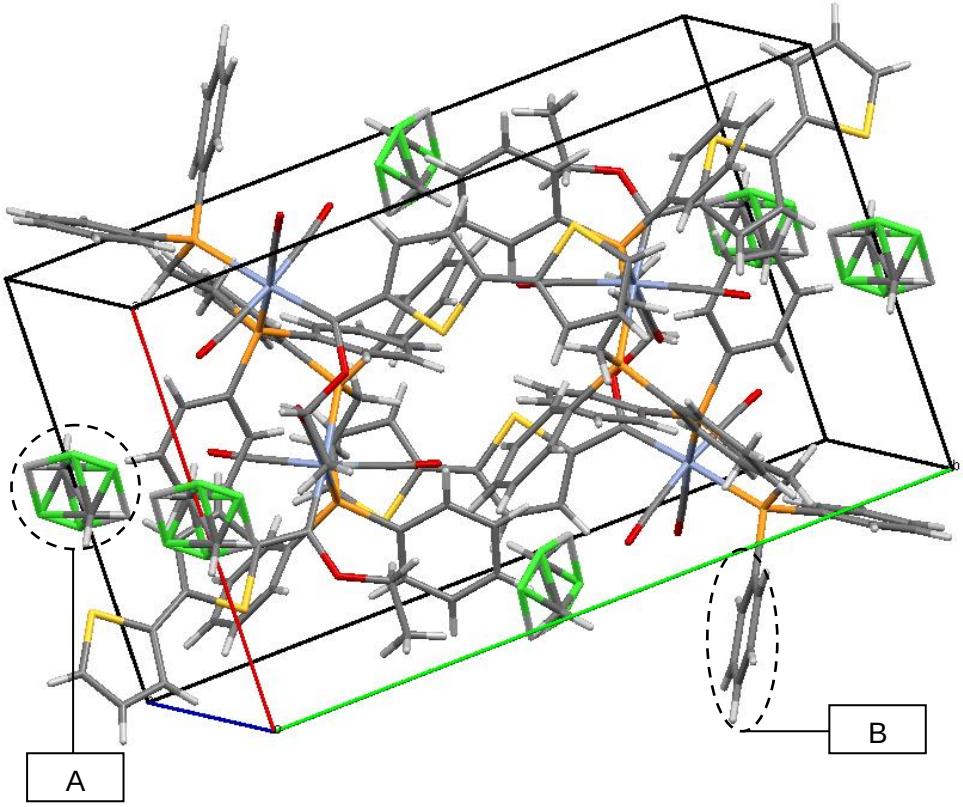

Figure 2.13. Packing structure of **1**

© University of Pretoria

As previously indicated, the packing structure of complex **1** contained molecules of dichloromethane (A) packed between individual molecules of the monocarbene complex. The contaminant fills pores not occupied by the complex itself and upon evaporation leaves tiny craters within the crystal structure. Due to symmetry, the dichloromethane can orientate itself in two directions and thus appears as dimers within the packing structure. Since complex **1** was exceptionally bulky, the entire unit cell could hold only two molecules per cell and thus portions of the molecules can be seen projecting into neighbouring cells (B).

Table 2.10. Selected bond lengths and angles for **1**

Bond	Bond length (Å)	Bond	Bond length (Å)
Cr(1)-C(4)	1.968(5)	S(1)-C(8)	1.727(6)
Cr(1)-C(3)	1.883(6)	C(8)-C(9)	1.443(8)
Cr(1)-P(1)	2.3537(15)	C(6)-C(7)	1.424(8)
Cr(1)-P(2)	2.3831(16)	C(9)-C(10)	1.426(8)
C(4)-C(5)	1.476(8)	C(11)-C(12)	1.341(9)
C(4)-O(4)	1.378(6)	C(10)-C(11)	1.424(8)
C(5)-C(6)	1.370(8)	C(9)-S(2)	1.714(6)
C(7)-C(8)	1.366(8)	S(2)-C(12)	1.709(6)
C(5)-S(1)	1.746(5)	C(15)-C(16)	1.523(8)
Angle	**Bond angle (°)**	**Angle**	**Bond angle (°)**
C(2)-Cr-C(4)	89.3(2)	C(9)-S(2)-C(12)	92.2(3)
P(1)-Cr-P(2)	83.44(5)	P(1)-C(15)-C(16)	109.8(4)
O(4)-C(4)-C(5)	103.0(4)	P(2)-C(16)-C(15)	110.3(3)
C(5)-S(1)-C(8)	92.9(3)		

Complex **1** had an average carbonyl bond length of 1.8687 Å and an average metal-phosphine bond length of 2.3684 Å.

© University of Pretoria

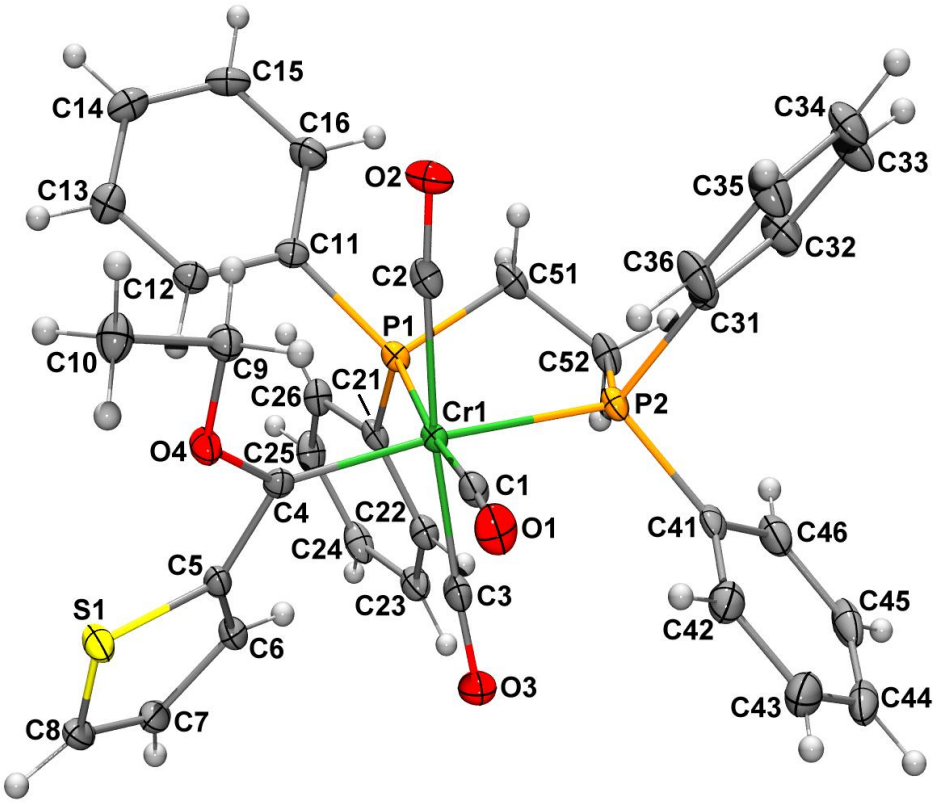

Figure 2.14. ORTEP + POV-Ray plot of **2**

The C(5)-C(6), C(6)-C(7), C(7)-C(8), C(5)-S(1) and C(8)-S(1) bond lengths of **2** measured 1.385(2) Å, 1.424(2) Å, 1.355(3) Å, 1.7456(17) Å and 1.7044(17) Å, respectively. The torsion angles, S(1)-C(5)-C(6)-C(7) and C(6)-C(7)-C(8)-S(1) have values of 0.20(18)° and 1.12(19)°, indicating a planar heteroarene ring, as expected from the aromaticity of the ring. A torsion angle of 158.26(9)° for Cr(1)-C(4)-C(5)-S(1) indicates that the heteroarene is rotated slightly out of the plane in which the metal is capsulated. All complexes show a close resemblance to the typical octahedral with some distortion, as shown by complex **2**. The angle C(1)-Cr(1)-C(4) is defined as 111.01(14)°, which deviates from the expected 90°. The unit cell also contains four distinct molecules per unit cell. Table 2.10 summarises selected bond lengths and angles.

Complex **2** had an average carbonyl bond length of 1.8709 Å and an average metal-phosphine bond length of 2.373 Å. Both average bond lengths are comparable to **1** and indicate a structural similarity between the two complexes.

© University of Pretoria

Table 2.11. Selected bond lengths and angles of **2**

Bond	Bond length (Å)	Angle	Bond angle (°)
Cr(1)-P(1)	2.3777(5)	C(3)-Cr(1)-P(1)	100.75(5)
Cr(1)-P(2)	2.3692(5)	P(1)-Cr(1)-P(2)	82.991(17)
Cr(1)-C(3)	1.8835(17)	C(8)-S(1)-C(5)	92.06(8)
C(4)-C(5)	1.478(2)	C(4)-Cr(1)-P(2)	174.27(5)
C(5)-C(6)	1.385(2)	C(5)-C(4)-O(4)	102.33(13)
C(6)-C(7)	1.424(2)	C(3)-Cr(1)-C(1)	85.44(7)
C(7)-C(8)	1.355(3)		
C(1)-O(1)	1.158(2)		
Cr(1)-C(4)	1.9902(16)		
S(1)-C(5)	1.7456(17)		
S(1)-C(8)	1.7044(17)		

Complex **3** contained a carbene bond length similar to that of **1** and **2**. The $C_{carbene}$-M length was measured to be 1.9944(17) Å, while the average carbonyl bond length was calculated as 1.8677 Å. The complex also displayed a similar bonding pattern to that of the other chelated carbene complexes, with one phosphine atom of the bidentate ligand coordinating adjacent to the carbene carbon atom. Three carbonyl ligands were present and the meridonial structural isomer was clearly favoured. The carbene substituents can arrange themselves into two orientations namely the *syn* and the *anti* orientations. The orientation is dependent on the position of both substituents (Figure 2.15). The oxygen atom of the furan ring orientated itself on the same side as the ethoxy carbene substituent, which proves to be an anomaly as it was expected to arrange in the *anti* position.[44] The torsion angles O(5)-C(5)-C(6)-C(7) and C(6)-C(7)-C(8)-O(5) have values of -0.3(2)° and 0.2(2)°, respectively, indicating that the heteroarene ring is planar.

[44] Landman, M., Unpublished results.

© University of Pretoria

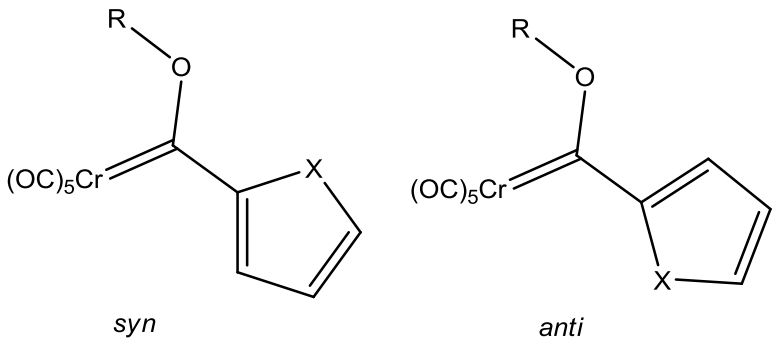

X = S, O
R = alkyl

Figure 2.15. *Syn* and *anti* orientations of the carbene substituents

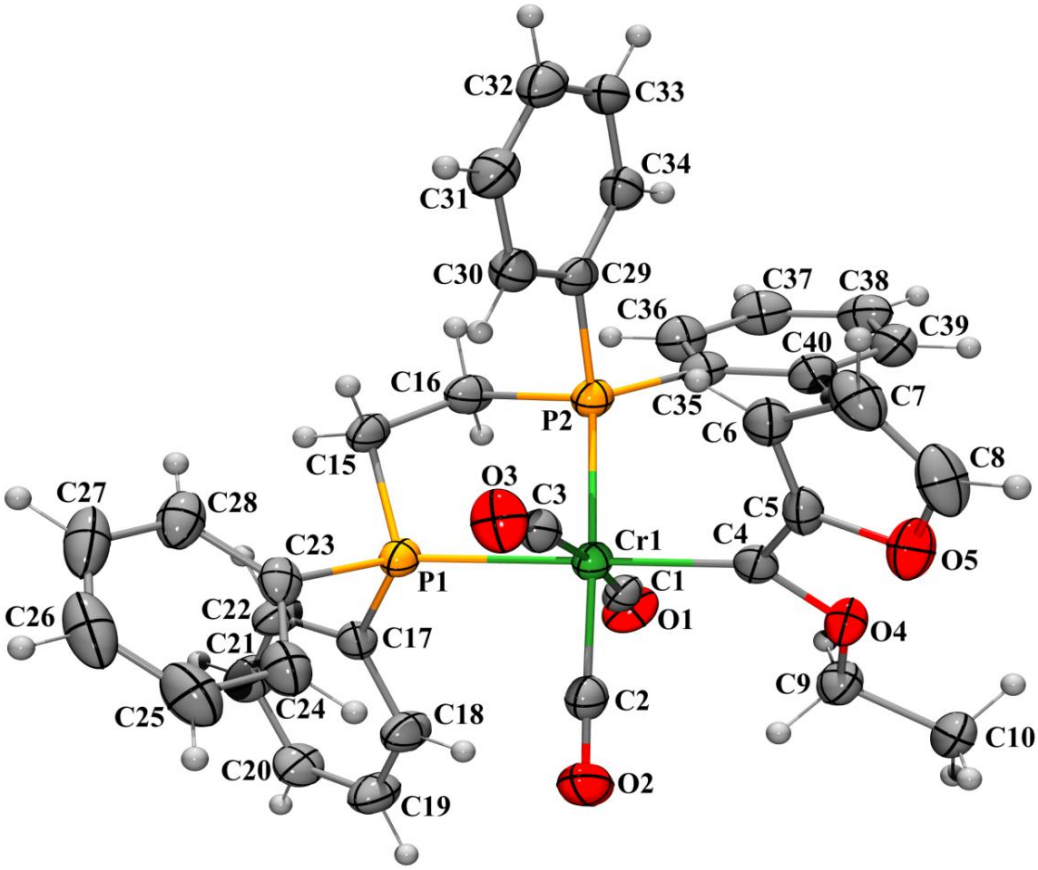

Figure 2.16. ORTEP + POV-Ray plot of **3**

© University of Pretoria

Table 2.12. Selected bond lengths and angles for **3**

Bond	Bond length (Å)	Angle	Bond angle (°)
Cr(1)-P(1)	2.3553(5)	C(3)-Cr(1)-P(1)	85.69(5)
Cr(1)-P(2)	2.3781(5)	P(1)-Cr(1)-P(2)	83.384(18)
Cr(1)-C(3)	1.8815(19)	C(8)-O(5)-C(5)	106.44(16)
C(4)-C(5)	1.467(2)	C(4)-Cr(1)-P(2)	98.62(5)
C(5)-C(6)	1.357(3)	C(5)-C(4)-O(4)	103.33(14)
C(6)-C(7)	1.425(3)	C(3)-Cr(1)-C(1)	172.68(8)
C(7)-C(8)	1.328(3)		
C(1)-O(1)	1.1549(19)		
Cr(1)-C(4)	1.9944(17)		
O(5)-C(5)	1.393(2)		
O(5)-C(8)	1.357(2)		

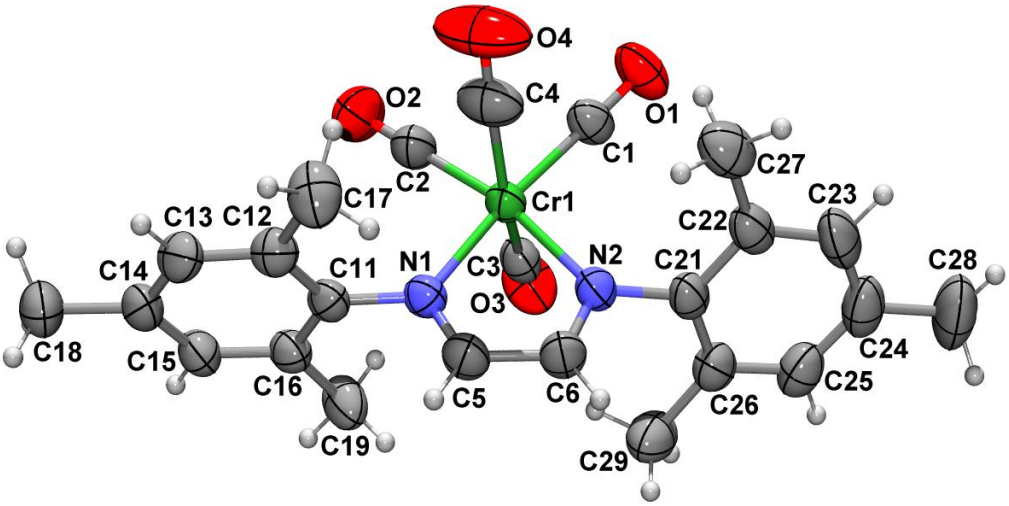

Figure 2.17. ORTEP + POV-Ray plot of **14**

Complex **14** was obtained as the major product of the bidentate-containing carbene synthetic methodology. The crystal structure revealed a tetracarbonyl coordinated complex without the carbene moiety. The average carbonyl bond length of the complex (C-O) was calculated as 1.1435 Å, with Cr-N lengths of 2.0737(18) Å and 2.0764(17) Å. The coordination of the bidentate ligand produced a bite angle of 75.84(7)°, illustrating the slight distortion in the structure from a perfect octahedral complex. Complex **14** crystallised in the *Cc* space group. All crystallographic data for complex **14** are summarised in Appendix D.

© University of Pretoria

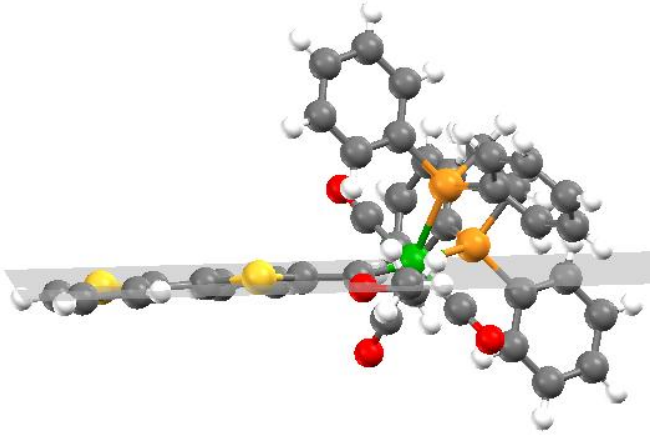

Complex 1

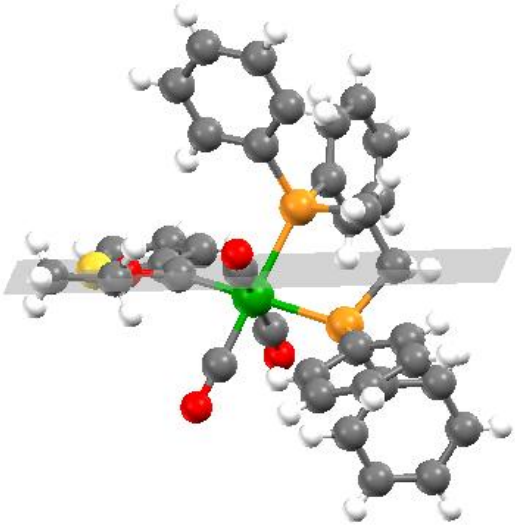

Complex 2

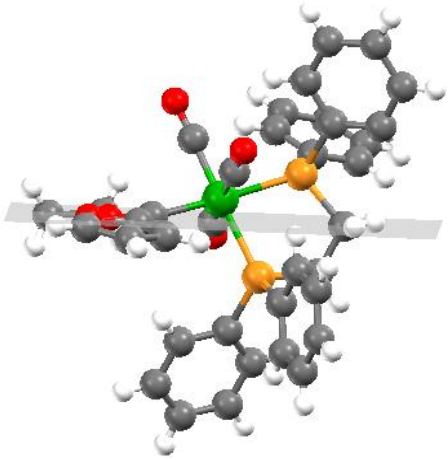

Complex 3

Figure 2.18. Plane dissection of the heteroarene

© University of Pretoria

Figure 2.18 shows a dissecting plane through the heteroarene of complexes **1–3**. The aspect to note is that in all three complexes the ethoxy and the heteroarene ring, both carbene substituents, lie in the same plane with respect to one another. It is clear from Figure 2.20 that both rings of bithiophene form a planar moiety with the sulfur atoms occupying the 'anti' geometry with respect to one another with a torsion angle of about 180°. Complexes **1–3** have numerous structural similarities between the molecules. The complexes crystallised with both carbene substituents in the same plane as the carbene carbon and the bidentate ligand coordinated in such a fashion as to produce the meridonial isomer. In comparison with literature complexes of similar structures, the most obvious feature to note is that the published studies indicate that the formation of the facial isomer is preferred above the meridonial structure obtained in this study. The study by Reinheimer *et al.*[24] produced numerous chromium carbene complexes containing phosphine bidentate ligands, all favouring the facial isomer. Barluenga *et al.*[23] produced meridonial methoxy chromium carbene complexes containing fluorinated phosphine bidentate ligands in aim of synthesising enantiomerically pure Fischer carbene complexes. Multiple carbene substituents were used in the study and the meridonial methoxyphenyl carbene isomer was obtained in a high yield; the structure is comparable to the complexes synthesised in this study (Figure 2.19). A similar methoxyphenyl carbene of molybdenum was also reported by Barluenga with a 90% yield of the facial isomer. Arrieta *et al.*[36] reported facial isomers of methoxy chromium carbene complexes containing bidentate phosphine ligands, also using dppe as bidentate ligand.

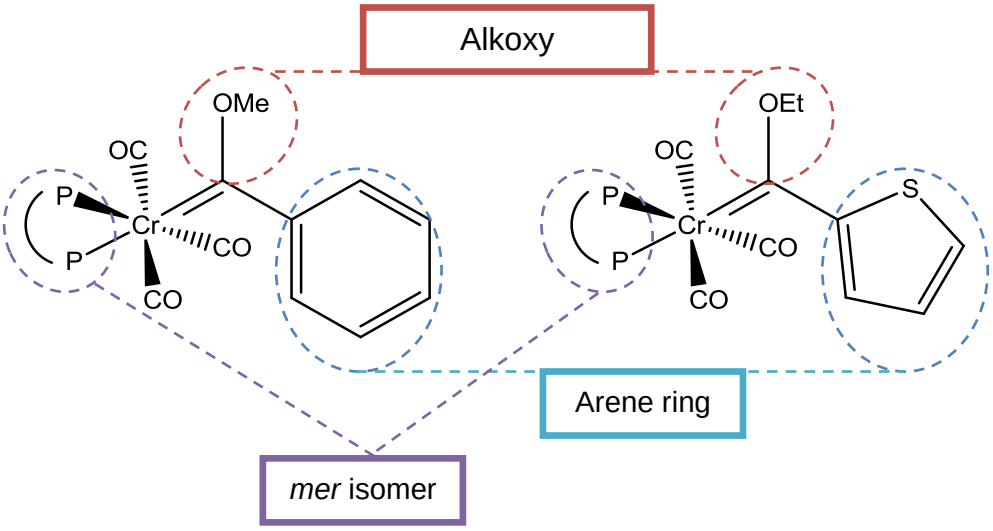

Figure 2.19. Structural similarities between Barluenga's methoxy carbene and complex **2**

© University of Pretoria

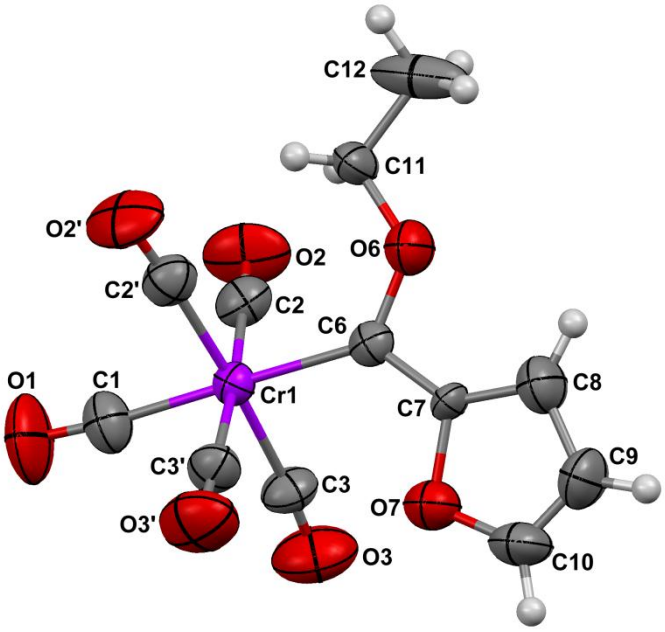

Figure 2.20. Crystal structure of complex **F**

The crystal structure of the starting carbene complex **F** was also afforded in this study and the crystal structure presented in Figure 2.20. The crystal structure presented with some disorder at C12 due to rotation around this carbon atom. The crystal structure clearly depicts the *anti* conformation expected by the by the furan carbene as well as a completely staggered conformation, as illustrated in Figure 2.21. Complex **F** crystallised in the orthorhombic crystal system with four units per unit cell. The complete crystallographic data is presented in appendix J.

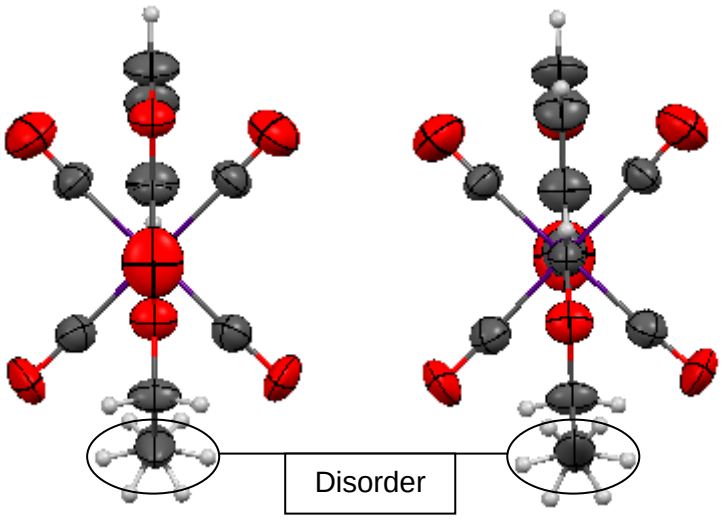

Figure 2.21. The staggered conformation of complex **F** (front and back)

© University of Pretoria

2.3.4 Mass spectrometry

Mass spectrometry analyses were done for complexes **1–3** and the results obtained are reported in Table 2.13.

Table 2.13. Mass spectrometry fragmentation of complexes **1–3**

Fragment	1	2	3
	m/z	**m/z**	**m/z**
M^+	758	676	660
-(CO)	732	649	632
-2(CO)	704	618	602
-3(CO)	674	592	576
-3(CO), OEt	658	547	531
-3(CO), S	466	466	466
-3(CO), L	450	450	450

L = carbene moiety; S = carbene heteroarene substituents

A molecular ion (M^+) peak was observed for all complexes but the fragmentation pattern indicating subsequent loss of carbonyl ligands followed by the loss of the ethoxy/methoxy or amino substituent did not prove consistent, as reported by Landman (2000).[45] Complexes underwent consecutive loss of the three remaining carbonyl ligands followed by the carbene substituents and lastly by the carbene carbon itself. The remaining fragment consists of the metal centre with atleast one of the chelating phosphorous atoms coordinated to the metal. It might also indicate that the chelate moiety remains intacted after fragmentation. This serves as a clear indication of the strength of the bidentate phosphine ligand. A key aspect of the bonding model applied in coordination complexes is that the chelate effect is one of the most important enthalpy principles. The chelate effect may thus be a possible explanation for the survival of the bidentate ligand coordinated to the metal centre after the fragmentation.

[45]Landman, M., *Synthesis of metal complexes with thiophene ligands,* PhD thesis, **2000**, University of Pretoria, Pretoria.

© University of Pretoria

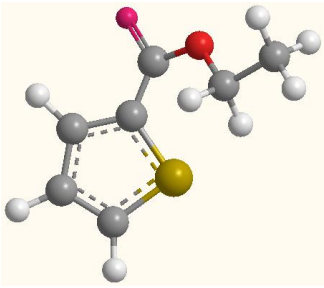

3 Evolution of Monocarbenes: Aminolysis

3.1 Background

Modification of Fischer carbene complexes via nucleophilic substitution at the alkoxy group is well known in the literature. In 1967 Helling and co-workers managed to produce two new chromium carbene complexes by substituting the methoxy substituent from a methylmethoxy pentacarbonyl chromium carbene firstly through reaction with an amine group or with a thiophenol moiety. Figure 3.1 illustrates the structures synthesised by the Helling group.[1]

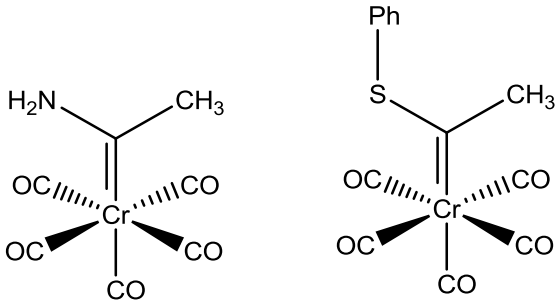

Figure 3.1. Structures of the modified Fischer pentacarbonyl chromium(0) carbene complexes

In the reaction of the Fischer carbene with gaseous ammonia, an immediate colour change was observed.

[1]Helling, J. F., Rennison, S. C., Merijan, A., *J. Am. Chem. Soc.,* **1967**, 89, 26.

© University of Pretoria

The classic bright red colour corresponding to the alkoxy Fischer carbene complex was spontaneously transformed into a yellow-orange coloured complex and upon removal of the solvent, yellow crystals were obtained.[1] The pioneering work of Fischer on the reaction of primary and secondary amines utilising alkynyl alkoxy metal carbenes[2] demonstrated significant chemical effects. The study explored kinetic versus thermodynamic control, as well as the addition of steric and electronic properties in the regiochemistry and stereochemistry (1-substitution vs. 3-addition) of the products obtained (Scheme 3.1).[3]

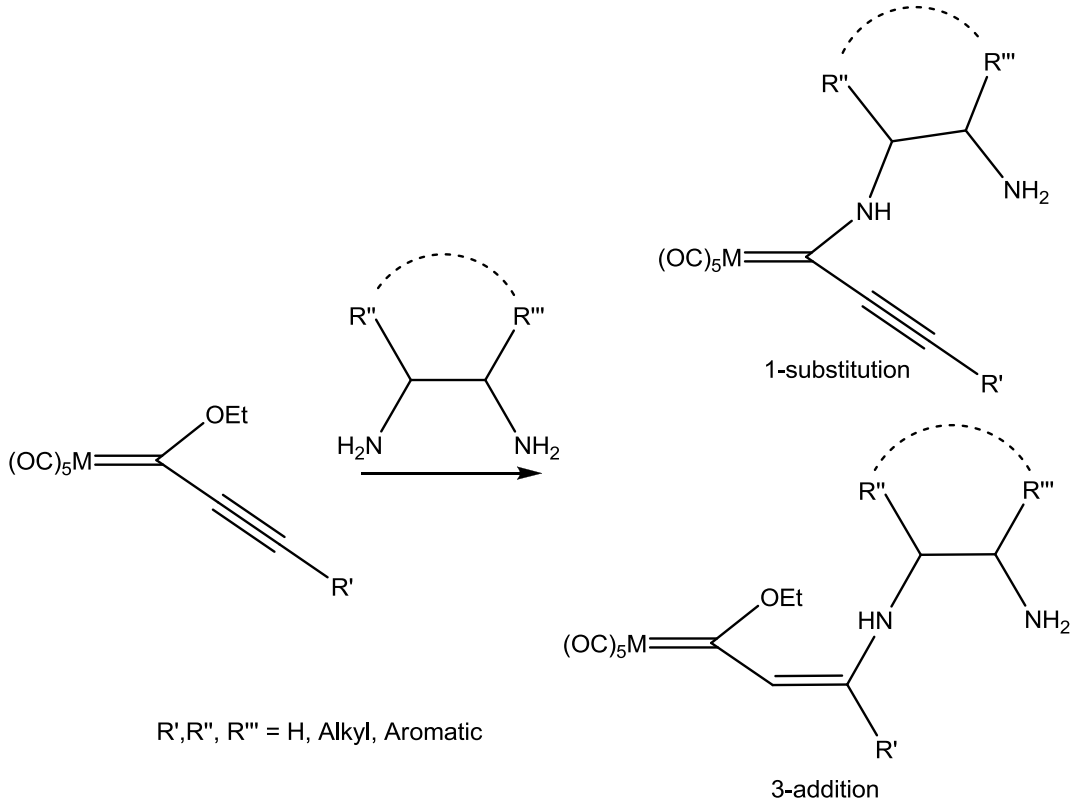

Scheme 3.1. Regiochemistry observed by Fischer

The lower electronegativity of both the nitrogen of the amine group and the sulfur of the thiol substituent increased the ease with which the group can donate electrons to the electron-poor carbene carbon atom, aiding in stabilisation.

The reaction of alkynyl alkoxy metal carbenes to produce the equivalent amino carbenes occurs readily and can be accomplished by the simple addition of the nucleophile to the

[2] (a) Fischer, E. O., Kreissl, F. R., *J. Organomet. Chem.,* **1972**, 35, C45–C51. (b) Fischer, E. O., Kalder, H. J., *J. Organomet. Chem.,* **1977**, 131, 57–64.
[3] (a) Duetsch, M., Stein, F., Lackmann, R., Pohl, E., Herbs-Irmer, R., De Meijere, A., *Chem. Ber.* **1992**, 125, 2051–2065. (b) Aumann, R., Hinterding, P., *Chem. Ber.,* **1992**, 125, 2765–2772. (c) Duetsch, M., Stein, F., Funke, F., Pohl, E., Herbs-Irmer, R., De Meijere, A., *Chem. Ber.,* **1993**, 126, 2535–2541.

© University of Pretoria

carbene starting material at room temperature. The Hegedus-Semmelhack approach has been employed with equal success to produce 2-furyl aminocarbene complexes, boasting yields of 96%,[4] as well as 3-furyl aminocarbene complexes with yields of only 63%.[5] Scheme 3.2 shows a typical aminolysis reaction with aliphatic amines, and Scheme 3.3 refers to the literature synthesis via the Hegedus-Semmelhack approach.

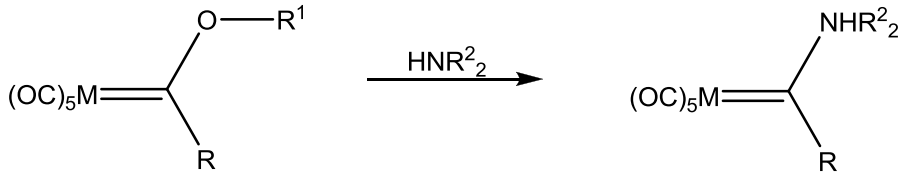

Scheme 3.2. Aminolysis of a Fischer carbene complex

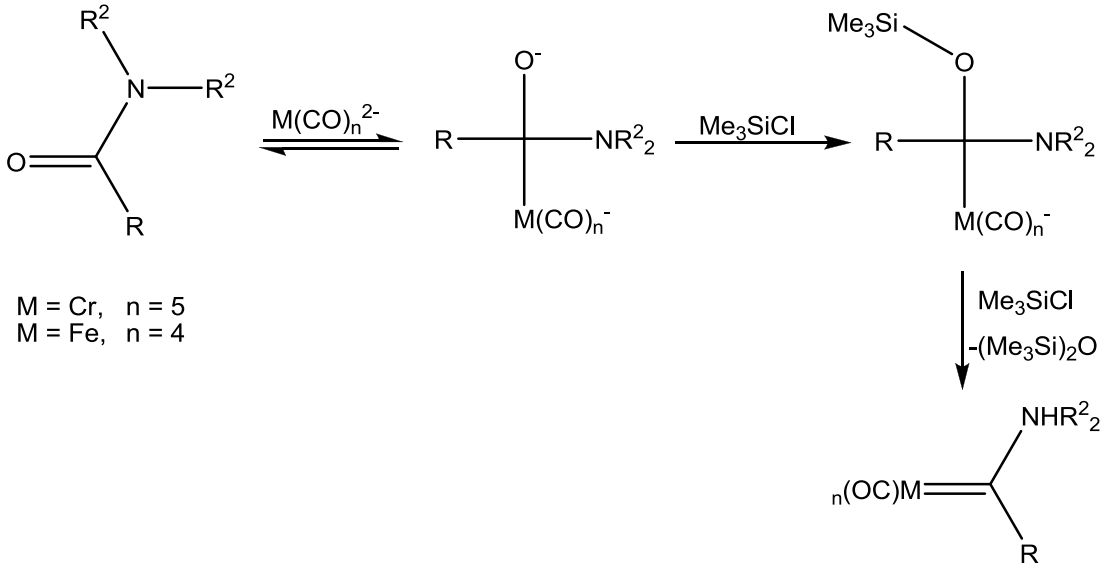

Scheme 3.3. Aminolysis via the Hegedus-Semmelhack approach

The original kinetic investigation into nucleophilic substitution of a Fischer carbene complex by multiple aliphatic amine groups was done by Fischer *et al.*[6]

Recent mechanistic studies by Andrada *et al.,*[7] utilising DFT calculations, demonstrated the reaction mechanism of aminolysis of Fischer alkoxycarbenes. Their results indicated that the most favourable pathway for modification via aminolysis follows a stepwise reaction through

[4] (a)Semmelhack, M. F., Lee, G. R., *Organometallics*. **1987**, 6, 1839. (b) Imwinkelried, R., Hegedus, L. S., *Organometallics*. **1988**, 7, 702.
[5]Schwindt, M. A., Lejon, T., Hegedus, L. S., *Organometallics*. **1990**, 9, 2814.
[6]Fischer, E.O., Heckl, B., Werner, J., *J. Organomet. Chem.,* **1971**, 28, 359.

© University of Pretoria

a zwitterionic intermediate produced by an initial nucleophilic attack. An ammonia-catalysed mechanism proved a considerably lower barrier for the rate-determining step in comparison with the uncatalysed version. When the alkoxycarbene dissolves in solution, the rate-determining step corresponds to the initial nucleophilic attack.[7] Figure 3.2 illustrates the proposed ammonia-catalysed mechanism of the B3LYP optimised pathway for the aminolysis reaction of the 'Fischer-type' monocarbene complex, [methoxy(methyl)carbene] pentacarbonyl chromium(0). Bond lengths are given in Angstrom (Å).[7]

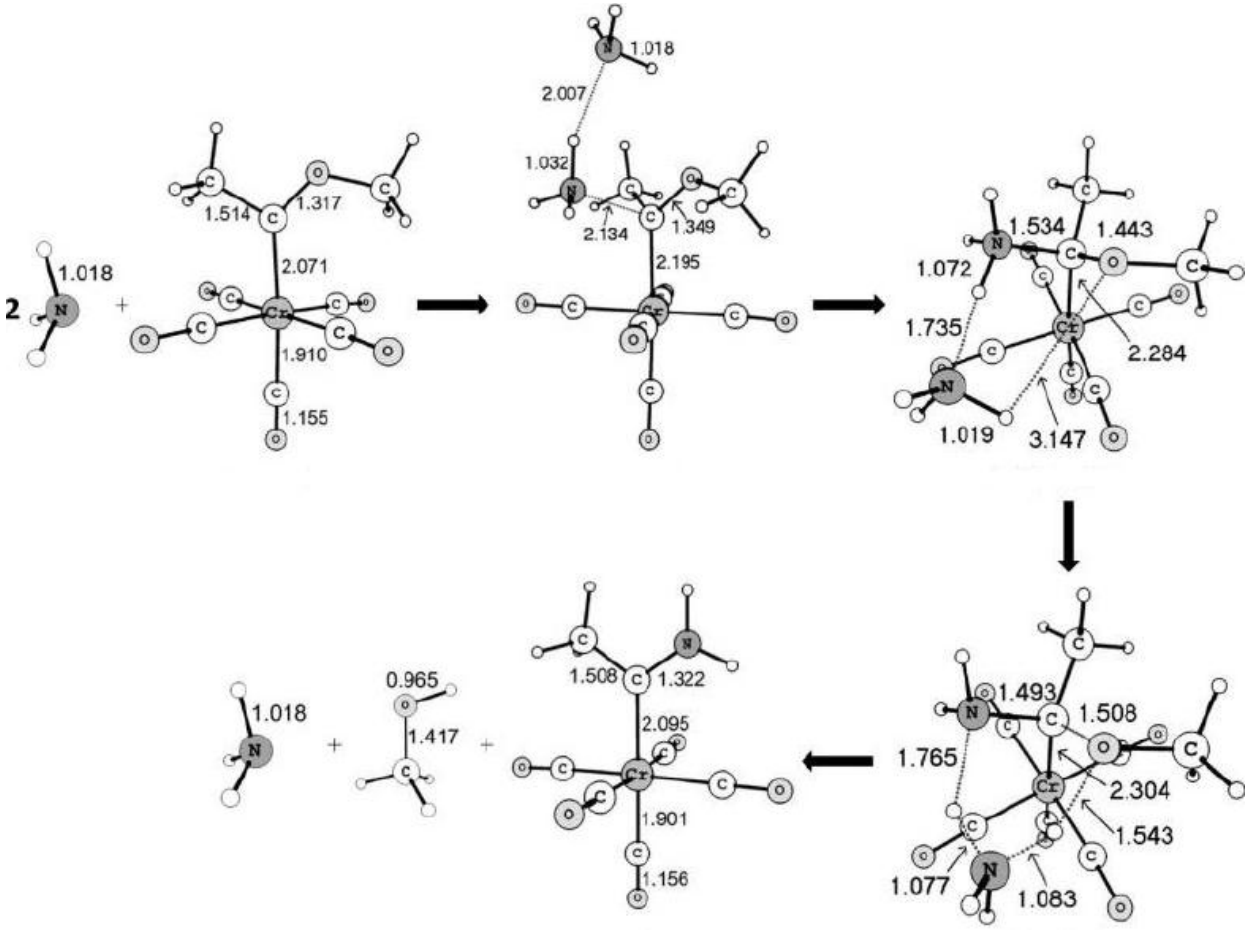

Figure 3.2. Ammonia-catalysed mechanism of the B3LYP optimised pathway for the aminolysis of the Fischer carbene complex, [methoxy(methyl)carbene] pentacarbonyl chromium(0)[7]

[7]Andrada, D. M.,Oscar, J., Jimenez-Halla, C., *J. Org. Chem.,* **2010**, 75, 5821–5836.

© University of Pretoria

3.2 Synthesis

3.2.1 Focus

Since the synthesis of the first aminocarbene complex by Klabunde,[8] numerous novel aminocarbene complexes have been prepared.[9, 10] In order to add novel aminolysis products to the already extensive range of complexes, as well as to give catalytic insight into these carbenes (chapter 5), aminolysis reactions were carried out on both the products and starting materials described in chapter 2, Section 2.2. The original synthesis focused on the simple aminolysis reactions of chromium(0) pentacarbonyl carbene complexes. Both furan and thiophene monocarbene complexes underwent aminolysis with ammonia gas which was found to be both simple and quick. Since the reaction proved highly successful, with an unmatched yield (99%) for complexes **A** and **B**, the aim shifted to producing aminolysis products of the bidentate ligated complexes. Complexes **4**, **5** and **8** all underwent modification with the bulkier cyclohexylamine ligand to produce a more sophisticated array of nitrogen-containing Fischer carbenes. Colour changes also provided an easy method of predicting reaction success since the typical red colour of the ethoxycarbene slowly turns to a yellow-orange colour. Originally, the aminolysis reaction was attempted only after the bidentate ligand had coordinated to the metal centre, which in turn produced a complex of higher polarity but little to no colour change. The approach was modified since, practically, it proved easier first to aminolise (observed colour was yellow-orange) and only then to coordinate the bidentate ligand to produce dark yellow-brown complexes **6**, **7** and **9**. All synthesised complexes were novel in character and formally characterised. The structural data obtained were compared with the literature characterisation to provide a sound reference. The aminocarbene complexes proposed in this chapter are depicted in Figure 3.3.

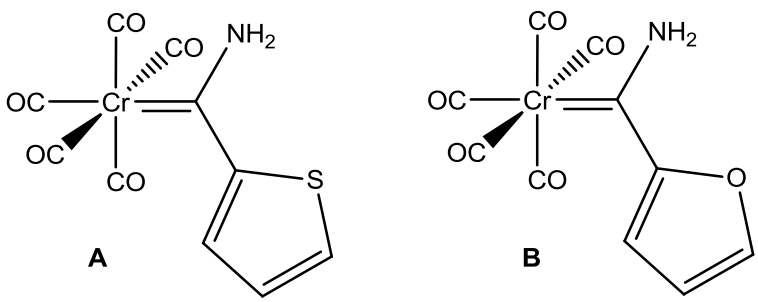

Figure 3.3 Aminocarbene complexes synthesised

[8] Klabunde, U., Fischer, E. O., *J. Am. Chem. Soc.,* **1967**, 89, 7141.
[9] Yamashita, A., *Tetrahedron Lett*., **1986**, 27, 5915.
[10] Borel, C., Hegedus, L. S., Krebs, S., Satoh, Y., *J. Am. Chem. Soc.,* **1987**, 109, 1101.

© University of Pretoria

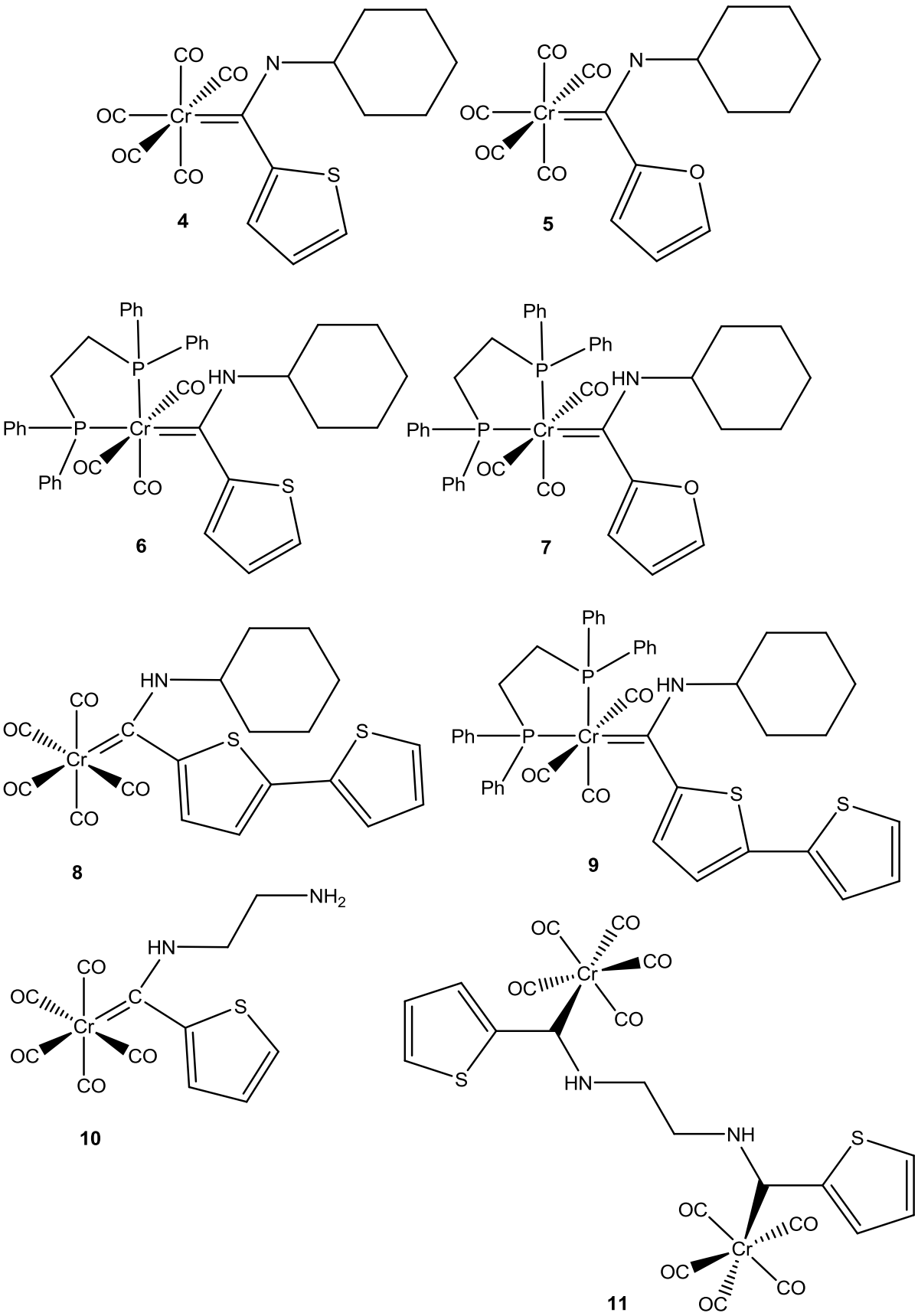

Figure 3.3 (continued). Aminocarbene complexes synthesised

© University of Pretoria

3.2.2 Synthetic methodology

The synthesis of aminocarbenes followed a literature procedure proposed by Klabunde and Fischer.[8] A steady flow of ammonia was passed through the furan and thiophene carbene complexes in ether solvent at room temperature to produce a yellow-orange coloured product. The product was dried under vacuum and the excess unreacted ammonia removed in the process (Scheme 3.4).

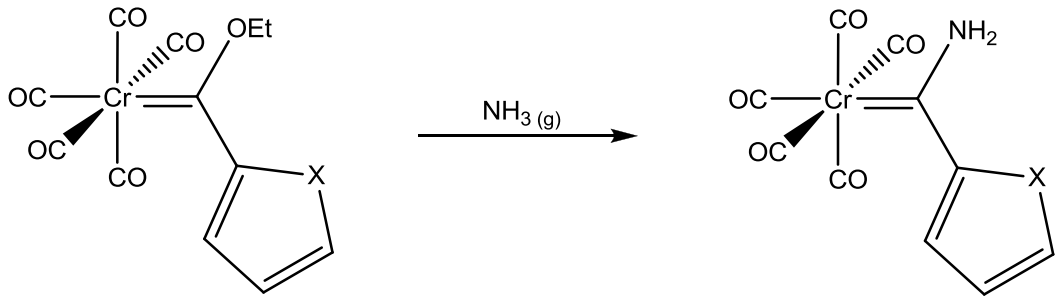

X= O, S

Scheme 3.4. Aminolysis of monocarbene complexes

The progress and advancement of the reaction was confirmed via thin layer chromatography and the developed tlc plate clearly illustrated conversion of the ethoxycarbene to the amino counterpart. The synthesis was practically flawless and yields greater that 98% were obtained for complexes **A**[11] and **B**[12]. Due to the fact that the reaction does not require any additional purification other than extraction of excess ammonia, high yields were expected. Complexes **4**, **5** and **8** were synthesised by adding cyclohexyl amine, in dry THF, to the thiophene (**E**), furan (**F**) and bithiophene (**G**) monocarbene complexes, respectively, at room temperature. The solution was stirred for an hour, after which a yellow solution was obtained and purified via silica gel chromatography. Complexes **4**, **5** and **8** were obtained in yields of 88%, 90% and 91%, respectively (Scheme 3.5). The synthesis of aminocarbenes containing a bidentate ligand followed a combination of the modified Klabunde and Fischer aminolysis[8] and the reaction in Scheme 2.3. Aminolysis was accomplished with addition of cyclohexyl amine to the mono carbene starting material in dry ether. The reaction was allowed to stir at room temperature until tlc analysis illustrated complete conversion to the aminocarbene. The solvent was extracted under vacuum and the residue dissolved in toluene. The bidentate

[11] Terblans, Y. M., PhD Thesis (and references therein), *Thiophene Bimetallic Carbene Complexes,* **1996**, University of Pretoria, Pretoria.
[12] Connor, J. A., Jones, E. M., *J. Chem. Soc., Part A,* **1971**, 1974

© University of Pretoria

ligand was added and the mixture allowed to react at 90 °C (Scheme 3.5). The progress of the reaction was continuously monitored via tlc and products purified using column chromatography with dry THF as eluent. In this case complete transformation from ethoxy to the aminocarbene was not achieved and some starting material was present in the reaction mixture. A yield range of 67-78% was obtained for complexes **6**, **7** and **9**. Products **6**, **7** and **9** were highly polar due to the electronic regions that both the aminolysis nitrogen and complexing phosphines provided.

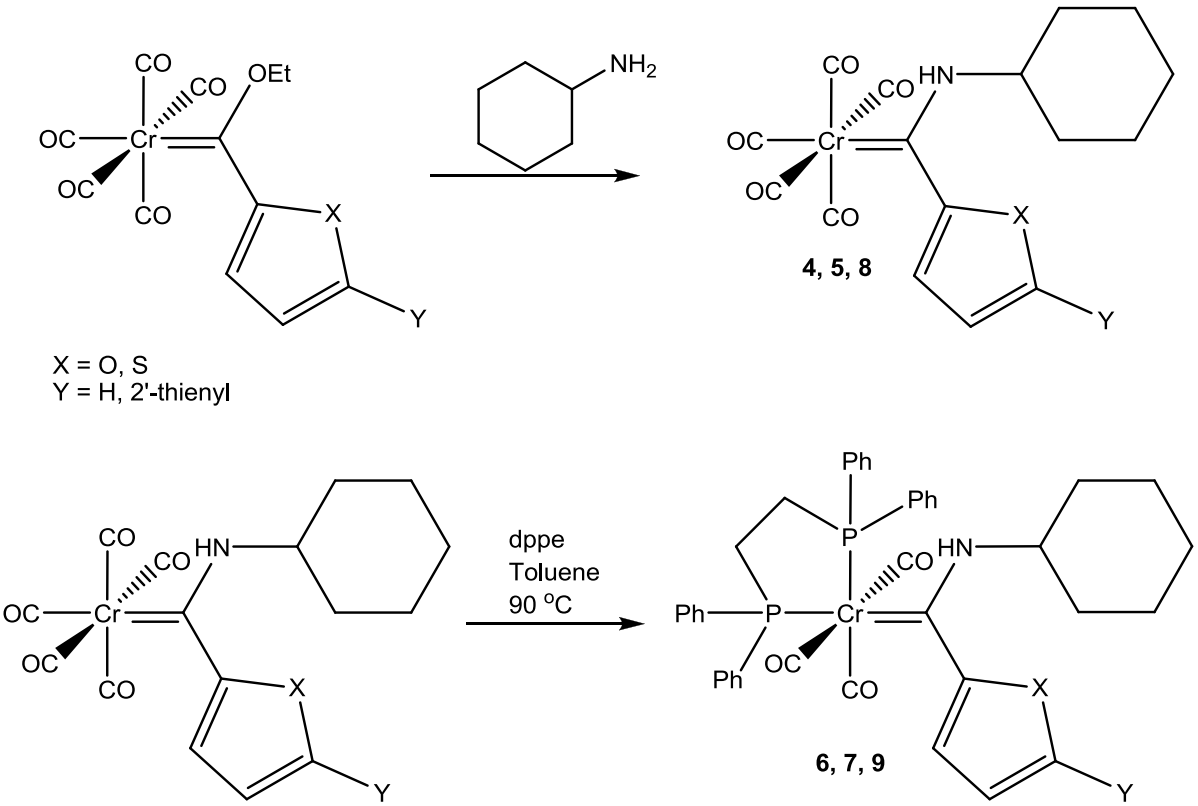

Scheme 3.5. Aminolysis and functionalisation of monocarbene complexes

Complexes **10** and **11** were afforded by the addition of ethylenediamine to the thiophene carbene complex and, after completion; the reaction produced a yellow aminocarbene (**10**) and a red binuclear bridged carbene complex (**11**). Complexes **10** and **11** were both exceptionally polar. Although a high yield was obtained for complex **10**, complex **11** was formed in a lower yield. Due to the exceptionally high polarity of the complexes, purification proved difficult but complex **11** could be isolated from the silica gel column by eluting with dry THF after eluting initially with hexane:DCM to afford **10**.

© University of Pretoria

3.3 Characterisation

All aminocarbene complexes (**4**-**11**) were fully characterised using deuterated solutions for NMR spectroscopy, KBr pellets for IR spectroscopy and solid state crystals for X-ray crystallography. Although complexes **A** and **B** are known compounds, characterisation of these complexes is incomplete in literature. Therefore, full characterisation of these complexes is reported here.

3.3.1 NMR spectroscopy

^{1}H NMR spectroscopy

The ^{1}H NMR shifts of the aminolysis products are presented in Table 3.1. Figure 3.4 shows the typical proton spectrum obtained for complex **B.** Since doubling of aromatic proton peaks was witnessed, it was deduced that certain aminolysis reactions yielded more than a single product (isomer).

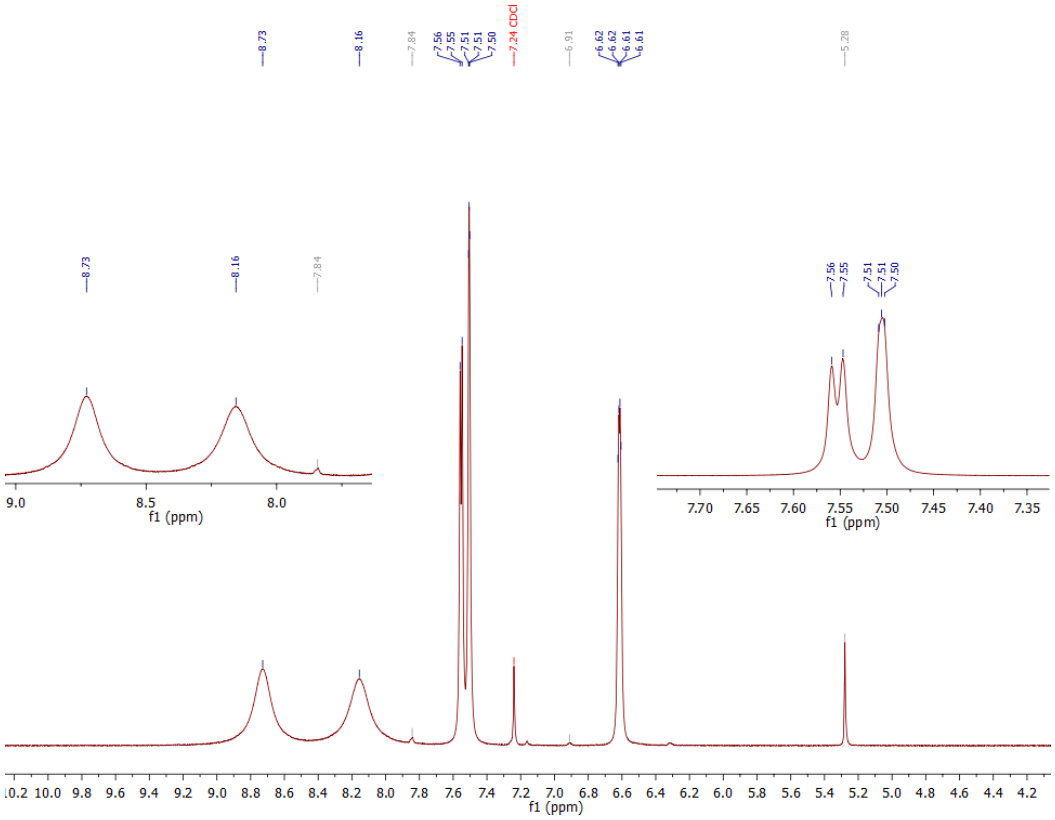

Figure 3.4. ^{1}H NMR spectrum of complex **B**

© University of Pretoria

Substituting the ethoxy substituent for an NH_2 moiety yielded broad NH peaks for complexes **A** and **B** in the chemical shift range δ = 8.16–8.73 ppm. These peaks are prominent in Figure 3.4 and exhibit the shape of broad singlet peaks in the proton spectrum. Typical aminolysis reactions with ammonia yield only a single product. However, isomerisation is a possibility in cases where asymmetrical nitrogen sources are available. Substitution of the ethoxy substituent for an amino ligand can yield both a *syn* and an *anti* isomer depending on the orientation of the R groups on the amino substituent to the heteroatom of the arene ring. This observed phenomenon is due to the extent of π-donation from the nitrogen atom that leads to an increase in the bond order between the C and N atoms to obtain double bond character (Figure 3.5).

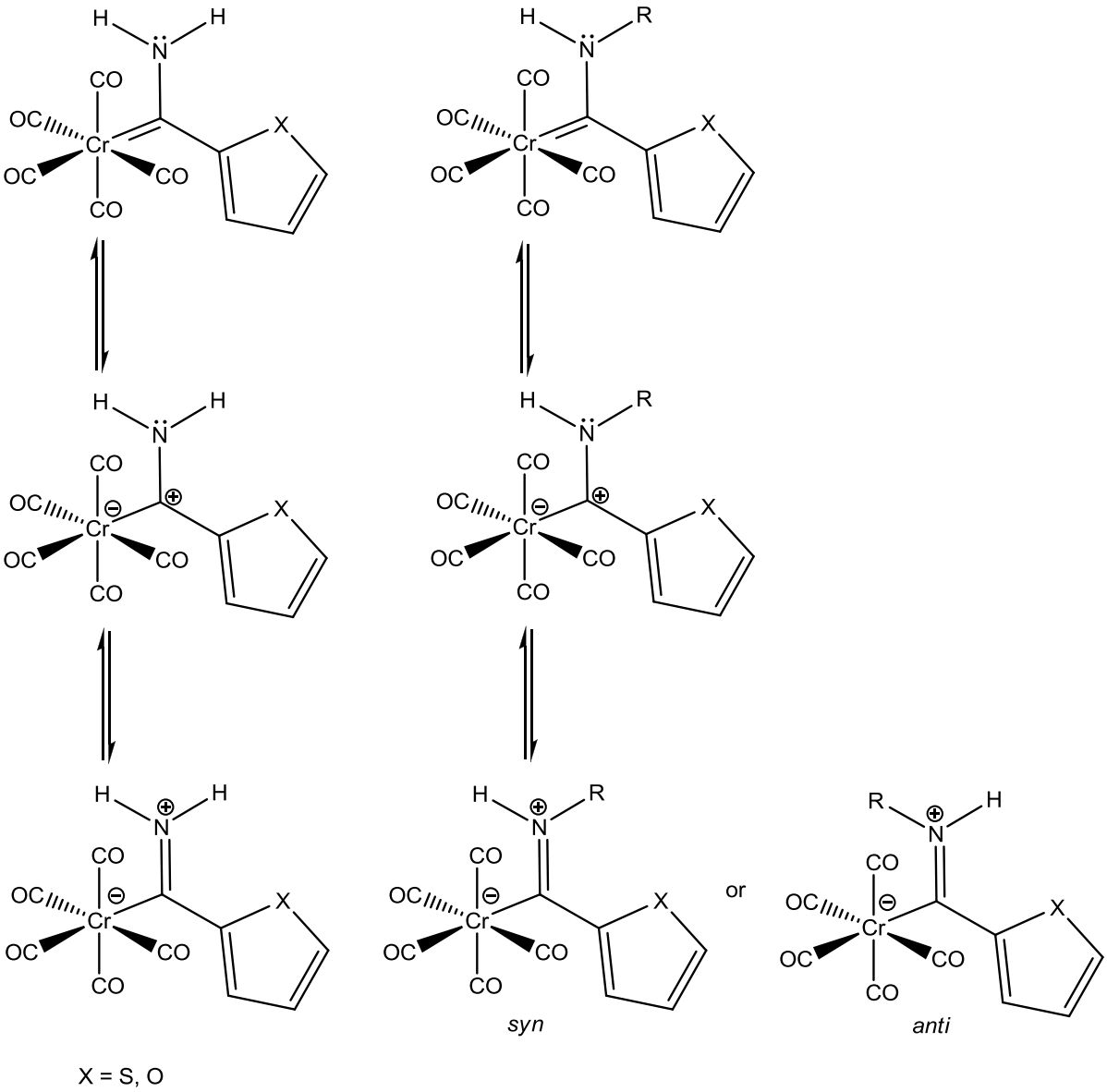

Figure 3.5. Resonance effects in aminocarbenes

© University of Pretoria

The heteroarene proton peaks remained fairly stationary and there is very little differentiation between the aminocarbene and the ethoxycarbene in all cases. The phenyl protons of complexes **6** and **7** also corresponded with the ethoxy Fischer carbene complexes in chapter 2 and the spectra illustrated a multiplet between 7.18 and 7.55 ppm, corresponding to 20 protons. The protons on the heteroarene of complexes **6** and **7** show a trend similar to that observed in chapter 2. H_1 of complex **4** is furthest downfield due to the close proximity to the carbene, resulting in a higher extent of deshielding. H_1 in general also has a downfield shift due to the resonance effect, leaving the proton in a state of higher deshielding than H_2. The chemical shift observed for H_3 of complex **5** is seen further downfield in comparison with H_1. This is mainly due to both the resonance effects as well as the location of this proton close to the electronegative oxygen atom. This proton shift is followed closely by the chemical shift of H_3 (relatively near to the carbene centre).

Table 3.1. ^{1}H NMR shifts of aminolysis products **A, B** and **4–11**

Assignment	**Complexes**			
	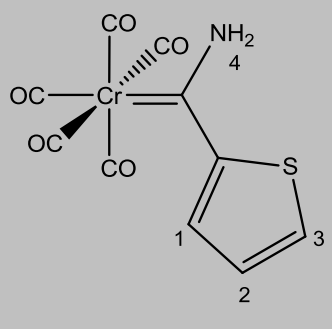		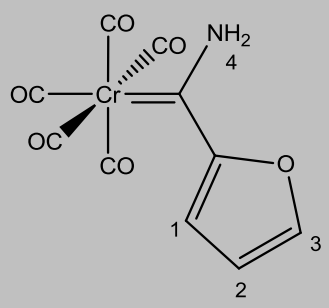	
	A		**B**	
Proton	**Chemical shift (δ,ppm)**	**Coupling constant (J,Hz)**	**Chemical shift (δ,ppm)**	**Coupling constant (J,Hz)**
H_1	7.69 (d)	3.9	7.51 (s, br)	-
H_2	7.19 (dd)	4.5	6.61 (dd)	3.7,1.8
H_3	7.62 (d)	5.1	7.55 (d)	3.7
$-NH_2$	8.2 (s, br)	-	8.73 (s, br)	-
			8.16 (s, br)	-

Solvent: $CDCl_3$

© University of Pretoria

Table 3.1 (continued). ^{1}H NMR shifts of aminolysis products **A, B** and **4-11**

Assignment	**Complexes**							
	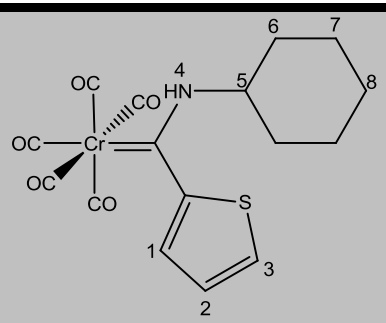				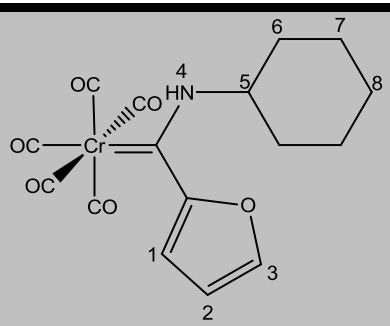			
	Isomer 4a		**Isomer 4b**		**Isomer 5a**		**Isomer 5b**	
Proton	**Chemical shift (δ, ppm)**	**Coupling constant (J, Hz)**	**Chemical shift (δ, ppm)**	**Coupling constant (J, Hz)**	**Chemical shift (δ, ppm)**	**Coupling constant (J, Hz)**	**Chemical shift (δ, ppm)**	**Coupling constant (J, Hz)**
H_1	7.42 (d)	5.1	7.40 (d)	4.5	7.10 (d)	3.6	7.43 (d)	3.6
H_2	7.07 (s, br)	-	6.79 (s)	-	6.58 (d, br)	4.4	6.57 (d, br)	4.4
H_3	7.32 (s)	-	7.03 (s, br)	-	7.62 (s, br)	-	7.44 (s, br)	-
H_4	8.47 (s, br)	-	8.87 (s, br)	-	8.35 (s, br)	-	9.12 (s, br)	-
H_5	4.49 (m)	-	3.74 (m)	-	4.11 (dt)	9.2, 4.5	4.47 (m)	-
H_6 - H_8	1.23-2.17 (m)	-	1.23-2.17 (m)	-	0.70-2.35 (m)	-	0.70-2.35 (m)	-

Solvent: $CDCl_3$

© University of Pretoria

Table 3.1 (continued). ^{1}H NMR shifts of aminolysis products **A, B** and **4–11**

Assignment	**Complexes**	**6**		**7**	
		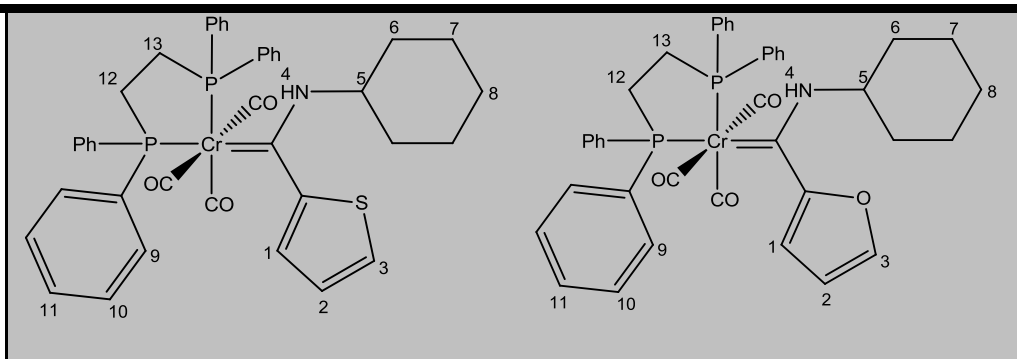			
Proton		**Chemical shift (δ, ppm)**	**Coupling constant (J, Hz)**	**Chemical shift (δ, ppm)**	**Coupling constant (J, Hz)**
H_1		7.46 (dd)	3.7,1.2	7.01 (d)	3.5, 0.8
H_2		7.03 (dd)	5.0, 3.7	6.50 (dd)	3.5, 1.8
H_3		7.42 (dd)	5.0, 1.1	7.45 (dd)	1.8, 0.9
H_4		8.40 (s, br)	-	8.65 (s, br)	-
H_5		3.93 (m)	-	3.70–3.83 (m)	-
H_6 – H_8		1.20–2.10 (m)	-	1.20–1.60 (m)	-
H_9 – H_{11}		7.20-7.40 (m)	-	7.25–7.70 (m)	-
H_9 – H_{11}		7.55-7.70 (m)	-	7.44-7.72 (m)	-
H_{12}		2.85–2.96 (m)	-	2.65 (m)	-
H_{13}		2.53-2.70 (m)	-	2.41-2.53 (m)	-

Solvent: CD_2Cl_2

© University of Pretoria

Table 3.1 (continued). ^{1}H NMR shifts of aminolysis products **A, B** and **4–11**

Assignment	**Complexes**	**8**	**10**		**11**
	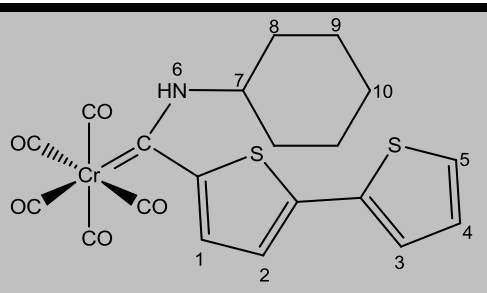		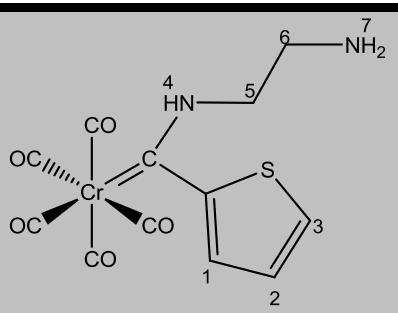		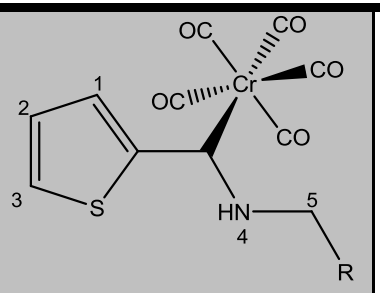
Proton	**Chemical shift (δ, ppm)**	**Coupling constant (*J*, Hz)**	**Chemical shift (δ, ppm)**	**Coupling constant (*J*, Hz)**	**Chemical shift (δ, ppm)**
H_1	7.25 (d)	4.0	7.77 (dd)	3.8, 1.2	7.46 (s, br)
H_2	7.15 (d)	4.0	7.11 (dd)	3.9, 1.3	n.o
H_3	7.25 (dd)	3.8, 1.3	7.53 (dd)	2.0, 1.1	6.85(s, br)
H_4	7.03 (dd)	5.1, 3.6	9.90 (s, br)	-	9.01 (s, br)
H_5	7.28 (dd)	5.3, 1.0	2.29 (m)	-	3.10 (s)
H_6	8.40 (s, br)	-	2.29 (m)	-	-
H_7	4.47 (m)	-	1.15 (s)	-	-
H_8- H_{10}	1.23–2.20(m)	-	-	-	-

Solvent: $CDCl_3$

© University of Pretoria

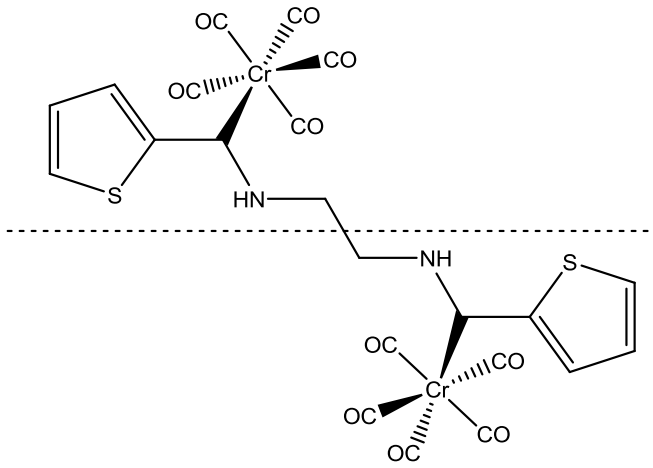

Figure 3.6. Plane of symmetry for complex **11**

Complexes **B**, **4** and **5** yielded isomeric products. This was deduced from the doubling of both amine proton peaks as well as the aromatic heteroarene peaks in the NMR spectrum. Four isomeric products are possible, as shown in Figure 3.7.

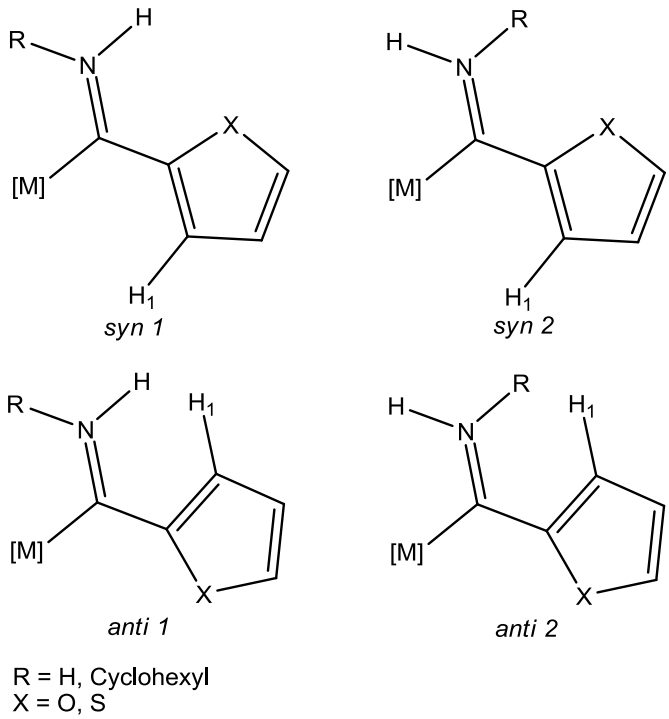

Figure 3.7. Showing the four possible isomeric products

In the *syn/anti 2* conformations, the amine proton will be more deshielded than this proton in the *syn/anti 1* conformations due to the proximity of this proton to the metal moiety. This proton is thus expected to shift downfield in the NMR spectra of the *syn/anti 2* conformations

© University of Pretoria

compared to the spectra of the *syn/anti 1* conformations. Similarly, H_1 will be observed at a more downfield chemical shift value on the spectra of the *syn 1/syn 2* conformations compared to its position on the *anti 1/anti 2* spectra. It was therefore determined that the major isomer (**4a**) of **4** displayed the *syn 1* conformation, whereas the minor isomer (**4b**) exhibited the *syn 2* conformation. In a similar fashion the major isomer (**5a**) of complex **5** was also determined to be in the *anti 1* conformation, while isomer (**5b**) was found in the *syn 2* conformation.

The proton and carbon NMR spectra of complex **9** could not be fully elucidated due to overlapping peaks in the aromatic region between 7.17-7.55 ppm and 7.60-7.80 ppm of the dppe ligand. The following proton peaks were, however, observed (proton numbering refers to complex **8**): H_2 δ = 7.03 ppm (s, br), H_3 δ = 7.15 ppm (d, *J*=3.4 Hz), H_4 δ = 6.93 ppm (s, br) and H_6 δ = 8.36 ppm (s, br).

Only a very small quantity of complex **11** remained for recharacterisation and thus only one proton spectrum was obtained. The proton spectrum indicated multiple broad peaks corresponding to thiophene protons, which could possibly indicate that two of the aromatic ring protons overlap. The H_5 protons for both complexes **10** and **11** display the expected triplet pattern and were found more downfield due to the proximity to the nitrogen carbene substituent. Complex **10** contained a second amine group located at the end of the heteroatom carbene substituent. This group increased the polarity of the complex in comparison with the cyclohexyl aminocarbene complexes (**4** and **5)**.

The N(H)R peak was located above 9.0 ppm for both products **10** and **11**. Mahapatra *et al.*[13] reported the N(H)R proton peak as a broad singlet and located at a chemical shift of 8.14 ppm. This peak is often absent. The additional amine protons are found at a chemical shift value of δ = 1.15 ppm for **10**. The ^{1}H NMR spectrum of **4** is presented in Figure 3.8.

[13] Mahapatra, D. K., Hazra, D., Puranik, V. G., Sarkar, A., *J. Organomet. Chem.,* **2004**, 689, 3501–3512.

© University of Pretoria

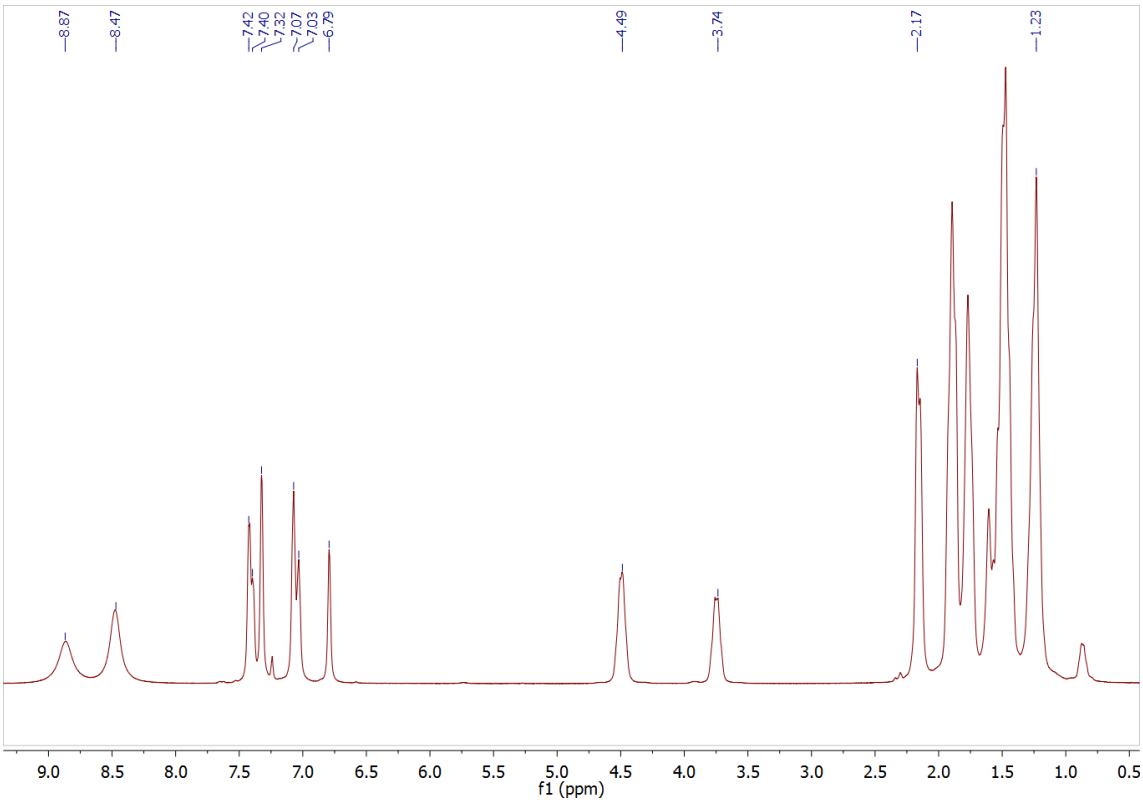

Figure 3.8. The ^{1}H NMR spectrum of **4**

^{13}C NMR spectroscopy

^{13}C NMR chemical shifts were obtained for complexes **A**, **B** and **4-11** and values are reported in Tables 3.2 and 3.3. Since doubling of carbon peaks was witnessed, the deduction was made that isomeric products have been obtained for **4** and **5**.

A heteronuclear single quantum coherence (HSQC) spectrum was analysed to aid in the assignment of the ^{13}C NMR peaks of complex **5** by cross-referencing with the relevant protons. Figure 3.10 depicts the HSQC spectrum obtained. Since complex **B** provided such a clear example of a typical aminocarbene ^{13}C NMR spectrum, this spectrum is shown in Figure 3.11, while the HSQC spectrum is shown in Figure 3.9. It should be noted that although many factors are similar to other monocarbene complexes, the major differentiation factor between amino- and alkoxycarbene complexes lies in the clear upfield shift of the carbene carbon. A noteworthy upfield shift is observed for all the carbene carbons of the amino analogue in comparison with the ethoxy version.

Upfield chemical shifts of between ± 30 and 50 ppm are witnessed for carbene carbons of the aminocarbene complexes and illustrate the superior electron donation of the nitrogen

© University of Pretoria

atom to the carbene carbon. The phenyl carbon atoms remained stationary in their original shifts and aminolysis had very few (if any) electronic effects on the phosphine ligands. Since the nitrogen lone pair is more adequate in supplying the carbene carbon with electron density than the oxygen atom of alkoxycarbene complexes, the net drainage from the heteroarene carbons is noted to be slightly less.

Upfield shifts of the carbons of the furan and thiophene substituents of 5-10 ppm can be ascribed to the donation effects of the nitrogen. The HSQC spectrum of complex **B** is also included in Figure 3.9 and can be compared to that of **5**. Both HSQC spectra show that C_4 is furthest downfield in comparison with the other H-containing carbons, followed by C_2 and lastly C_3. The carbonyl ligand displays shifts similar to the ethoxycarbene complexes and thus no change in shift was recorded.

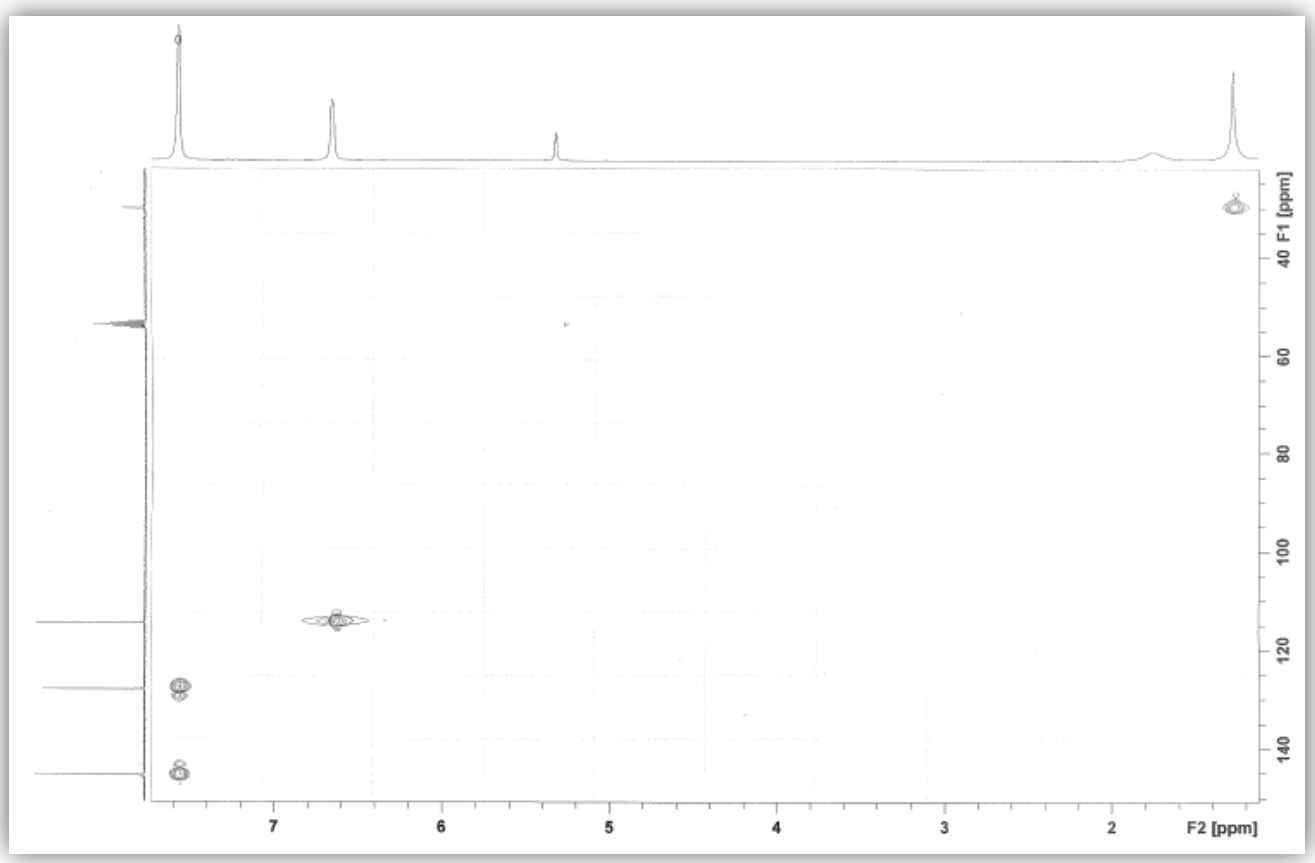

Figure 3.9. HSQC of complex **B**

© University of Pretoria

Table 3.2. ^{13}C NMR shifts of complexes **A** and **B**

Assignment	**Complexes**	
	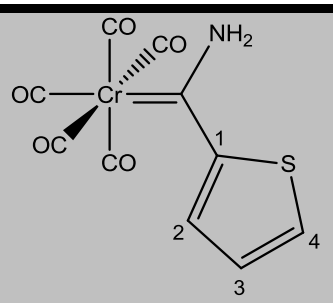	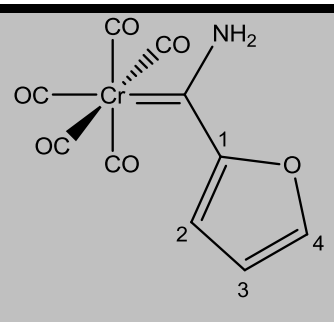
Carbon	**Chemical shift (δ,ppm)**	**Chemical shift (δ,ppm)**
Carbene	268.3	253.3
C_1	151.4	157.3
C_2	131.7	128.0
C_3	129.0	114.5
C_4	132.8	145.5
CO (*cis*)	217.4	218.4
CO (*trans*)	222.7	223.3

Solvent: $CDCl_3$

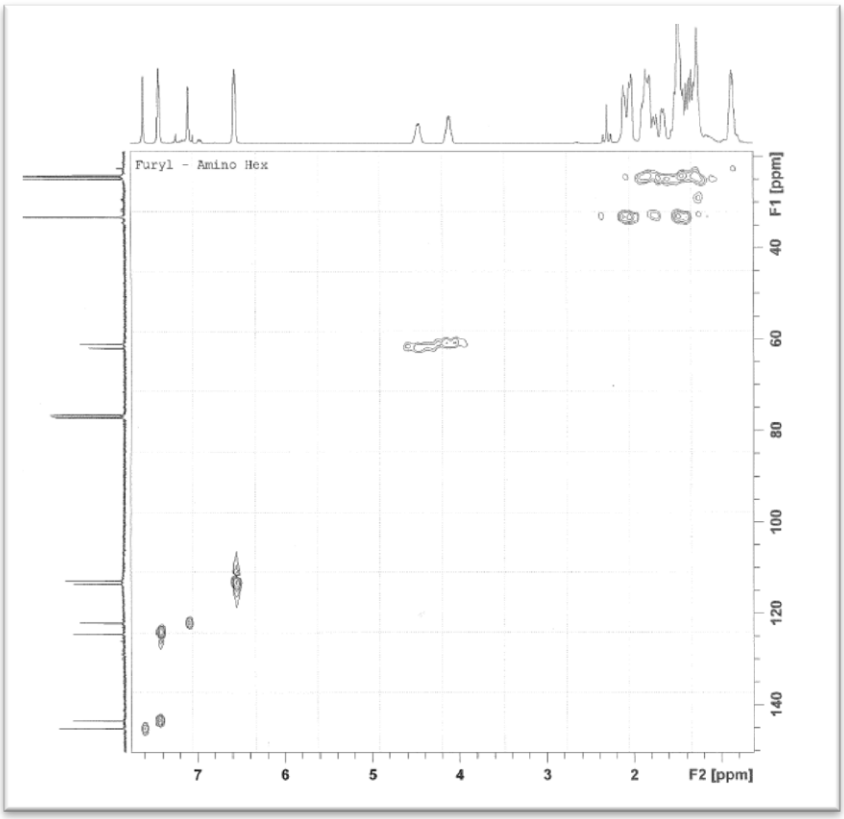

Figure 3.10. HSQC spectrum of complex **5**

© University of Pretoria

Table 3.3. ^{13}C NMR shifts of aminolysis products **4-11**

Assignment **Complexes**

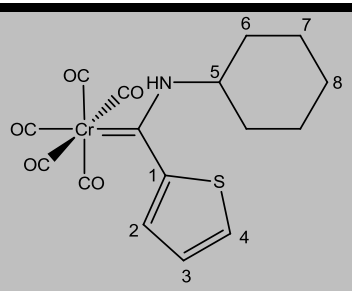

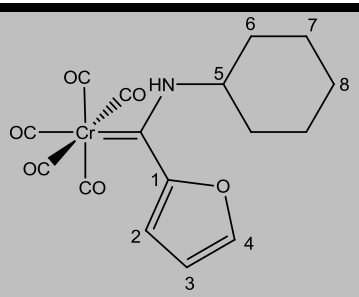

Carbon	4a Chemical shift (δ, ppm)	4b Chemical shift (δ, ppm)	5a Chemical shift (δ, ppm)	5b Chemical shift (δ, ppm)
Carbene	257.2	270.9	249.2	239.6
C_1	156.0	148.7	157.5	156.1
C_2	127.2	121.9	124.5	122.1
C_3	126.3	126.2	112.9	113.6
C_4	128.3	128.2	145.2	143.6
C_5	62.7	59.9	61.1	62.1
C_6	33.3	33.5	33.4	33.3
C_7	24.5	24.2	24.3	24.6
C_8	25.0	24.8	25.0	25.0
CO (*cis*)	217.5	217.2	218.1	218.0
CO (*trans*)	223.2	223.1	222.8	222.9

Solvent: $CDCl_3$

© University of Pretoria

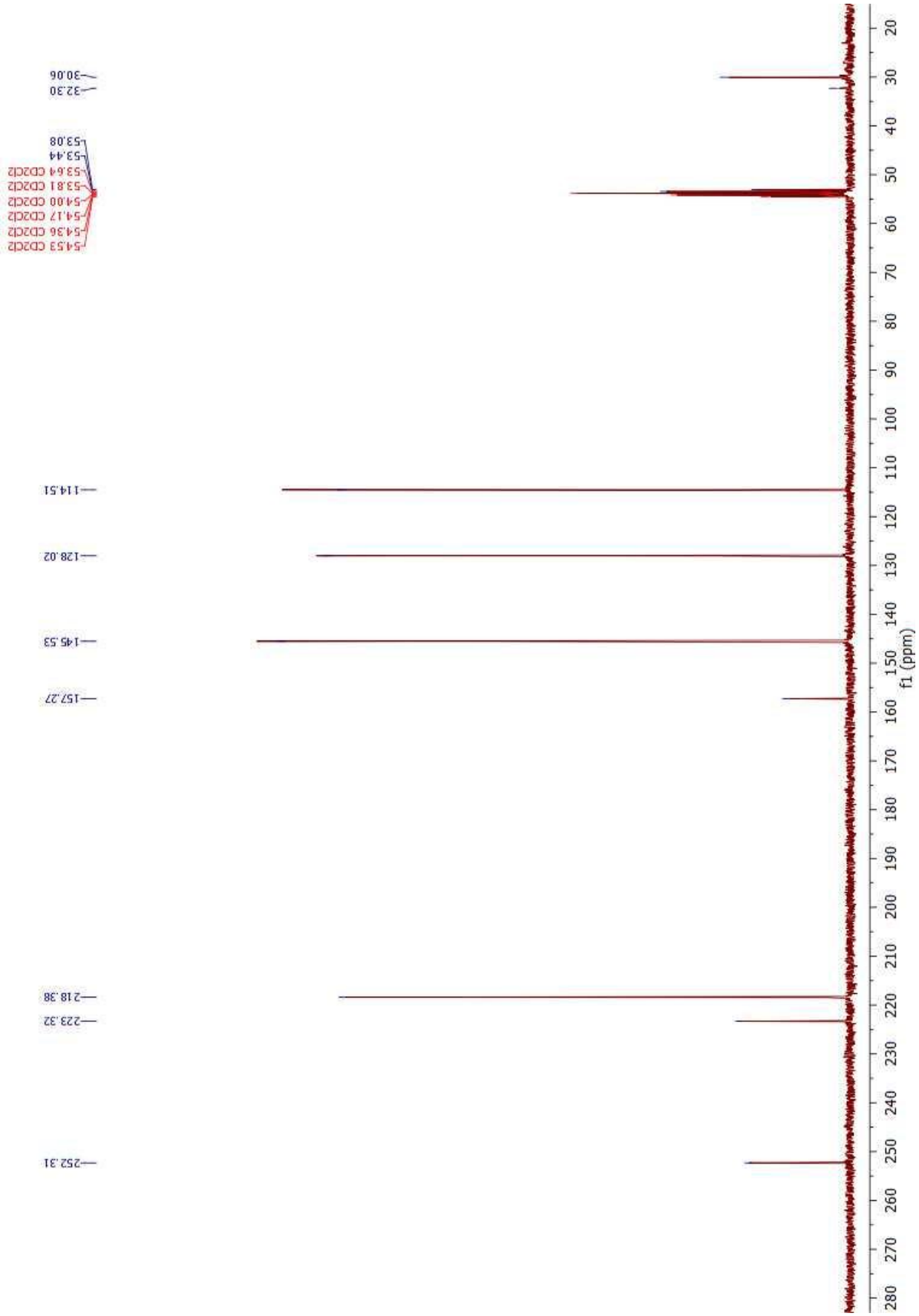

Figure 3.11. ^{13}C NMR spectrum of complex **B**

© University of Pretoria

Table 3.3 (continued). ^{13}C NMR shifts of aminolysis products **4-11**

Assignment	**Complexes**	
	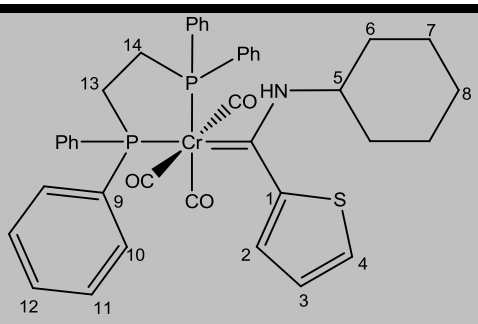	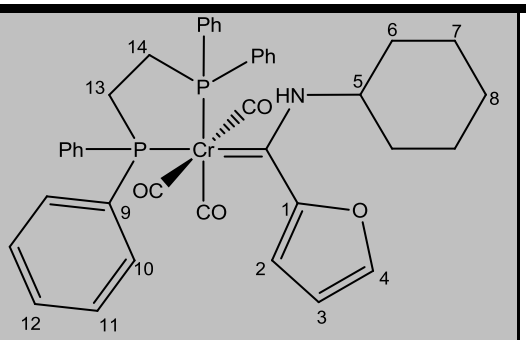
	6	**7**
Carbon	**Chemical shift (δ, ppm)**	**Chemical shift (δ, ppm)**
Carbene	277.7	262.6
C_1	150.6	157.8
C_2	123.0	129.7
C_3	119.2	118.7
C_4	126.1	143.5
C_5	58.1	59.8
C_6	30.3	30.7
C_7	25.0	24.4
C_8	25.6	25.5
C_9	138.0	138.5
C_{10}	132.7	131.8
C_{11}	129.2	129.1
C_{12}	131.4	131.3
C_{13}	31.7	31.5
C_{14}	33.1	33.2
CO (1)	220.1	220.1
CO (2)	229.0	229.0
CO (3)	234.4	235.5

Solvent: $CDCl_3$,CO (1) & CO (2) *trans* to each other, CO (3) *trans* to phosphine

© University of Pretoria

Table 3.3 (continued). ^{13}C NMR shifts of aminolysis products **4-11**

Assignment	**Complexes**	
	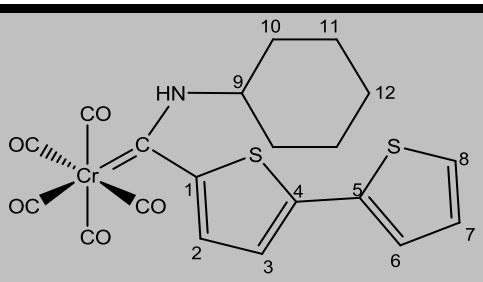	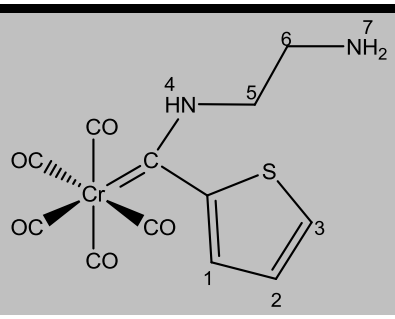
	8	**10**
Carbon	**Chemical shift (δ, ppm)**	**Chemical shift (δ, ppm)**
Carbene	254.3	278.6
C_1	132.4	137.8
C_2	129.3	129.9
C_3	124.5	127.8
C_4	128.3	129.0
C_5	128.1	41.0
C_6	126.1	61.90
C_7	128.2	217.0
C_8	125.1	221.2
C_9	53.4	-
C_{10}	33.5	-
C_{11}	24.5	-
C_{12}	29.7	-
CO (*cis*)	217.5	-
CO (*trans*)	223.1	-

Solvent: $CDCl_3$

© University of Pretoria

Table 3.3 (continued). ^{13}C NMR shifts of aminolysis products **4-11**

Assignment	**Complex**
	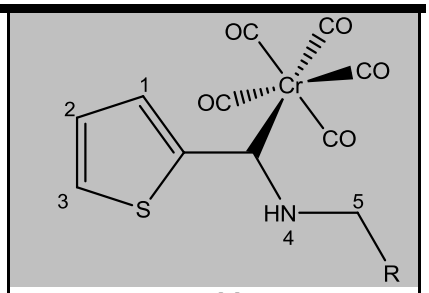
	11
Proton	**Chemical shift (δ, ppm)**
Carbene	271.0
C_1	153.5
C_2	131.8
C_3	128.7
C_4	129.3
C_5	40.7
CO (*cis*)	218.8
CO (*trans*)	220.8

Solvent: $CDCl_3$

The^{13}C NMR spectra of both complexes **10** and **11** display a carbene carbon peak in the same chemical shift range as the aminocarbene complexes **6** and **7**. The carbene peaks are found at chemical shifts of δ = 277.1 ppm and δ = 262.6 ppm, respectively, with carbonyls in the δ = 220 ppm region. The aromatic carbon peaks of these two carbenes are similar in nature and, in addition, complex **11** contains a plane of symmetry (Figure 3.6) - hence the biscarbene only indicates, as expected, a single carbene peak.

Complexes **6** and **7** contain carbon peaks at chemical shifts similar to those of **1–3**. Carbonyl carbon peaks are witnessed at chemical shifts of δ = 220.1 ppm, 229.0 ppm and 234.4 ppm for complex **6** and at δ = 220.1 ppm, 229.0 ppm and 235.5 ppm for **7**. For both complexes, the carbonyl peaks as well as the carbene carbon peaks displayed a multiplet splitting pattern indicating that C-P coupling occurred. Mahapatra *et al.*[13] synthesised amino Fischer carbenes containing conjugated double bonds. The ethoxy pentacarbonyl chromium carbene complexes displayed carbonyl carbon chemical shifts of δ = 217.6 ppm and 223.5 ppm and a carbene carbon shift of δ = 269.6 ppm. The ^{13}C NMR shifts are similar in nature to those of

© University of Pretoria

complexes **4**, **5**, **8, 10** and **11**. Klapdohr *et al.*[14] synthesised phosphine-bearing aminocarbene complexes with the aim of finding application for the aminolysis of alkoxycarbene complexes. The tetracarbonyl phosphine aminocarbene complex displayed carbon shifts at δ = 221.7 ppm, 228.1 ppm and 230.01 ppm for the carbonyl ligands and δ = 287.1 ppm for the carbene carbon. These chemical shifts correspond to the reported peaks of **6** and **7**. Complex **9** presented difficulty in the assigning of peaks due to the aromatic groups on the dppe ligand overlapping with the bithiophene rings. The carbene peak was, however, observed at a chemical shift of δ = 276.3 ppm and the three carbonyl ligands at δ = 224.9 ppm, δ = 234.3 ppm and δ = 236.6 ppm. Carbon chemical shifts could also be assigned to the cyclohexyl amine carbons and the shifts were witnessed at δ = 58.2 ppm, δ = 33.8 ppm, δ = 25.1 ppm and δ = 29.7 ppm. Merlic *et al.*[15] synthesised and examined the structure of cyclic arene chromium carbene complexes containing amino groups as carbene substituents. The pentacarbonyl arene chromium carbene complexes displayed the carbonyl ^{13}C chemical shifts at δ = 216.8 and 223.6 ppm and a carbene carbon shift at δ = 277.1 ppm. The chemical structures of the arene chromium carbene complexes were similar to those of complexes **4** and **5** and also displayed analogous ^{13}C chemical shifts.

^{31}P NMR spectroscopy

^{31}P NMR spectroscopy was preformed for complexes **6, 7** and **9** and the chemical shifts reported in Table 3.4.

Table 3.4. ^{31}P NMR of **6**, **7** and **9**

	P_1 Chemical shift (δ, ppm)	**P_2 Chemical shift (δ, ppm)**
6	79.4	77.3
7	78.9	77.6
9	80.1	76.8

Solvent: $CDCl_3$

Similar to the ethoxy carbene analogues described in chapter 2, distinct chemical shifts are observed which corresponds to P_1 (*trans* to the carbene) and P_2 (*trans* to a carbonyl). P_1 is observed further downfield due to the electron withdrawing ability of the carbene centre, leaving the P-atom more deshielded whilst P_2 is slightly more upfield and competing for electron density with a carbonyl ligand.

[14] Klapdohr, S., Dötz, K. H., Assenmacher, W., Hoffbauer, W., Hüsing, N., Nieger, M., Pfeiffer, J., Popall, M., Schubert, U., Trimmel, G., *Chem. Eur. J.,* **2000**, 6, 3006–3017.
[15] Merlic, C. A., Xu, D., Khan, S. I., *Organometallics,***1992**, 11, 412–418.

© University of Pretoria

3.3.2 Infrared spectroscopy

In a similar fashion and method to that described in chapter 2, infrared spectroscopy with reference carbonyl patterns was employed to provide structural insight into all the aminolysis products synthesised. A full theoretical argument on the ν_{CO} of three carbonyl complexes was previously given in chapter 2. KBr pellets were used to characterise products **6-11** to limit the impact of solvent polarity and the complexity of solubility. Products **4**, **5**, **8**, **10** and **11** show the typical five carbonyl stretching pattern with four bands visible, whereas complexes **6**, **7** and **9** only show three bands. IR data was obtained for all complexes (**4-11**) and the stretching frequencies are listed in Table 3.5.

Table 3.5. IR data for complexes **4-11**

Complex	Carbonyl stretching frequency (ν_{CO}, cm^{-1})			
	$A_1^{(1)}$	$A_1^{(2)}$	B_1	E
4	2054 (s)	1872 (s)	1983 (s)	1916 (s)
5	2054 (m)	1884 (s)	1988 (s)	1918 (s)
6	2005 (w)	1805 (s)	1909 (s)	-
7	2005 (w)	1825 (s)	1911 (s)	-
8	2059 (m)	1903 (s)	1963 (s)	1938 (s)
9	2007 (w)	1827 (s)	1944 (m)	-
10	2051 (m)	1884 (s)	1995 (s)	1918 (s)
11	2053 (m)	1860 (s)	2003 (s)	1910 (s)
A	2057 (m)	-	2009 (s)	1986 (s)
B	2060 (m)	1946 (s)	1991 (s)	1961 (s)

The $A_1^{(2)}$ band of complex **5** is superimposed on the E_1 band, whereas a clear peak is visible for complex **4**. Complexes **6** and **7** both displayed an exceptionally large separation between the $A_1^{(1)}$ and the E band, and complex **6** also contains a very high-frequency E band. The literature IR stretching frequencies of aminocarbene complexes are presented in Table 3.6. The $A_1^{(1)}$ band for pentacarbonyl complexes is similar to literature values, while the same band of tricarbonyl complexes **6**, **7** and **9** is comparable with the tetracarbonyl complex of Table 3.6.

© University of Pretoria

Table 3.6. Infrared stretching frequencies of literature aminocarbene complexes

Complex	Stretching frequencies (cm^{-1})			
$(CO)_5Cr$(aminocarbene)[16]	2056	1976	1932	-
$RPPh_2(CO)_4Cr\{C(Ph)(N^iBu_2)\}$[14]	2002	1917	1892	1875

3.3.3 X-ray crystallography

X-ray diffraction analysis established the molecular arrangement of complexes **4**, **5** and **7**. All single crystals were obtained by the diffusion method proposed in chapter 2. Diffusion was achieved between dichloromethane (good solvent) and hexane (reduced solubility) and yielded orange-red crystals for complexes **A** and **B**. Complex **6** produced brownish single crystals. Figures 3.12 and 3.14 illustrate the ORTEP + POV-Ray plots of the absolute geometries of the amino monocarbene complexes **4** and **5,** while Figure 3.13 illustrates the packing pattern for complex **A**. Complexes **A** and **B** both crystallised in the monoclinic crystal system and contained a P2(1)/c space group. The unit cell of complex **A** was occupied by a total of eight independent molecules, while complex **B** was packed by four structures per unit cell. Noteworthy bond lengths and angles were determined and are summarised in Tables 3.7. and 3.8. The complete crystallographic data of complexes **A**, **B** and **6** are given in Appendices E, F and G, respectively. The carbene-chromium bond lengths of complexes **A** and **B** are defined as 2.0916(13) Å and 2.0958(13) Å, respectively and are comparable to those of **1** and **2**. The short carbon-nitrogen bond should be noted. The average C-N bond length of 1.3165 Å for complexes **A** and **B** is significantly shorter than expected for a single bond; through π-donation to the carbene moiety, the bond can be redefined as having double bond characteristics[17]. The length of the C-N bond is comparable to that of the C-C double bonds of the heteroarene, which also displayed a π-system. The heteroarene bond lengths for C(7)-C(8), C(8)-C(9), C(9)-C(10), S(1)-C(7) and S(1)-C(10) are observed as 1.4199(18) Å, 1.4203(19) Å, 1.359(2) Å, 1.7364(13) Å and 1.6909(19) Å, respectively for complex **B**. The bond lengths for the furan counterpart were comparable. Distortion within the aromatic ring can be ascribed to the effects of the carbene fragment on the π-system.

[16] Hoskovcová, I., Zvěřinová, R., Roháčová, J., Dvořák, D., Tobrman, T., Záliš, S., Ludvík, J.,*ElectrochimicaActa.,* **2011**, 56, 6853–6859.
[17] Reinheimer, E. W., Kantardjieff, K. A., Ouyang, X., Herron, S. R., Lu, T., Casalnuovo, J. A., *J. Chem. Crystallogr.***2007**, 37, 507–515.

© University of Pretoria

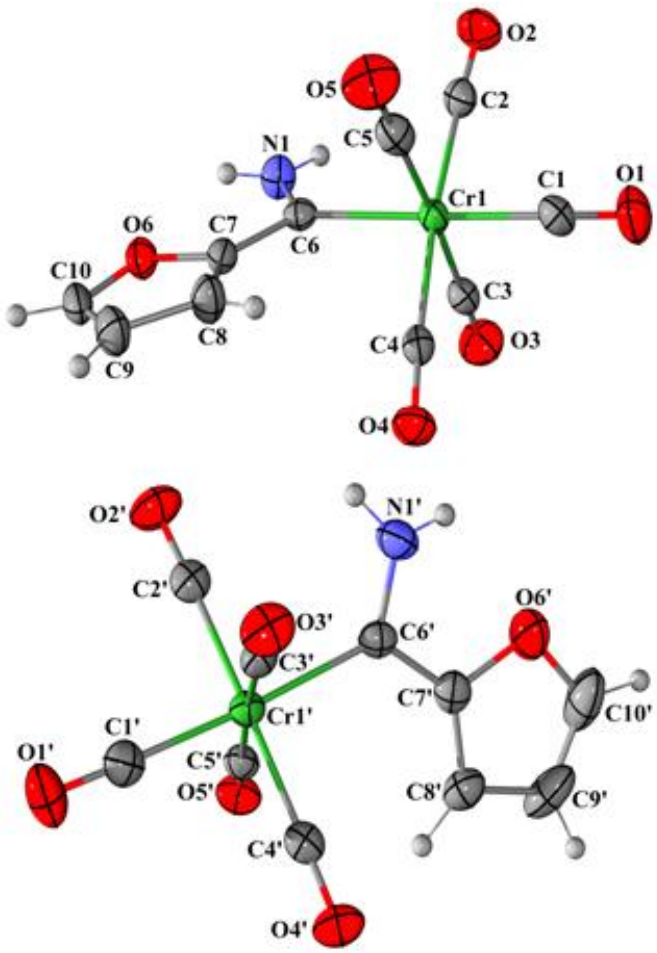

Figure 3.12. ORTEP + POV-Ray plot of the structure of complex **B**

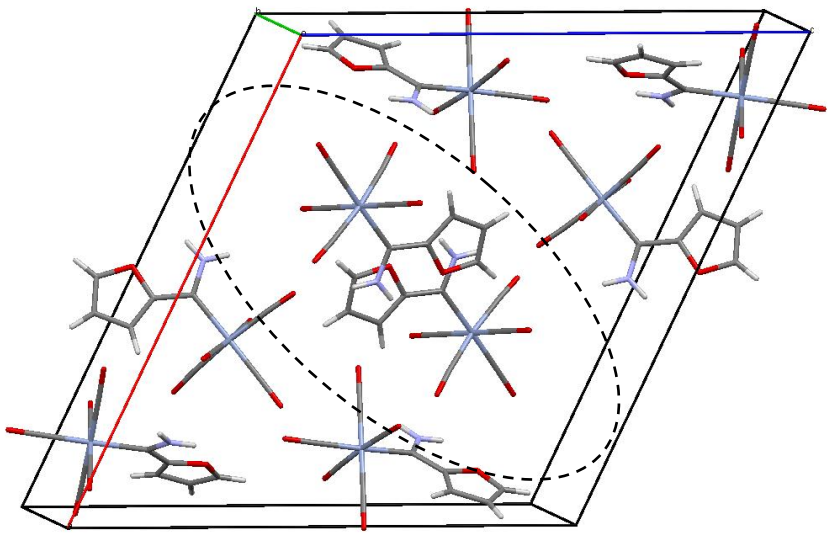

Figure 3.13. Capped stick representation of the packing displayed by complex **B**

© University of Pretoria

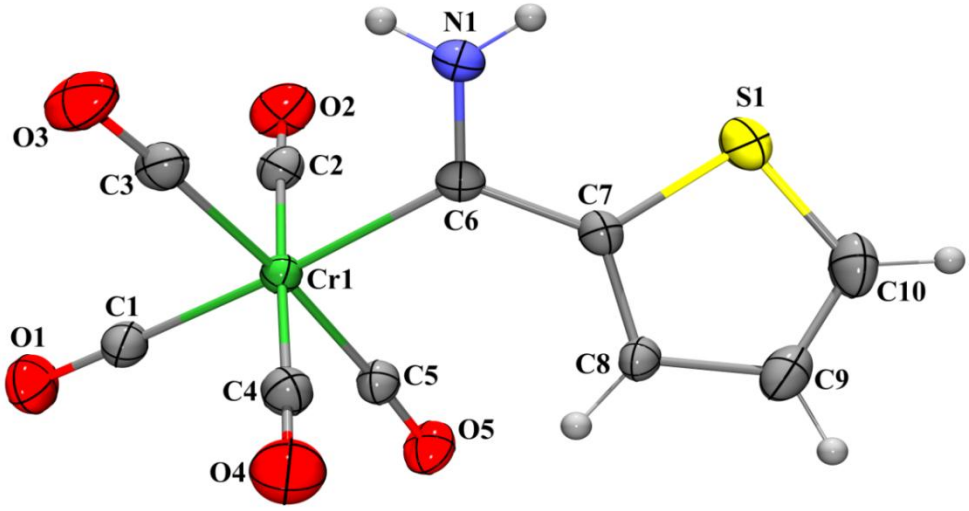

Figure 3.14. ORTEP + POV-Ray plot of the structure of complex **A**

The carbene complexes were found in a slightly distorted octahedral arrangement. The thiophene and furan moieties were coplanar to the amino substituent in each case.

Table 3.7. Selected bond lengths for complexes **A** and **B**

Bond definition	**Bond lengths (Å)**	
	Complex A	**Complex B**
Cr(1)-C(1)	1.8738(14)	1.8767(14)
Cr(1)-C(6)	2.0912(13)	2.0912(13)
C(6)-N(1)	1.3169(17)	1.3147(16)
C(6)-C(7)	1.4656(18)	1.4520(17)
C(7)-C(8)	1.4198(18)	1.3595(18)
C(7)-O(6)	-	1.3868(15)
C(8)-C(9)	1.4203(19)	1.4194(19)
C(9)-C(10)	1.359(2)	1.333(2)
C(10)-O(6)	-	1.3582(16)
C(7)-S(1)	1.7366(13)	-
C(10)-S(1)	1.6907(19)	-
C(1)-O(1)	1.1439(18)	1.1482(14)

© University of Pretoria

Table 3.8. Selected bond angles for complexes **A** and **B**

Angle definition	Bond angles (°)	
	Complex A	**Complex B**
C(1)-Cr(1)-C(4)	91.29(6)	86.95(6)
Cr(1)-C(6)-C(7)	125.61(9)	124.19(9)
C(7)-S(1)-C(10)	92.64(8)	-
C(7)-O(6)-C(10)	-	106.56(10)
C(1)-Cr(1)-C(6)	175.52(6)	177.85(6)
C(7)-C(6)-N(1)	113.12(12)	112.44(11)

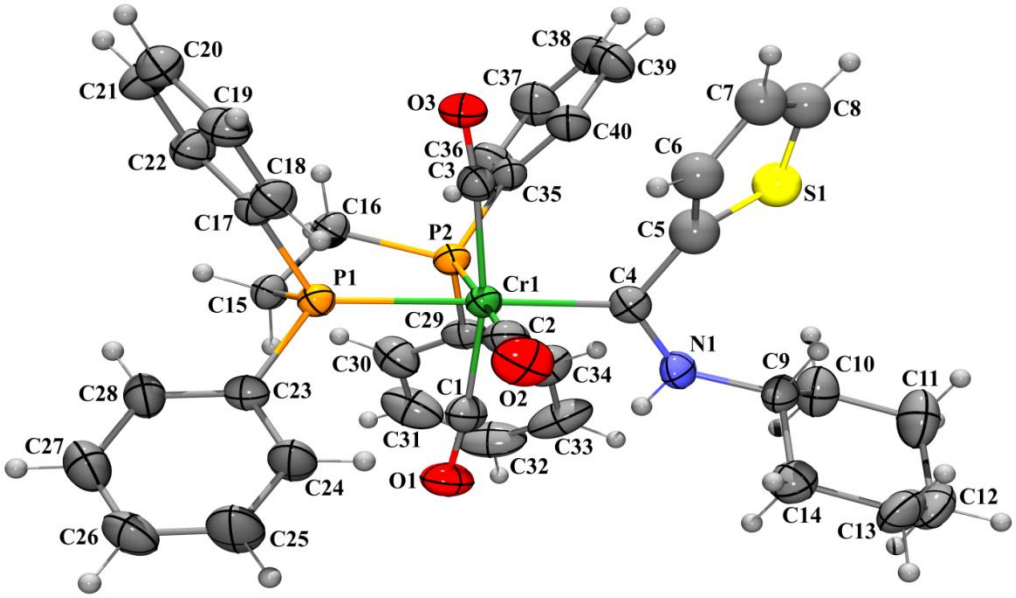

Figure 3.15. ORTEP + POV-Ray plot of the structure of complex **6**

Figure 3.15 displays the ORTEP + POV-Ray plot of complex **6**. The crystal structure confirmed not only the presence of an amino carbene substituent, but also the fact that two carbonyl ligands have been substituted for a bidentate phosphine group.

The carbene bond length of complex **6** was determined to be 2.035(5) Å, which is comparable to that of both aminocarbenes **A** and **B,** but elongated in comparison with the ethoxycarbenes (**1**-**3**). The elongation can be ascribed to the double bond characteristics of the C(4)-N(1) bond which results in the lengthening of the metal-carbene bond, producing a

© University of Pretoria

connection more closely resembling a single bond.[15] The complex had an average calculated carbonyl bond length of 1.155 Å with a bidentate ligand bite angle of 84.03 (5)°.

There were a total of eight molecules per unit cell and the crystal displayed a larger unit cell in comparison with complexes **A** and **B**. The complex crystallised in a pattern similar to that of complex **1**, with DCM asymmetric units packed in between the molecules of complex **6**. An additional anomaly of the complex is an asymmetric hydrogen molecule located as part of the single molecular structure. Figure 3.16 displays key aspects of the ellipsoid structure of Complex **6** and selected bond lengths and angles are summarised in Table 3.9.

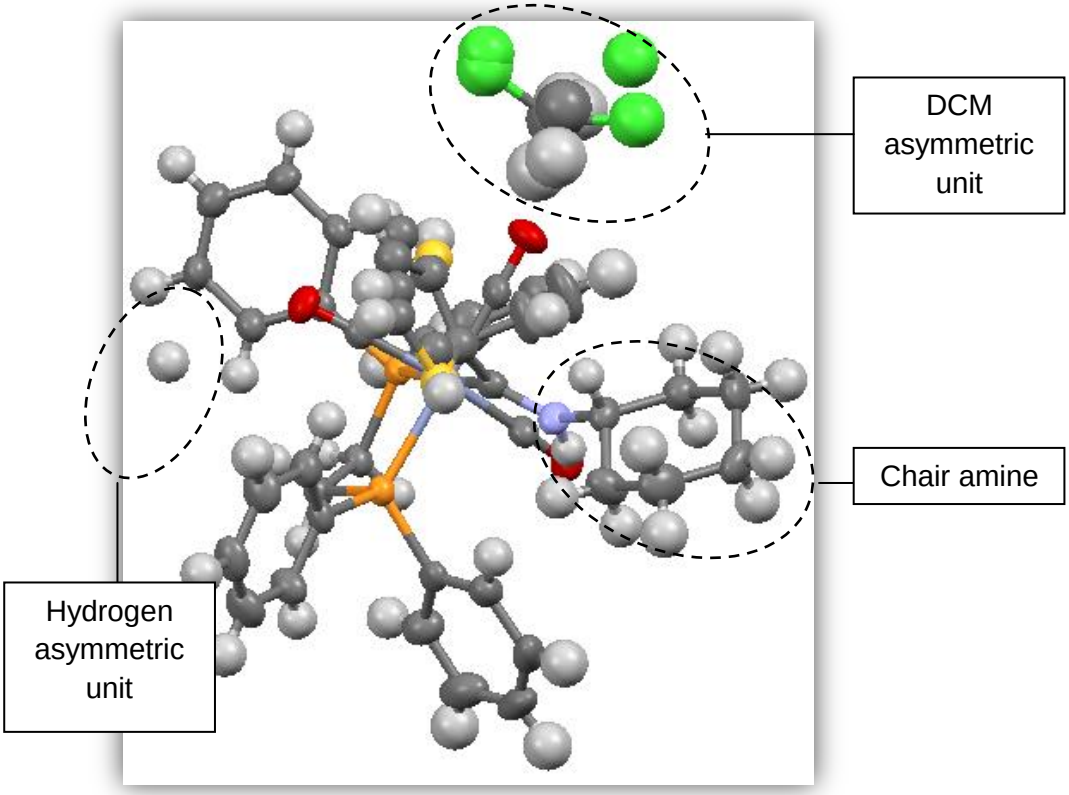

Figure 3.16. Ellipsoid structure of complex **6**

© University of Pretoria

Table 3.9. Selected bond lengths and angles for complex **6**

Bond definition	Bond length (Å)	Angle definition	Bond angle (°)
Cr(1)-P(1)	2.3109(15)	C(3)-Cr(1)-P(1)	84.77(15)
Cr(1)-P(2)	2.3558(15)	P(1)-Cr(1)-P(2)	84.03(5)
Cr(1)-C(3)	1.887(6)	C(8)-S(1)-C(5)	98.8(4)
C(4)-C(5)	1.498(8)	C(4)-Cr(1)-P(2)	97.85(14)
C(5)-C(6)	1.412(11)	C(5)-C(4)-N(1)	113.4(5)
C(6)-C(7)	1.387(12)	C(3)-Cr(1)-C(1)	168.8(2)
C(7)-C(8)	1.313(11)	-	-
C(1)-O(1)	1.151(6)	-	-
Cr(1)-C(4)	2.035(5)	-	-
S(1)-C(5)	1.685(6)	-	-
S(1)-C(8)	1.545(9)	-	-

Reinheimer *et al.*[17] successfully synthesised and obtained crystal structures for multiple dppe coordinated amino carbene complexes of chromium. Both pyrrolidino and dimethylamino carbene complexes of chromium containing dppe or 1,3-bis(diphenylphosphino)propane (dppp) were synthesised in a *fac/mer* isomeric mixture. Crystal structure studies indicated dppe amino carbenes crystallised in the monoclinic crystal system and favoured the *fac* isomer. The space groups determined corresponding to the crystal structure were P21/n and P21/c for the pyrrolidino and dimethylamino complexes, respectively. By contrast, the crystal structure of complex **6** crystallised in the orthorhombic crystal system and favoured the *mer* isomer. The crystal structures of complexes **A** and **B** both crystallised in the monoclinic crystal system with P2(1)/n space group and are comparable to the pentacarbonyl metallocene aminocarbenes synthesised by Siemeling *et al.*[18] (Figure 3.17)

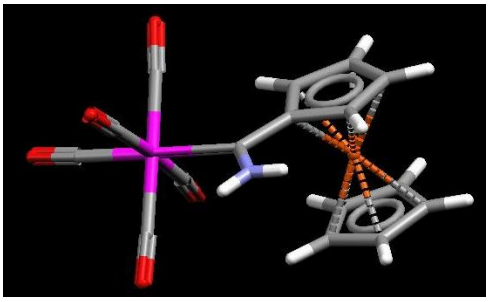

Figure 3.17 Amino carbene synthesised by Siemeling

[18] Siemeling, U., Färber, C., Bruhn, C., Fürmeier, S., Schulz, T., Kurlemann, M., Tripp, S., *Eur. J. Inorg. Chem.* **2011**, 0000.

© University of Pretoria

3.3.4 Mass spectrometry

Mass spectrometry analyses were done for complexes **A, B, 4, 5, 6, 7** and **9** and the results obtained are reported in Table 3.10.

Table 3.10. Mass spectrometry fragmentation of complexes **A–7**

Fragment	A	B	4	5	6	7	9
	m/z	m/z	m/z	m/z	m/z	m/z	m/z
M^+	301	286	385	369	730	716	809
$-NH_2$	289	270	-	-	-	-	-
-(CO)	273	258	357	341	702	686	781
-2(CO)	245	230	329	313	674	658	753
-3(CO)	218	203	301	285	645	629	725
-4(CO)	190	174	273	256	-	-	-
-5(CO)	165	146	244	229	-	-	-
-3(CO), Tf/Fr/Bt	-	-	-	-	510	510	560
-3(CO), S	-	-	-	-	463	463	463
-3(CO), S	-	-	-	-	451	451	-

S= carbene substituents

The fragmentation of **A**, **B**, **4** and **5** follows a trend of consecutive loss of the carbonyl ligands. The pattern for **6**, **7** and **9** however, follows the same trend as indicated in chapter 2. The results indicate that the molecular ion forms fragments with the loss of a carbonyl ligand, followed by the carbene substituents and lastly by the carbene carbon atom itself. Since the fragmentation pattern corresponds to that of the complexes in chapter 2, it clearly reinforces the deduction that the M-P bonds survive as a result of the strength of these bonds.

.

© University of Pretoria

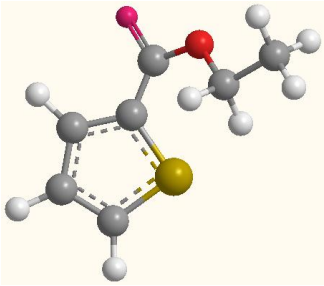

4 Synthesis of N-Heterocyclic Carbene Complexes

4.1 Background and Theoretical Synthesis

Arduengo carbenes have invoked extensive research interest since the discovery of the diverse chemical reactivity displayed by these novel molecules. The implementation of these ligands as phosphine mimics has continued to arouse interest in catalysis engineering and modification.[1] In comparison with the classic phosphine analogues, NHC ligands are significantly lower in toxicity[2] and form stronger coordination bonds to metals.[3] Arduengo

[1] (a) Weskamp, T., Böhm, V. P. W., Herrmann, W. A., *J. Organomet. Chem.,* **2000**, 600, 12. (b) Jafapour, L., Nolan, S. P., *Adv. Organomet. Chem.,* **2001**, 46, 181.

[2] (a) Waltman, A. W., Grubbs, R. H., *Organometallics*, **2004**, 23, 3105. (b) Dharmasena, U. L., Foucault, H. M., Dos Santos, E. N., Fogg, D. E., Nolan, S. P., *Organometallics*, **2005**, 24, 1056. (c) Hu, X., Castro-Rodriguez, I., Olsen, K., Meyer, K., *Organometallics,* **2004**, 23, 755. (d) Dorta, R., Stevens, E. D., Hoff, C. D., Nolan, S. P., *J. Am. Chem. Soc.,* **2003**, 125, 10490. (e) Nakai, H., Hu, X., Zakhorov, L. N., Rheingold, A. L., Meyer, K., *Inorg. Chem.,* **2004**, 43, 855. (f) Castarlenas, R., Esteruelas, N. A., Onate, E. *Organometallics*, **2005**, 24, 4343. (g) Buchgraber, P., Toupet, L., Guerchais, V., *Organometallics*, **2003**, 22, 5144. (h) Caddick, S., Cloke, F. G. N., Hitchcock, P. B., Lewis, A. K. D., *Angew. Chem., Int. Ed. Engl.,* **2004**, 43, 5824. (i) Danopoulos, A. A, Hankin, D. M., Wilkinson, G., Cafferkey, S. M., Sweet, T. K. N., Hursthouse, M. B., *Polyhedron*, **1997**, 16, 3879. (j) Voges, M. H., Rømming, C., Tilset, M., *Organometallics,* **1999**, 18, 529.

[3] Various PhD theses filed under the supervision of W. A. Herrmann (all Technische Universität München): (a) Mihalios, D., PhD thesis (**1992**). (b) Roesky, P. W., PhD thesis (**1994**). (c) Elison, M., PhD thesis (**1995**). (d) Fischer, J., PhD thesis (**1996**). (e) Artus, G. R. J., PhD thesis (**1996**). (f) Reisinger, C.-P., PhD thesis (**1997**). (g) Köcher, C., PhD thesis (**1997**). (h) Steinbeck, M., PhD thesis (**1997**). (i) Booβen, L. J. PhD thesis (**1997**). (j) Runte, O. PhD thesis (**2000**). (k) Weskamp, T.

© University of Pretoria

carbenes also display a broad range of chemical versatility by the substitution of the heteroatom substituents by different alkyl or aryl groups. These variations lead to differentiation in chirality, solubility and functionalisation possibilities.[4]

Various examples of NHC complexes of chromium(0) have been reported in the literature through the use of both metal carbonyl ligands and metallocene starting materials (see Figure 4.1 for examples).[5]

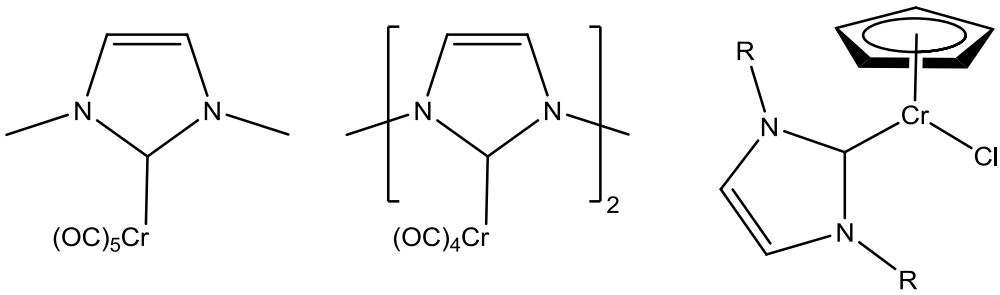

Figure 4.1. Examples of NHC complexes of Cr

N-heterocyclic carbene complexes (normal NHC complexes) have been extensively described in chapter 1. This chapter will thus focus on the properties and complexes of alternative versions of this class of compound.

4.1.1 Abnormal NHC complexes

In chapter 1, complexes containing diaminocarbene ligands were described, with the chemistry focusing mainly on the metalation on the central carbon atom flanked by heteroatoms. Abnormal NHC complexes arise when carbene formation by metalation is stabilised by only one heteroatom at a time. The NHC ligand is derived from an imidazolium cation and subsequent metalation is achieved at either carbon 4 or carbon 5, in comparison with the classic, normal NHC complexes.[6] Figure 4.2 clearly illustrates the different carbene formation possibilities for a given NHC ligand. The key factor in the formation of abnormal carbene complexes is the interplay of steric, electronic and kinetic considerations. Cases are

PhD thesis (**1999**). (l) Schwarz, J. PhD thesis (**2000**). (m) Böhm, V. P. W., PhD thesis (**2000**). (n) Köhl, F., J., PhD thesis (**2000**). (o) Prinz, M., PhD thesis (**2001**).

[4] (a) Hermann, W. A., Weskamp, T., Böhm, V. P. W., *Adv. Organomet. Chem.,* **2002**, 48, 1. (b) Bourissou, D., Guerret, O., Gabbaï, F. P., Bertrand, G., *Chem. Rev.,* **2000**, 100, 39.

[5] Herrmann, W. A., Weskamp, T., Böhm, V. P. W., *Adv. Organomet. Chem.,* **2001**, 48, 12–16.

[6] Arnold, P. L., Pearson, S., *Coord.Chem. Rev.,* **2007**, 251, 596–609.

© University of Pretoria

also noted where the counter-ion of the imidazolium salt, as well as the base utilised for deprotonation, play a significant role.[6]

The first example of an abnormal NHC complex was prepared and isolated by Crabtree *et al*. and was achieved by the reaction of N-(2-pyridylmethyl)-substituted imidazolium salt metalated with an iridium complex.[7]

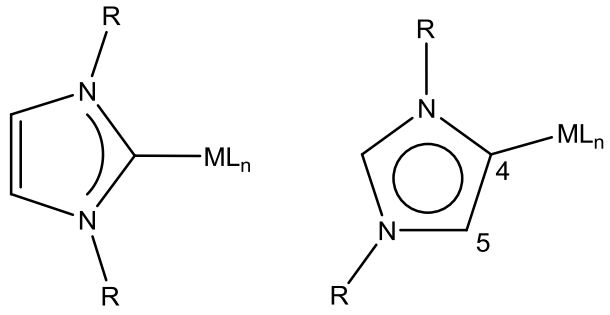

Figure 4.2. Structural classification of a normal NHC complex (left) *vs*. an abnormal NHC complex (right)

4.1.2 Remote NHC complexes (rNHCs)

In contrast to both normal and abnormal NHC complexes, remote NHCs contain no heteroatom directly neighbouring the carbene carbon. Despite the fact that complexes of these ligands have been synthesised, no free version has been isolated. Multiple rNHC complexes have been produced by Raubenheimer *et al.*[8] by oxidative addition of chloropyridinium cations to d^{10} metal spheres and calculations with regard to these complexes have shown that the carbene carbon-metal bond is stronger than the comparable complexes of normal NHCs.[8] Figure 4.3 shows the complexes prepared by Raubenheimer *et al.*[8] Remote NHC complexes of palladium have also been synthesised through oxidative addition of iodopyrazolium iodide to the metal by the Han and Huynh group.[9]

[7] Gründemann, S., Kovacevic, A., Albrecht, M., Faller, J. W., Crabtree, R. H., *Chem. Commun.,* **2001**, 2274–2275.
[8] (a) Meyer, W. H., Deetlefs, M., Pohlmann, M., Scholz, R., Esterhuysen, M. W., Julius, G. R., Raubenheimer, G. G., *J. Chem. Soc., Dalton Trans.,* **2004**, 413–420. (b) Schneider, S. K., Julius, G. R., Loschen, C., Raubenheimer, H. G., Frenking, G., Herrmann, W. A., *J. Chem. Soc., Dalton Trans.,* **2006**, 1226–1233. (c) Schneider, S. K., Roembke, P., Julius G. R., Loschen, C., Raubenheimer, H. G., Frenking, G., Herrmann, W. A., *Eur. J. Inorg. Chem.,* **2005**, 2973–2977. (d) Raubenheimer, H. G., Cronje, S., *J. Chem. Soc., Dalton Trans.,* **2008**, 1265–1272.
[9](a) Han, Y., Huynh, H. V., *Chem Commun.,* **2007**, 1089-1091. (b) Han, Y., Huynh, H. V., Tan, G. K., *Organometallics,* **2007**, 26, 6581–6585.

© University of Pretoria

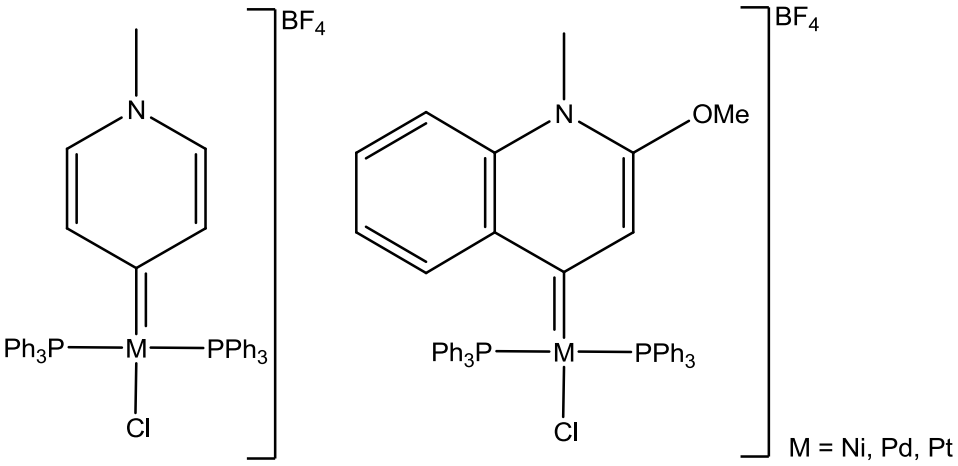

Figure 4.3. Remote NHC complexes prepared by Raubenheimer *et al.*

4.1.3 Synthesis of NHC complexes

As stated in chapter 1, there are multiple routes for the synthesis to both the free NHC ligand and the NHC complex. The synthesis of the free NHC ligand has been largely covered in chapter 1 (Section 1.4) and thus this chapter will focus more on the incorporation of the NHC ligand into a complex molecule. There is an extraordinarily large variety of transition metal-NHC complexes with a diverse range of both ligands and oxidation states. NHC ligands react with a broad series of organometallic precursors through direct addition or through substitution of two electron-donating ligands. Displacements of nitriles, phosphines, carbonyls, THF molecules, pyridines and dimethyl sulphide (DMS) have been noted as some of the most common ligands displaced by the NHC moiety.[10] Scheme 4.1 illustrates the typical approach of ligand substitution by free NHCs in metal complexes.

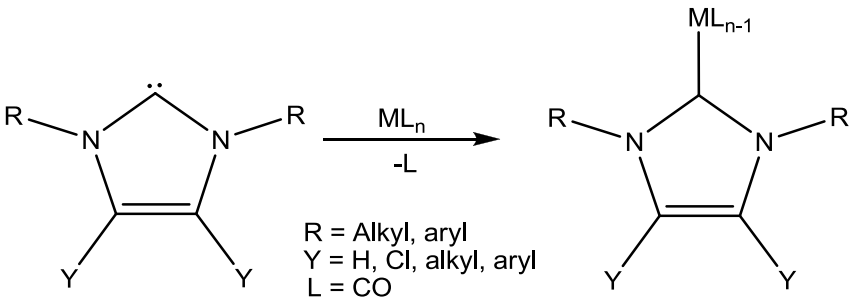

Scheme 4.1. Typical approach of ligand substitution by free NHCs in metal complexes

[10] De Frémont, P., Marion, N., Nolan, S. P., *Coord. Chem. Rev.,* **2009**, 253, 862–892

© University of Pretoria

Under thermal conditions, Wanzlick and Schönherr[11], and Öfele[12] produced NHC complexes by reacting metal carbonyl hydride complexes with an NHC ligand. The mechanism in Scheme 4.2 shows the substitution of a hydride substituent by the NHC ligand with liberation of hydrogen gas.[9,10] This reaction also produced the first ever example of a Cr(0) NHC complex.

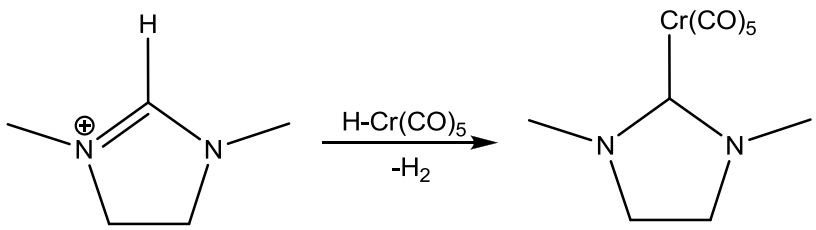

Scheme 4.2. First NHC complex synthesised by Wanzlick and Schönherr, and Öfele

As noted above, ligand exchanges in carbonyl complexes are possible (Scheme 4.3). Complexes such as $Cr(CO)_6$, $Mo(CO)_6$, $W(CO)_6$, $Fe(CO)_6$ or $Ni(CO)_4$ all have the ability to substitute either one or two carbonyl ligands for NHC fragments under thermal conditions; thereafter further substitution requires the utilisation of photolysis techniques.[13,14,15,16,17]

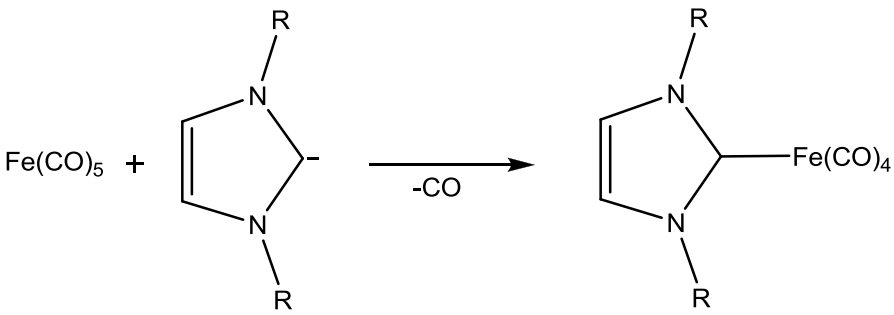

Scheme 4.3. Synthesis of an NHC complex through carbonyl substitution

[11] Wanzlick, H. W. Schönherr, H., J. *Angew. Chem.,* **1968**, 80,154.; *Angew. Chem. Int. Ed. Engl.,* **1968**, 7, 141
[12] Öfele, K., *J. Organomet. Chem.,* **1968,** 12, 42.
[13] Herrmann, W. A., Köcher, C., Gooβen, L. J., Artus, G. R. J., *Chem. Eur. J.,* **1996**, 2, 1627.
[14] Herrmann, W. A., Elison, M., Fischer, J., Köcher, C., Artus, G. R. J., *Chem. Eur. J.,* **1996**, 2, 772.
[15] Öfele, K., Herrmann, W. A., Mihalios, D., Elison, M., Herdtweck, E., Scherer, W., Mink, J., *J. Organomet. Chem.,* **1993**, 459, 177.
[16] Kuhn, N., Kratz, T., Boese, R., Bläser, D., *J. Organomet. Chem.,* **1994**.,470, C8.
[17] Kuhn, N., Kratz, T., Boese, R., Bläser, D., *J. Organomet. Chem.,* **1994**.,479, C32.

© University of Pretoria

This was also the technique employed in the synthesis of NHC complexes in this project. Subsequent metalation after deprotonation of the NHC fragment by a strong base leads to the desired complex.

Weakly coordinated η^5-cyclopentadienyl anions can also function as the base to deprotonate the imidazolium salts. Chromocene can react with imidazolium chloride in THF to produce a 14-electron complex [(η^5-C_5H_5)Cr(NHC)Cl] containing only a single cyclopentadienyl moiety (Scheme 4.4).[1] This synthetic route is also accessible for other metallocenes. Nickelocene generates the corresponding [(η^5-C_5H_5)Ni(NHC)Cl] via the same mechanism.[18]

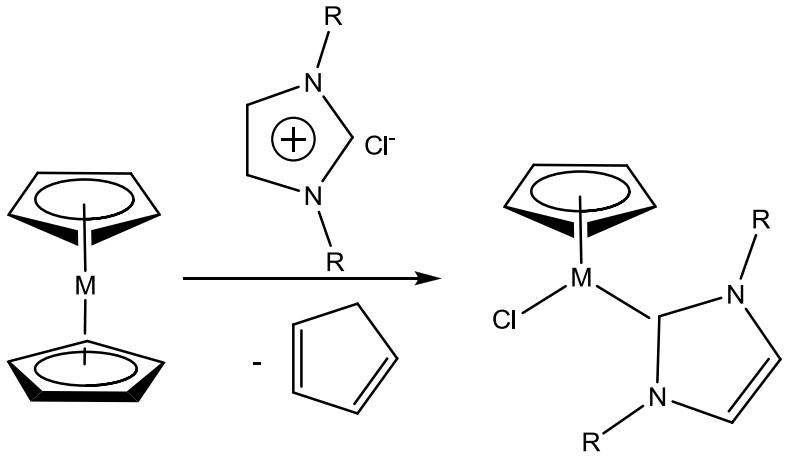

Scheme 4.4. NHC complex formation from metallocene precursor

2-Carboxylate NHC precursors (Figure 4.4) are both air stable and have the particular ability to transfer the NHC to a metal without the necessity for deprotonation by a base. At about 80 °C these compounds react with Rh, Ir, and Pd substrates to form NHC complexes in high yields, in less than an hour.[19]

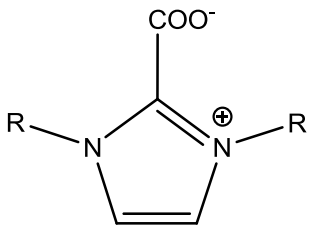

Figure 4.4. Structure of a 2-carboxylate NHC precursor

[18] Abernethy, C. D., Cowley, A. H., Jones, R. A., *J. Organomet. Chem.*, **2000**, 596, 3.
[19] Duong, H. A., Tekavec, T. N., Arif, A. M., Louie, J., *Chem. Commun.*, **2004**, 112.

© University of Pretoria

4.2 Synthesis

4.2.1 Focus

The synthesis of NHC ligand precursors is moderately uncomplicated and a number of these compounds are now commercially available. The increasing use of metal-containing NHC complexes in synthesis has led to a broad selection of techniques through which these complexes can be synthesised.[20] Numerous examples of chromium-containing NHC complexes have been reported.[11,12,21,22] Nonnenmacher *et al.*,[23] in particular, synthesised larger, bulkier Chromium(0) NHC complexes with an extended aromatic system (Figure 4.5). The carbene atom was found to be exceptionally rich in electron density, as proven by the ^{13}C NMR signal and the strong upfield shift that was observed.[23] *In situ* deprotonation of the NHC fragment with an external base in combination with either photolysis or thermal labilisation of metal carbonyl ligands proved an easy alternative to more strenuous synthetic procedures. By utilising THF solvent and photolysis conditions, the substitution of carbonyl ligands for a more labile THF moiety can be achieved. This labile THF ligand can, in turn, be subsequently substituted for an NHC ligand,[1] The main focus of this chapter was, firstly, to produce several novel pentacarbonyl Chromium(0) NHC complexes and, secondly, further functionalisation of these novel NHC compounds by substituting the remaining labile carbonyl ligands with bidentate counterparts (Figure 4.6).

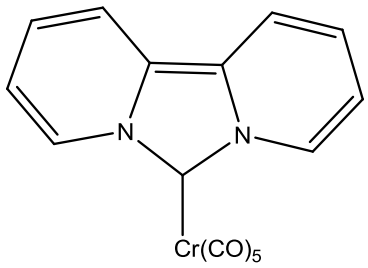

Figure 4.5. NHC carbene synthesised by Nonnenmacher *et al.*[23]

[20] (a) Viciano, M., Mas-Marzá, E., Poyatos, M., Sanaú, M., Crabtree, R. H., Peris, E., *Angew. Chem., Int. Ed. Engl.,* **2005**, 44, 444. (b) Arduengo, A. J., Tamm, M., McLain, S. J., Calabrese, J. C., Davidson, F., Marshall, W. J., *J. Am. Chem. Soc.,* **1994**, 116, 7927. (c) Lin, I. J. B., Vasam, C. S., *Comments Inorg. Chem.,* **2004**, 25, 75. (d) Lappert, M., Pye, P., Mclaunghlin, G., *J. Chem. Soc., Dalton Trans.,* **1977**, 1271. (e) Centikaya, B., Dixneuf, P., Lappert, M. F., *J. Chem. Soc., Dalton. Trans.,* **1974**, 1827. (f) Trnka, T. M., Morgan, J. P., Sanford, M. S., Wilhelm, T. E., Schroll, M., Choi, T. L., Ding, S., Day, M. W., Grubbs, R. H., *J. Am. Chem. Soc.,* **2003**, 125, 2546. (g) Csihony, S., Culkin, D. A., Sentman, A. C., Dove, A. P., Waymouth, R. M., Hedrick, J. L., *J. Am. Chem. Soc.,* **2005**, 127, 9079.

[21] Herrmann, W. A., Michalios, D., Öfele, K., Kiprof, P., Belmedjahed, F., *Chem. Ber.,* **1992**, 125, 1795.

[22] Öfele, K., Hermann, W. A., Mihalios, D., Elison, M., Herdtweck, E., Priermeier, T., Kliprof, P., *J. Organomet. Chem.,* **1995**, 498, 1.

[23] Nonnenmacher, M., Kunz, D., Rominger, F., Oeser, T., *J. Organomet. Chem.,* **2005**, 690, 5647.

© University of Pretoria

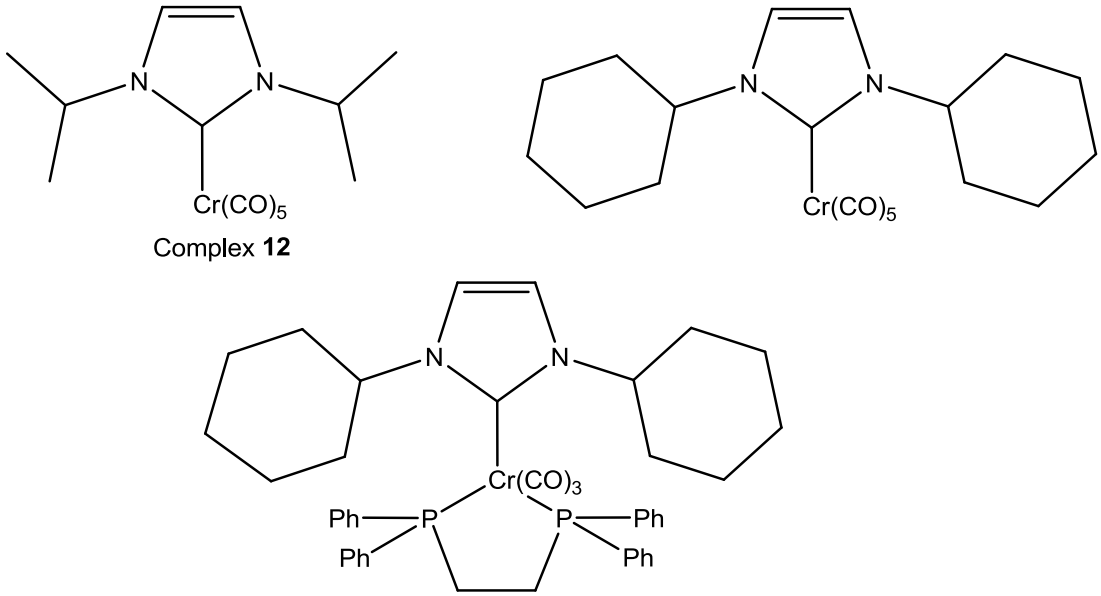

Figure 4.6. Proposed NHC complexes

Several different methods were attempted to produce stable monocarbenes with sufficient yields to enable reliable characterisation data to be obtained. First the NHC ligand had to be synthesised. Deprotonation by a strong base and the subsequent reaction with a metal carbonyl substrate resulted in the formation of the target complex.

4.2.2 Synthetic methodology

4.2.2.1 Synthesis of 1,3-bis(cyclohexyl)imidazolium chloride

Synthesis of imidazolium salts follows a relatively simple and reliable two-step method[24,25] (Scheme 4.5). The Schiff base (glyoxal-bis(cyclohexyl)imine) is synthesised in the first step by the reaction of the corresponding primary amine (cyclohexyl amine, 71 mmol) and glyoxal (40 %, 28 mmol, 4 ml) in water to produce a white shiny solid. The second reaction step involves the condensation of paraformaldehyde (5 mmol) with the imine (5 mmol) and finally acidification by the addition of HCl (1 ml, 4 M) in dioxane. The reaction produces an off-white solid precipitate after 4-7 days of stirring. This is filtered off and washed with cold diethyl

[24] (a) Arduengo, A. J., Harlow, R. L., Kline, M., *J. Am. Chem. Soc.,* **1991**, 113, 361. (b) Arduengo, A. J., Kline, M., Calabrese, J. C., Davidson, F., *J. Am. Chem. Soc.,* **1991**, 113, 9704. (c) Arduengo, A. J., Krafczyk, R., Schmutzler, R., Craig, H. A., Goerlich, J. R., Marshall, W. J., Unverzagt, M., *Tetrahedron*, **1999**, 55, 14523.
[25] (a) Jafarour, L., Steven, E. D., Nolan, S. P., *J. Organomet. Chem.,* **2000**, 606, 49. (b) Hintermann, L., J., *Org. Chem.* **2007**, 3, 22. (c) De Frémont, P., Scott, N. M., Steven, E. D., Ramnial, T., Lightbody, O. C., MacDonald, C. L. B., Clybure, J. A. C., Nolan, S. P., *Organometallic,* **2005**, 24, 6301.

© University of Pretoria

ether and THF. The off-white solid is then recrystallised from ethanol and diethyl ether and produces a white solid.

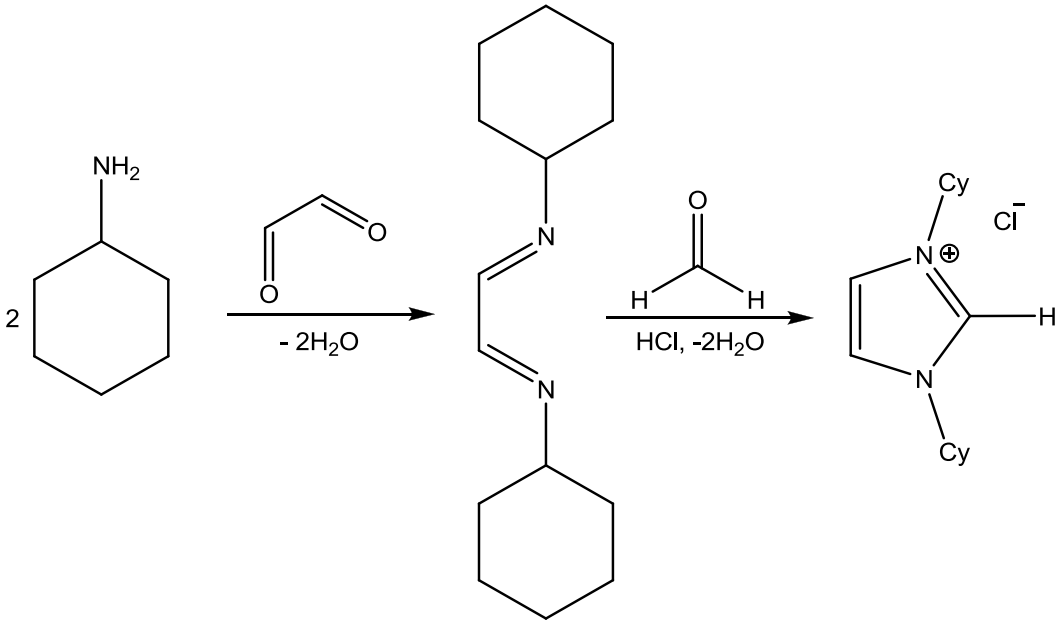

Scheme 4.5. Synthesis of 1,3-bis(cyclohexyl)imidazolium chloride

4.2.2.2 Synthesis of pentacarbonyl chromium NHC complexes

Synthesis of NHC complexes requires the combination of the in situ deprotonated imidazolium salt and [$Cr(CO)_5(THF)$], prepared by the photolysis of $Cr(CO)_6$ in THF. In this study the NHC precursors (imidazolium salts) were deprotonated either by potassium *tert*-butoxide or n-BuLi at -30 °C for 30 minutes. Photolysis of the hexacarbonyl chromium was achieved by dissolving the complex in a 40 ml dry hexane:10 ml dry THF solution under inert conditions. The solution was irradiated for 30 min, after which the orange solution was cooled to -30 °C and the deprotonated NHC precursor gradually added. The solvent was removed under vacuum and the reaction yielded a yellow solid (Scheme 4.6). A persistent pink by-product was obtained in each case and in initial reactions observed to be the major product. Deprotonation with either of the strong bases under varied temperatures all produced this pink by-product and only by applying an excess of strong bases was this pink by-product observed as a trace contaminant. It is only suspected that excess HCl contaminated the imidazolium salt, breaking down the NHC complex to produce product **13.** The formation of **13** is circumvented only through neutralisation by excess base. The imidazolium salt was recrystallised from an ethanol and diethyl ether solution and, in addition, placed under high vacuum to remove excess acid together with any moisture

© University of Pretoria

obtained through storage. The additional precautions ensured the formation of the yellow NHC complex as the major product and limited the pink coordination complex to a trace contaminant. Literature on the possible origin or characteristics of this pink product has proved elusive. Other synthetic methods were also experimented with but proved less viable and often led to low yields, no reaction or severe oxidation of the metal complex. A silver transfer reaction was attempted. However, after the silver NHC complex had been produced, the transfer of the NHC fragment to the hexacarbonyl chromium failed. The decomposition of the NHC ligand to produce the bidentate cyclohexyl amine ligand and subsequent coordinates to the metal centre, produced product **13**.

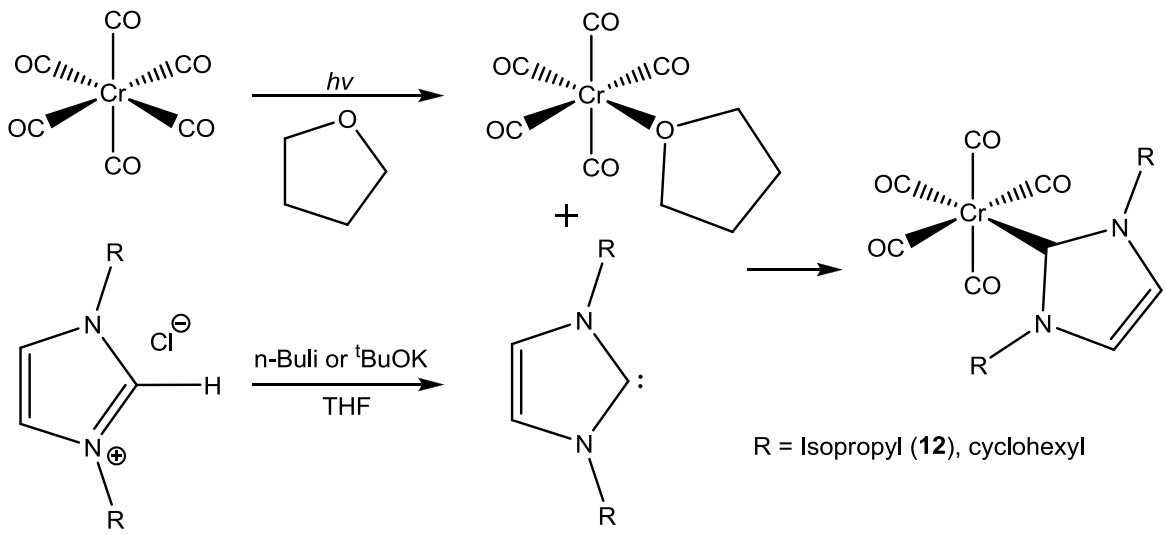

Scheme 4.6. Synthesis of NHC complexes

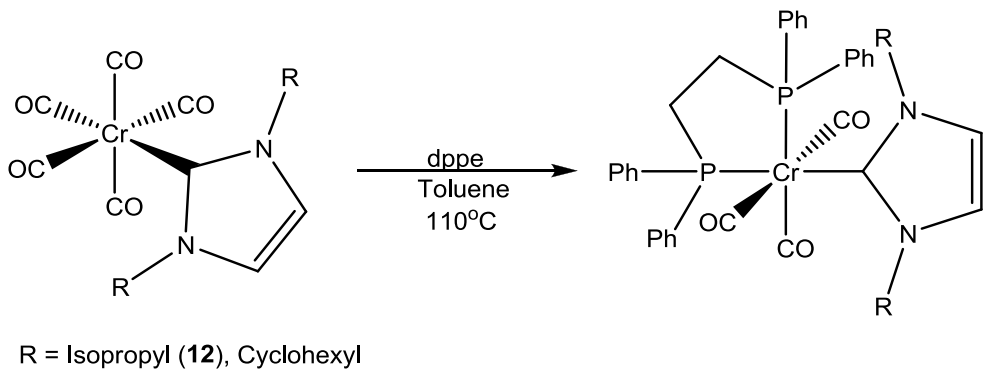

Scheme 4.7. Proposed modification of NHC complexes

Unfortunately, due to severe decomposition, only **12** could be obtained in sufficient yields for characterisation. Further modification of the NHC complexes was attempted, aimed at the substitution of two labile carbonyl ligands for the bidentate ligand dppe (Scheme 4.7). The

© University of Pretoria

NHC complex was dissolved in toluene and reacted with the dppe ligand but no reaction ensued. Kim *et al.* also attempted substitution of carbonyl ligands after the NHC complex had formed, but also had no success in producing a higher substituted NHC compound.[26]

4.3 Characterisation

The NHC complex **12** as well as the by-product (**13**), were fully characterised using deuterated solutions for NMR spectroscopy, KBr pellets for IR spectroscopy, and solid state crystals for X-ray crystallography.

4.3.1 NMR spectroscopy

^{1}H NMR spectroscopy

One of the most applicable methods for the synthesis of free and coordinated NHC complexes relies on the deprotonation of the equivalent azolium salt by a strong base. The resulting carbene is characterised by the disappearance of the acidic proton in the ^{1}H NMR spectrum.[27] The ^{1}H NMR data of the imidazolium salt precursor and complex **12** are presented in Table 4.1.

Table 4.1. ^{1}H NMR data of the imidazolium salts

Complex

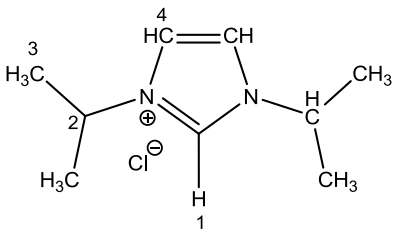

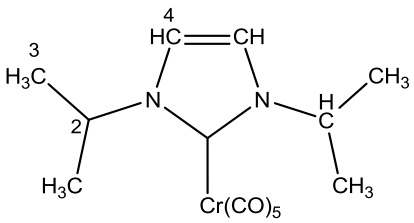

Proton assignment	Imidazolium salt		**12**	
	Chemical shift (δ, ppm)	**Coupling constant (J, Hz)**	**Chemical shift (δ, ppm)**	**Coupling constant (J, Hz)**
H_1	10.96 (s)	-	-	-
H_2	4.93 (h)	6.6	5.34 (m)	-
H_3	1.54 (d)	6.7	1.62 (d)	3.7
H_4	7.48 (s)		7.90 (s)	-

Solvent: $CDCl_3$

[26] Kim, S., Choi, S. Y., Lee, Y. T., Park, K. H., Sitzmann, H., Chung, Y. K., *J. Organomet. Chem.*, **2007**, 692, 5390–5394.
[27] Tapu, D., Dixon, D. A., Roe, C., *Chem. Rev.*, **2009**, 109, 3385–3407.

© University of Pretoria

The key difference between saturated vs. unsaturated NHC complexes lies in the alkene double bond fragment incorporated into the cyclic ring. Numerous articles typically place the chemical shift of the unsaturated carbon protons at δ = 8.56 ppm,[28] while H_1 is found at δ = 8.56 ppm.[28] The major difference between the chemical shifts observed between the imidazolium salt and **12** is the clear downfield shift of the protons associated with the carbene complexes. The disappearance of the single peak above δ = 10 ppm serves as a clear indication that the deprotonation step was successful. Both the disappearance of the NCHN proton peak and the downfield shift in proton peaks serve as indications that the carbene complex has formed. Table 4.2 present the ^{1}H NMR data of **13** which was obtained as the major product in the synthesis of the NHC complex.

Table 4.2. ^{1}H NMR data of **13**

Coordination Complex

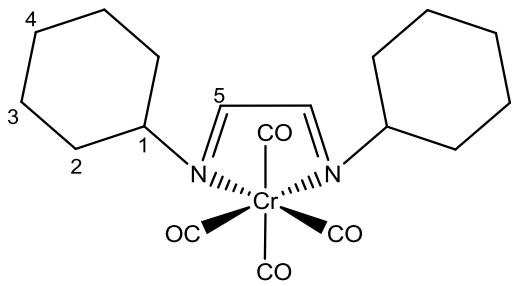

Proton assignment	13 Chemical shift (δ, ppm)	Coupling constant (J, Hz)
H_1	2.40 (t)	9.9
H_2	1.57-1.78 (m)	-
H_3	1.10-1.21 (m)	-
H_4	1.38-1.53 (m)	-
H_5	4.66 (s)	-

Solvent: $CDCl_3$

^{13}C NMR spectroscopy

On deprotonation of the imidazolium salt, a significantly downfield-shifted carbon peak is observed in correlation to the protonated precursor. The carbonic N-C-N carbon atom is typically witnessed in the range δ = 206-220 ppm for the unsaturated free carbenes, usually

[28]Arduengo III, A. J., Krafczyk, R., Schmutzler, R., *Tetrahedron*,**1999**, 55, 14523–14534.

© University of Pretoria

shifted by 75-88 ppm downfield from the protonated salt.[29,30,31,32] Substitution on the heteroatoms exerts minute influences on the chemical shifts, although saturation of the ring carbons does play a role in the shifts as well. The single-triplet energy gap becomes minor upon saturation of the C-C bond, since five-centre, six-electron π-delocalisation as a stabilising factor is no longer feasible.[27] Saturated imidazol-2-ylidenes show resonances for the carbene centre shifted further downfield and peaks located between 236 and 244 ppm. This is consistent with a higher anisotropy at the carbene centre, due mainly to the carbene p_{π}-orbital containing a lower density of electrons.[27] Table 4.3 gives the carbon chemical shifts for the imidazolium salt and NHC complex **12.**

Table 4.3. ^{13}C NMR data of the imidazolium salt and corresponding complex **12**

Complex

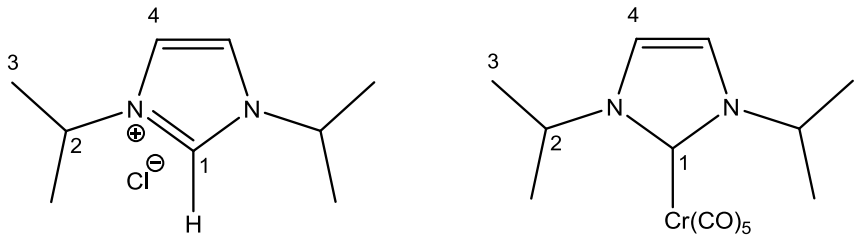

Carbon	1,3-Bis(isopropyl)imidazolium chloride **Chemical shift (δ, ppm)**	**12*** **Chemical shift (δ, ppm)**
C1	136.2	189.9
C2	53.2	54.9
C3	23.1	23.2
C4	119.7	129.6
CO (*cis*)	-	215.9
CO (*trans*)	-	226.1

Solvent : $CDCl_3$, *d-Acetone

Tapu *et al.* reported the carbene carbon shifts of both the free and ligated carbenes bearing isopropyl and cyclohexyl substituents on the heteroatoms.[27] The free carbene, containing an isopropyl substituent, presented a shift of 210.5 ppm, while a cyclohexyl N-ligated NHC showed a slightly lower shift of 210.1 ppm. On complexation with a metal fragment, the

[29]Arduengo, A. J., Bock, H., Chen, H., Denk, M., Dixon, A. D., Green, J. C., Herrmann, W. A., Jones, N. L., Wagner, M., West, R., *J. Am. Chem. Soc.,* **1994**, 116, 6641.
[30]Nieheus, M., Kehr, G., Erker, G., Wibbeling, B., Fröhlich, R., Blacque, O., Berke, H., *J. Organomet. Chem.,* **2002**, 663, 192.
[31] Alder, R. W., Blake, M. E., Bortolotti, C., Bufali, S., Butts, C. P., Linehan, E., Oliva, J. M., Orpen, A. G., Quayle, M. J., *Chem. Commun.*, **1999**, 241.
[32]Saravanakumar, S., Kindermann, M. K., Heinicke, J., Köckerling, M., *Chem. Commun.,* **2006**, 640.

© University of Pretoria

electron density is displaced towards the metal centre through σ-donation and thus results in a dislocation of the chemical shift to a downfield position.[27] Group trends in metal-carbene formation are also visible. Metal-ligated NHC complexes of group 6 metals (Cr, Mo, W) show upfield shifts of the carbene fragment upon replacement of lighter metal spheres with heavier counterparts.[27] ^{13}C NMR data of complex **13** is presented in Table 4.4.

Table 4.4. ^{13}C NMR data of **13**

Coordination Complex

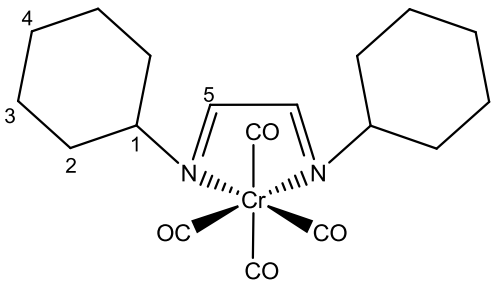

Carbon	13 Chemical shift (δ, ppm)
C1	63.8
C2,	34.4
C3	25.6
C4	25,8
C5	116.7
CO (*cis*)	217.1
CO (*trans*)	217.40

Solvent: $CDCl_3$

The ^{13}C spectra obtained from the NHC carbene did not indicate the presence of the carbene peak. Both NHC complexes were fairly unstable in solution at room temperature and thus reliable ^{13}C NMR spectra seemed difficult to obtain. The complexes decomposed in a variety of deuterated solvents and ultimately resulted in poor spectra. Carbonyl groups as well as the NHC carbons were visible and provided certainty that the complex did indeed form prior to decomposition. The *trans* carbonyl peak of complexes **12** were δ = 226.1 ppm and fell within the literature range.[23]

© University of Pretoria

4.3.2 Infrared spectroscopy

In a comparable approach and method, IR spectroscopy with predictable carbonyl patterns was utilised to provide structural data on all the NHC products synthesised. A complete theoretical argument on the ν_{CO} of the five carbonyl complexes was previously given in chapter 2. KBr pellets were utilised to characterise products **12** to minimise considerations of polarity and complexity of solubility. Table 4.5 summarises the key stretching frequencies. The $A_1^{(1)}$ band features a lower stretching frequency in the comparison to the typical 2060 cm^{-1} domain as expected for pentacarbonyl chromium complexes. Complex **13** shows four individual frequencies corresponding to the $A_1^{(1)}$, B_1, $A_1^{(2)}$ and the very strong E vibrational bands. The stretching frequencies of complex **12** are lower than those found by Nonnenmacher *et al.* but illustrate pentacarbonyl chromium carbene complexes[23] with IR carbonyl vibration bands at 2053, 1970 and 1899 cm^{-1}.

Table 4.5. The stretching frequencies for complexes **12** and **13**

Band **Stretching vibrational frequencies ν_{CO}, cm^{-1}**

	12	**13**
$A_1^{(1)}$	2031 (m)	2011 (m)
B_1	n.o.	1922 (vs)
$A_1^{(2)}$	1895 (s)	n.o.
E	1867 (vs)	-
B_2	-	1866 (m)

4.3.3 X-ray crystallography

Single crystals were obtained for complexes **13** and **15**. Complex **13** was the major product of the NHC complex synthesis and the pink, prismatic crystals acquired from diffusion of DCM and hexane and **15** from a hexane and ether diffusion. Finally, the molecular structures were confirmed by single-crystal X-ray diffraction (Figure 4.7 and Figure 4.9).

© University of Pretoria

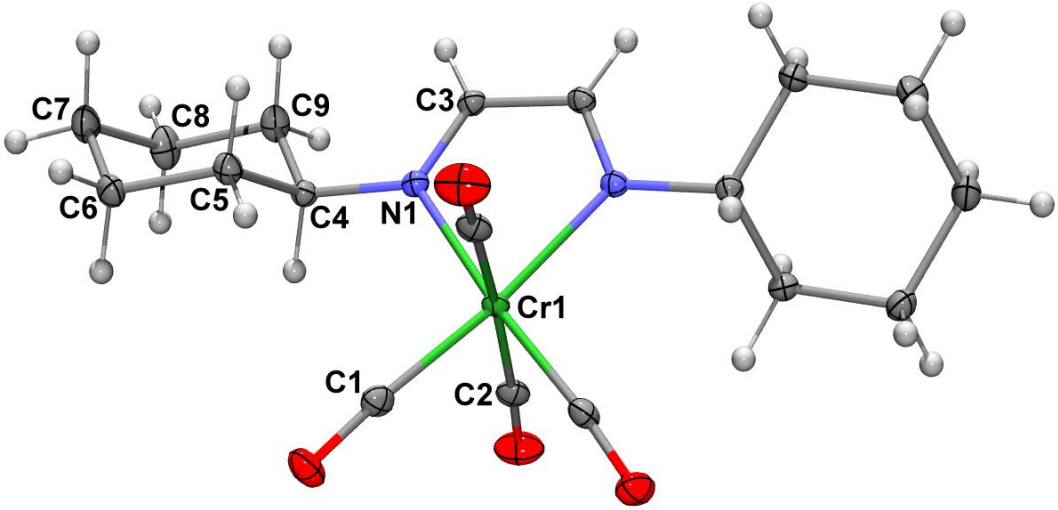

Figure 4.7. ORTEP + POV-Ray plot of the structure of Complex **13**

Complex **13** crystallised in a monoclinic crystal system with four units per cell and the space group was determined to be C2/c. The octahedral geometry is slightly distorted, with the angle between the carbonyl ligands being smaller than the expected 90° but larger between the carbonyl ligand and the *cis* nitrogen group. The two chair substituents on the nitrogen atoms are orientated perpendicular to one another to limit steric interaction and the bite angle produced by the bidentate ligand was measured to be 76.08(5)°. The average carbonyl bond length was calculated as 1.15225 Å with individual carbonyl lengths for C(1)-O(1) and C(2)-O(2) measured at 1.1622(15)Å and 1.423(16) Å, respectively.

The full crystal data for complex **13** are given in Appendix H. Selected bond lengths and angles for complex **13** are summarised in Table 4.6.

Table 4.6. Selected bond lengths and angles for complex **13**

Bond	Bond length (Å)	Angle	Angle (°)
Cr-C(1)	1.8472(12)	C(1)-Cr-N(1)	98.60(4)
Cr-C(2)	1.9103(12)	C(2)-Cr-N(1)	89.35(4)
Cr-N(1)	2.0927(10)	C(1)-Cr-N'(1)	173.79(4)
C(3)-C'(3)	1.453(2)	N(1)-Cr-N'(1)	76.08(5)

© University of Pretoria

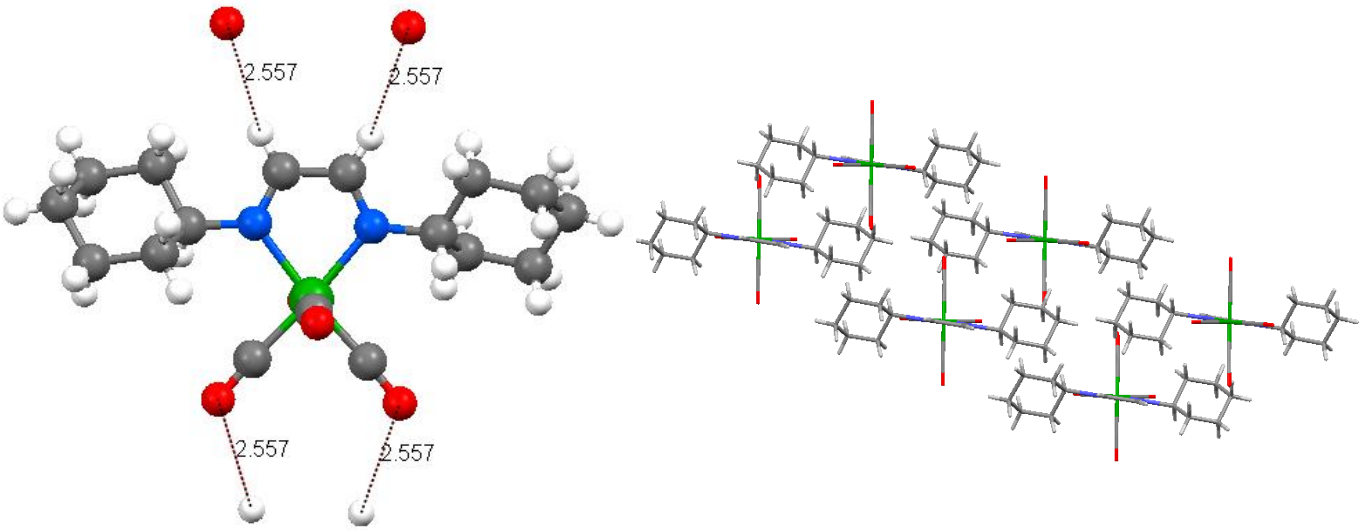

Hydrogen bonding **Packing pattern**

Figure 4.8. Intermolecular interactions in complex **13**

As shown in Figure 4.8, the main feature of intermolecular interaction in **13** is hydrogen bonding resulting in the packing pattern observed. The hydrogen interaction with a sister molecule in close proximity is only witnessed to a limited extent and the main interaction takes place between the carbonyl ligand's oxygen and the alkene fragment's hydrogen atoms. The bond distance between the participants was measured to be 2.557 Å. The packing pattern, in turn, shows a grid-type arrangement in which individual molecules will form square orientations, producing a network of grids.

Complex **15** was produced as the major yellow product in the attempt to synthesise a cyclohexyl NHC complex and crystallised in a monoclinic crystal system with sixteen units per cell. The space group was determined to be C2. The octahedral geometry is slightly distorted, with the angle between the carbonyl ligands being smaller than the expected 90°. Due to symmetry restrictions, the unit cell has four discrete molecules as shown in Figure 4.9. The average carbonyl bond length was calculated as 1.15225 Å with individual carbonyl lengths for C(1)-O(1) and C(2)-O(2) measured at 1.1622(15)Å and 1.423(16) Å, respectively. The full crystal data for complex **15** is given in Appendix I. Selected bond lengths and angles for complex **15** are summarised in Table 4.7.

© University of Pretoria

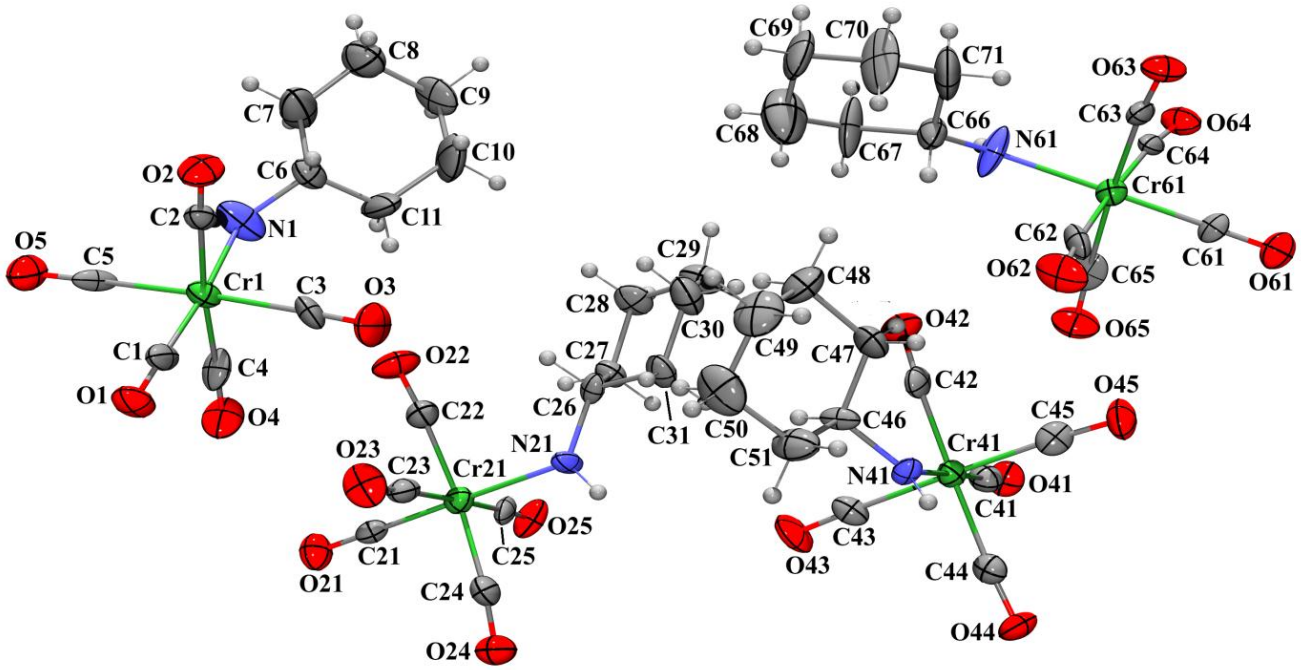

Figure 4.9. Intermolecular interactions in complex **15**

Table 4.7. Selected bond lengths and angles of complex **15**

Bond	Bond length (Å)	Angle	Angle (°)
Cr-C(1)	1.817(12)	C(1)-Cr-C(4)	88.2(5)
Cr-C(2)	1.886(12)	C(1)-Cr-C(2)	91.3(5)
Cr-C(3)	1.891(12)	C(4)-Cr-C(2)	174.6(5)
Cr-C(4)	1.863(12)	C(1)-Cr-C(3)	89.2(5)
Cr-C(5)	1.904(12)	C(1)-Cr-N(1)	174.9(4)
Cr-N(1)	2.171(12)	C(4)-Cr-N(1)	92.4(4)

Figure 4.10 illustrates the dissecting plane through the central metal and carbonyl ligands as well as hydrogen interactions present between molecules. The planes clearly show the close resemblance to a perfect octahedron with only slight distortions while the H-interaction indicates intermolecular forces.

© University of Pretoria

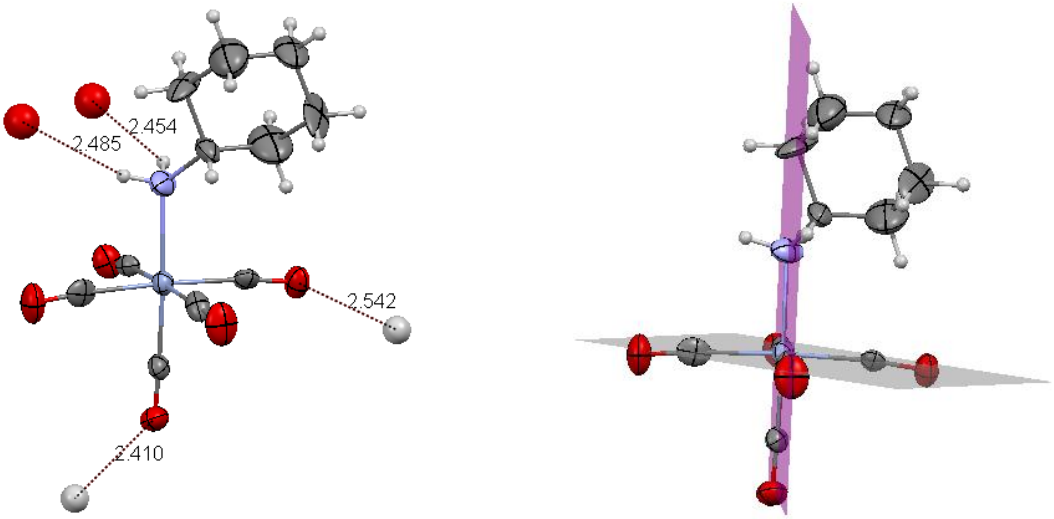

Figure 4.10. Structural properties of complex **15** (H-interactions left, dissecting planes right)

4.3.4 Mass spectrometry

A mass spectrometry analysis was done for complex **12** and the results obtained are reported in Table 4.8.

Table 4.8. Mass spectrometry fragmentation of complex **12**

Fragment	12
	m/z
M^+	344.2472
-5(CO)	154.1446
-5(CO), R(Iso)	111.0938

R(Iso)= isopropyl N-substituent

The fragmentation pattern of complex **12** produced a spectrum with little analytical information. Only three regions were clearly discernible and corresponded to the metal ion, an NHC ligand fragment and the NHC ligand without one of the isopropyl-groups. The low resolution and few peaks obtained might indicate decomposition of complex **12** and for this reason very little sample remained before the solution was analysed with mass spectrometry.

© University of Pretoria

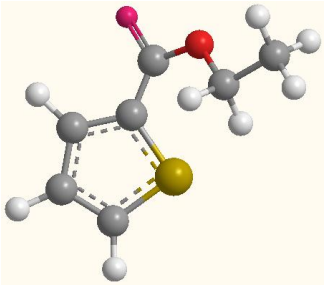

5 Application Study: Catalytic Ability

5.1 Application Background

5.1.1 Fischer carbenes

For centuries traditional Chinese and Japanese medicines have focused on tannin-containing plant extracts for the management of infections and diseases.[1] Natural products such as tannins and flavonoids contain the fragment 4-aryldihydrocoumarins in their carbon skeleton.[2] Dihydrocoumarin derivatives possess important biological activities (inhibition of HIV replication,[3] antiherpetic activity,[4] etc.) and this class of compounds has been isolated as attractive candidates for biological testing. The production of dihydrocoumarins (DHCs) has been accomplished through many different methods[5] and here Fischer carbenes find high applicability.[6]

---

[1] (a) Yoshida, T., Ohbayashi, G., Ishihara, K., Ohwashi, W., Haba, K., Okano, Y., Shingu, T., Okuda, T., *Chem. Pharm. Bull.,* **1991**, 39, 2233. (b) Okuda, T., Hantano, T., Yakazi, K., *Chem. Pharm. Bull.,* **1983**, 31, 333. (c) Saijio , R., Nonaka, G. I., Nishioka, I., *Chem. Pharm. Bull.,* **1989**, 37, 2063.
[2] (a) Iinuma, M., Tanaka, T., Asai, F., *Phytochemistry,***1994**, 36, 941. (b) Nonaka, G. I., Kawahara, O., Nishioka, I., *Chem. Pharm. Bull.,* **1982**, 30, 4277.
[3] Tillekeratne, L. M. V., Sherette, A., Grossmann, P., Hupe, L., Hupe, D., Hudson, R. A., *Bioorg. Med. Chem. Lett.,* **2001**, 11, 2763.
[4] Takechi, M., Tanaka, Y., Takehara, M., Nonaka, G. I., Nishioka, I., *Phytochemistry,***1985**, 24, 2245.
[5] (a) Donnelly, D. M. X., Boland, G., In *The Flavonoids. Advances in Research since 1986,* Hardborn, J. B. (Ed.), Chapman & Hall, London, **1993**. (b) Wagner, H., Seligmann, O., Chari, M. V., Wollenweber, E., Dietz, V. H., Donnelly, D. M. X., Meegan, M. J., O'Donnell, B., *Tetrahedron Lett.,* **1979**, 20, 4269. (c) Iinuma, M., Matsura, S., Asai, F., *Heterocycles,***1983**, 20, 1923. (d) Stephan, E., Rocher, R., Aubouet, J., Pourcelot, G., Cresson, P., *Tetrahedron: Asymmetry,***1994**, 5, 41.
[6] Barluenga, J., Andina, F., Aznar, F., *Org. Lett.,* **2006**, 8, 13.

© University of Pretoria

Noteworthy examples of their diverse chemistry are their participation in multi step synthesis of numerous natural products,[7] their capability to form differently sized carbocycles[8] and heterocycles[9] from pre-functionalised initial materials, as well as their relevance in multi-component and flow reactions.[10] Chromium Fischer carbene complexes have been employed in reactions with ketene materials to produce functionalised versions of dihydrocoumarins using a one-pot, open-air reaction methodology.[6] The ease of this reaction clearly shows the absolute power of even toxic carbenes in the field of medicinal chemistry. Synthesis of peptides and protection of the α-amino function group have been accomplished by the introduction of alkoxycarbenes to yield aminocarbene-labelled peptides.[11] This, in turn, has led to the ability to label proteins[12] and finally the design of a bioactive surface for protein immobilisation.[13] Transmetalation is perhaps one of the most significant processes in organometallic chemistry and, in particular, finds application in reactions catalysed by transition metals.[14] The straightforward transfer of the carbene moiety from a metal-carbene complex to another metal is exceptional.[15] Carbene complexes of palladium, rhodium, platinum, copper and silver have been synthesised by the transfer of diaminocarbene ligands from Group 6 metal carbene complexes.[2,16,17] Studies by Sierra *et al*. have proposed

---

[7] (a) Barluenga, J., Fernández-Rodriguez, M. A., Aguilar, E.,Fernández-Mari, F., Salinas, A., Olano, B., *Chem. Eur. J.,* **2001**, 7, 3533. (b) Minatti, A., Dötz, K. H., *J. Org. Chem.,* **2005**, 70, 3745. (c) Gupta, A., Sen, S., Harmata, M., *J. Org. Chem.,* **2005**, 70, 7422.

[8] (a) Barluenga, J., Diéguez, A., Rodriguez, F., Florez, J., Fañanás, F. J., *J. Am. Chem. Soc.,* **2002**, 124, 9056. (b) Barluenga, J., López, S., Trabanco, A. A., Fernández-Aceves, A., Florez, J., *J. Am. Chem. Soc.,* **2000**, 122, 8145. (c) Barluenga, J., Aznar, F., Palomero, M. A., *Angew. Chem., Int. Ed. Engl.,* **2000**, 39, 4346. (d) Barluenga, J., Alonso, J., Rodriguez, F., Fañanás, F. J., *Angew. Chem., Int. Ed. Engl.,* **2000**, 39, 2460. (e) Barluenga, J., Aznar, F., Valdés, C., Martin, A., Garcia-Granda, S., Martin, E., *J. Am. Chem. Soc.,* **1993**, 115, 4403. (f) Barluenga, J., Aznar, F., Martin, A., Vázqquez, J. T., *J. Am. Chem. Soc.,* **1995**, 117, 9419.

[9] Barluenga, J., Santamaría, M., Tomás, M., *Chem. Rev.*, **2004**, 104, 2259–2283.

[10] Barluenga, J., Fernández-Rodriguez, M. A., Aguilar, E. J., *Organomet.Chem.,* **2005**, 690, 539.

[11] (a) Weiss, K., Fischer, E. O., *Chem. Ber.*, **1973**, 106, 1277. (b) Weiss, K., Fischer, E. O., *Chem. Ber.,* **1976**, 109, 1868.

[12] (a) Licandro, E., Maiorana, S., Capella, L., Manzotti, R., Papagni, A., Vandoni, B., Albinati, A., Chuang, S. H., Hwu, J. R., *Organometallics*, **2001**, 20, 485. (b) Samanta, D., Sawoo, S., Patra, S., Ray, M., Salmain, M., Sarkar, A., *J. Organomet. Chem.,* **2005**, 690, 5581. (c) Baldoli, C., Cerea, P., Giannini, C., Licandro, E., Rigamonti, C., Maiorana, S., *Synlett*., **2005**, 1984. (d) Licandro, E., Maiorana, S., Pericchia, D., Baldoli, C., Graiff, C., Tiripicchio, A., *J. Organomet. Chem.,* **2001**, 399, 617–618. (e) Salmain, M., Jaouen, G. C. R., *Chim.,* **2003**, 6, 249.

[13] Sawoo, S., Dutta, P., Chakraborty, A., Mukhopadhyay, R., Boulussa, O., Sarkar, A., *Chem. Commun.,* **2008**, 5957.

[14] (a) Hegedus, L. S., *Transition Metals in the Synthesis of Complex Organic Molecules,* University Science Books, Sausalito, CA, US, **1999**. (b) Boudier, A., Bromm, L. O., Lotz, M., Knochel, P., *Angew. Chem.,* **2000**, 112, 4584; *Angew.Chem. Int. Ed. Engl.,* **2000**, 39, 4414.

[15] Liu, S. T., Reddy, K. R., *Chem. Soc. Rev.,* **1999**, 28, 315.

[16] Ku, R. Z., Huang, J. C., Cho, J. Y., Kiang, F. M., Reddy, K. R., Chen, Y. C., Lee, K. J., Lee, J. H., Peng, S. M., Liu, S. T., *Organometallics,* **1972**, 105, 162.

[17] Arduengo III, A. J., Dias, H. V. R., Calabrese,J. C., Davidson, F., *Organometallics*, **1993**, 12, 3405.

© University of Pretoria

palladium biscarbene complexes as the active transitional complex in the Pd-catalysed dimerisation of alkoxycarbene chromium(0) complexes.[18,19]

5.1.2 N-heterocyclic carbene complexes

Stable metal-containing NHC complexes have recently attracted increasing interest in medicinal applications. Various transition metal-coordinated NHC complexes, including silver, gold, palladium, rhodium and ruthenium, have shown vast medicinal applications in antimicrobial and antitumor activity and the suppression of bacterial growth.[20] Silver complexes have been recognised as effective antimicrobial agents since the 17th and 18th centuries.[21] Silver NHC complexes have found application as transfer agents, prospective anti-microbials and catalysts.[22] The earliest examples of Ag(I)-NHC complexes possessing antimicrobial activity against bacterial infections, such as *Escherichia coli, Staphylococcus aureus* and *Pseudomonas aeruginosa*, were produced by Youngs in 2004 and possessed a pincer geometry linked by pyridine.[23] Apart from antimicrobial properties, silver-NHC complexes also have antitumor abilities and silver metal-containing NHC complexes are currently undergoing efficiency tests against ovarian, breast and cervical cancers.[24] In addition, modern medicine has found application for the bacteriostatic and medicinal properties of numerous gold complexes.[25] Gold complexes are still widely considered the most successful obtainable remedy for the management of rheumatoid arthritis.[26] Similarly to the silver counterpart, Cetinkaya *et al.* reported Au(I)-NHC complexes (Figure 5.1) to contain antimicrobial properties.[27] Baker and co-workers investigated the possible antimitochondrial antitumor capability of Au(I) NHCs since mitochondrial regulation of programmed cell death

[18] Sierra, M. A., del Amo, J. C., Mancheño, M. J., Gómez-Gallego, M., *J. Am. Chem. Soc.,* **2001**, 123, 851. (b) Sierra, M. A., Mancheño M. J., Sáez, E., del Amo, J. C., *J. Am. Chem. Soc.,* **1998**, 120, 6812. (c) Casey, C. P., Anderson, R. L., *J. Chem. Soc., Chem. Commun.,* **1975**, 895.
[19] (a) Göttker-Schnetmann, I., Aumann, R., *Organometallics,* **2001**, 20, 346. (b) Aumann, R., Göttker-Schnetmann, I., Fröhlich, R., Meyer, O., *Eur. J. Org. Chem.,* **1999**, 2545.
[20] Hindi, K. M., Panzner, M. J., Tessier, C. A., Cannon, C. L., Youngs, W. J., *Chem. Rev.,* **2009**, 109(8), 3859–3884.
[21] Baba, E., Cundari, T. R., Firkin, I., *Inorg. Chim. Acta,* **2005**, 358, 2867–2875.
[22] Garrison, J. C., Youngs, W. J., *Chem. Rev.,* **2995**, 105, 3978–4008.
[23] Melaiye, A., Simons, R. S., Milsted, A., Pingitore, F., Wesdemiotis, C., Tessier, C. A., Youngs, W. J., *J. Med. Chem.,* **2004**, 47, 973–977.
[24] Medvetz, D. A., Hindi, K. M., Panzner, M. J., Ditto, A. A. J., Yun, Y. H., Youngs, W. J., *Metal-based Drugs,* **2008**, 384010–384016.
[25] Fricker, S. P., *Gold Bulletin,* **1996**, 29, 53–60.
[26] Shaw III, C. F., *Chem. Rev.,***1999**, 99, 2589–2600.
[27] Özdemir, I., Denizci, A., Öztürk, T. H., Çetinkaya, B., *Appl. Organometal. Chem.,* **2004**, 18, 318–322.

© University of Pretoria

(apoptosis) in tumour cells could possibly be manipulated for beneficial therapeutic gain.[28] Ruthenium-containing complexes are currently in use for the development of new antitumor drugs.[20] The complex *trans*-[$RuCl_4(Im)_2$](HIm), better known as the Keppler-type complex, proved to have tumour-inhibition activity superior to that of cyclophosphamide, cisplatin or 5-fluorouracil when tested against P388 leukaemia, B16 melanoma and platinum-resistant colorectal tumours.[20] The antimicrobial activity of Ru-NHC complexes was evaluated against *Enterococcus faecalis, Pseudomonas, Escherichia coli* and *Staphylococcus aureus* bacterial species with ampicillin employed as reference.[29, 30] It was found that none of these complexes showed any comparable antimicrobial action to that of ampicillin.[20] NHC complexes are highly appropriate for pharmaceutical application and interest in their utilisation in more relevant medicinal processes is increasing. They possess the ability to coordinate to both hard and soft metals and are frequently functionalised, adding to the possibility of creating new target drugs and pharmaceuticals. NHCs and most of their metal complexes have adequate lipophilicity, which contributes to both their antimicrobial and antitumor properties.[20]

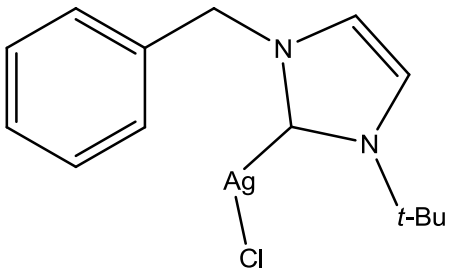

Figure 5.1. A typical antimicrobial Ag(I)-NHC complex

5.1.3 Focus of the study

It was envisaged that appropriate applications for the newly synthesised carbenes might be found. Although the main aim of the project was to synthesise Fischer and NHC carbenes, catalytic studies were employed as a screening tool for their application as catalysts. A basic

[28] Baker, M. V., Barnard, P. J., Berners-Price, S. J., Brayshaw, S. K., Hickey, J. L., Skelton, B. W., White, A. H., *J. Chem Soc., Dalton Trans.,* **2006**, 2708–3715.
[29] Çentinkaya, B., Ozemir, I. Binbasioglu, B., Durmaz, R., Gunal, S., *Arzneim-Forsch/Drug Res.,* **1999**, 49, 538–540.
[30] Çetinkaya, B., Çetinkaya, E., Kucukbay, H., Durmaz, R., *Arzneim-Forsch/Drug Res.,* **1999**, 46, 821–823.

© University of Pretoria

investigation was undertaken to produce an overall view of the different applicabilities and abilities of complexes **2** and **6** in both metathesis and polymerisation reactions (these complexes were both air stable and available in adequate quintities). The information obtained would then serve as experimental data to compare with the results of theoretical studies with the aim of establishing a model to predict activity based on computational methods. The catalytic action, rate and catalysis products were all compared with information from the known studies of the Grubbs first-generation catalyst (Grubbs 1).[31] Metathesis reaction of 1-octene using the Grubbs 1 catalyst was performed to obtain the profile of the reaction products for comparison with the profile of products obtained with pre-catalysts **2** and **6**. It was expected that the products obtained through catalysis would be the *cis* and *trans* forms of 7-tetradecene. The catalytic products can be analysed using gas chromatography/mass spectrometry (GC/MS) at about 14 min (retention time) and serve as primary metathesis products (PMP) (Figure 5.2).

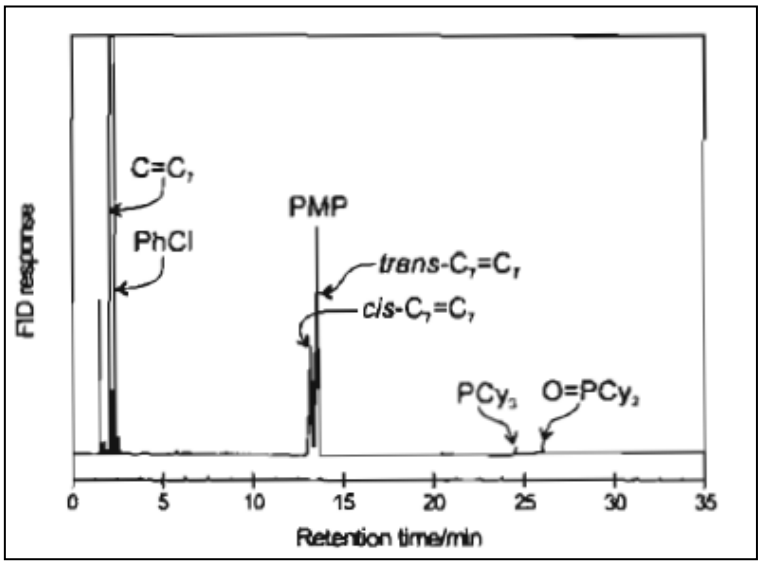

Figure 5.2. GC/MS of the metathesis of 1-octene in the presence of Grubbs 1 catalyst (solvent: chlorobenzene)[31]

Complexes **2** and **6** were also used in polymerisation reactions. Polymerisation of phenyl acetylene was attempted using the same method as with the metathesis reactions for possible polymer product formation.

[31] Jordaan, M., PhD Thesis. *Experimental and theoretical investigation of new Grubbs-type catalysts for the metathesis of alkenes,* **2007**, University of the North-West, Potchefstroom, South Africa.

© University of Pretoria

5.2 Methodology

5.2.1 Metathesis and polymerisation reactions

The procedure for the preliminary small-scale metathesis reactions is shown in Figure 5.3. The mini-reactor was filled with inert argon gas and the pre-catalyst weighed and added. Nonane (0.25 ml) and 1-octane (5 ml) were added to the reactor with Hamilton GASTIGHT® syringes. The nonane served both as solvent and as internal standard and, although the complexes were poorly soluble, a completely homogeneous solution was obtained after the reactor had been placed on a heating source at 60 °C. The temperature was raised from 60 to 70 °C and finally to 90 °C. Samples were drawn at the start (0 min) and at 5, 30 and 60 min intervals to gauge the progression of the metathesis reaction. The drawn samples were first quenched in a solution of toluene (0.3 ml) and 2 drops of tert-butyl-hydrogen peroxide and then placed on a gas chromatograph (GC) for analysis. The acquired chromatograms were compared with the Grubbs 1 catalyst standard. A polymerisation reaction was attempted using the same procedure as with the metathesis reaction, with only a slight deviation. All solutions were prepared in a similar fashion with phenyl acetylene (5 ml) replacing the 1-octene. The solution was allowed to stir for 24 h at 70 °C and then quenched with methanol added directly to the mini-reactor. If any form of polymerisation were to be achieved, the addition of methanol would precipitate out the newly formed polymer.

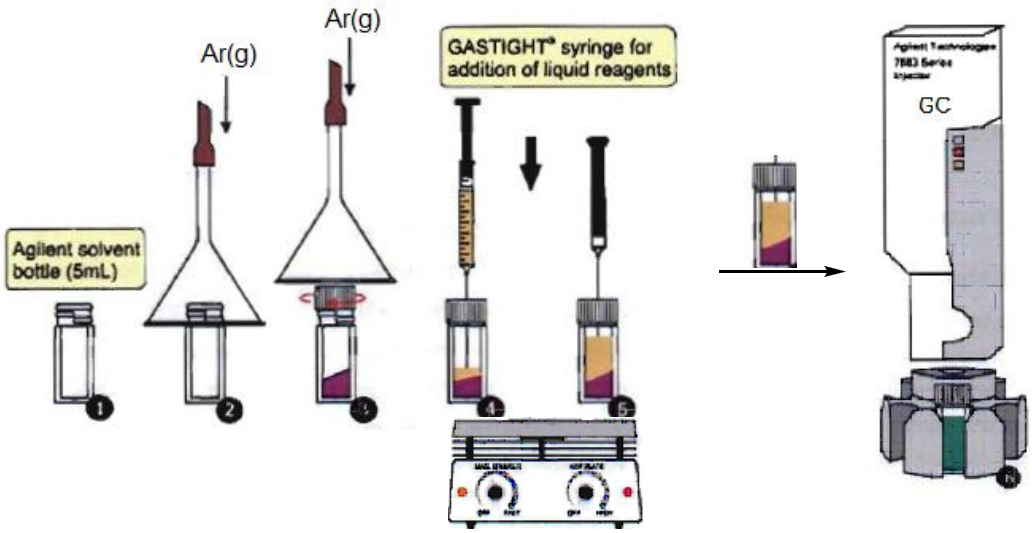

Figure 5.3. Metathesis reaction sequence[31]

© University of Pretoria

5.2.2 Analysis: gas chromatography

Samples taken at the initiation of the metathesis reactions, after 5 min and at half-hourly and hourly intervals were all quenched, as mentioned above, and analysed on both an Agilent 2890 and an Agilent 6850 gas chromatograph equipped with an Agilent 7683 auto injector, HP-5 capillary column (30 m × 320 µm × 0.25 µm) and a flame ionisation detector (FID). The specific GC settings were as follows:

Inlet temperature	250 °C
N_2 carrier gas flow rate	1.9 ml/min
Inject volume	2.0 µl (auto inject)
Split ratio	50.4:1
Oven programming	Initial: 60° for 5 min
	Ramp 1: 60 to 110 °C for 10 min at 25 °C/min
	Ramp 2: 110 to 29 0 °C at 25 °C/min
	Ramp 3: 290 to 300 °C for 5 min at 25 °C/min
Detector	FID @ 250 °C
H_2 flow rate	40 ml/min
Air flow rate	450 ml/min

5.3 Results

5.3.1 Metathesis reactions

The results from theoretical metathesis reactions using Grubbs 1 give two major products, namely the *cis*- and *trans* 7-tetradecenes. Any successful catalytic ability of complexes **2** and **6** with 1-octene would result in either a similar product profile to that of Grubbs 1 or a measurable change in any additional products not observed in the theoretical Grubbs 1 study. The GC results for complexes **2** and **6** obtained after both the initial point as well as 3 h later (samples 8 and 6, respectively) showed no difference in either 1-octene concentration and there were no additional peaks.

The peak profile remained unchanged over time and the only differences can be attributed to the quantity of sample placed in the GC instrument. No product peaks were visible to compare with those of Grubbs 1 and thus the results obtained for both complexes **2** and **6**

© University of Pretoria

show that no catalytic process took place. In an attempt to aid the process by finding a more optimum temperature, the reaction was heated to 70 °C with no observed impact and to 90 °C, at which temperature catalyst decomposition occurred. Figures 5.4 and 5.5 show the GC chromatograms obtained for samples 1 (0 min) and 8 (145 min) (complex **2**).

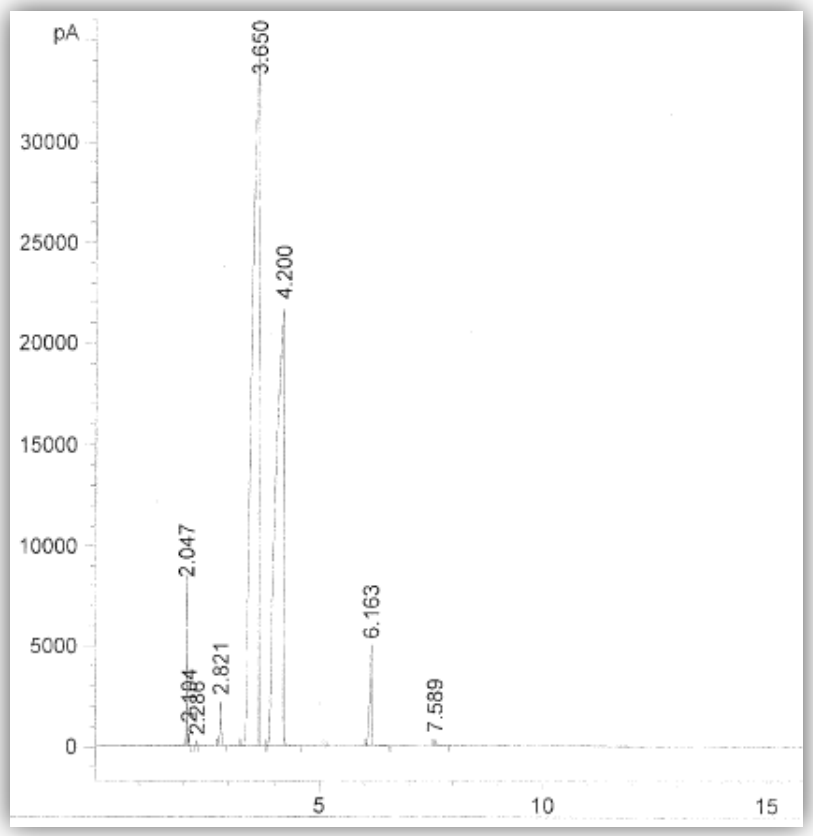

Figure 5.4. Gas chromatogram for complex **2** (initial point)

From the GC-MS results obtained, it became clear that starting material, solvent and unidentified molecules was present in the initial point solution. No new compound was produced in reference to the Grubbs standard. Figure 5.5 shows the GC spectrum after two hours. The two spectra (Figure 5.4 and 5.5) are nearly superimposable onto one another and thus the deduction was made that no catalytic process was initiated.

© University of Pretoria

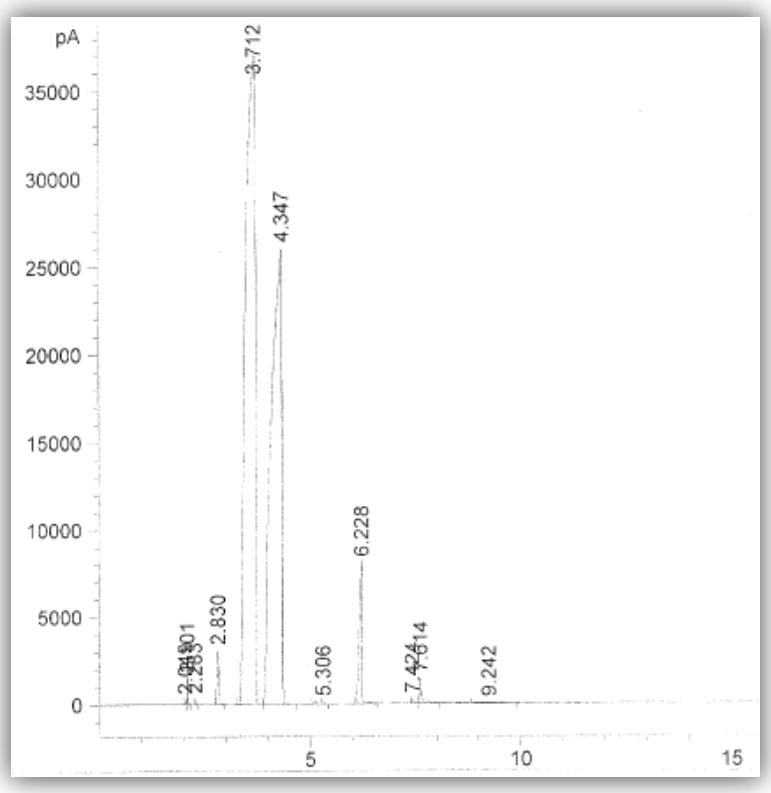

Figure 5.5. Gas chromatogram for complex **2** (sample 8)

Table 5.1. Main gas chromatogram peaks for complex **2** (initial point)

Peak	Retention time (min)	Width (min)	Area (%)	Identification
5	3.650	0.1306	56.07	Toluene
6	4.200	0.1451	39.47	1-octene
7	6.163	0.0440	2.52	Nonane
8	7.589	0.0472	0.16	Contaminant

Table 5.2. Main GC chromatogram peaks for complex **2** (sample 8)

Peak	Retention time (min)	Width (min)	Area (%)	Identification
5	3.712	0.1859	54.08	Toluene
6	4.347	0.2024	40.93	1-octene
8	6.228	0.0604	3.47	Nonane
10	7.614	0.0426	0.42	Decane
11	9.242	0.4505	0.067	Contaminant

© University of Pretoria

Table 5.3. Main gas chromatogram peaks for complex **6** (initial point)

Peak	Retention time (min)	Width (min)	Area (%)	Identification
3	3.305	0.0836	47.17	Toluene
4	3.663	0.1143	47.85	1-octene
5	5.674	0.0526	3.20	Nonane
7	7.366	0.0336	0.73	Decane
8	10.836	0.4587	0.042	Contaminant

Table 5.4. Main gas chromatogram peaks for complex **6** (sample 6)

Peak	Retention time (min)	Width (min)	Area (%)	Identification
3	3.317	0.0832	51.47	Toluene
4	3.657	0.0999	44.16	1-octene
5	5.672	0.0500	3.07	Nonane
7	7.360	0.0604	0.54	Decane

Although many small contaminant peaks do appear on the GC chromatogram, they show exceptionally low area percentages. These peaks are present in single cases and are completely absent in others and thus the focus fell only on the identification of the main peaks with noticeable area sizes. Both the chromatograms and the data in Tables 5.1 to 5.4 provide clear evidence that there was no catalytic action, with only solvent and starting material peaks visible.

5.3.2 Polymerisation reactions

In an attempt to produce a polymer product through the catalytic ability of complex **2**, the product was dissolved in nonane and phenyl acetylene was then added to the reaction mixture. The reaction was left for 24 h to produce polyphenylacetylene (Figure 5.6). The success of the reaction is dependent on the precipitation of the polymer product on the introduction of methanol.

© University of Pretoria

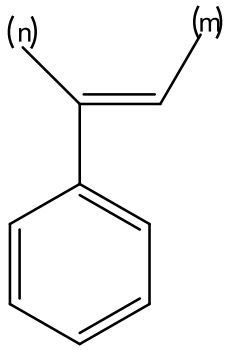

Figure 5.6. Structure of polyphenylacetylene

In this study, however, the polymer product was not obtained and the initial brown solution returned to the original yellow colour. Since no polymeric ability was induced at a lower initial temperature of 70 °C, the temperature was raised to 90 °C, at which temperature the pre-catalyst decomposed.

5.4 Discussion

Neither the polymerisation nor the metathesis reactions proved successful. Literature theoretical models predict that Fischer carbenes containing a LUMO on the metal and a HOMO distribution on the carbene indicate catalytic properties, but in this study no direct correlation was proved. Preliminary theoretical calculations indicated a lower concentration of the LUMO spread residing on the metal spheres in comparison with the carbene carbon atom. Since a LUMO concentration did exist on the metal centre of complexes **2** and **6**, these complexes might have displayed catalytic ability. The location and density of the LUMO unfortunately cannot be seen as the only indication of catalytic ability and multiple other factors also proved vital as indicated by the experimental results. Lability of ligands and molecular energies also have to be taken into consideration. The mechanism for ruthenium alkene metathesis might prove helpful in explaining the complete failure of the metathesis activity of complexes **2** and **6**. The mechanism requires the opening of a coordination site for the approach and coordination of the alkene molecule in the case of an dissociative mechanism or smaller, less buiky ligands for associative mechanisms. Only after coordination of this approaching ligand is the metathesis pathway available.[32,33] A simplified mechanism is presented in Scheme 5.1.

[32] Dias, E. L., Nguyen, S. T., Grubbs, R. H., *J. Am. Chem. Soc.*, **1997**, 119, 3887.

© University of Pretoria

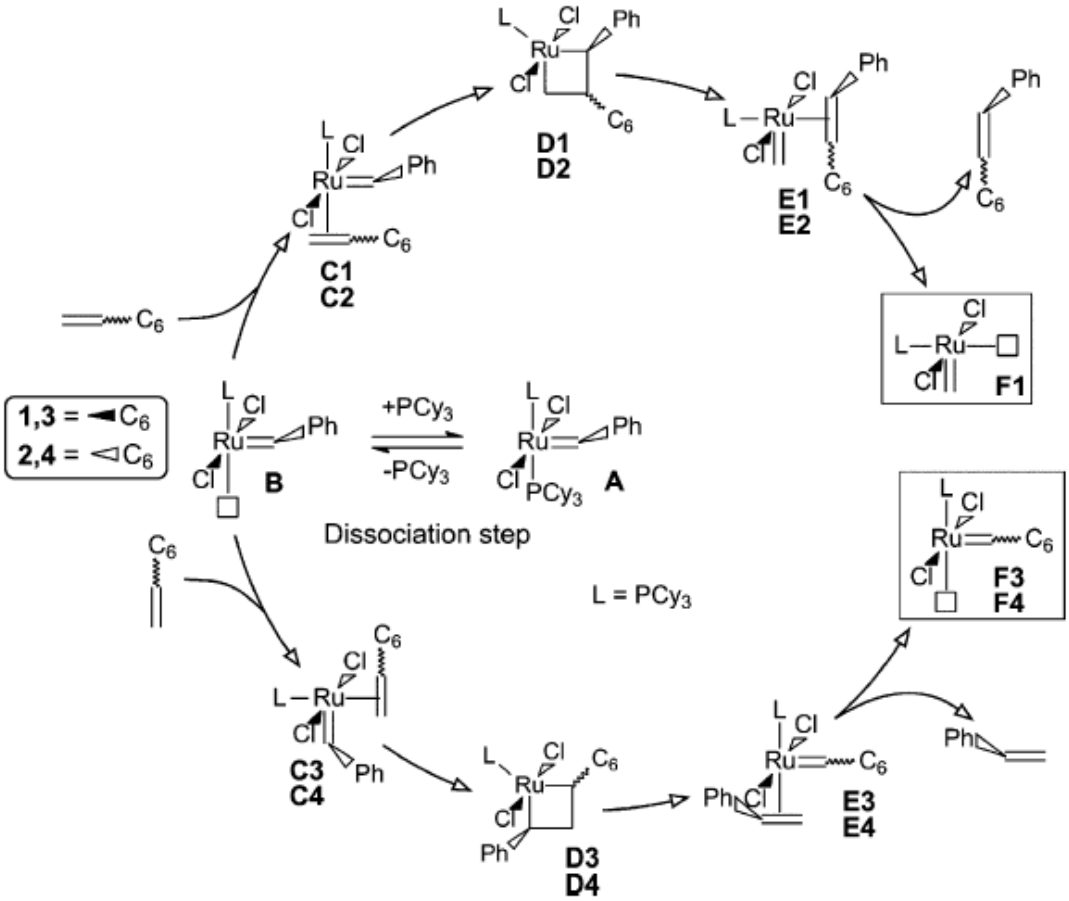

Scheme 5.1. Mechanism for alkene metathesis by a ruthenium catalyst[34]

In both complexes tested there is no such labile ligand. All three available carbonyl ligands are inertly bound to the metal sphere since excess electron density is shifted onto these ligands from the metal centre. Neither of the phosphine atoms is labile enough to dissociate and stabilise further chelate. Since both complexes have basically inert surroundings, with no possible associative or dissociative mechanism available to form the coordinated alkene bond, the result is a complex with limited metathesis or polymerisation ability.

Another possible disadvantage lies in the sheer complexity of the molecule. The molecule is steric and bulky, hindering the approach of any incoming alkene into the active site. In conclusion, from the results of this study, a few valuable lessons were learned. Multiple adaptations to the Fischer complexes should be made to improve on any catalytic ability. Firstly, chelates can be synthesised containing heteroatomic ligation sites. Chelates

[33] Sanford, M. S., Ulman, M., Grubbs, R. H., *J. Am. Chem. Soc.,* **2001**, 123, 749.
[34] Jordaan, M., van Helden, P., van Sittert, C. G. C. E., Vosloo, H. C. M., *J. Mol. Catal. A: Chem.* **2006**, 254, 145-154

© University of Pretoria

containing both oxygen and a nitrogen atom, bearing lone pairs, would already be an improvement. The nitrogen atom on the chelate serves only as a σ-donating atom and will therefore be hemi-labile in nature. Dissociation of the nitrogen will open a coordination site through which the alkene ligand can coordinate. This dissociation will initiate the metathesis or polymerisation cascade and terminate the reaction by the final back-chelation of the nitrogen atom before the catalyst is recovered. Another obvious modification would be the synthesis of a less bulky coordination complex which would allow sufficient space for any associating group to ligate easier and faster. Carbene complexes containing less bulky bidentate ligands would thus be more efficient in metathesis or polymerisation reactions.

© University of Pretoria

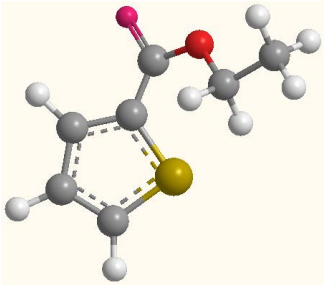

6 Theoretical Study: Molecular Modelling

6.1 Theoretical Modelling

Theoretical and computational chemistry simulates chemical structures and reactions numerically, based on the elementary laws of physics. It enables chemists to study chemical phenomena by implementing calculations on computers rather than exploring reactions and complexes experimentally. Computational chemistry provides insight about molecules and reactions that would have proved unfeasible to attain through inspection.[1]

6.1.1 Modelling methods

Two main simulation methods apply to computational chemistry. Molecular mechanics exploits the laws of conventional physics to forecast the construction and properties of molecules, while the electronic structure methods obey the laws of quantum mechanics.[1] Molecular mechanics utilises a simplified system by mainly considering only the nuclei involved in the molecule; electronic considerations are only implied through parameterisation. Contradictorily, quantum mechanics states that all related properties of a molecule may be derived from the solution of the Schrödinger equation. Electronic structure methods are pigeonholed by their vast mathematical approximations to the solution.[1]

[1]Foresman, J. B., Frisch, Æ., *Exploring Chemistry with Electronic Structure Methods,* 2nd edn., Gaussian, Inc. Pittsburgh USA, **1996**.

© University of Pretoria

Electronic structure methods are divided into three main categories, namely semi-empirical, *ab initio* and density functional theory (DFT) methods. DFT methods have become ever more attractive because of the inclusion of the effects of electron correlations, as well as their limited computational costs.[1]

6.1.2 Theoretical calculations: Fischer carbenes

DFT calculations by Irshaidat *et al.* provided insight into the distinctive elementary organic/organometallic aspects of both free and Cr, Mo and W tetracarbonyl metal coordinated carbenes. Their study demonstrated interesting results with an intermediate stabilised by an agnostic interaction.[2] Wang *et al*. calculated the bond dissociation energies of typical pentacarbonyl carbene complexes using DFT calculations, and the relative orbital energies were also compared with photoelectron spectroscopy data. Values based on DFT calculations by means of transition-state estimations gave the best agreement with experimental findings.[3] A dual computational (TD-DFT) investigative study of the UV-vis spectroscopy of alkoxycarbene chromium(0) complexes correctly assigns the vertical transitions accountable for the experimental spectra of these compounds. The study showed that the substituent is also connected with the equilibrium arrangement of the complexes and the occupation of the p-atomic orbital of the electrophilic carbene carbon.[4] Photocarbonylation reactions of Group 6 carbene complexes have been studied utilising DFT and experimental measurements. It was found that the progression occurs by an intersystem crossing from the lowest possible excited singlet state (S_1) to the smallest possible triplet state (T_1), with the latter configuration being critical for the result of the reaction.[5] Examples of organic catalytic cycles utilising Fischer-type carbenes have also been modelled.

Transmetalation processes from chromium (0) complexes to late transition metal complexes (Pd(0), Cu(I) and rhodium(I)) have been modelled by DFT and the computational data compared with experimental findings.[6] The reaction profiles in connection with the transmetalation reaction to both copper and palladium proved quite similar, but the

[2] Irshaidat, T., *E-Journal of Chemistry*, **2010**, 7(2), 437–444.
[3] Wang, C. C., Wang, Y., Liu, H. J., Lin, K. J., Chou, L. K., Chan, K. S., *J. Phys. Chem.,* **1997**, 101, 8887–8901.
[4] Marta, L. L.,Fernández, I., Mancheño, M. J., Sierra, M. A., *Inorg. Chem.,* **2008**, 47(12), 5253–5258.
[5] Fernández, I., Sierra, M. A., Gómez-Gallego, M., Mancheño, M. J., Cossío, F. P., *J. Chem., Eur.,* **2005**, 11, 5988–5996.
[6] Fernández I., Mancheño, M. J., Vicente, R., López, L. A., Sierra, M. A., *J. Chem., Eur.,* **2008**, 14, 11222–11230.

© University of Pretoria

computational energy values specify that the method using palladium as catalyst is more favourable than the copper counterpart.[6]

6.1.3 Theoretical calculations: N-heterocyclic carbenes

It is well established that DFT methods are exceptionally efficient in reproducing X-ray arrangements of transition metal complexes[7] (Table 6.1). Studies by Jacobsen *et al*. demonstrated the method's effectiveness in predicting both the M-NHC bond distances and the energetics of this bond[7] (Table 6.2). Currently, theoretical and experimental evidence indicates that, to produce a stable carbene, the carbonic carbon is required to bond to strong π-donor atoms.[8] Nevertheless, the notable stability of the primary isolated carbene was entirely unanticipated at the time. *Ab initio* studies enabled Dixon and Arduengo to hypothesise that p(π)-p(π) delocalisation is not widespread and that the bonding in these ligands should, in reality, be considered to be carbonic since ylidic resonance modes are not prevailing contributors.[9] In terms of complexing to Group 6 metals, an experimental-theoretical charge-density study combination on $(IMe)Cr(CO)_5$ revealed the σ-donor/π-acceptor character of the NHC ligand.[10] It was concluded that the bond distances in the five-membered ring of the free NHC moiety were not in any way significantly different after complexation to the metal. This fact seems inconsistent with only σ-donation M-(NHC) interaction, which should have resulted in a shortening of the C-N bond of the NHC after the complex was formed. Frenking and co-workers undertook a more wide-ranging bonding investigation of $(NHC)M(CO)_5$ complexes with 'normal' and 'abnormal' NHC molecules through DFT calculation at a BP86/TZ2P level.[11] In reference to this analysis, the measured d^6 metal systems present a π-contribution to the orbital interface between the metal and the NHC group of about 17–18% of the overall orbital interaction; about 77–78% of the π orbital interaction has been attributed to the M→NHC π*-back-donation. Although ruthenium, nickel and iridium metals do not constitute any part of this project and since accurate DFT calculations for Cr metal complexes have been evasive, Tables 6.1 and 6.2 are included to provide supplementary insight into the power and accuracy of DFT calculations.

---

[7] Jacobsen, H., Correa, A., Poater, A., Costabile, C., Cavallo, L., *Coord. Chem.,* **2009**, 253, 687–703.
[8] (a) Lavallo, V., Canac, Y., Präsan, C., Donnadieu, B., Bertrand, G., *Angew.Chem., Int. Ed. Engl.,* **2005**, 44, 5705. (b) Lavallo, V., Canac, Y., De Hope, A. C., Donnadieu, B., Bertrand, G., *Angew. Chem., Int. Ed. Engl.,* **2005**, 44, 7236.
[9] Dixon, D. A., Arduengo III, A. J., *J. Phys. Chem.,* **1991**, 95, 4180.
[10] Tafipolsky, M., Scherer, W., Öfele, K., Artus, G., Pedersen, B., Herrmann, W. A., McGrasy, G. S., *J. Am. Chem. Soc.,* **2002**, 124, 5865.
[11] Tonner, R., Heydenrych, G., Frenking, G., *J. Chem. Asian.,* **2007**, 2, 1555.

© University of Pretoria

Table 6.1. Comparison between X-ray data and DFT calculation[12]

	Complex	M–(NHC), X-ray	M–(NHC), DFT
1	$Cp^*Ru(ITol)Cl$	2.068	2.044
2	$Cp^*Ru(IMes)Cl$	2.105	2.086
3	$Cp^*Ru(SIMes)Cl$	2.083	2.076
4	$Cp^*Ru(IPr)Cl$	2.086	2.093
5	$Cp^*Ru(SIPr)Cl$	2.087	2.078
6	$(TIME^{Me})_2Cu_3$[a]	1.912	1.901
7	$(TIME^{Me})_2Ag_3$[a]	2.082	2.087
8	$(TIME^{Me})_2Au_3$[a]	2.028	2.054
9	$(IMes)Ni(CO)_3$	1.971	2.005
10	$(SIMes)Ni(CO)_3$	1.960	1.969
11	$(IPr)Ni(CO)_3$	1.979	1.967
12	$(SIPr)Ni(CO)_3$	1.962	1.967
13	$(ItBu)Ni(CO)_2$	1.957	1.964
14	$(IAd)Ni(CO)_2$	1.953	1.964
15	$(IMes)Ir(CO)_2Cl$	2.108	2.099
16	$(SIMes)Ir(CO)_2Cl$	2.121	2.103
17	$(IPr)Ir(CO)_2Cl$	2.079	2.096
18	$(SIPr)Ir(CO)_2Cl$	2.071	2.098
19	$(ItBu)Ir(CO)_2Cl$	2.114	2.121

All distances in Å.

Table 6.2. Comparison between experimental bond dissociation energies and DFT calculated BDEs[12]

	Complex	Relative BDE, experimental	Relative BDE, DFT
1	$Cp^*Ru(ITol)Cl$	18.8	26.2
2	$Cp^*Ru(IMes)Cl$	15.6	19.2
3	$Cp^*Ru(SIMes)Cl$	16.8	19.2
4	$Cp^*Ru(IPr)Cl$	11.1	11.6
5	$Cp^*Ru(SIPr)Cl$	12.1	10.9
6	$(ItBu)Ni(CO)_2$	39 ± 3	44.3
7	$(IAd)Ni(CO)_2$	43 ± 3	46.5

All BDEs are in kcal/mol.

[12] (a) Barluenga, J., Fernández-Rodriguez, M. A., Aguilar, E.,Fernández-Mari, F., Salinas, A., Olano, B., *Chem. Eur. J.,* **2001**, 7, 3533. (b) Minatti, A., Dötz, K. H., *J. Org. Chem.,* **2005**, 70, 3745. (c) Gupta, A., Sen, S., Harmata, M., *J. Org. Chem.,* **2005**, 70, 7422.

© University of Pretoria

Studies into isolobal atoms to carbon have also been done.[13] Complexation of CuCl, AgCl and AuCl to carbenes, silylenes and germylenes showed that metal→ligand bond dissociation energies (BDEs) follow the trend C > Si > Ge. The stiffest bond is predicted for the carbene-AuCl complex, which contains a higher BDE than the typical Fischer complex $(CO)_5W$-CH(OH). The most significant modification of the ligand geometries is the reduction of the N-X (X=C, Si, Ge) bond, indicating a heftier π-donation. Although the σ-donation is still the dominant factor, metal→ligand π-back-bonding becomes slightly more significant for silylenes and germylenes, while being negligible for carbenes.[14] Figure 6.1 shows the structures of a typical silylene and germylene.

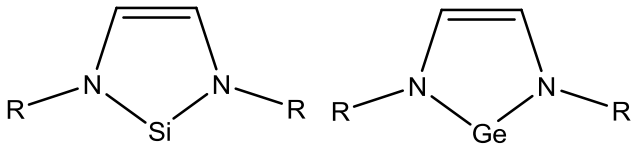

R= alkyl groups

Figure 6.1. Typical structure of a silylene and a germylene

6.2 Intention of this Study

This study focused mainly on the computational modelling of the numerous synthesised carbene complexes. Both Fischer carbene complexes and NHCs were modelled in an attempt to gain an in-depth understanding of the structural and electronic properties of these complexes. Through computational calculations, theoretical HOMO and LUMO determination became possible and the structural energies could be resolved. Energy calculations and analyses demonstrated preferred geometries in cases where both the facial and meridonial isomers were possible. The structure obtained from single-crystal diffraction studies can also be superimposed on theoretical models to enable a visible indication of the accuracy and confidence level of the structural arrangement implied by computational methods. Theoretical models provide valuable opportunities to evaluate catalytic ability and forecast the possibility for such applications.

[13] Boehme, C., Frenking, G., *Organometallics*,**1998**, 17, 5801.
[14] Strassner, T., *Topics Organomet. Chem.,* **2004**, 13, 1–20.

© University of Pretoria

All complexes were modelled with the aid of ground-state DFT calculations using the B3LYP functional and the GEN basis set (6-31G* for C, H, O, P, S and N, and LANL2DZ for Cr) with a neutral charge and singlet spin state. Modelling was executed using Gaussian 03 software.[15]

The global minimum and global maximum correspond to the lowest and highest structural energy points, respectively, while both the local maxima and minima flag the configuration of intermediate energies (Figure 6.2). Saddle points are valleys located in between maxima in one direction and minima in the other and correlate to a transition structure connecting two equilibrium structures.[15] At both the saddle point and any minima, the first derivative of the energy is zero and thus locating favourable states will focus on these basis-finding geometries where the first derivative is zero. The aim of any optimisation would be to circumvent finding local minima or saddle points and to find an energy valley corresponding to the minimum energy possible to be associated with a given structure.[15]

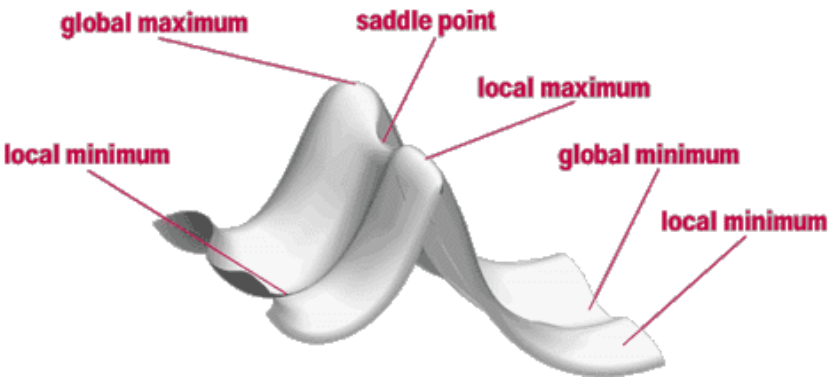

Figure 6.2. Potential energy surface[15]

[15] Frisch, M. J., Trucks, G. W., Schlegel, H. B., *et al*. cuseria, *Gaussian 03*, Revision C.02, Gaussian, Inc., Wallingford, CT, US, **2004**.

© University of Pretoria

6.3 Structural Study

6.3.1 Structures investigated

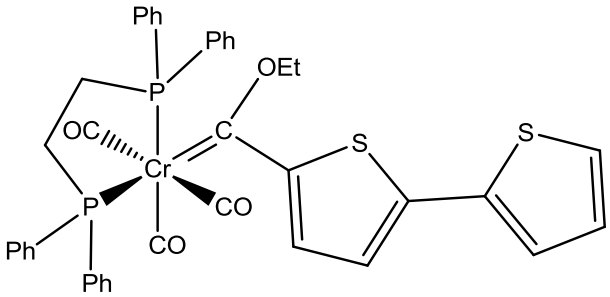

Complex 1

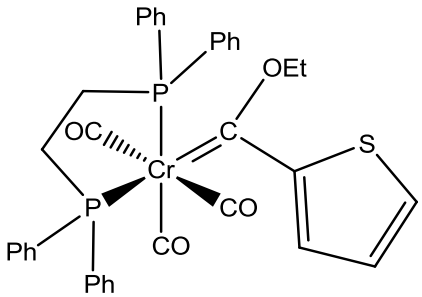

Complex 2

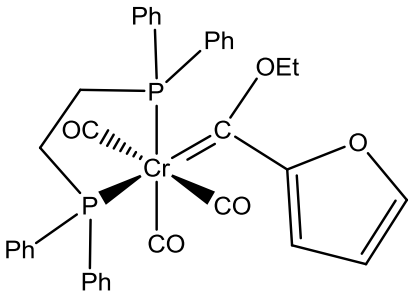

Complex 3

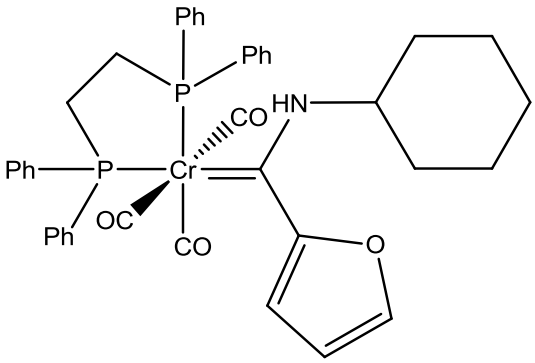

Complex 7

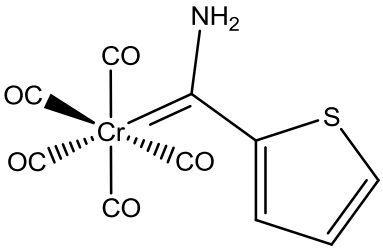

Complex A

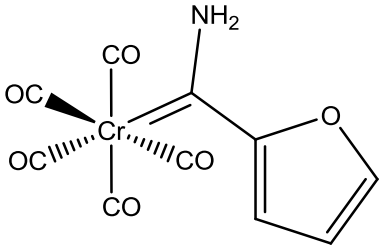

Complex B

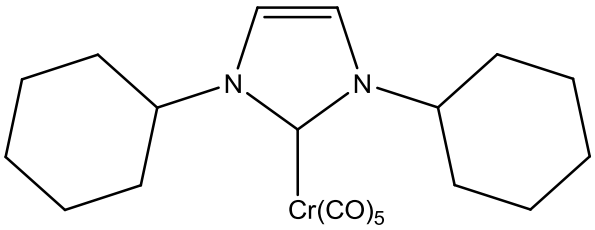

Cyclohexyl NHC

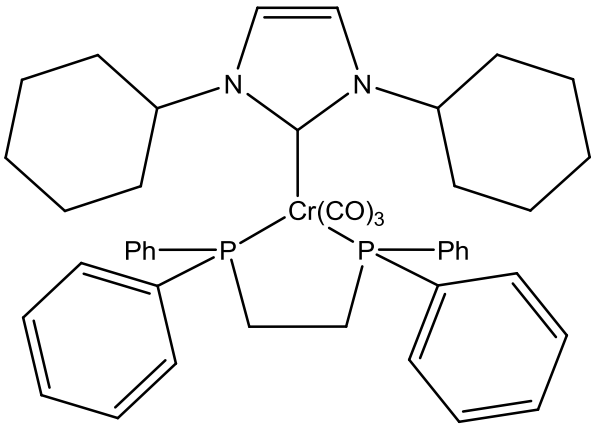

(Dppe)NHC

© University of Pretoria

6.3.2 Bidentate coordination

Coordination of the bidentate ligand can occur at two main positions (Figure 6.3). Removal of the labile carbonyl at either the facial or meridonial position of the carbene is plausible, producing the two isomers. In the case of the dppe bidentate ligand, both sterics and ligand characteristics need to be taken into consideration. Dppe is a larger, bulky ligand and thus positioning further away (*trans*) from the carbene would be expected, while the strong π-accepting ability of the ligand would allow for coordination across from a weaker accepting counterpart. The prevailing factor in the observation that strong π-accepting ligands prefer to coordinate with ligands with weaker ability, or even with only σ-donating characteristics, is that electron density competition is limited or even completely restricted. Theoretically calculated energies for both the *mer* and *fac* isomers, as well as the energy difference between the two isomers, are given in Table 6.3.

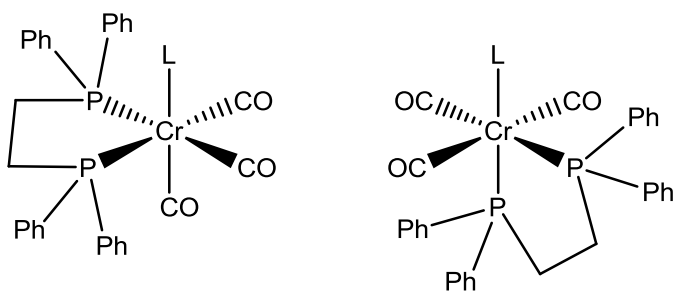

L = Fischer Carbene, NHC

Figure 6.3. Bidentate-containing isomers

Table 6.3. Calculated energy differences of the *fac* and *mer* isomers

Carbene (L)	*fac* kJ/mol	*mer* kJ/mol	Δ kJ/mol E_{mer}-E_{fac}	Dipole (Debye) *fac*	Dipole (Debye) *mer*
Bithiophene (**1**)	-8955513.13	-8955509.29	+3.84	7.72	4.91
Thiophene (**2**)	-7506738.81	-7506755.23	-17.84	7.44	5.30
Furan (**3**)	-6658743.33	-6658766.06	-22.73	6.62	5.29
Furan amino(**7**)	-7016352.10	-7016330.10	+22.00	7.40	3.11
Dppe NHC	-7377101.38	-7377100.66	+0.72	8.01	4.41

© University of Pretoria

Structural data clearly indicate the meridonial isomer as the more energetically favourable geometry in larger carbene complexes. Sterically, the bulky phenyl rings are located further away from the Fischer carbene, providing a less strained environment with ligation angles of approximately 90 and 180°, while the *fac* configuration has both phosphine ligation angles of 90° in reference to the carbene carbon. Structurally the *fac* isomer would likely be preferred energetically in situations where the carbene fragment is small or has less bulky substituents. This is supported in literature where complexes containing carbene substituents such as methyl groups[16] were found in a *fac* arrangement whereas complexes containing phenyl rings preferred the *mer* isomeric form.[17] Computational energy values, however, designate the *mer* isomer as the favoured conformation of the thiophene dppe (**2**) and furan dppe (**3**) ethoxycarbene complexes only. Computed energy values of the bithiophene dppe ethoxycarbene (**1**) as well as the furan dppe cyclohexyl aminocarbene (**7**) gave the *fac* isomer as the preferred arrangement. Since the computational results and the structural information contradict one another in certain cases, it is clear that further computational studies should include transition state calculations to determine activation energies associated with the formation of both isomers. This will be included in future work.

Only phosphine-containing carbene complexes were modelled, since selected complexes from this range were also applied in catalytic studies in chapter 5. The NHC pentacarbonyl complex was also optimised and energy determination utilising ground-state DFT calculations served to produce a reference molecule. Since only meridonial crystal structures were obtained, all computational calculations were done on this isomer.

6.3.2.1 HOMO, LUMO and potential energy surfaces

The HOMO (highest occupied molecular orbital) is defined, by the build-up principle, as the frontier orbital to be occupied lastly by electrons. The molecular orbital directly higher in energy is unoccupied and termed the LUMO (lowest unoccupied molecular orbital).[18] Both frontier orbitals play a vital role in determination of reactive centres on the molecule and, in particular, the susceptibility of a complex towards nucleophilic or electrophilic attack.[19] The

[16] Arrieta, A., Cossío, F. P., Fernández, I., Gómez-Gallego, M., Lecea, B., Mancheño, M. J., Sierra, M. A., *J. Am. Chem. Soc.* **2000**, 122, 11509–11510
[17] Barluenga, J., Muñiz, K., Tomás, M., Ballesteros, A., García-Granda, S., *Organometallics,* **2003**, 22, 1756–1760.
[18] Atkins, P., Overton, T., Rourke, J., Weller, M., Armstrong, F., *Inorganic Chemistry, 4th edn,* Oxford University Press, Oxford, UK, **2006**, p 58.
[19] (a) Fukui, K., Fujimoto, H., *Bull. Chem. Soc. Jpn,* **1969**, 42, 3399. (b) Klopman, G., Hudson, R. F., *Theor. Chim. Acta,* **1967**, 8, 165.

© University of Pretoria

highest-energy occupied orbitals of the attacking nucleophile are likely to be close in energy to the lowest unoccupied orbitals of the attacked electrophile.

Thus the HOMO occupies the nucleophilic reaction centre, while the LUMO is the special localisation of electrophilic characteristics.[20] Calculations aimed at determining the HOMO and LUMO of all the carbene complexes in this chapter were done using DFT calculations. Figure 6.4 provides a visual representation of the HOMO and LUMO of complex **2**.

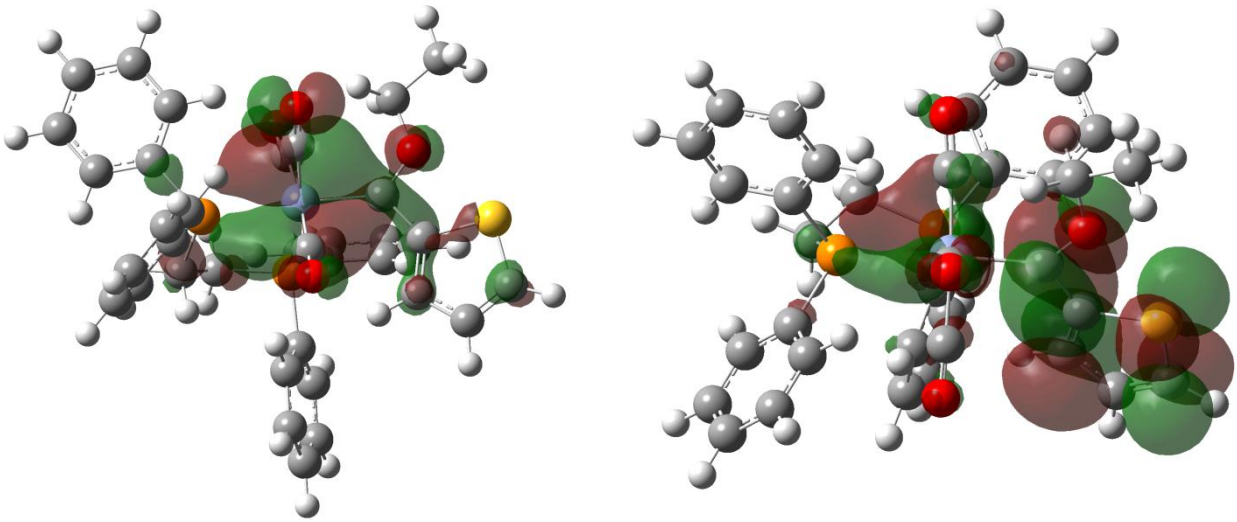

Figure 6.4. The HOMO (left) and LUMO (right) of complex **2**

The thiophene Fischer carbene complex depicted in Figure 6.4 indicates a HOMO located on the metal centre. Additional contribution to the HOMO is also found around the *cis* carbonyl (to the carbene) ligand and the *trans* phosphine atom. The largest contributor to the HOMO is a 3d atomic orbital of the chromium centre with a contribution of 44%. The LUMO is orientated around the carbene carbon with a 2pz orbital playing the major role and displaying a contribution of 30%. Additional LUMO character is also located on the heteroarene ring and both the carbene as well as portions of the arene would be expected to be electrophilic regions. Nucleophilic attack according to the computed model is characteristic of the metal centre.

[20] Clayden, J., Greeves, N., Warren, S., Wothers, P., *Organic Chemistry,*1st edn, Oxford University Press, Oxford, UK **2001**, p 118.

© University of Pretoria

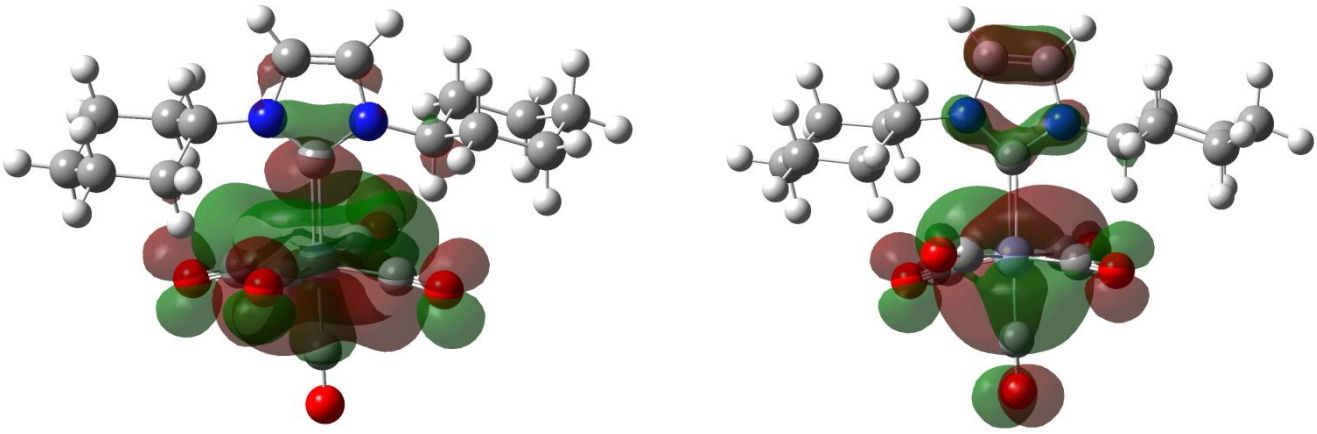

Figure 6.5. The HOMO (left) and LUMO (right) of cyclohexyl NHC complex

The cyclohexyl NHC complex contains a very interesting HOMO and LUMO distribution (Figure 6.5). The NHC complex illustrates a concentrated HOMO density around the metal centre and *cis* carbonyls, but with no spread located on the *trans* carbonyl ligand. Since the highest distribution of the LUMO is orientated around the carbene carbon, this would also be the electrophilic region. The metal-carbonyl coordination bonds bear LUMO density if located beneath the two chair structures, while only the *cis* carbonyl oxygen atoms contain a small allocation if coordinated in the meridonial orientation. The HOMO distribution is, as expected, located on the alkene bond of the NHC fragment, on the metal centre as well as on all the oxygen atoms of the carbonyl ligands. The largest contributor to the HOMO is a 3d atomic orbital of the chromium metal sphere and to the LUMO a 3s orbital of the carbene carbon. The contributions are 43% in both cases.

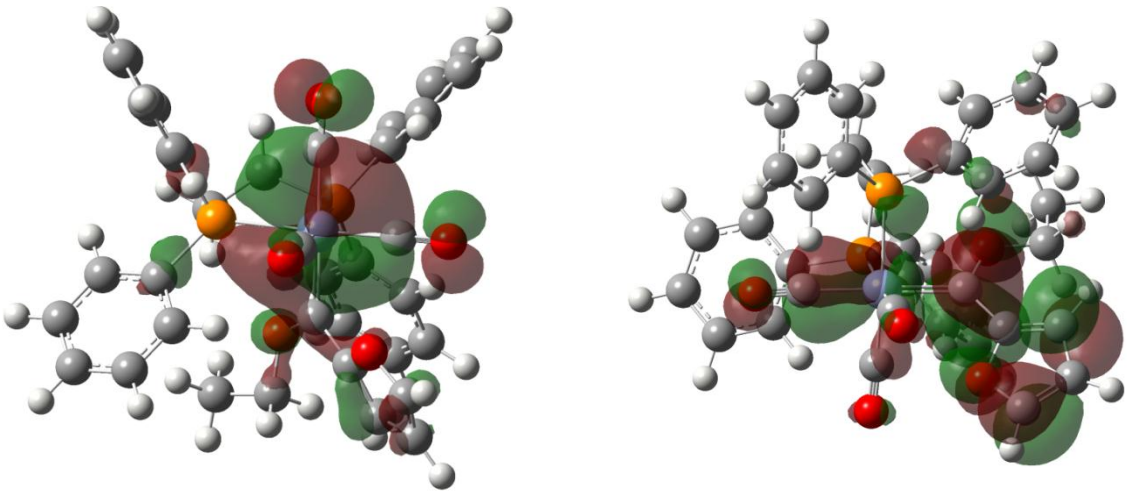

Figure 6.6. The HOMO (left) and LUMO (right) of complex **3**

© University of Pretoria

Theoretical modelling indicates that the HOMO of complex **3** is orientated around the Cr metal sphere with a 3d atomic orbital contributing the most to this orbital (42%) (Figure 6.6). The 2pz orbital of the carbene carbon atom makes the largest contribution towards the LUMO (26%). The heteroarene, the ethoxy substituents and, in particular, the carbene carbon also demonstrate HOMO characteristics, while some LUMO density is orientated around the *trans* phosphine atom. The HOMO orientation around the oxygen of the ethoxy substituent is in accordance with the nucleophilic characteristics as attributed in chapter 1. From the energy values in Table 6.3, it is clear that the meridonial isomer is favoured over the facial equivalent. According to the total electron density map (Figure 6.7), the main electronically active regions are located on the meridonial carbonyl ligands. The electron negativity of these groups, in conjunction with the metal→CO back-bonding, ensures a thick cloud of electron density located around these groups. The electron density is distributed more evenly over the remaining coordinated groups, with intermediate density for atoms and moieties closer to the carbonyl ligands.

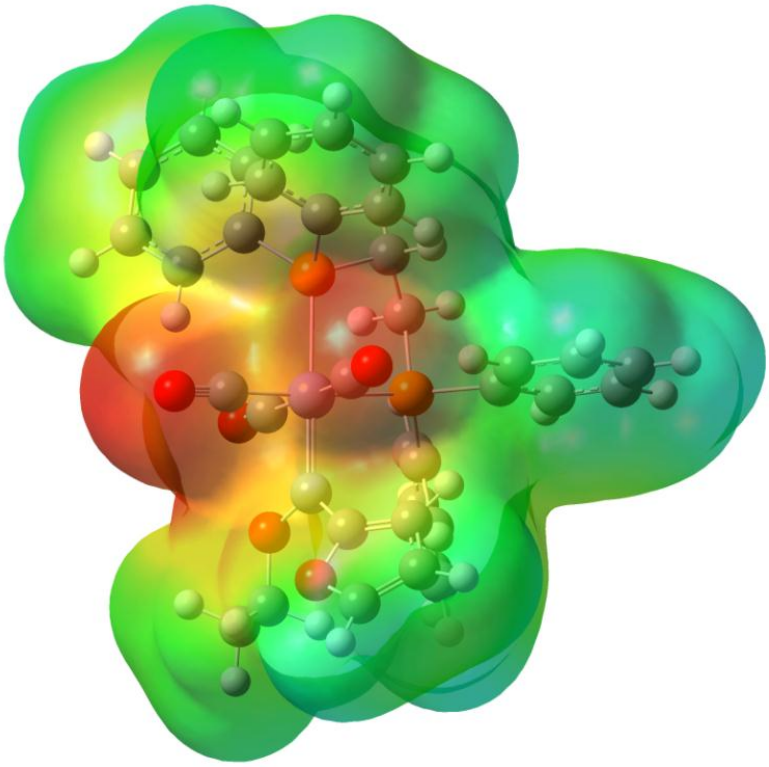

Figure 6.7. Electrostatic potential energy map for **3**

© University of Pretoria

DFT calculations indicated that for complex **7** the facial isomer is the preferred isomer, however, theoretical calculations were done for the meridonial isomer with the aim of comparing all the computed structures. The HOMO and LUMO orientations are thus presented for the meridonial isomer in Figure 6.8 and Table 6.4.

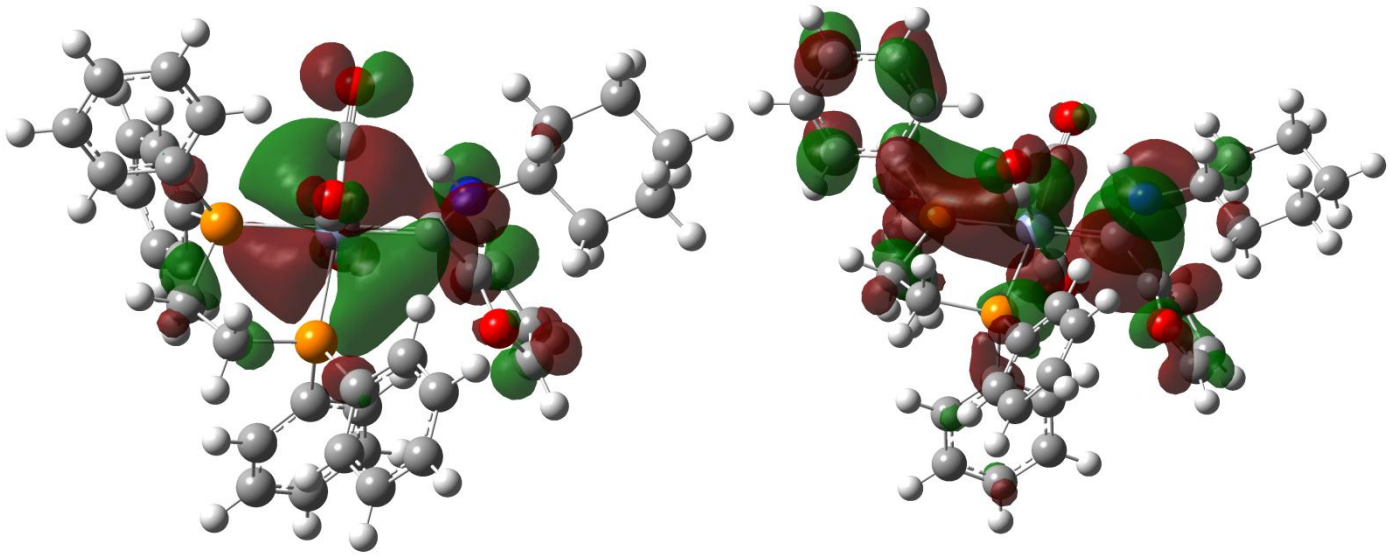

Figure 6.8. The HOMO (left) and LUMO (right) of complex **7**

The HOMO is distributed around the metal centre, while the LUMO density is located around an H atom on a C atom of the P-C-C-P backbone with a 2s orbital as the largest contributor. The atomic contribution associated with the LUMO is allocated as 54%.

Table 6.4. Theoretical results for complexes dppe containing complexes

Complex	HOMO distribution	Contribution	LUMO distribution	Contribution
1	Cr (3d)	58%	Carb C(2pz)	36%
2	Cr (3d)	44%	2pz	30%
3	Cr (3d)	42%	2pz	26%
7 (*mer*)	Cr (3d)	32%	P-CH*-C-P	54%
(dppe)(*fac*)NHC	Cr (3d)	41%	P-C*-C-P (2py)	28.5%

*Indicates the atom contributing the most significantly towards the LUMO

© University of Pretoria

The fac-(dppe)NHC complex presented the typical HOMO and LUMO orientation trends as observed for other complexes. As expected from all the results provided in this chapter, the HOMO also surrounded the Cr metal atom, with its d orbital providing the majority density. As Table 6.4 indicates, the LUMO is located around a carbon atom of the phosphine bidentate ligand. Figure 6.9 depicts the HOMO (left) and LUMO (right) of the NHC complex. Figure 6.10 shows that the electron distribution around the NHC molecule in the electron density map is fairly comparable to Figure 6.6.

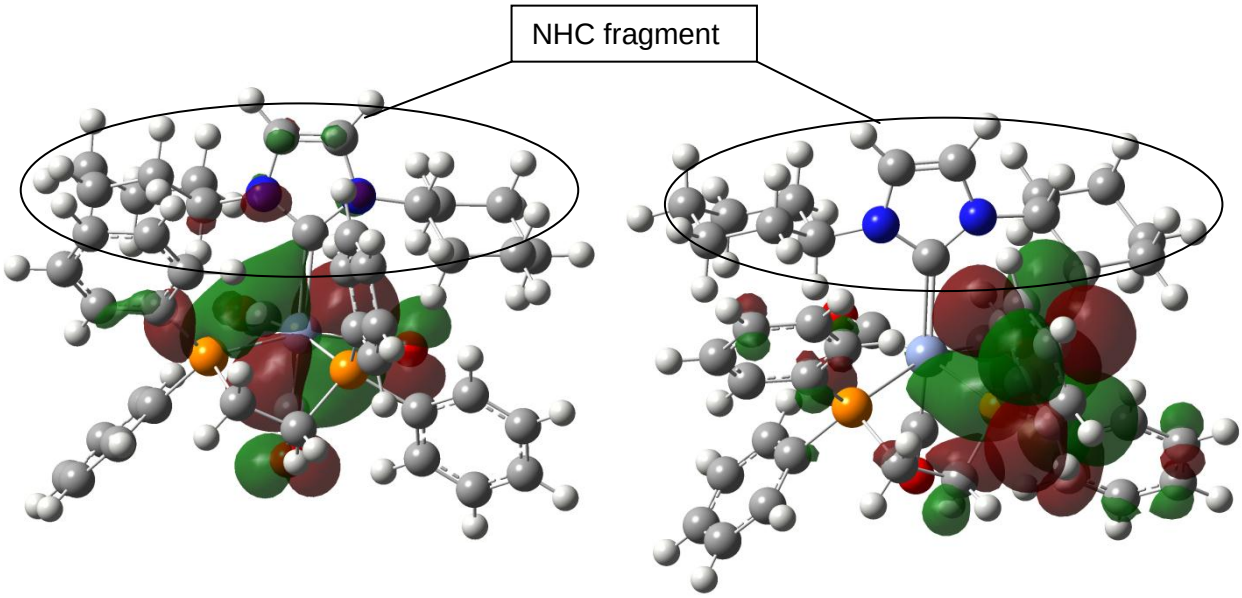

Figure 6.9. The HOMO (left) and LUMO (right) of the NHC complex

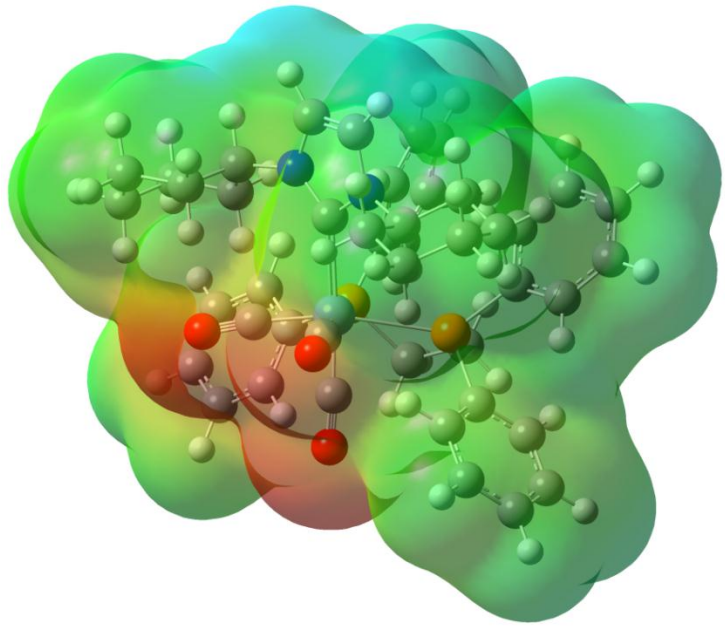

Figure 6.10. Electrostatic potential energy map of dppe NHC molecule

© University of Pretoria

6.3.2.2 Bonding characteristics

All complexes were optimised using DFT calculations and the theoretical bond lengths of classic Fischer carbene complexes were compared with the NHC counterparts. The strength of the combination of σ-donation to the metal centre from the Fischer carbene carbon atom, with the π-back-donation from the metal will determine the M-$C_{carbene}$ bond length. As stated by Frenking *et al*.,[21] the degree of electron deficiency at the carbene carbon is a direct effect of the strength of σ-donation from the carbene fragment to the metal. In the case of NHC complexes, enlarging the extent of σ-donation increases the π-electron donation from heteroatoms to the carbon atom in an attempt to stabilise the electron-poor carbene centre, and thus ultimately decreases the heteroatom-carbon bond. In effect, the C-N bond decreases as the $C_{carbene}$→M σ-bond increases. Table 6.5 provides the calculated bond lengths of selected Fischer carbene and NHC complexes. The theoretical meridonial isomer of a bidentate ligated NHC complex was selected to serve as comparison with complex **2** (meridonial).

Table 6.5. Theoretical bond lengths of selected complexes

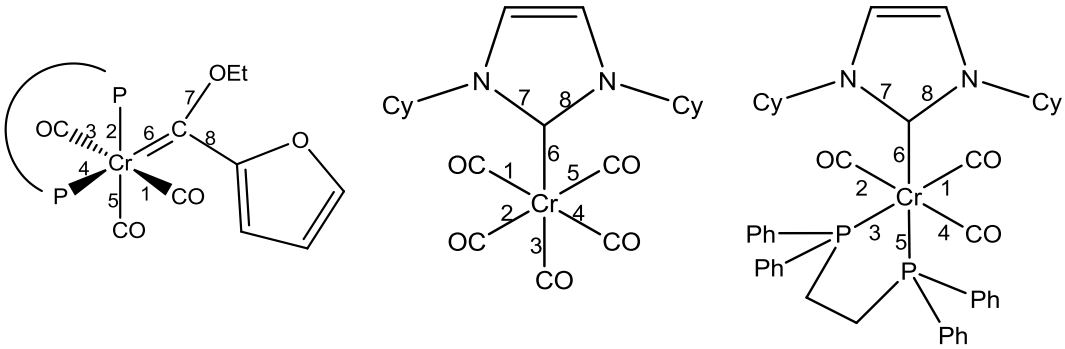

Bond	3	Cyclohexyl NHC	*mer*-dppe NHC
		Bond length (Å)	
1	1.87685	1.89764	1.84885
2	2.42160	1.89723	1.89020
3	1.88470	1.85960	2.54223
4	2.43306	1.89446	1.86916
5	1.85540	1.90199	2.53556*
6	1.96101	2.25447	2.23484
7	1.13511	1.37948	1.38721
8	1.46896	1.38241	1.39309

* Phosphine bond is *trans* to carbene bond

[21] Frenking, G., Solá, M., Vyboishchikov, S. F., *J. Organomet.Chem.*, **2005**, 290, 6178.

© University of Pretoria

6.3.2.3 Vibrational analysis and spectra

Computational modelling allows the prediction of carbonyl stretching frequencies after molecular optimisation is completed. The frequencies obtained from theoretical calculations are not always in accordance with experimental results but serve as an indicator of the expected region and number of bands to be observed. Theoretical modelling relies on the different media in which the data is collected and hence will have different frequency results. A full theoretical argument surrounding carbonyl stretching frequencies was provided in Chapter 2. The main aim of the vibrational analysis was to illustrate the effects of ligand substitution on the remaining carbonyl ligand sphere. Substitution of a single carbonyl ligand by an NHC moiety results in a pentacarbonyl complex. Stretching frequencies corresponding to the $A_1^{(1)}$, B_1, E and $A_1^{(2)}$ bands are expected for such complexes and there are normally strong E and $A_1^{(2)}$ vibration bands. The corresponding frequencies are 2123.00 cm^{-1}, 2048.12 cm^{-1}, 2032.95 cm^{-1}, 2030.70 cm^{-1} and 2010.79 cm^{-1}, respectively. Stretching of the carbonyl ligands in opposing vectors results in destructive interference and hence the $A_1^{(1)}$ and B_1 bands may appear minute. All complexes under study in this chapter, except for the cyclohexyl NHC complex and **B**, contained only three carbonyl ligands. Subsequent modification or substitution of labile carbonyl ligands resulted in the tricarbonyl substituted carbene complex. Although the experimental results showed only two vibrational bands, the computational model differentiated between three independent vibrations – $A_1^{(1)}$, $A_1^{(2)}$ and E. Theoretical calculations also indicated limited variation between the carbonyl stretching frequencies of the Fischer and NHC complexes containing a similar ligand sphere. The calculations signify that all complexes bearing only three carbonyl ligands contain vibrations at ± 2050, 2000 and 1975 cm^{-1}. Nonnenmacher *et al.* did, however, state that saturated NHC complexes are simultaneously more σ-basic and π-acidic in comparison with the unsaturated versions and thus may result in higher CO stretching frequencies.[22] Table 6.6 provides the calculated CO stretching frequencies for all complexes in this study.

Table 6.6. CO stretching frequencies for the complexes in this study

Assignment	**Complex**					
	1	**2**	**3**	**B**	Cy-NHC	dppe NHC *fac*
$\mathbf{A_1^{(1)}}$	2050.75	2038.56	2047.89	2079.30	2042.24	2050.75
$\mathbf{B_1}$	1975.14	1958.95	1970.24	2064.87	-	1975.14
E	-	-	-	2055.16	1953.02	-
$\mathbf{A_1^{(2)}}$	2000.38	1968.09	1999.44	2054.52	1973.71	2000.75

[22] Nonnenmacher, M., Kunz, D., Rominger, F., Oeser, T., *J. Organomet. Chem.*, **2005**, 690, 5647.

© University of Pretoria

Usually the values of the calculated vibrations cannot be compared directly with experimental values. Usually a scaling factor is necessary for direct comparison.[23,24]

Figure 6.11 shows a typical IR spectrum obtained from theoretical modelling. It indicates the expected region, band strength and number of visible bands for complex **3**.

Figure 6.11. Calculated IR spectrum for complex **3**, highlighting the CO region

6.3.2.4 Conformations of the pentacarbonyl carbene complexes

Metal pentacarbonyl carbene complexes can exist in two main conformations in reference to their carbene substituents. When the heteroatom of the arene ring orientates itself on the same side as the heteroatom carbene substituent, the *syn* conformation is produced whereas the opposite is true for the *anti* conformation. In this theoretical study the conformations of both the ethoxy and the aminocarbene complexes were studied (Figure 6.12).

[23] Scott, A.P., Random, L., *J. Phys. Chem.* **1996**,100, 16502
[24] Zhang, L., Zhang, Y., Tao, H., Sun, X., Guo, Z., Zhu, L., *Journal of Molecular Structure (Theochem).* **2002**, 617, 87

© University of Pretoria

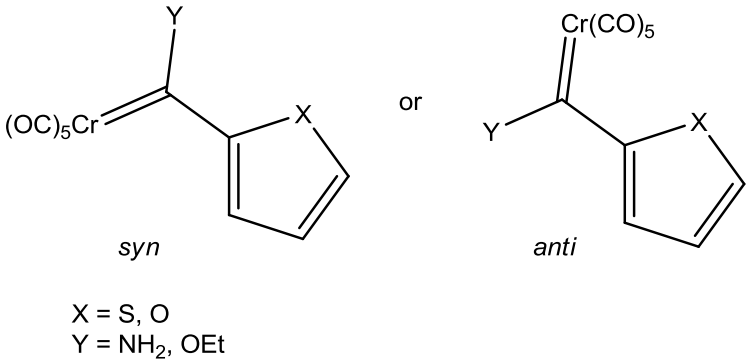

Figure 6.12. *Syn* and *anti* conformations of a pentacarbonyl carbene complex

In all cases the *syn* conformation is favoured, except for complex **F**. This complex exclusively favours the *anti* conformation. For all the theoretical calculations of the pentacarbonyl complexes, the conformation of the crystal structure corresponds to the lowest energy calculated complex. No standard numbering system was used to number atoms. Numbers were used as shown in individual figures. The conformations, crystal structures and energies associated with the different conformations of the thiophene carbene complexes (**E** and **A**) are displayed in Figures 6.13 and 6.14.

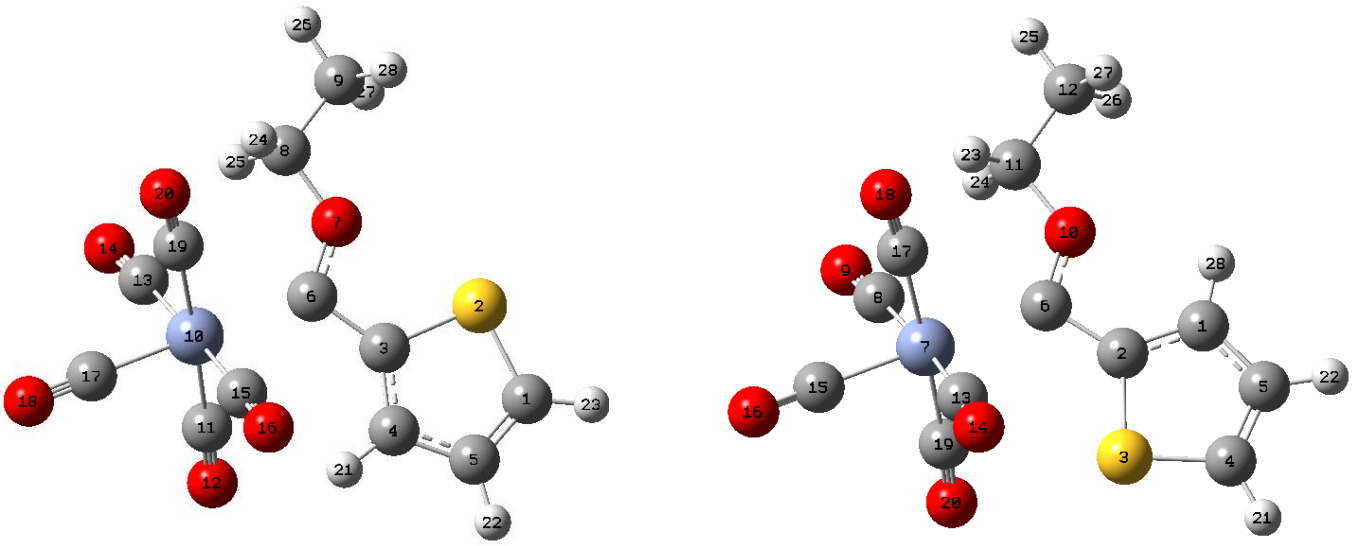

***Syn* E, *E* = 0 kJ/mol** **_Anti_ E, *E* = +12.66 kJ/mol**

Figure 6.13. Conformations and energies of thiophene carbene complexes (**E** and **A**)

© University of Pretoria

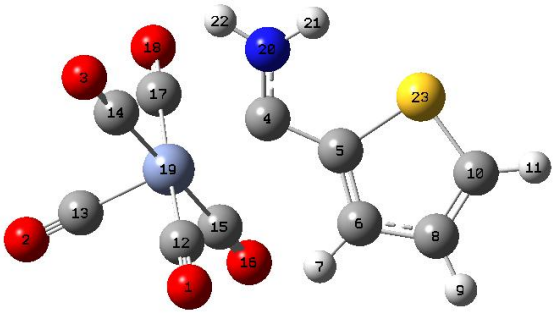

***Syn* A, *E* = 0 kJ/mol**

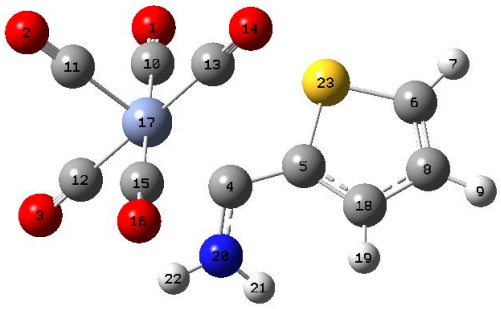

***Anti* A, *E* = +6.49 kJ/mol**

Figure 6.13 (continued). Conformations and energies of thiophene carbene complexes (**E** and **A**)

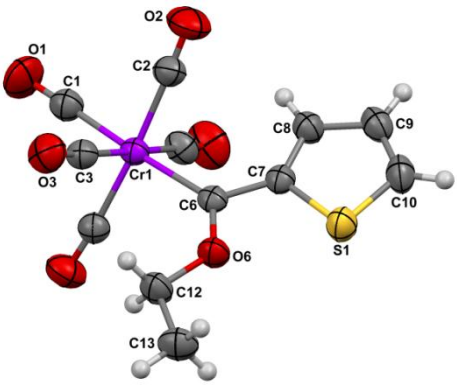

E

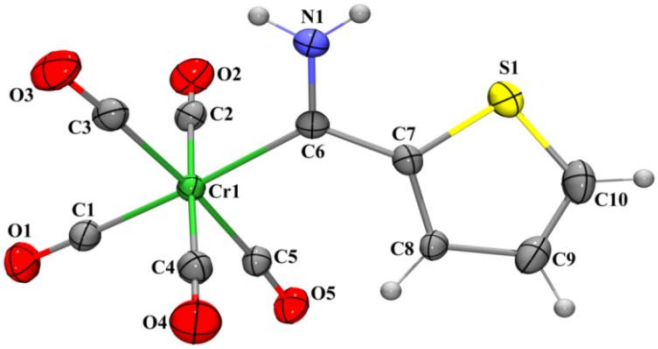

A

Figure 6.14. The crystal structures of thiophene carbene complexes (**E** and **A**)

The conformations, crystal structures and relative energies associated with the different conformations of the furan carbene complexes (**F** and **B**) are displayed in Figures 6.15 and 6.16.

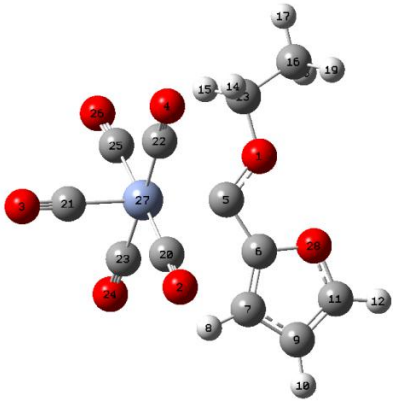

***Syn* F, *E* = +6.92 kJ/mol**

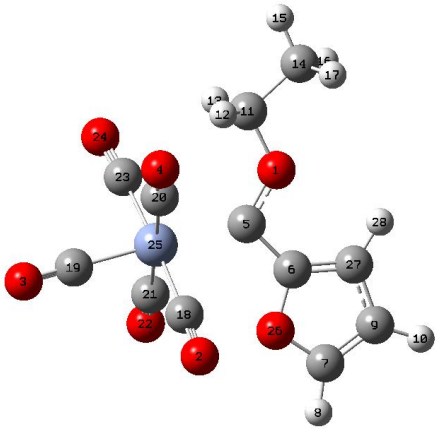

***Anti* F, *E* = 0 kJ/mol**

Figure 6.15. Conformations and energies of furan carbene complexes (**F** and **B**)

© University of Pretoria

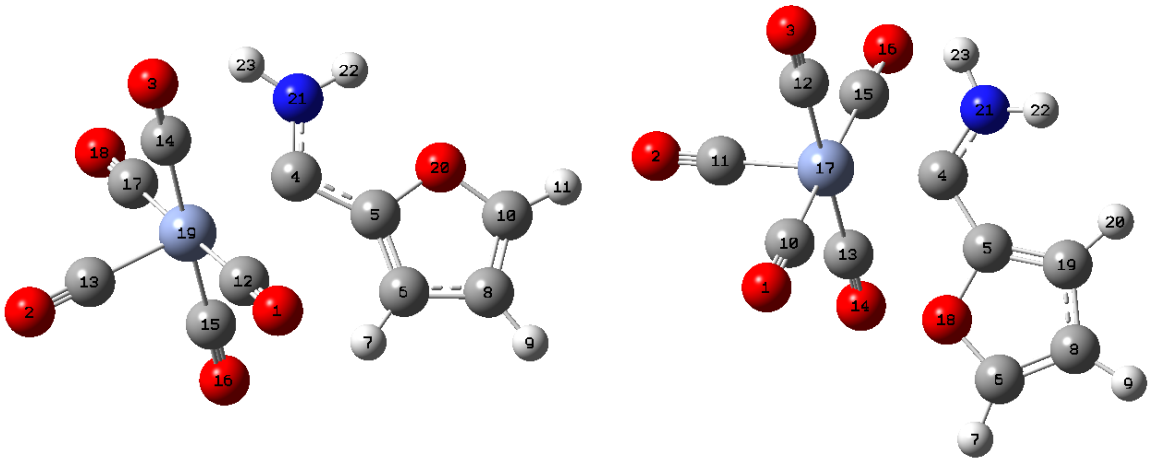

***Syn* B, *E* = 0 kJ/mol** ***Anti* B, *E* = +13.97 kJ/mol**

Figure 6.15 (continued). Conformations and energies of furan carbene complex (**F** and **B**)

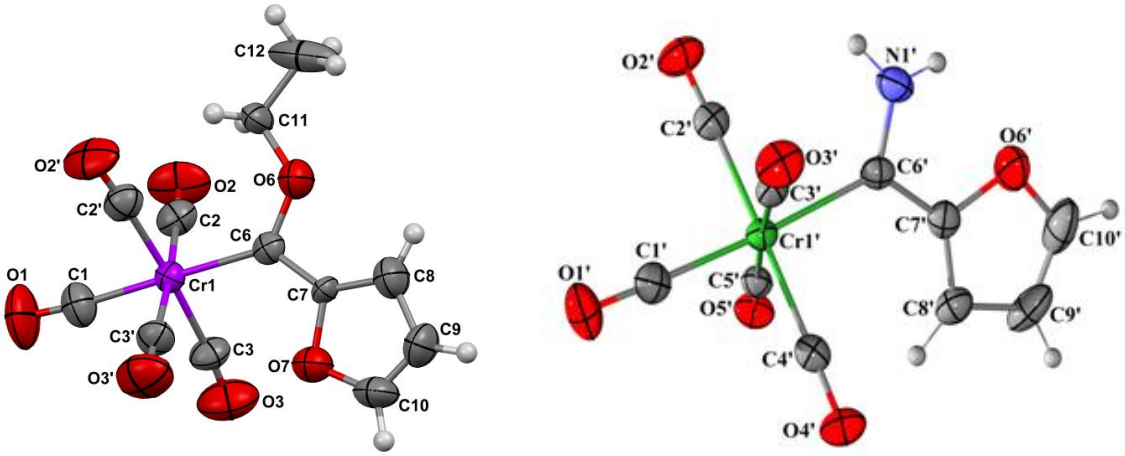

F **B**

Figure 6.16. The crystal structures of furan carbene complexes (**F** and **B**)

For the thiophene complexes, a certain percentage of the molecules were found in the *anti* conformation (±15%). This was not true for the furan complexes. Only one isomer was found in the crystal structure analysis and complex **F**, was only found in the *anti* conformation. No minor *syn* conformation was present in the crystal structure. NBO analysis of this complex indicated an interaction between the lone pair electrons on the O26-atom of the heteroarene ring and the anti-bonding orbitals on the carbonyls C21-O22 and C18-O2 (Figure 6.15). The associated energy of this interaction is around 9.2 kJ/mol, which may contribute to the preference of only this conformation in the solid state crystal structure (Figure 6.17).

© University of Pretoria

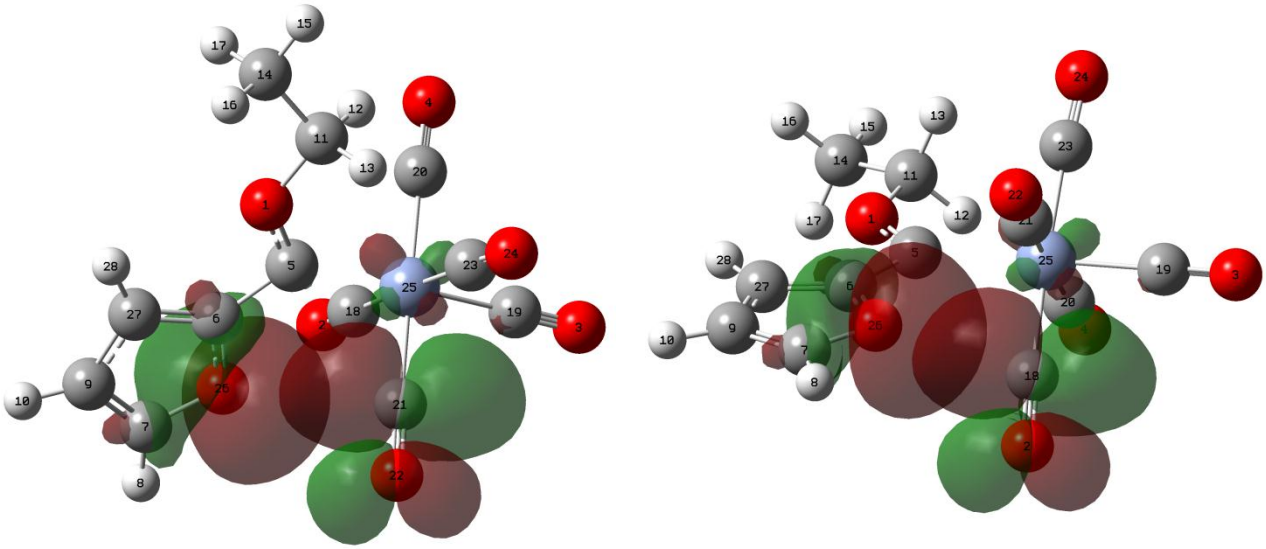

Figure 6.17. The interaction between the heteroarene oxygen's lone pair and the antibonding orbitals of carbonyls C21-O22 and C18-O2

Another attributing factor may be the short distance of 2.49 Å observed in *syn* **F** between O1 and O28. Both O atoms have lone pairs, which may repel one another, leading to the preference for the *anti* conformation. The similar distance between S2 and O7 in *syn* **E**, is 2.72 Å (Figure 6.18).

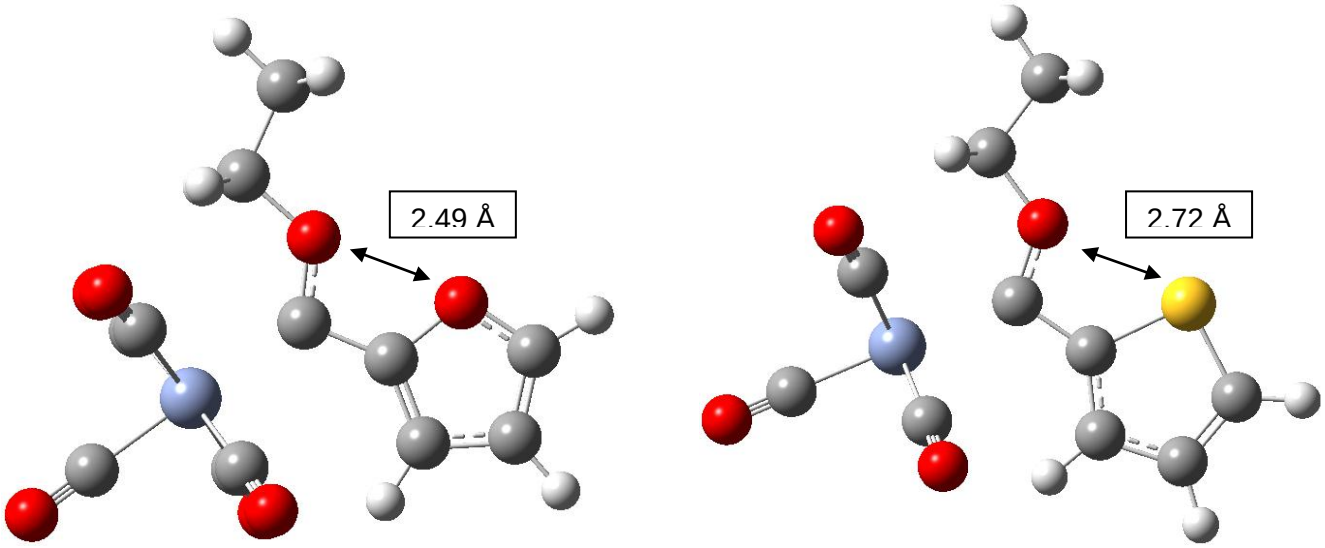

Figure 6.18. The interaction between the heteroarene oxygen's lone pair and the antibonding orbitals of the carbonyls

© University of Pretoria

7 Conclusions

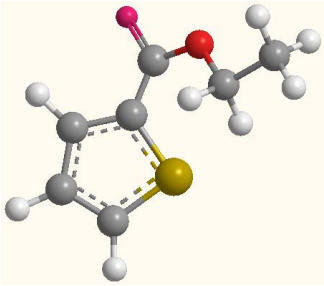

The objectives of this study were achieved in that numerous new functionalised monocarbene complexes of thiophene, furan and bithiophene were successfully synthesised. Synthetic procedures were also employed to synthesise novel N-heterocyclic carbene (NHC) complexes containing isopropyl and cyclohexyl substituents on the N-heteroatom. All carbene complexes were characterised and studied in solution, together with solid state analysis. Valuable information and insight were obtained from the spectroscopic data.

7.1 Synthesis

Monocarbene complexes of thiophene, furan and bithiophene were all prepared in a similar fashion (Fischer synthesis). The heteroarene substrates were all lithiated, directly metalated with $Cr(CO)_6$ and subsequently alkylated with an ethyl oxonium salt to yield red monocarbene complexes. The monocarbene starting material was further modified by the substitution of two labile carbonyl ligands with dppe, 2,2'-bipy, (Z)-N',N',N'',N''-tetramesitylethene-1,2-diamine or N'N'N''N''-tetramethylethane-1,2-diamine (TEMED) bidentate ligands to produce bidentate functionalised carbenes for the phosphine-containing ligands and coordination complexes for the amine-containing ligands. Although synthesis of these complexes was not particularly difficult, purification proved more challenging and both the 2,2'-bipy and the TEMED ligated complexes could only be isolated by washing with cold hexane. After characterisation was completed, it was found that the amine ligands substituted the carbene moiety and produced bidentate coordination complexes. In the case of EDA, aminolysis products were obtained instead of either substituted carbene complexes or coordination compounds. Even under inert conditions, synthesis and purification of the NHC complexes led to immense complications. Direct substitution of a labile metal substituent by the deprotonated NHC molecule produced the NHC-$Cr(CO)_5$ complexes in low yields. Higher numbers of carbonyl ligands could not be substituted after the formation of the NHC complexes and attempts to ligate dppe failed. Extreme inert conditions and the use of a glove box are advised for this synthesis. Characterisation of these compounds was

© University of Pretoria

problematic due to low yields. Figure 7.1 displays the synthetic pathways attempted as well as the outcomes obtained for the Fischer carbene complexes. Figure 7.2 shows the outcomes obtained for the NHC carbene reactions. Low solubility, air and moisture sensitivity, side reactions and the low yields obtained proved challenging to overcome for all compounds synthesised. Future work should focus on finding synthetic routes that enable both high obtainable yields and an easier practical approach.

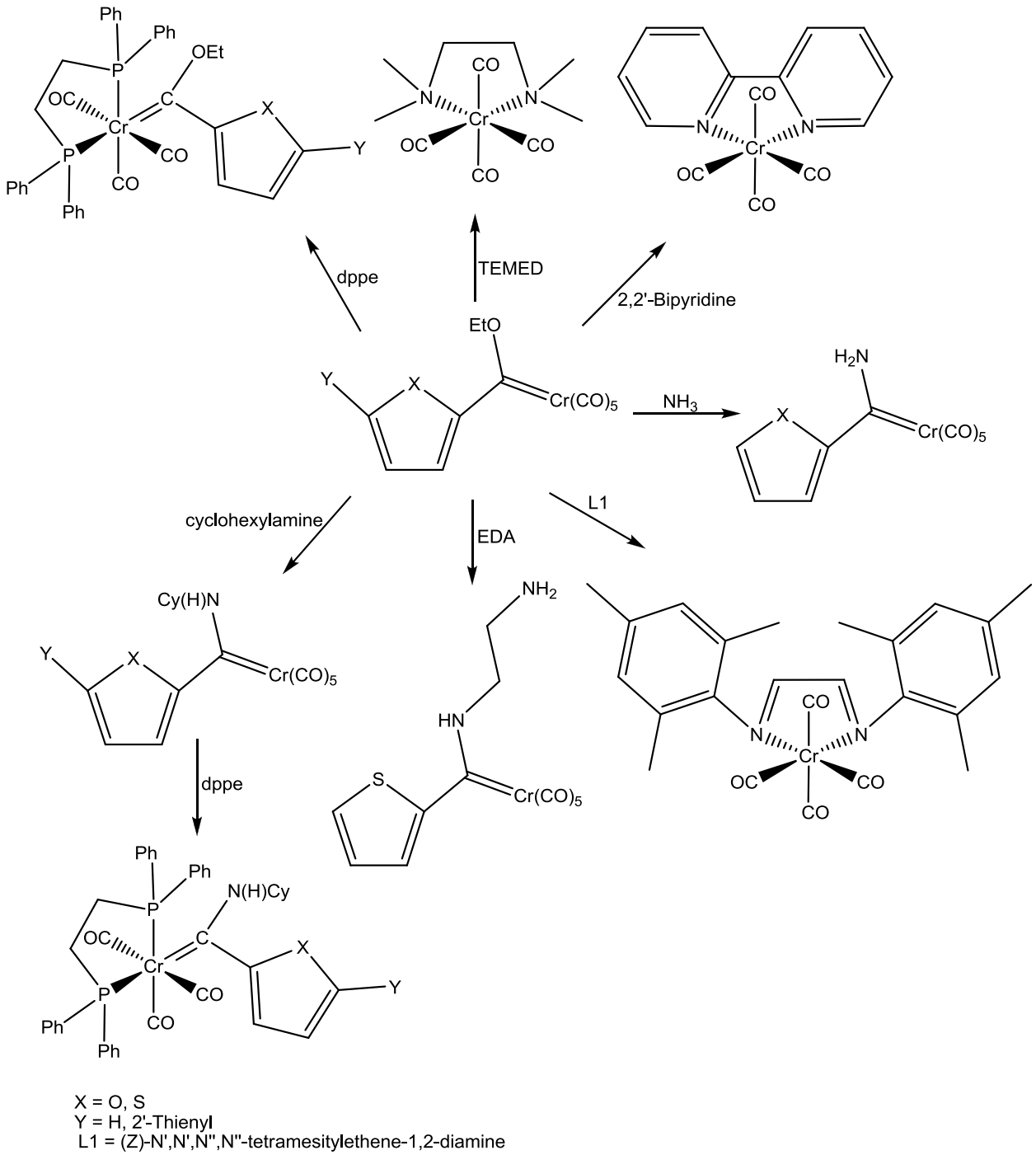

Figure 7.1. The synthesis and outcomes of all Fischer carbene reactions attempted

© University of Pretoria

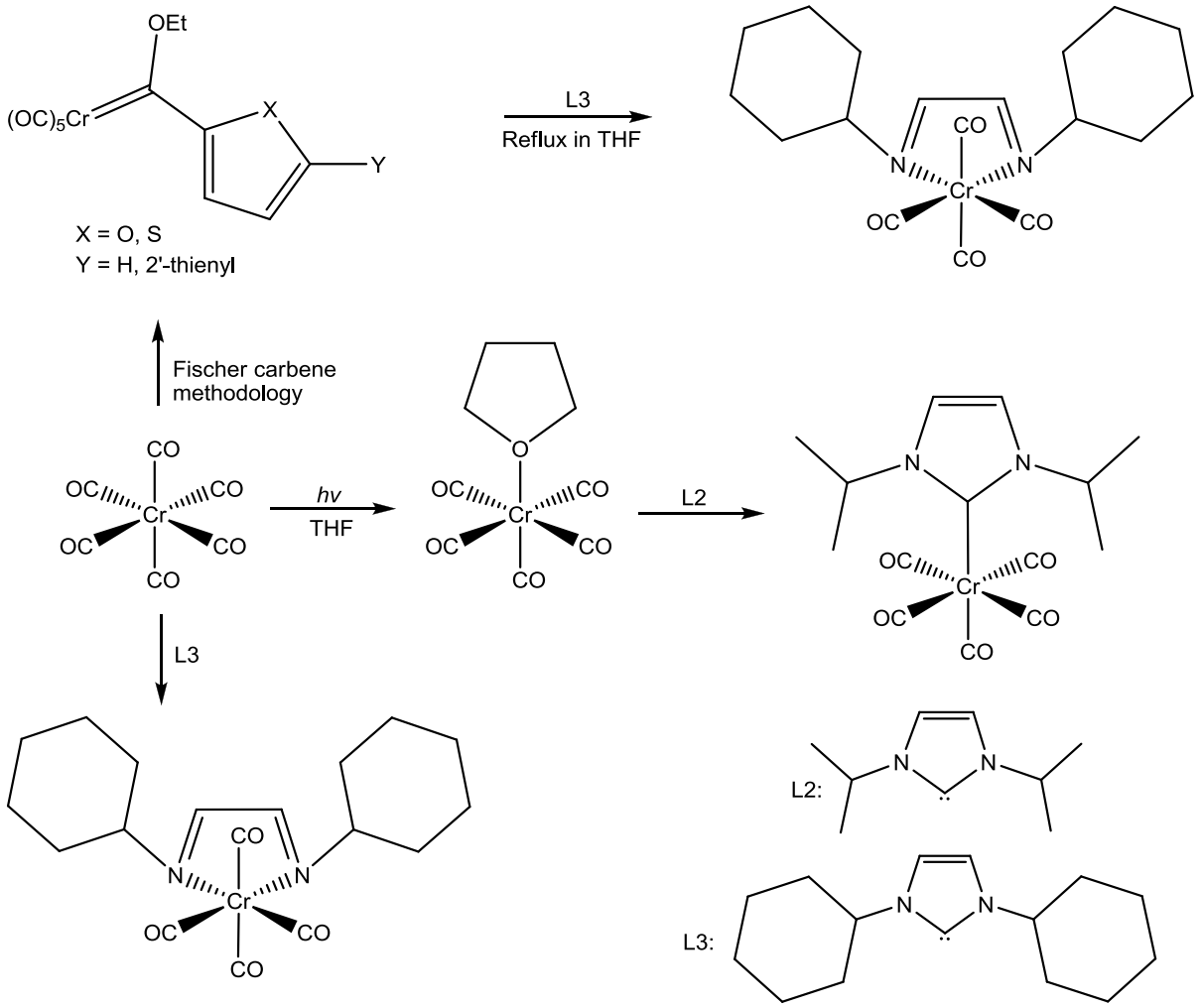

Figure 7.2. The synthesis and outcomes of all NHC complex reactions attempted

7.2 Characterisation

7.2.1 NMR spectroscopy

NMR characterisation confirmed the proposed structures of the compounds synthesised. Carbonyl ligands of the phosphine substituted ethoxycarbene complexes (**1**, **2**, **3**) showed three distinctive carbonyl peaks in the region 220-235 ppm, more downfield compared to the two carbonyl resonances observed for the pentacarbonyl analogues (**E**, **F**, **G**) in the 217-223

© University of Pretoria

ppm region.[1,2] Also, in changing the carbene substituent from an ethoxy group to an amino group left the carbonyl chemical shifts virtually unchanged for both the pentacarbonyl (**A**, **B**, **E**, **F**, **G**, **4**, **5**, **8**, **10**, **11**) as well as the dppe substituted tricarbonyl complexes (**1**, **2**, **3**, **6**, **7**, **9**). Changing the metal coordination sphere had negligible influence on the chemical shifts of the carbene heteroarene substituents in both ^{1}H and ^{13}C NMR spectra. The carbene carbons of the phosphine substituted ethoxycarbene complexes, in general, showed only slightly more downfield shifts compared to the pentacarbonyl analogues.[1,2] The carbene carbons of the ethoxycarbene complexes were observed 50 ppm more downfield than any of the aminocarbene carbon peaks. In the ^{13}C spectrum of the NHC complex, the carbene carbon resonance was observed at 189.9 ppm. The spectra of this complex had distinguishable peaks, which corresponded exceptionally well with the literature values. Table 7.1 summarises the carbonyl regions as well as the carbene carbon region on the ^{13}C NMR spectra.

Table 7.1. ^{13}C NMR summary

Complex	Carbonyl ligands	Carbene carbon
Pentacarbonyl ethoxycarbene **E, F, G**	217-223 ppm	312-314 ppm
Tricarbonyl dppe ethoxycarbene **1, 2, 3**	220-235 ppm	312-316 ppm
Pentacarbonyl aminocarbene **A, B, 4, 5, 8, 10, 11**	217-223 ppm	250-280 ppm
Tricarbonyl dppe aminocarbene **6, 7, 9**	220-234 ppm	260-280 ppm

7.2.2 Infrared spectroscopy

Good infrared spectra were generally obtained. The IR data clearly showed the relationship between the number of remaining carbonyl ligands and the number and position of vibrational bands. All modified Fischer carbenes had three remaining carbonyls corresponding to the $A_{(1)}$, $B_{(1)}$ and $A_{(2)}$ vibrating bands. These bands were also significantly lower in wavenumber than the hexacarbonyl or pentacarbonyl bands (Table 7.2).

[1] van Staden, M., MSc Dissertation, *Synthesis and structure of bithiophene complexes,* **2001**, University of Pretoria, Pretoria.
[2] Crause, C., *Synthesis and application of carbene complexes with heteroaromatic substituents,* **2004**, University of Pretoria, Pretoria.

© University of Pretoria

Table 7.2. v_{CO} summary

Complex	CO stretching frequency range
Pentacarbonyl ethoxycarbene[1,2] **E, F, G**	1945-2061 cm^{-1}
Tricarbonyl dppe ethoxycarbene **1, 2, 3**	1837-2007 cm^{-1}
Pentacarbonyl aminocarbene **A, B, 4, 5, 8, 10, 11**	1910-2060 cm^{-1}
Tricarbonyl dppe aminocarbene **6, 7, 9**	1805-2007 cm^{-1}

7.2.3 X-ray crystallography

Suitable crystals and crystal structures could be obtained for four dppe coordinated carbene complexes, one ethoxycarbene, two aminocarbenes and three coordination complexes. Structural and electronic features could be derived from the crystal structures. Upon carbene formation, electron delocalisation in the heteroarene rings leads to bond lengthening of the formal double bonds, resulting in bond lengths of intermittent single-double bond character. The heteroatom also acquired a specific special orientation, i.e. *syn* or *anti* with regards to the heteroatom carbene substituent. In general the *syn* conformation is favoured. The only exception found in this study was the furan ethoxycarbene, **F**, which was found exclusively in the *anti* conformation. The average carbonyl bond lengths of **1**-**3** were comparable to one another and were measured to be in the region of ± 1.86 Å, which is similar to values found for the thiophene aminocarbene complex **6**. All the complexes containing dppe crystallised as the meridonial isomer, having one coordinating phosphorous atom *trans* to that of a carbonyl, while the other phosphorous atom attained a *trans* position to the carbene. The Cr-P bond length, *trans* to the carbene, was found to be slightly shorter by 0.03 Å (average) compared to the Cr-P bond length *trans* to a carbonyl.

7.2.4 Mass spectrometry

All complexes with presentable quantities were dissolved in acetonitrile and analysed with mass spectrometry. Fragmentation generally occurred with the loss of subsequent carbonyl ligands.

© University of Pretoria

7.3 Theoretical modelling

Theoretical modelling of the complexes was achieved via DFT calculations and the results obtained proved the adequacy of the model applied. The bond lengths, geometry and bond angles were all comparable with those of the crystallographic data. Energy calculations showed that modelling methods provide good estimations of energetically favourable geometries, and that accurate DFT calculations can also predict HOMO and LUMO locations on the structure. Results from computational calculations indicated that the *fac* isomer of **1** should be energetically favoured while the crystal structure showed the meridonial isomer as the preferred isomer in solid state. Computational conformational energy values provided excellent correlation with crystal structures obtained for complexes **A**, **B**, **E** and **F**. Molecular orbital calculations indicated the chromium 3d atomic orbitals as the major contributor towards the HOMO whereas in many cases, the carbene carbon atom contributed towards the LUMO. Electron potential energy maps of complex **3** provided a visual representation of the electron density distribution in a dppe monocarbene complex. Another interesting result obtained from theoretical calculations was the large difference in dipole moment between the *fac* and *mer* isomers of the calculated structures. The *fac* isomer displayed a considerable larger dipole moment in comparison to the *mer* isomer. The *fac* isomer assembled ligands together in such a manner that the electron withdrawing carbonyl ligands were packed closely together on one face of the molecule. The net effect is a strong electron draining towards the metal moiety, leaving this area highly electron rich.

7.4 Catalytic studies

Both metathesis and polymerisation catalytic reactions were attempted on complex **2,** while only metathesis studies were attempted for complex **6**. Both complexes were found to be inert to either of the reactions and there was no evidence of catalytic ability. Gas chromatography was utilised to study the progress of the reactions and the chromatograms presented evidence that neither pre-catalyst found application in metathesis or, in the case of complex **2**, polymerisation.

© University of Pretoria

8 Experimental: Standard Operational Procedures and Specifications

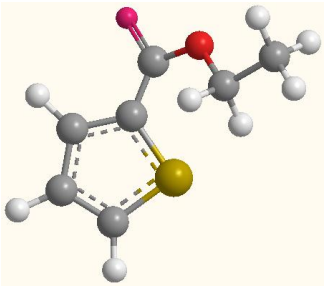

8.1 Products

Table 8.1. Product information (values refer to page numbers)

Complex	Colour	^{1}H NMR	^{13}C NMR	IR	Structure	Synthesis
	Dppe modified Fischer carbenes					
1	Brown-purple	51	58	63	65	171
2	Brown-orange	51	58	63	67	171
3	Brown-orange	52	59	63	69	171
	Amino Fischer carbenes					
4	Yellow	86	94	100	-	173
5	Yellow	86	94	100	-	173
6	Brown-orange	87	96	100	104	174
7	Brown-orange	87	96	100	-	174
8	Yellow	88	97	100	-	173
9	Brown-orange	90	99	100	-	174
10	Yellow	88	97	100	-	173
11	Red-orange	88	98	100	-	173
A	Yellow	85	93	100	103	173
B	Yellow	85	93	100	102	173

© University of Pretoria

Table 8.1 (continued). Product information (values refer to page numbers)

Complex	Colour	^{1}H NMR	^{13}C NMR	IR	Structure	Synthesis
	NHC Complexes					
12	Yellow	118	120	122	-	175
	Coordination Complexes					
13	Pink	119	121	122	123	175
14	Blue	52	59	63	70	177
15	Yellow	-	-	-	125	175
	Monocarbene Starting Material					
F	Red-orange	-	-	-	73	-

8.2 Information and Specifications

8.2.1 NMR spectroscopy

All complexes were dissolved in deuterated solvents and the NMR spectra were obtained by running the samples on the spectrometer. Solvation occurred under inert conditions by filling the reaction flask with dry argon. The reference signals of the deuterated solvents[1] are presented in Table 8.2.

Table 8.2. Solvent references[1]

Deuterated solvent	^{1}H NMR (ppm)	^{13}C NMR (ppm)
Acetone-d^6	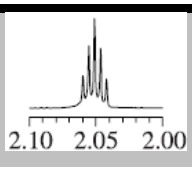	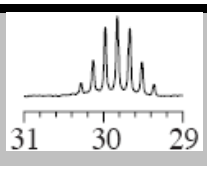
THF-d^8	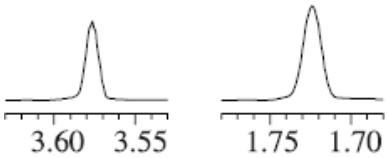	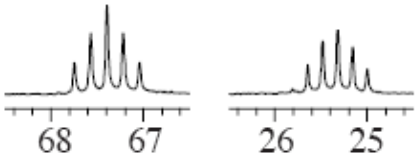
Chloroform-d	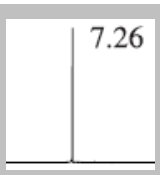	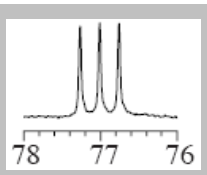

[1] Pretsch, E., Bühlmann, P., Badertscher, M., *Structure Determination of Organic Componds, 4th edn,* Springer-Verlag, Berlin, Heidelberg, **2009**.

© University of Pretoria

The specifications of the spectrometers utilised for chemical analysis are indicated in Table 8.3.

Table 8.3. NMR spectrometer specifications

Spectrometer	^{1}H NMR (MHz)	^{13}C NMR (MHz)
Bruker ARX-300	300.135	75.469
Bruker Ultrashield 400 Plus. Avance III.	400.21	100.63
AVANCE 500	500.139	125.75

8.2.2 Infrared spectroscopy

Infrared spectra were obtained in solid state on a Perkin-Elmer Spectrum RXI FT-IR spectrophotometer using KBr pellets. A pellet of pure KBr functioned as a reference sample and the region between 400 and 4000 cm^{-1} was recorded. Carbonyl bands, visible in the region 1800–2100 cm^{-1}, were reported.

8.2.3 X-ray crystallography

X-ray diffraction was utilised to confirm the true structure of all complexes from which a single crystal was obtainable. The following universities took part in obtaining crystal structures: University of Johannesburg, University of Stellenbosch, University of the Witwatersrand and University of Cambridge (UK).

8.2.4 Gas chromatography

GC analysis was performed on both an Agilent 2890 and an Agilent 6850 gas chromatograph equipped with an Agilent 7683 auto-injector, HP-5 capillary column (30 m × 320 µm × 0.25 µm) and a flame ionisation detector (FID). The precise GC settings were as follows:

Inlet temperature	250 °C
N_2 carrier gas flow rate	1.9 ml/min
Inject volume	2.0 µl (auto inject)
Split ratio	50.4 : 1

© University of Pretoria

Oven programming	Initial: 60 °C for 5 min
	Ramp 1: 60 to 110 °C for 10 min at 25°C/min
	Ramp 2: 110 to 290 °C at 25°C/min
	Ramp 3: 290 to 300 °C for 5 min at 25°C/min
Detector	FID @ 250 °C
H_2flow rate	40 ml/min
Air flow rate	450 ml/min

8.2.5 Mass spectroscopy

The mass spectroscopy was done utilising a SYNAPT G2 HDMS with the following parameters:

- TOF MS method
- Sampling time of 4 min with direct infusion inlet method
- Source : electron spray ionisation
- Positive polarity: Acquisition mode
- Resolution: Analyser mode

8.2.6 Reactions

All synthetic reactions were carried out under an inert atmosphere (argon or nitrogen) using classic Schlenk techniques.[2] Inert solvents were required and were therefore dried immediately prior to use. Fischer methodology[3] was followed to synthesise the monocarbene starting material complexes through an organolithium nucleophile addition to a metal carbonyl to form the acyl metalate. O-alkylation with triethyl oxonium salt accomplished alkylation. Thermal substitution of labile carbene carbonyls to form bidentate ligated Fischer carbene complexes followed the synthetic approach proposed by Barluenga *et al*.[4] Direct substitution of a labilised metal carbonyl ligand by deprotonated NHC molecules produced the NHC-Cr complex in diminished yields. Synthesis of NHC ligands was attempted following

[2] Schriver, D. F., Drezdon, M. A., *The Manipulation of Air-sensitive Compounds, 2nd edn,* Wiley, New York, US, **1980**.
[3] Fischer, E. O., Maasböl, A., *Angew. Chem., Int. Ed. Engl.,* **1964**, 3, 580.
[4] Barluenga, J., Muñiz, K., Tomás, M., Ballesteros, A., García-Granda, S., *Organometallics,* **2003**, 22, 1756–1760.

© University of Pretoria

the methodology proposed by Nonnenmacher *et al.*[5] Further modifications of the NHC complexes by thermal substitution of carbonyl ligands for bidentate counterparts were again attempted following the methods proposed by Barluenga *et al.*[4] Purification of the synthesised carbene complexes was achieved either via silica gel (particle size 0.063-0.200 nm) chromatography or by multiple cold hexane washes.

8.3 Preparation of Bidentate-containing Fischer Carbene Complexes

Monocarbene complexes of furan, thiophene and bithiophene were synthesised prior to the attempt at chelation substitution reactions. The synthesis of these monocarbene starting materials was based on the details given in the thesis by Crause[6]. Thiophene, furan and bithiophene were all bought from Sigma-Aldrich. 2,2'-Bipyridine, TEMED and dppe reagents were also purchased from Sigma-Aldrich.

8.3.1 1,2-Bis(diphenylphosphino)ethane chelated monocarbene complexes (1-3)

An oven-dried 50 ml round-bottomed flask was filled with inert argon gas and 20 ml of dried toluene (20 ml) was added as solvent. $Cr(CO)_5$heteroarene carbene (1.0 mmol) was dissolved in toluene and 1,2-bis(diphenylphosphino)ethane (1.0 mmol, 0.398 g) was added in a single portion. The reaction mixture was allowed to reflux at 90 °C until the reaction had proceeded to completion. The solvent was removed *in vacuo*, resolvated with dry DCM (15 ml) and inert silica gel, and finally dry loaded onto a column for purification. Purification via silica gel chromatography was achieved and the contaminates were removed by eluting first with hexane and secondly with a hexane:DCM (8:2) mixture. The product was recovered from the column with a hexane:DCM mixture (8:2) as eluent. Product fraction: Brown-orange (chelated monocarbene complexes **1**-**3**).

<u>Carbene quantities reacted:</u>

Complex **E** (1.0 mmol, 0.332 g) for complex **2**

Complex **F** (1.0 mmol, 0.316 g) for complex **3**

Complex **G** (1.0 mmol, 0.498 g) for complex **1**

[5] Nonnenmacher, M., Kunz, D., Rominger, F., Oeser, T., *J. Organomet. Chem.,* **2005**, 690, 5647
[6] Crause, C., *Synthesis and application of carbene complexes with heteroaromatic substituents,* **2004**, University of Pretoria, Pretoria.

© University of Pretoria

Yields:

Complex **1** = 60%; Brown-purple colour

Complex **2** = 65%; Brown-orange colour

Complex **3** = 63%; Brown-orange colour

8.3.2 2,2'-Bipyridine chelated monocarbene complex

The same procedure was followed as for the bidentate phosphine ligation to a carbene complex. $Cr(CO)_5$heteroarene carbene (1.0 mmol) was dissolved in toluene (15 ml) and 2,2'-bipy (1.0 mmol, 0.156 g) added in a single portion. No additional changes were made.

Purification could only be achieved with multiple cold hexane washes. Product fraction: Peach-red (coordination compound).

Note: The bidentate ligand substituted the monocarbene fragment and yielded an incorrect coordination complex, **C**, instead.

Yield:

Complex **C** : 60%; Peach-red colour

8.3.3 TEMED chelated monocarbene complex

Again a similar procedure was followed as for the bidentate phosphine and 2,2'-bipy ligation to a carbene complex. $Cr(CO)_5$heteroarene carbene (1.0 mmol) was dissolved in toluene (20 ml) and N'N'N''N''-(tetramethyl)ethane-1,2-diamine (1.0 mmol, 0.116 g) added in a single portion. No additional changes were made.

Purification could only be managed with several cold hexane washes. Product fraction: Yellow-brown (coordination compound).

Note: The bidentate ligand substituted the monocarbene fragment and yielded an incorrect coordination complex, **D**, instead.

Yield:

Complex **D**: 55%; Yellow-brown colour

© University of Pretoria

8.4 Preparation of Aminocarbene Complexes

Monocarbene complexes of furan and thiophene were again synthesised as starting material for further modification to produce aminocarbene complexes. Both simple aminolysis with NH_3 and chelation substitution reactions were attempted. Aminolysis with NH_3 was achieved by bubbling ammonia gas through a solution of the carbene starting material. The cyclohexylamine aminolysis reagent was purchased from Sigma-Aldrich.

8.4.1 Ammonia aminocarbene complexes (A and B)

An oven-dried Schlenk flask was filled with inert argon gas and 15 ml of dried ether was added to function as solvent. $Cr(CO)_5$heteroarene carbene (1.0 mmol) was dissolved in dry ether (15 ml) and ammonia gas bubbled through the reaction mixture until all the alkoxycarbenes had been converted to the amino version and an yellow-orange product obtained. Excess ammonia was removed under vacuum and no additional purification was needed or attempted.

<u>Carbene quantities reacted:</u>

Complex **E** (1.0 mmol, 0.332 g) for complex **A**

Complex **F** (1.0 mmol, 0.316 g) for complex **B**

<u>Yields:</u>

Complex **A**= 98%; Yellow colour

Complex **B**= 97%; Yellow colour

8.4.2 Mono aminocarbene complexes (4, 5, 8, 10 and 11)

Complexes **4**, **5**, **8**, **10** and **11** were all prepared by stirring the appropriate monocarbene complex (1 mmol) with the corresponding amine (1 mmol) at room temperature. After the reaction had turned yellow and all starting material had been converted to the aminocarbene, the reaction mixtures were dried under vacuum and purified via silica gel chromatography. Complexes **4**, **5** and **8** were separated by first eluting with hexane and secondly with a 50:50 mixture of hexane:DCM. Since products **10** and **11** were so polar, a hexane:DCM (50:50) mixture was used from the start and complex **11** was only eluted using dry THF as solvent.

© University of Pretoria

Carbene quantities reacted:

Complex **E** (1.0 mmol, 0.332 g) for complexes **4**, **10** and **11**

Complex **F** (1.0 mmol, 0.316 g) for complexes **5**

Complex **G** (1.0 mmol, 0.498 g) for complex **8**

Amine quantities reacted:

Cyclohexyl amine (1.0 mmol, 0.100 g) for complex **4**, **5** and **8**

Ethylene diamine (1.0 mmol, 0.061 g) for complexes **10** and **11**

Yields:

Complex **4** = 88%; Yellow colour

Complex **5** = 90%; Yellow colour

Complex **8** = 91%; Yellow colour

Complex **10** = 55%; Yellow colour

Complex **11** = 10%; Red-orange colour

8.4.3 Bidentate ligated aminocarbene complexes (6, 7 and 9)

An oven-dried Schlenk flask was filled with inert argon gas and 20 ml of dried dichloromethane was added. $Cr(CO)_5$heteroarene carbene (1.0 mmol) was dissolved in the DCM, cyclohexyl amine (1.0 mmol, 0.100 g) added in a single portion and the reaction mixture stirred until a yellow product was obtained. The solvent was removed, the product resdissolved in toluene and dppe (1.0 mmol, 0.398 g) added in a single portion. The reaction mixture was allowed to reflux at 90 °C until all the yellow aminocarbene had been converted to a brown-orange product. The solvent was removed again under vacuum and the products transferred to a column. The products were purified with silica gel chromatography and both the aminocarbene starting material and the chelated aminocarbene product were obtained. Separation was achieved by first eluting with hexane, thereafter with a hexane:DCM (1:1) mixture and finally with dried THF. Product fractions: Yellow (aminocarbene); Brown-red (chelated aminocarbene product).

Carbene quantities reacted:

Complex **E** (1.0 mmol, 0.332 g) for complexes **6**

© University of Pretoria

Complex **F** (1.0 mmol, 0.316 g) for complexes **7**

Complex **G** (1.0 mmol, 0.498 g) for complex **9**

Yields:

Complex **6** = 67%; Brown-orange colour

Complex **7** = 72%; Brown-orange colour

Complex **9** = 78%; Brown-orange colour

8.5 Preparation of N-Heterocyclic Carbene Complexes

8.5.1 Formation of NHC complex (12)

Step 1: Formation of the THF-Cr(CO)$_5$ complex

$Cr(CO)_6$ + THF → THF-$Cr(CO)_5$

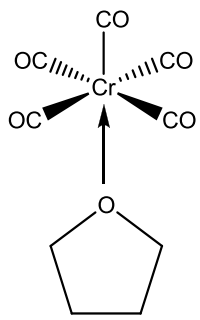

Figure 8.1. Formation of the THF-$Cr(CO)_5$ complex

Chromium(0) hexacarbonyl (1 mmol, 0.220 g) was dissolved in a hexane:THF (5:1) solvent mixture and placed under a UV light (photolysis conditions) to stir for 30 min. The clear solution turned orange and a highly unstable THF-$Cr(CO)_5$ coordination complex formed. The solution was immediately cooled to -30 °C.[5]

© University of Pretoria

Step 2: Deprotonation of the NHC fragment

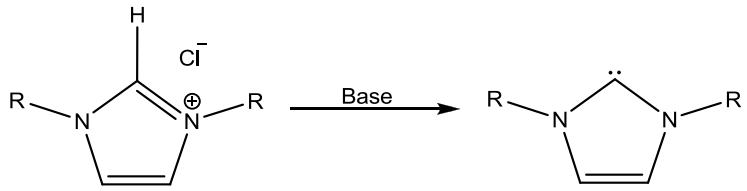

R = Isopropyl, cyclohexyl
Base = KO^{t}Bu, n-Buli

Figure 8.2. Deprotonation of the NHC fragment

The 1,3-bis(isopropyl)imidazolium chloride salt (1.0 mmol, 0.202 g) and 1,3-bis(cyclohexyl)imidazolium chloride (1.0 mmol, 0.247 g), each in turn, were deprotonated with ^{t}BuOK (1.2 mmol, 0.089 g) in dry THF (20 ml) for 30 min in an acetone bath at -30 °C.[5]

The deprotonated imidazolium salt was then slowly added to the freshly prepared THF-$Cr(CO)_5$ coordination complex formed and a bright yellow product formed immediately. The solvent was removed under vacuum and the product transferred to a column.

Purified silica gel chromatography was achieved and complex **12** as well as **13** were successfully purified. Separation was achieved by first eluting with hexane, subsequently with a hexane:DCM (1:1) mixture and finally with dried THF. Product fractions: Pink (complex **13**); Yellow (NHC complexes).

Note: Alternatively, the deprotonated 1,3-bis(isopropyl)imidazolium chloride can be added directly to hexacarbonyl chromium(0) (1 mmol, 0.220 g) to produce the corresponding NHC complex (complex **12**). In the reaction of 1,3-bis(cyclohexyl)imidazolium chloride, only the coordination compound **13** could be isolated. Most of the NHC complex decomposed on the column and upon crystallisation of the residue produced yellow crystals, which were identified as compound **15**.

<u>Yields:</u>

Complex **12** = 5%; Yellow colour

© University of Pretoria

8.6 Preparation of Coordination Complexes

8.6.1 Formation of complex 14

Complex **14** was produced by the substitution of the carbene moiety and a carbonyl ligand by the bidentate ligand, (Z)-N',N',N'',N''-tetramesitylethene-1,2-diamine. This ligand (1 mmol, 0.564,72 g) was reacted with $Cr(CO)_5$thiophene carbene (1.0 mmol, 0.332 g) at 90 °C in toluene for 2 h to produce a blue coordination complex. The solvent was removed *in vacuo* and the product purified via silica gel chromatography with a hexane:DCM (6:4) mixture as eluent. The reaction yielded a blue powder and a single crystal apon crystalisation.

<u>Yield:</u>

Complex **14** = 45%; Blue colour

© University of Pretoria

APPENDICES: All crystal data tables available on the included CD

Appendix A: Crystal data and structure refinement for complex 1

Identification code	up1105n	
Empirical formula	$C_{81}H_{70}Cl_2Cr_2O_8P_4S_4$	
Formula weight	1598.39	
Temperature	180(2) K	
Wavelength	0.71073 Å	
Crystal system	monoclinic	
Space group	$P2_1/n$	
Unit cell dimensions	a = 11.8067(3) Å	a= 90°
	b = 18.7663(6) Å	b= 99.640(2)°
	c = 17.2967(5) Å	g = 90°
Volume	3778.28(19) $Å^3$	
Z	2	
Density (calculated)	1.405 Mg/m^3	
Absorption coefficient	0.610 mm^{-1}	
F(000)	1652	
Crystal size	0.14 x 0.12 x 0.07 mm^3	
Theta range for data collection	3.67 to 26.74°.	
Index ranges	-14<=h<=14, -23<=k<=23, -21<=l<=21	
Reflections collected	30 646	
Independent reflections	7871 [R(int) = 0.1975]	
Completeness to θ = 26.74°	98.2%	
Absorption correction	Semi-empirical from equivalents	
Max. and min. transmission	0.995 and 0.797	
Refinement method	Full-matrix least-squares on F^2	
Data / restraints / parameters	7871 / 3 / 454	
Goodness-of-fit on F^2	0.974	
Final R indices [I>2σ(I)]	R1 = 0.0757, wR2 = 0.1662	
R indices (all data)	R1 = 0.1703, wR2 = 0.1985	
Extinction coefficient	0	
Largest diff. peak and hole	1.108 and -1.058 $e.Å^{-3}$	

© University of Pretoria

Appendix B: Crystal data and structure refinement for complex 2

Identification code	ml_rf1_p21n	
Empirical formula	$C_{36}H_{32}CrO_4P_2S$	
Formula weight	674.62	
Temperature	100(2) K	
Wavelength	0.71073 Å	
Crystal system	Monoclinic	
Space group	$P2_1/n$	
Unit cell dimensions	a = 15.5785(10) Å	a= 90°
	b = 11.6413(7) Å	b= 96.252(2)°
	c = 17.2518(11) Å	g = 90°
Volume	3110.1(3) $Å^3$	
Z	4	
Density (calculated)	1.441 Mg/m^3	
Absorption coefficient	0.578 mm^{-1}	
F(000)	1400	
Crystal size	0.33 x 0.28 x 0.23 mm^3	
θ range for data collection	1.67 to 28.30°	
Index ranges	-20<=h<=20, -15<=k<=12, -22<=l<=23	
Reflections collected	25 756	
Independent reflections	7716 [R(int) = 0.0343]	
Completeness to θ = 28.30°	99.9%	
Absorption correction	Semi-empirical from equivalents	
Max. and min. transmission	0.8775 and 0.8321	
Refinement method	Full-matrix least-squares on F^2	
Data / restraints / parameters	7716 / 0 / 398	
Goodness-of-fit on F^2	1.046	
Final R indices [I>2σ(I)]	R1 = 0.0329, wR2 = 0.0824	
R indices (all data)	R1 = 0.0418, wR2 = 0.0878	
Extinction coefficient	0	
Largest diff. peak and hole	0.435 and -0.379 $e.Å^{-3}$	

© University of Pretoria

Appendix C: Crystal data and structure refinement for complex 3

Identification code	up1206n	
Empirical formula	$C_{36}H_{32}CrO_5P_2$	
Formula weight	658.56	
Temperature	180(2) K	
Wavelength	0.71069 Å	
Crystal system	Monoclinic	
Space group	$P2_1/n$	
Unit cell dimensions	a = 15.1358(4) Å	a= 90°
	b = 11.7118(4) Å	b= 97.573(2)°
	c = 17.4351(5) Å	g = 90°
Volume	3063.72(16) $Å^3$	
Z	4	
Density (calculated)	1.428 Mg/m^3	
Absorption coefficient	0.522 mm^{-1}	
F(000)	1368	
Crystal size	0.28 x 0.14 x 0.14 mm^3	
Theta range for data collection	3.55 to 27.47°.	
Index ranges	-19<=h<=19, -14<=k<=15, -22<=l<=22	
Reflections collected	18 837	
Independent reflections	6911 [R(int) = 0.0374]	
Completeness to θ = 25.24°	99.7%	
Absorption correction	Semi-empirical from equivalents	
Max. and min. transmission	0.931 and 0.827	
Refinement method	Full-matrix least-squares on F^2	
Data / restraints / parameters	6911 / 0 / 398	
Goodness-of-fit on F^2	0.925	
Final R indices [I>2θ(I)]	R1 = 0.0334, wR2 = 0.0791	
R indices (all data)	R1 = 0.0582, wR2 = 0.0824	
Extinction coefficient	0	
Largest diff. peak and hole	0.403 and -0.288 e.$Å^{-3}$	

© University of Pretoria

Appendix D: Crystal data and structure refinement for complex 14

Identification code	ml06_cc	
Empirical formula	$C_{24}H_{24}CrN_2O_4$	
Formula weight	456.45	
Temperature	293(2) K	
Wavelength	0.71073 Å	
Crystal system	monoclinic	
Space group	*Cc*	
Unit cell dimensions	a = 19.3119(18) Å	a= 90°
	b = 7.5303(7) Å	b= 100.912(2)°
	c = 16.0769(15) Å	g = 90°
Volume	2295.7(4) $Å^3$	
Z	4	
Density (calculated)	1.321 Mg/m^3	
Absorption coefficient	0.530 mm^{-1}	
F(000)	952	
Crystal size	0.46 x 0.38 x 0.36 mm^3	
Theta range for data collection	2.58 to 26.42°.	
Index ranges	-23<=h<=15, -8<=k<=9, -18<=l<=15	
Reflections collected	5 932	
Independent reflections	2836 [R(int) = 0.0214]	
Completeness to θ = 25.24°	99.1%	
Absorption correction	Semi-empirical from equivalents	
Max. and min. transmission	0.826 and 0.676	
Refinement method	Full-matrix least-squares on F^2	
Data / restraints / parameters	2836 / 2 / 286	
Goodness-of-fit on F^2	1.066	
Final R indices [I>2σ(I)]	R1 = 0.0294, wR2 = 0.0750	
R indices (all data)	R1 = 0.0295, wR2 = 0.0753	
Absolute structure parameter	0.018(14)	
Extinction coefficient	0	
Largest diff. peak and hole	0.204 and -0.200 e.$Å^{-3}$	

© University of Pretoria

Appendix E: Crystal data and structure refinement for complex B

Identification code	up1106n	
Empirical formula	$C_{10}H_5CrNO_6$	
Formula weight	287.15	
Temperature	180(2) K	
Wavelength	0.71073 Å	
Crystal system	monoclinic	
Space group	$P2_1/c$	
Unit cell dimensions	a = 19.7407(3) Å	a= 90°
	b = 6.72900(10) Å	b= 114.9270(10)°
	c = 18.9860(3) Å	g = 90°
Volume	2287.07(6) $Å^3$	
Z	8	
Density (calculated)	1.668 Mg/m^3	
Absorption coefficient	1.019 mm^{-1}	
F(000)	1152	
Crystal size	0.23 x 0.12 x 0.07 mm^3	
Theta range for data collection	3.61 to 32.03°.	
Index ranges	-29<=h<=29, -10<=k<=9, -28<=l<=28	
Reflections collected	22 520	
Independent reflections	7882 [R(int) = 0.0362]	
Completeness to θ = 32.03°	99.3%	
Absorption correction	Semi-empirical from equivalents	
Max. and min. transmission	0.932 and 0.831	
Refinement method	Full-matrix least-squares on F^2	
Data / restraints / parameters	7882 / 0 / 337	
Goodness-of-fit on F^2	0.956	
Final R indices [I>2σ(I)]	R1 = 0.0311, wR2 = 0.0738	
R indices (all data)	R1 = 0.0530, wR2 = 0.0768	
Extinction coefficient	0	
Largest diff. peak and hole	0.300 and -0.533 e.$Å^{-3}$	

© University of Pretoria

Appendix F: Crystal data and structure refinement for complex A

Identification code	up1107n	
Empirical formula	$C_{10}H_5CrNO_5S$	
Formula weight	303.21	
Temperature	180(2) K	
Wavelength	0.71070 Å	
Crystal system	monoclinic	
Space group	$P2_1/c$	
Unit cell dimensions	a = 9.33320(10) Å	a= 90°
	b = 12.3299(2) Å	b= 90.3200(10)°
	c = 10.3982(2) Å	g = 90°
Volume	1196.58(3) $Å^3$	
Z	4	
Density (calculated)	1.683 Mg/m^3	
Absorption coefficient	1.141 mm^{-1}	
F(000)	608	
Crystal size	0.30 x 0.25 x 0.23 mm^3	
Theta range for data collection	3.84 to 33.14°	
Index ranges	-14<=h<=14, -18<=k<=18, -15<=l<=15	
Reflections collected	19486	
Independent reflections	4541 [R(int) = 0.0303]	
Completeness to θ = 33.14°	99.6%	
Absorption correction	Semi-empirical from equivalents	
Max. and min. transmission	0.775 and 0.703	
Refinement method	Full-matrix least-squares on F^2	
Data / restraints / parameters	4541 / 0 / 170	
Goodness-of-fit on F^2	1.046	
Final R indices [I>2σ(I)]	R1 = 0.0339, wR2 = 0.0929	
R indices (all data)	R1 = 0.0415, wR2 = 0.0977	
Extinction coefficient	0.026(2)	
Largest diff. peak and hole	0.633 and -0.515 $e.Å^{-3}$	

© University of Pretoria

Appendix G: Crystal data and structure refinement for complex 6

Identification code	up1202n	
Empirical formula	$C_{41}H_{41}Cl_2CrNO_3P_2S$	
Formula weight	812.65	
Temperature	180(2) K	
Wavelength	0.71073 Å	
Crystal system	Orthorhombic	
Space group	*Pbcn*	
Unit cell dimensions	a = 28.6325(6) Å	a= 90°
	b = 11.2991(2) Å	b= 90°
	c = 24.0498(5) Å	g = 90°
Volume	7780.6(3) $Å^3$	
Z	8	
Density (calculated)	1.387 Mg/m^3	
Absorption coefficient	0.607 mm^{-1}	
F(000)	3376	
Crystal size	0.18 x 0.16 x 0.12 mm^3	
Theta range for data collection	3.61 to 25.04°.	
Index ranges	-34<=h<=34, -13<=k<=13, -27<=l<=28	
Reflections collected	24 112	
Independent reflections	6492 [R(int) = 0.1030]	
Completeness to θ = 25.04°	94.1%	
Absorption correction	Semi-empirical from equivalents	
Max. and min. transmission	0.976 and 0.525	
Refinement method	Full-matrix least-squares on F^2	
Data / restraints / parameters	6492 / 16 / 437	
Goodness-of-fit on F^2	0.923	
Final R indices [I>2σ(I)]	R1 = 0.0744, wR2 = 0.2097	
R indices (all data)	R1 = 0.1196, wR2 = 0.2378	
Extinction coefficient	0	
Largest diff. peak and hole	1.554 and -0.910 $e.Å^{-3}$	

© University of Pretoria

Appendix H: Crystal data and structure refinement for complex 13

Identification code	ml_rf2_c2c	
Empirical formula	$C_{18}H_{24}CrN_2O_4$	
Formula weight	384.39	
Temperature	100(2) K	
Wavelength	0.71073 Å	
Crystal system	Monoclinic	
Space group	C2/c	
Unit cell dimensions	a = 19.5914(18) Å	a= 90°.
	b = 8.2944(7) Å	b= 121.457(2)°
	c = 13.0126(12) Å	g = 90°
Volume	1803.8(3) $Å^3$	
Z	4	
Density (calculated)	1.415 Mg/m^3	
Absorption coefficient	0.659 mm^{-1}	
F(000)	808	
Crystal size	0.281 x 0.147 x 0.085 mm^3	
θ range for data collection	2.74 to 28.29°	
Index ranges	-26<=h<=26, -10<=k<=11, -17<=l<=17	
Reflections collected	22 582	
Independent reflections	2237 [R(int) = 0.0277]	
Completeness to θ = 28.29°	99.6%	
Absorption correction	Semi-empirical from equivalents	
Max. and min. transmission	0.946 and 0.871	
Refinement method	Full-matrix least-squares on F^2	
Data / restraints / parameters	2237 / 0 / 114	
Goodness-of-fit on F^2	1.203	
Final R indices [I>2σ(I)]	R1 = 0.0231, wR2 = 0.0671	
R indices (all data)	R1 = 0.0250, wR2 = 0.0682	
Extinction coefficient	0	
Largest diff. peak and hole	0.486 and -0.354 e.$Å^{-3}$	

© University of Pretoria

Appendix I: Crystal data and structure refinement for complex 15

Identification code	12m_up3_rfiso	
Empirical formula	$C_{11}H_{13}CrNO_5$	
Formula weight	291.22	
Temperature	173(2) K	
Wavelength	0.71069 Å	
Crystal system	Monoclinic	
Space group	*C*2	
Unit cell dimensions	a = 31.126(5) Å	α = 90°.
	b = 11.567(5) Å	β = 124.513(5)°.
	c = 17.690(5) Å	γ = 90°.
Volume	5248(3) $Å^3$	
Z	16	
Density (calculated)	1.474 Mg/m^3	
Absorption coefficient	0.883 mm^{-1}	
F(000)	2400	
Crystal size	0.272 x 0.095 x 0.069 mm^3	
θ range for data collection	1.40 to 28.00°.	
Index ranges	-31<=h<=41, -15<=k<=15, -23<=l<=23	
Reflections collected	26344	
Independent reflections	12641 [R(int) = 0.1702]	
Completeness to θ = 28.00°	100.0 %	
Absorption correction	Analytical	
Max. and min. transmission	0.9408 and 0.7964	
Refinement method	Full-matrix least-squares on F^2	
Data / restraints / parameters	12641 / 1 / 650	
Goodness-of-fit on F^2	0.744	
Final R indices [I>2σ(I)]	R1 = 0.0628, wR2 = 0.0754	
R indices (all data)	R1 = 0.1952, wR2 = 0.1062	
Absolute structure parameter	-0.07(4)	
Extinction coefficient	0	
Largest diff. peak and hole	0.462 and -0.487 e.$Å^{-3}$	

© University of Pretoria

Appendix J: Crystal data and structure refinement for complex F

Identification code	phvr13_ama2	
Empirical formula	$C_{12}H_8CrO_7$	
Formula weight	316.18	
Temperature	293 K	
Wavelength	0.71069 Å	
Crystal system	Orthorhombic	
Space group	Ama2 (No. 40)	
Unit cell dimensions	a = 7.6779(11) Å	α = 90°.
	b = 12.1661(18) Å	β = 90°.
	c = 14.7560(18) Å	γ = 90°.
Volume	1378.4(3) $Å^3$	
Z	4	
Density (calculated)	1.524 Mg/m^3	
Absorption coefficient	0.856 mm^{-1}	
F(000)	640	
Crystal size	0.48 x 0.39 x 0.29 mm^3	
θ range for data collection	3.3 to 26.10°.	
Index ranges	-4<=h<=9, -11<=k<=14, -17<=l<=17	
Reflections collected	3465	
Independent reflections	1342 [R(int) = 0.0408]	
Completeness to θ = 26.06°	94.4 %	
Absorption correction	Analytical	
Refinement method	Full-matrix least-squares on F^2	
Data / restraints / parameters	1342 / 1 / 112	
Goodness-of-fit on F^2	1.082	
Final R indices [I>2σ(I)]	R1 = 0.0457, wR2 = 0.1140	
R indices (all data)	R1 = 0.0480, wR2 = 0.1186	
Absolute structure parameter	0.45(4)	
Extinction coefficient	0.96(5)	
Largest diff. peak and hole	-0.60 and 0.31 $e.Å^{-3}$	

© University of Pretoria